SIMULATION AND ANALYSIS OF THE WEAR OF METAL ON METAL ARTICULATIONS IN ARTIFICIAL HIP JOINTS

Richard FARRAR BEng CEng MIMechE DipEM

Submitted in accordance with the requirements for the degree of

Doctor of Philosophy

The University of Leeds
School of Mechanical Engineering

March 2001

The candidate confirms that the work submitted is his own and that appropriate credit has been given where reference has been made to the work of others

ACKNOWLEDGEMENTS

Six years go by as quickly as you bat your eyelid and especially when you have a few more years under your belt to start with, whilst on the other hand it seems an awfully long time ago since 1995 when the work started: Life can be strange sometimes!

I would like to acknowledge a number of people who have helped directly or, just because they are such a significant part of my life, have helped by being there.

One summers afternoon in 1992 I met for the first time someone who was to have a greater influence and presence in my life than I could then have imagined. The advice he gave me that day and on many occasions since was sound. Professor John Fisher, advisor, academic supervisor, intellectual giant, and good friend: Thankyou!

Dr Mary Beth Schmidt, Research Scientist at J&J Raynham, Mass, USA, and favourite co worker on the metal on metal programme.

Dr Allan Ritchie, Director of Research and Development at DePuy in Leeds and my industrial supervisor, who, even after interviewing me, offered me my first bioengineering job at J&J in New Milton! It has been my pleasure to report to him for all but 2 of my years with the company.

Dr Don Evans, former VP of Research, Development and Operations at J&J New Milton, by whom the idea of a PhD was given the nod of approval over dinner and belly dancing entertainment in Morocco, Epcot. Wow, was that so long ago?

Robert Scott, Senior Bioengineer and colleague during my early years at J&J, who taught me so much about bioengineering, and handed over to me the metal on metal programme on his departure, and remains my good friend.

All the lads who worked so hard with me at J&J in New Milton to make the metal on metal programme happen including Mike Harvey, Dave Smith, Ian Roberts, Len Mutter, Tony Hargreaves, Danny Ingrem, Dennis "broom stick handle" Turner (happy retirement), Adrian Dyer, Colin Wellman, Trevor Burley, Brian Griffiths, and Bruno Hiernard. Boy, we had some laughs! Thanks to you all from "Yorkie", let me know if I missed anyone, and all the best for the future!

Thanks to the orthopaedic surgeons around the world with whom it was such a pleasure to work. To Mr Nolan, Mr Phillips, and Mr Tucker in Norwich UK, Mr Villar in Cambridge UK, Mr Bhamra in Rotherham UK, Dr Dick in Bavaria Germany, Prof. Honnart in Paris France, and Dr Jacobs in Baltimore USA. I certainly retain many fond memories of trips and meetings.

Thanks to Cath Goulborn, Professor Fishers Secretary for making many arrangements for meetings and organizing the parking ("Your name's not down so you ain't coming in!" was only said to me once by the security guard). Thanks also to Pat Richardson, mechanical Engineering Post Graduate Secretary at Leeds University for going out of

her way to make the registration process painless for me each year whilst I lived and worked so far from Leeds.

Thanks to my parents who have always supported me and always shown delight when even the smallest thing has turned out well. Also to the rest of my kin who always enquire with interest as to how its all going: Brian and Mandy Farrar, Phillip and Janette Harrison, John and Linda Irvine, Paul and Julie Stephens, Graham and Val Wilford, and of course my mother in law Jean Harrison (no son in law could have wished for a better one!).

I acknowledge some special friends, since teenage years, who have always been there and with whom I have felt most comfortable to talk about even the "difficult things" of life. Thanks Paul and Jackie Johnston and Andy and Ruth Wilson.

To all my good friends at the Family Church Christchurch with whom we met for 7 very happy years whilst living in Lymington, Hampshire. This PhD was just one of my reasons for not being able to spend more time with you! Thanks Tony and Sue Goodman, John and Pat Bament, Peter and Ann Bassett, Peter and Jayne Herbert, John and Beryl Braime, and many, many more.

And finally, and most of all, those one could call "longsuffering" through this six year task: My Family. To my children I owe a fortune of gratitude for not being too critical when I had to decline the various offers to "Come and play". They maybe didn't feel so bad about that but I know I did. During this period, Adam has gone from 4 to 10, Oliver from 2 to 8, and Elliot has arrived and reached 5 years old. Thanks boys!

And especially to my wife Shirley who is just so grateful that, in the 10 years or so between my bachelors degree and this PhD, the computer revolution has meant that she didn't have to type this thesis up by hand as she did with my final year project all those years before. Her dedication towards me has not waned though and I have no clue what I would have done without her.

2 Corinthians 9v15 "Thanks be to God for his indescribable gift!" Thanks Father.

Richard Farrar
Leeds
2001

ABSTRACT

Metal on metal articulations used in hip joint replacement were demonstrated through the 1960's and 70's to perform adequately and comparably to metal on plastic articulations but their use then fell into decline as orthopaedic surgeons preferred metal on polyethylene articulations. However, one of the main causes of failure of prosthetic hip joints was then discovered to be aseptic loosening due to particle induced osteolysis, such particles arising from wear of the prosthetic components, and in particular from polyethylene bearing surfaces. Through the late 1980's and the 1990's the concept of metal on metal bearings has re-emerged as one potential solution to the clinical problems associated with polyethylene particle induced osteolysis.

In this thesis both theoretical analysis and practical testing using a 12 station MMED hip joint simulator were employed to investigate how metal on metal articulations may be optimized so as to reduce the amount of wear debris generated through their use. Hence, such articulations should function effectively within the environment of a human hip joint when they form part of a total hip replacement design. To this end the effect of diametral clearance, head size, and material composition were both tested and analyzed. Finally a modular clinical design of hip joint replacement was tested to assess its performance.

Wear was found to be strongly related to bearing clearance in practical tests as predicted by the theory. A lower limit of clearance existed due to deviations from perfect form which were unavoidable with current manufacturing technology. A band of clearance was defined for 22, 28, and 35mm diameter bearings within which reduced wear was exhibited. Steady state wear rates, following the initial bedding in period, were generally equal regardless of total wear volume. High carbon against high carbon content cobalt chromium articulations did not produce the lowest wear contrary to previous studies in the literature. The mean hardness of, and hardness difference between, bearing surfaces influenced the wear performance of metal on metal articulations. It was possible to design a clinical metal on metal bearing having modular femoral (head and stem) and acetabular (insert and shell) components with optimized metal on metal articulation. This metal on metal device has been introduced into clinical use throughout the world.

CONTENTS

		Page
	Acknowledgements	i
	Abstract	iii
	Contents	iv
	List of Figures and Tables	viii
	Nomenclature	xxv
1.	Introduction	1
2.	Literature Review	4
2.1	Introduction	4
2.2	A historical Review of Metal on Metal Devices	5
2.1.1	McKee-Farrar	5
2.1.2	Ring	10
2.3	Design Critique of Early Devices	15
2.3.1	McKee-Farrar	15
2.3.2	Ring	15
2.4	Review of Clinical Performance of Early Devices	16
2.4.1	McKee-Farrar	16
2.4.2	Ring	19
2.5	Review of Clinical Performance of Modern Designs	20
2.6	In Vitro and Theoretical Studies	21
2.6.1	Simulator Studies	21
2.6.2	Retrieval Analysis	23
2.6.3	Theoretical Studies	24
2.7	Discussion	25
3.	Research Hypothesis	29
3.1	Research Hypothesis	29
3.2	Research Objectives	29
3.2.1	Diametral Clearance Objective	29
3.2.2	Material Composition Objective	29
3.2.3	Head Diameter Objective	29
3.2.4	Clinical Product Objective	30

3.3	Structure of Thesis	30
4.	Theoretical Analysis and Design of Articulating Geometry	31
4.1	Introduction	31
4.2	The Influence of Geometrical Errors (Walker and Gold)	31
4.3	Analysis of Lubricating Film Thickness and Contact Mechanics (Jin, Dowson, and Fisher)	34
5.	Materials, Equipment, and Methods	43
5.1	Introduction	43
5.2	Materials	43
5.3	Equipment	45
5.3.1	Microfinishing Machine	45
5.3.2	Co-ordinate Measuring Machine	50
5.3.3	Profilometer	53
5.3.4	Balance	55
5.3.5	Hip Simulator	55
5.4	Methods	62
5.5	Summary	69
6.	Investigation of the Effect of Diametral Clearance on Wear for a 28mm Articulation in a Hip Simulator Test	71
6.1	Introduction	71
6.2	Method	71
6.3	Materials	72
6.4	Test Pieces	72
6.5	Pre Test Surface Finish	74
6.6	Pairing of Test Pieces	75
6.7	Results	76
6.8	Discussion	83
6.9	Conclusions	97
7.	Investigation of the Effect of Material Composition on Wear in a Hip Simulator Test	99
7.1	Introduction	99
7.2	Method	100
7.3	Materials	101

7.4	Test Pieces	101
7.5	Pre Test Surface Finish	103
7.6	Results	103
7.7	Discussion	121
7.8	Conclusions	135
8.	Investigation of the Effect of Head Diameter on Wear in a Hip Simulator Test	137
8.1	Introduction	137
8.2	Method	137
8.3	Materials	137
8.4	Test Pieces	139
8.5	Pre Test Surface Finish	140
8.6	Pairing of Test Pieces	140
8.7	Results	141
8.8	Discussion	155
8.9	Conclusions	159
9.	Investigation of the Long Term Wear Performance of a Clinical Metal on Metal Product Design in a Hip Simulator Test	161
9.1	Introduction	161
9.2	Device Design	162
9.3	Method	166
9.4	Materials	166
9.5	Test Pieces	166
9.6	Pre Test Surface Finish	167
9.7	Results	167
9.8	Discussion	174
9.9	Conclusions	178
10.	Conclusions of the Study, Discussion, and Recommendations for Further Work	179
10.1	Introduction	179
10.2	Discussion	180
10.3	Recommendations for Further Work	183

Bibliography 184

Appendices

Appendix A: Preliminary Wear Test

Appendix B: Figures and Tables

Appendix C: Derivations and Calculations

Appendix D: Abstracts, Proceedings, and Papers

Appendix E: Procedure for Operation of Surfanalyzer 5000 Profilometer

LIST OF FIGURES AND TABLES

1. Figures

Figure 4.1: Relationship of spherical socket and ball. Figure shows the relationship when the ball is fractionally larger than the socket as could be the case due to imperfections of sphericity. Reproduced from Walker and Gold (1971)

Figure 4.2: Base Clearance 'e' between Ball and Socket against values of Radial Interference where Effective Diameter of the Ball exceeds that of the Socket. Figure shows the relationship when the ball is fractionally larger than the socket as could be the case due to imperfections of sphericity. Reproduced from Walker and Gold (1971)

Figure 4.3a: Relationship Between Predicted Film Thickness, Nominal Bearing Diameter, and Diametral Clearance. Figure shows curves of diametral clearance on axes of nominal diameter and predicted film thickness for a cobalt chromium alloy metal on metal spherical articulation.

Figure 4.3b: Relationship Between Predicted Lubrication Regime, Nominal Bearing Diameter, and Diametral Clearance. Figure shows curves of diametral clearance on axes of nominal diameter and lambda ratio for a cobalt chromium alloy metal on metal spherical articulation.

Figure 4.4a: Relationship Between Contact Half Width, Nominal Bearing Diameter, and Diametral Clearance. Figure shows curves of diametral clearance on axes of nominal diameter and Hertzian contact half width for a cobalt chromium alloy metal on metal spherical articulation.

Figure 4.4b: Relationship Between Peak Pressure, Nominal Bearing Diameter, and Diametral Clearance. Figure shows curves of diametral clearance on axes of nominal diameter and peak pressure within the Hertzian contact zone for a cobalt chromium alloy metal on metal spherical articulation.

Figure 4.5: Replication of Figure 4.3b but with Better Surface Finish. Figure shows curves of diametral clearance on axes of nominal diameter and lambda ratio for a cobalt chromium alloy metal on metal spherical articulation.

Figure 5.1: Thielenhaus Type KF50F2 (No 1.1.002453) Microfinishing Machine.

Figure 5.2: Thielenhaus Microfinishing Machine Suitable for Microfinishing the Cup Inserts.

Figure 5.3: Plane Section through a Sphere. Figure shows that any plane section through a sphere is circular in form.

Figure 5.4: Microfinishing a Cup. Figure shows the relationship of the cup work piece and the stone during microfinishing. Note that the working edge of the stone is the external corner and note the angle of about 45° between the axes of the cup and the stone.

Figure 5.5: Arrangement of In Process Measurement Calliper Arms. Figure shows the Thielenhaus machine with work holding jaws, microfinishing spindle, and in process measurement calliper arms.

Figure 5.6: Mitutoyo CMM model BH305.

Figure 5.7: CMM Trigger Probe and Ceramic Calibration Master Ball.

Figure 5.8: Surfanalyzer 5000 profilometer.

Figure 5.9: Typical Printout from The Surfanalyzer. Figure shows the input, and output information for the measurement of a metal on metal cup bearing surface. The figure is not to scale.

Figure 5.10: Sartorius balance model MC210S.

Figure 5.11: MMED EW12 Hip Simulator.

Figure 5.12: MMED EW12 Hip Simulator Station. The arrangement of a single station during a test showing test fixtures and fluid retention. 5.12a (left) shows a photograph of a station during test whilst 5.12b (right) shows a cutaway CAD model of a station clearly showing the internal arrangement.

Figure 5.13: Paul walking Cycle. The figure shows the form of the Paul walking cycle used in the study at a peak load of 2000N.

Figure 5.14: MMED EW12 Hip Simulator Station Side View. Figure shows a CAD representation of the side view of a station during test. The geometrical orientation of the parts is clear and the temperature probe can be seen inserted through the lid.

Figure 5.15: MMED EW12 Hip Simulator Station Pair Diagrammatic. Figure shows the arrangement of a pair of stations during a test.

Figure 6.1a: Hip Simulator Test Pieces. Three dimensional cut away model of the hip simulator metal on metal test sample pairings. Note that in the simulator the head would be exactly as illustrated but the cup would be rotated by 22.5° about the head centre

Figure 6.2: Total Wear for 28mm Samples. Figure shows a weight loss against number of cycles of the hip simulator for the 12 samples having variation of clearance between head and cup

Figure 6.3a: 3 Dimensional Total Wear Plot. Figure shows a weight loss against number of cycles of the hip simulator for the 12 samples having variation of clearance between head and cup in a three dimensional format which clearly illustrates the lowest wear samples

Figure 6.3b: 3 Dimensional Total Wear Plot . The positive clearance test piece data of Figure 6.3a is shown against a linear X axis

Figure 6.4: Effect of Diametral Clearance on Temperature. Each curve represents the temperature profile for all samples at a particular number of cycles through the test. The legend indicates the particular number of cycles and for how long the simulator had continuously run prior to taking the temperatures. It was considered that these times were long enough to ensure steady state temperatures were recorded

Figure 6.5a-f: Fluorescing Photographs of Sample Heads. Figure shows a photograph for a selection of the sample heads taken looking directly on the pole. The fluorescence technique allows the condition of the articulating surface to be shown clearly. Heads are identified by head number and diametral clearance

Figure 6.6a-f: Fluorescing Photographs of Sample Cups. Figure shows a photograph for a selection of the sample cups taken looking directly on the pole. The fluorescence technique allows the condition of the articulating surface to be shown clearly. Cups are identified by cup number and diametral clearance

Figure 6.7: Wear Volume Against Contact Radius. Values of wear volume (V) plotted against radius of conforming contact patch (Rcp) for theoretical 28mm head diameter with diametral clearance of 0.014, 0.060, and 0.322mm

Figure 6.8: Replication of the "Low Wear" Samples of Figure 6.2. In order to see on a larger vertical scale how the lowest wear samples performed, these are shown in isolation

Figure 7.1: Pin on Disk Test Results. Test results for metal on metal pin on disk testing as presented by Schmidt et al (1996) as evidence that metal on metal spherical bearing pairings should be designed and manufactured using high against high carbon materials. Materials A to G represent CoCrMo alloys from different manufacturers. H/H represents high carbon content (0.20-0.30%) and L/L low carbon content (0.05-0.08%) combinations. Material A is cast and B to G are hot rolled

Figure 7.2a: Total Wear for 28mm Variable Carbon Content Samples (Test 1). Figure shows weight loss against number of cycles of the hip simulator for the 28mm variable carbon content wear test samples for the first of three such tests.

Figure 7.2b: Total Wear for 28mm Variable Carbon Content Samples (Test 2). Figure shows weight loss against number of cycles of the hip simulator for the 28mm variable carbon content wear test samples for the second of three such tests.

Figure 7.2c1: Total Wear for 28mm Variable Carbon Content Samples (Test 3). Figure shows weight loss against number of cycles of the hip simulator for the 28mm variable carbon content wear test samples for the third of three such tests.

Figure 7.2c2: Replication of the Lower Wear Samples of Fig 7.2c1. Figure shows the data of Figure 7.2c1 but without the obviously high wear sample.

Figure 7.3a: Total Wear at 2 Million Cycles for 28mm Variable Carbon Content Samples (Test 1). Figure shows weight loss at about 2 million cycles of the hip simulator for the 28mm variable carbon content wear test samples for the first of three such tests.

Figure 7.3b: Total Wear at 2 Million Cycles for 28mm Variable Carbon Content Samples (Test 2). Figure shows weight loss at about 2 million cycles of the hip simulator for the 28mm variable carbon content wear test samples for the second of three such tests.

Figure 7.3c: Total Wear at 2 Million Cycles for 28mm Variable Carbon Content Samples (Test 3). Figure shows weight loss at about 2 million cycles of the hip simulator for the 28mm variable carbon content wear test samples for the third of three such tests.

Figure 7.4a-f: Fluorescing Photographs of Sample Heads. Figure shows a photograph for a selection of the sample heads taken looking directly on the pole. The fluorescence technique allows the condition of the articulating surface to be shown clearly. Heads are identified by head number.

Figure 7.5a-f: Fluorescing Photographs of Sample Cups. Figure shows a photograph for a selection of the sample cups taken looking directly on the pole. The fluorescence

technique allows the condition of the articulating surface to be shown clearly. Cups are identified by cup number.

Figure 7.6: Cup form Plots Near Bearing Surface Edge. Figure shows actual and theoretical form plots for cups MC073 and MC079 from CMM data of table 7.9 with cup axis of revolution shown horizontal. The cup lead in chamfer is clearly visible and should intersect the spherical form below the spherical centre at the zero level as shown on MC073.

Figure 7.7: Mean Material Hardness for High and Low Carbon Content Materials Used in the Carbon Content Variation Study. Figure shows the estimate of population means for high and low carbon cobalt chromium alloy materials of chapters 6 and 7. The error bars represent the 95% confidence levels for the population means (Appendix C3).

Figure 7.8a: Mean Wear Against Sample Hardness Difference for 28mm Variable Carbon Content Samples. Figure shows weight loss at about 2 million cycles of the hip simulator for the 28mm variable carbon content wear test samples plotted against difference in hardness between cup and head for all 34 samples.

Figure 7.8b: Mean Wear Against Mean Sample Hardness for 28mm Variable Carbon Content Samples. Figure shows weight loss at about 2 million cycles of the hip simulator for the 28mm variable carbon content wear test samples plotted against the mean hardness of cup and head for all 34 samples.

Figure 7.8c: Mean Wear Against Sample Hardness Difference for 28mm Variable Carbon Content High/High Samples. Figure shows weight loss at about 2 million cycles of the hip simulator for the 28mm variable carbon content wear test samples plotted against difference in hardness between cup and head for all 10 high/high carbon content samples.

Figure 7.8d: Mean Wear Against Mean Sample Hardness for 28mm Variable Carbon Content High/High Samples. Figure shows weight loss at about 2 million cycles of the

hip simulator for the 28mm variable carbon content wear test samples plotted against the mean hardness of cup and head for all 10 high/high carbon content samples.

Figure 7.8e: Mean Wear Against Sample Hardness Difference for 28mm Variable Carbon Content Low/Low Samples. Figure shows weight loss at about 2 million cycles of the hip simulator for the 28mm variable carbon content wear test samples plotted against difference in hardness between cup and head for all 8 low/low carbon content samples which includes the three optimum clearance samples from chapter 6.

Figure 7.8f: Mean Wear Against Mean Sample Hardness for 28mm Variable Carbon Content Low/Low Samples. Figure shows weight loss at about 2 million cycles of the hip simulator for the 28mm variable carbon content wear test samples plotted against the mean hardness of cup and head for all 8 low/low carbon content samples which includes the three optimum clearance samples from chapter 6.

Figure 7.8g: Mean Wear Against Sample Hardness Difference for 28mm Variable Carbon Content High/Low and Low/High Samples. Figure shows weight loss at about 2 million cycles of the hip simulator for the 28mm variable carbon content wear test samples plotted against difference in hardness between cup and head for all 19 high/low and low/high carbon content samples.

Figure 7.8h: Mean Wear Against Mean Sample Hardness for 28mm Variable Carbon Content High/Low and Low/High Samples. Figure shows weight loss at about 2 million cycles of the hip simulator for the 28mm variable carbon content wear test samples plotted against the mean hardness of cup and head for all 19 high/low and low high carbon content samples.

Figure 8.1: Total Wear at 2 Million Cycles for 22mm Samples. Figure shows weight loss against number of cycles of the hip simulator for the 22mm variable diametral clearance wear test samples

Figure 8.2: Total Wear at 2 Million Cycles for 35mm Samples. Figure shows weight loss against number of cycles of the hip simulator for the 35mm variable diametral clearance wear test samples

Figure 8.3: Replication of Figure 8.2. Figure shows weight loss against number of cycles of the hip simulator for the 35mm variable diametral clearance wear test samples as Figure 8.2 but with same scale as Figure 8.1 for easier direct comparison.

Figure 8.4: Fluorescing Photographs of Sample Heads. Figure shows a photograph for a selection of the sample heads taken looking directly on the pole. The fluorescence technique allows the condition of the articulating surface to be shown clearly. Heads are identified by head number and diametral clearance.

Figure 8.5: Fluorescing Photographs of Sample Cups. Figure shows a photograph for a selection of the sample cups taken looking directly on the pole. The fluorescence technique allows the condition of the articulating surface to be shown clearly. Cups are identified by cup number and diametral clearance.

Figure 8.6: Mean Total Wear at 2 Million Cycles for 22, 28, and 35mm Samples. Figure shows mean weight loss against number of cycles of the hip simulator for the 22, 28, and 35mm variable diametral clearance wear test samples with diametral clearance between 0.03 and 0.09mm. Note that sample MH/MC031 excluded at final interval due to unusually high wear rate over final interval.

Figure 9.1: CAD Image of Metal on Metal Cup. Figure shows a partially cut away CAD model of a Metal on Metal shell, augmented insert, and femoral head.

Figure 9.2: Photograph of Typical Metal on Metal Total Hip. Photograph shows a typical combination of the metal on metal cup with augmented insert and coupled with a cemented TPS stem.

Figure 9.3: Total Wear for Final Design Samples. Figure shows weight loss against number of cycles of the hip simulator for the final design test samples. The red curves represent standard and the blue curves augmented samples. The black curves represent the control samples.

Figure 9.4: Mean Total Wear for Final Design Samples. Figure shows weight loss against number of cycles of the hip simulator for the final design test samples. The red curve represents the mean wear for standard and the blue curve for augmented samples. Error bars shown for samples greater than 4.

Figure 9.5: Mean Total Wear for Final Design Samples Compared to Previous Test. Figure shows weight loss against number of cycles of the hip simulator for the final design test samples compared to the same data for the high/low and low high carbon content test samples of chapter 7. The red curve represents the mean wear for standard and the blue curve for augmented samples and the green curve for the samples of chapter 7.

Figure 9.6: Wear Rate for MOM against that for MOP
Figure shows the wear rate for metal on metal designs compared with those for metal on polyethylene articulations either sterilized by gamma irradiation in air or in a vacuum foil pouch.

Figure A.1: Cup Weight Loss for Preliminary Wear Test. Figure shows cup weight loss against number of cycles of the hip simulator for the preliminary study wear test samples

Figure A.2: Head Weight Loss for Preliminary Wear Test. Figure shows head weight loss against number of cycles of the hip simulator for the preliminary study wear test samples

Figure A.3: Total Weight Loss for Preliminary Wear Test. Figure shows total weight loss against number of cycles of the hip simulator for the preliminary study wear test samples

Figure B5.15a: Hip Simulator Test Fixture Drawing (Base). The test fixture base used for the hip simulator tests made in accordance with drawing E03496.

Figure B5.15b: Hip Simulator Test Fixture Drawing (Lid). The test fixture header disc or lid used for the hip simulator tests made in accordance with drawing E03560.

Figure B5.15c: Hip Simulator Test Fixture Drawing (Rod). The test fixture head shaft or rod used for the hip simulator tests made in accordance with drawing E03562.

Figure B6.1b: Hip Simulator Test Cup Drawing. The test piece cups used for the hip simulator tests using wrought material were made in accordance with the test piece drawing E02931

2. Tables

Table 4.1: Base Clearance 'e' between Ball and Socket against values of Radial Interference Δ where Effective Diameter of the Ball exceeds that of the Socket

Table 5.1: List of material suppliers used in the study

Table 5.2: List of materials used in the study

Table 6.1: Material details for the 28mm variable diametral clearance wear test samples

Table 6.2: Geometrical details of the articulating surfaces for the 28mm variable diametral clearance wear test samples

Table 6.4: Sample heads and cups matched to give required variation of diametral clearance

Table 6.8: The data of Table 6.2 repeated after completion of the wear test is presented

Table 6.9: Comparison of the articulating surface geometry's pre and post testing

Table 6.10: Problems encountered during the simulator wear test

Table 6.11: Information from a post test visual inspection of the wear test heads and cups

Table 7.1: Material details for the 28mm variable carbon content wear test samples

Table 7.2: Material and geometrical bearing surface details of the test piece samples for the 28mm variable carbon content wear test samples including detail of simulator run number.

Table 7.5: The geometry data of Table 7.2 repeated after completion of the wear test is presented.

Table 7.6: Comparison of articulating surface geometry's pre and post testing.

Table 7.7: Problems encountered during the simulator wear tests.

Table 7.8a: Information from a post test visual inspection of the wear test heads MH017 to MH028

Table 7.8b: Information from a post test visual inspection of the wear test heads MH060 to MH071

Table 7.8c: Information from a post test visual inspection of the wear test heads MH072 to MH084

Table 7.8d: Information from a post test visual inspection of the wear test cups MC017 to MC028

Table 7.8e: Information from a post test visual inspection of the wear test cups MC060 to MC071

Table 7.8f: Information from a post test visual inspection of the wear test cups MC072 to MC084

Table 7.9: Actual and theoretical points on the bearing surface and lead in chamfer of cups MC073 and MC079.

Table 7.10: Hardness data for the materials used for the carbon content variation test.

Table 7.11a: Hardness data for the materials used for the carbon content variation test. Note that mean hardness values are rounded down to nearest whole or half Rockwell.

Table 7.11b: Mean wear versus hardness data for all materials used for the carbon content variation test. Note that mean hardness values are rounded down to nearest whole or half Rockwell.

Table 7.11c: Mean wear versus mean hardness data for the high/high carbon materials used for the carbon content variation test. Note that mean hardness values are rounded down to nearest whole or half Rockwell.

Table 7.11d: Mean wear versus mean hardness data for the low/low materials used for the carbon content variation test. Note that mean hardness values are rounded down to nearest whole or half Rockwell.

Table 7.11e: Mean wear versus mean hardness data for the high/low and low/high materials used for the carbon content variation test. Note that mean hardness values are rounded down to nearest whole or half Rockwell.

Table 8.1: Material details for the 22 and 35mm variable diametral clearance wear test samples.

Table 8.2: Geometrical details of the articulating surfaces for the 22 and 35mm variable diametral clearance wear test samples

Table 8.4: Problems encountered during the simulator wear test.

Table 8.5: The geometry data of Table 8.2 repeated after completion of the wear test is presented.

Table 8.6: Comparison of articulating surface geometry's pre and post testing.

Table 8.7a: Information from a post test visual inspection of the 22mm wear test heads MH029 to MH040.

Table 8.7b: Information from a post test visual inspection of the 35mm wear test heads MH044 to MC056.

Table 8.7c: Information from a post test visual inspection of the 22mm wear test cups MC029 to MC040

Table 8.7d: Information from a post test visual inspection of the 35mm wear test cups MC044 to MC056

Table 8.8: 22, 28, and 35mm diametral clearance variation wear test results for samples between 0.030 and 0.090mm diametral clearance inclusive. Note that the data point at 2026464 cycles for sample MH/MC031 was excluded since it exhibited an unusually high wear rate over the final interval.

Table 9.1: Material details for the final design wear test samples.

Table 9.2: Insert type and geometrical bearing surface details of the test piece samples for the final design wear test.

Table 9.5: The geometry data of Table 9.2 repeated after completion of the wear test is presented.

Table 9.6: Comparison of articulating surface geometry pre and post testing.

Table 9.7: Problems encountered during the simulator wear test.

Table 9.8a: Information from a post test visual inspection of the wear test heads MH100 to MH113

Table 9.8b: Information from a post test visual inspection of the wear test inserts MC100 to MC113

Table A.1: Geometrical details of the articulating surfaces for the preliminary wear test samples

Table A.2: Wear test samples pairings to give variation in diametral clearance

Table A.3: Preliminary hip simulator wear test results with wear in grams

Table A.4: Preliminary hip simulator wear test results with wear in mm^3

Table A.5: Steady state temperature of serum in hip simulator stations associated with specific diametral clearance wear test samples through the test

Table B6.3a: Pre test surface finish data for 28mm diametral clearance variation wear test heads

Table B6.3b: Pre test surface finish data for 28mm diametral clearance variation wear test cups

Table B6.5: 28mm diametral clearance variation wear test results

Table B6.6: Steady state temperature of serum in hip simulator stations associated with specific diametral clearance wear test samples through the test

Table B6.7: Pre test surface finish data for 28mm diametral clearance variation wear test head and cup samples.

Table B7.3a: 28mm carbon content variation wear test results, Test 1 of 3

Table B7.3b: 28mm carbon content variation wear test results, Test 2 of 3

Table B7.3c: 28mm carbon content variation wear test results, Test 3 of 3

Table B7.4a: 28mm carbon content variation mean wear test results at about 2 million cycles, Test 1 of 3

Table B7.4b: 28mm carbon content variation mean wear test results at about 2 million cycles, Test 2 of 3

Table B7.4c: 28mm carbon content variation mean wear test results at about 2 million cycles, Test 3 of 3

Table B7.4d: 28mm carbon content variation mean wear test results at about 2 million cycles, Sum of All 3 Tests

Table B7.4e: 28mm carbon content variation mean wear test results at about 2 million cycles, Sum of All 3 Tests as Table B7.4d but combining the H/L and L/H samples

Table B7.4f: 28mm carbon content variation mean wear test results at about 2 million cycles, Sum of All 3 Tests and including the 3 optimum clearance Low/Low samples from Chapter 6 (Figure 6.8)

Table B8.3a: 22mm diametral clearance variation wear test results

Table B8.3b: 35mm diametral clearance variation wear test results

Table B9.3a: Final design wear test results from 0 to 2 million cycles

Table B9.3b: Final design wear test results from 2 to 5 million cycles

Table B9.4a: Standard insert final design mean wear data. Appendix C3 details the statistical method used.

Table B9.4b: Augmented insert final design mean wear data. Appendix C3 details the statistical method used.

Table B9.9: Mean wear data for the high/low and low/high carbon content samples of chapter 7 interpolated linearly to give data at the cycle intervals as used for the data of chapter 9.

Table C2.1: Values of wear volume (V), radius of conforming contact patch (Rcp), and linear penetration (a) for a theoretical 28mm head diameter with diametral clearance of 0.014, 0.060, and 0.322mm. Data is colour coded to clarify which values of Rcp and a correspond to which diametral clearance.

NOMENCLATURE

1. Alphabetical

a	Contact half width or radius of circular contact area
Ah	Curved surface area of a hemisphere
As	Surface area of a sphere
ASTM	American Society for Testing and Materials
b	Linear penetration of R_1 into R_2
C	Chemical symbol for Carbon
	Units of temperature: degrees Celsius
CMM	Coordinate Measuring Machine
Co	Chemical symbol for Cobalt
Cr	Chemical symbol for Chromium
D	Test specimen diameter
	Equivalent diameter of spherical articulating surfaces
D_1	Diameter of the male spherical bearing surface (head)
D_2	Diameter of the female spherical bearing surface (cup)
e	Base clearance at pole of cup between head and cup due to form errors
E_i	A single measurement of a single sample drawn randomly from a population
Ë	The mean of the measured values of a sample of size n
E'	Equivalent elastic modulus of mating bearing surfaces
E_1	Elastic modulus of the male spherical bearing surface (head)
E_2	Elastic modulus of the female spherical bearing surface (cup)
El%	Percentage elongation of test sample at fracture (ductility indicator)
Fe	Chemical symbol for Iron
g	Units of mass: Gramme
h_{min}	Minimum lubricating film thickness
HRc	Hardness of a material according to the Rockwell Scale C
Hz	Units of frequency: Hertz (1Hz = 1cycle/second)
kg/m^3	Units of density: kilogramme/cubic metre

kg	Units of mass: kilogramme (1kg=1000g)
l	Linear distance from the pole of a spherical surface along the polar axis
L	Linear distance from the pole of a spherical surface along the polar axis defining a portion of the sphere of which the volume is to be calculated
m	units of length: metre (1m=1000mm)
MC	Hip simulator test cup sample designation meaning Metal Cup
MH	Hip simulator test head sample designation meaning Metal Head
mm	Units of length: millimetre
mm^3	Units of volume: cubic millimetre
Mn	Chemical symbol for Manganese
Mo	Chemical symbol for Molybdenum
n	Number of parts in a sample
N	Units of Force: Newton Chemical symbol for Nitrogen
N/A	Not Available
Ni	Chemical symbol for Nickel
P	Chemical symbol for Phosphorus
q_o	Peak pressure at centre of Hertzian contact zone
r	Radial distance to a point on a spherical surface from and perpendicular to the polar axis
R	Radius of a sphere
Ra	Surface roughness parameter: The arithmetic average of the absolute values of the measured profile height deviations taken within the measurement length and measured from the mean line. Used also as the composite surface roughness of a bearing pair
R_{a1}	Surface roughness of the male spherical bearing surface (head)
R_{a2}	Surface roughness of the female spherical bearing surface (cup)
RA%	Percentage reduction in area of test sample
Rb	Instantaneous radius of an imperfectly formed ball or head
Rcp	Radius of conforming contact patch between 2 mating spherical surfaces, one male and one female
Rp	Surface roughness parameter: The maximum profile peak

	height measurement provides the distance between the highest point of the roughness profile and the mean line within the sampling length
Rs	Radius of socket or cup
Rsk	Surface roughness parameter: The skewness measurement provides a measure of the symmetry of the roughness profile about the mean line Rsk<0: surfaces with peaks removed, or with deep scratches Rsk=0: surfaces with equal form and size of peaks and valleys Rsk>0: surfaces dominated by peaks or with valleys filled in
Rv	Surface roughness parameter: The maximum profile valley depth measurement provides the distance between the lowest point of the roughness profile and the mean line within the sampling length
Ry	Surface roughness parameter: The maximum height of profile measurement provides the distance between the line of roughness profile peaks and the line of roughness profile valleys within the sampling length
R_1	Radius of male sphere
R_2	Radius of female sphere
s	The standard deviation of a sample of size n drawn from a population
š	The standard deviation of a population from which a sample of size n is drawn
S	Chemical symbol for Sulphur
Si	Chemical symbol for Silicon
t	Statistical distribution used rather than the normal distribution when sample sizes are below 30.
u	Entraining velocity ($u_1/2$)
u_1	Sliding velocity of male in the female bearing surface (head in cup)
UTS	Ultimate Tensile Strength
V	Volume of wear between two spherical mating surfaces, one male and one female
V_{R1}	The volume for 2 intersecting spheres, one male and one female, between the apex of the male sphere and the plane of intersection of the spheres
V_{R2}	The volume for 2 intersecting spheres, one male and one female,

	between the apex of the female sphere and the plane of intersection of the spheres
w	Load applied to bearing
WQ	Water quench
X	The distance from the apex on the male sphere to the intersection plane between two mating spherical surface, one male and one female, where the male sphere has penetrated the surface of the female sphere

2. Greek Symbols

α	Angle used in calculation of spherical surface area measured from equator to pole of a hemisphere
$\delta\alpha$	included angle of arc δl
δA	Surface area of a very thin annulus used in calculation of total sphere surface area
δl	Width of annular ring of area surface δA
Δ	Difference between the radius of imperfectly formed ball Rb and the socket radius Rs
ΔR	difference in radius between two mating spherical surfaces, one male and one female
η	Lubricant viscosity
λ	Ratio of fluid film thickness to surface roughness of bearings
μ	The mean of the population from which a sample of size n measurements of the are taken
μm	Units of length: micrometre (1000μm=1mm)
ν_1	Poisson's ratio for the male spherical bearing surface material (head)
ν_2	Poisson's ratio for the female spherical bearing surface material (cup)
π	Constant used in calculation of areas, volumes etc. approximately 3.141592654

3. Other

°	Units of angle: Degrees (360° in a circle)
	Units of temperature: Degrees. Generally coupled with C eg °C

CHAPTER 1

Introduction

Human beings have always suffered from disease and injury to natural synovial joints. However it is only within the last 150 years that any progress has been made in the field of joint replacement. Initial progress was to find materials which the body would not reject or which did not fracture under load, and to find ways of preventing infection during joint replacement surgery. Subsequently the issues were around prevention of early loosening. Entering the 20th century joint replacement surgery had an extremely high chance of failure, but at the beginning of the 21st century the average person having hip joint replacement surgery should enjoy a greater than 95% chance of the implant lasting for 10 years or more, and many implants have survived for 20 and even 30 years. However the fact that not all implants attain such longevity remains a cause for concern and a driver for improvement of device design.

There are a number of goals in hip joint replacement which, completely fulfilled in a single product, would mean that a perfect product had been created. These are:-

Restoration of Anatomy
Restoration of Function
Relief of Pain
Ease of Implantation
Longevity

Over the years orthopaedic surgeons and engineers have striven to attain these goals with numerous products of many different styles and whilst some obviously perform much better than others, with every device there remained problems. Sir John Charnley led the way in the 1960's with the development of a prosthesis which has remained relatively unchanged in 30 years or more of use. However whilst at the time of its development the use of polyethylene was seen as the answer to most of the problems of articulation, today a great deal more is understood about the effects of the billions of particles which are shed from the articulating surfaces during the lifetime of a product.

Indeed it may even be that these same particles are a direct limitation upon the longevity of the device.

Today it is believed that the body will treat any particle as a foreign body. Large particles such as the prosthetic devices themselves will be tolerated if the materials presented to the body tissues are reasonably biocompatible. Smaller particles of the same materials are dealt with by the body by a mechanism of digestion whereby the body attempts to absorb the particle into a cell and there digest it. The problem appears to be that some materials are not easily digested and amongst these are most of the biomaterials used today including polyethylene, PMMA, titanium and its alloys, and cobalt chromium alloys. It seems that the body can cope with a certain level of particle contamination without any apparent effect. However, a threshold exists beyond which the body begins a destructive reaction whereby chemicals are released which initiate a bone resorbing effect. This bone resorption process, known as osteolysis, can be dramatic and quite catastrophic, often leading to loosening of the implant and sometimes to fracture of the weakened bone. This effect is now strongly accredited to the presence of polyethylene debris in the amounts typically associated with the wear of total hip replacements of perhaps 5 years plus, though some survive with no effects for many more years. It has however not been possible as yet to determine that metallic debris released in the quantities normally associated with a metal on metal prosthesis after many years in service illicit a similar response. Indeed many are postulating that metal on metal prostheses do not show the same sort of bone resorbing and granulomatous response by the host bone. Whether this is a real effect, or whether it is related to the type of debris or to the volume of debris released is not completely clear.

Around the time that Charnley was at work, George McKee was working on a slightly different approach to addressing the 5 goals of prosthetic design. He opted to work with what are now commonly called metal on metal articulations and saw some success. For varied and complex reasons, over the course of time it was the metal on polyethylene articulations which came to the fore whilst the metal on metal all but disappeared from use. Looking back and examining all the facts today, the conclusion is that the problems associated with polyethylene debris could potentially be reduced dramatically by a careful revisit of the metal on metal philosophy.

This thesis describes the research work to investigate how metal on metal articulations may be optimized so as to reduce the amount of wear debris generated through their use and so lead to effective function within the environment of a human hip joint when it forms part of a hip system design.

CHAPTER 2

Literature Review

2.1 Introduction

Many developments in joint replacement technology are described in the literature and yet there remains a large number of questions unanswered. In the case of a metal on metal hip prostheses many features of the product are substantially described in the available literature, some of it dating back to the 1950's. Indeed, whilst the idea of a metal on metal articulation in the 1990's seems novel, there is in truth little of a major nature which has in fact never before been previously clinically tried. However, as is common with many medical implants, an understanding of how and why metal on metal bearings perform, and how certain design parameters influence that performance is lacking.

The application of 1990's bioengineering and surgical knowledge, research laboratory technology, materials technology, and manufacturing capability to a product first conceptualised in the 1950's by McKee and others is the real advantage investigators have today over those early entrepreneur surgeons. The other great benefit today is that there is the opportunity to look back at the performance of those early, first generation, metal on metal devices in the hope of answering some of the questions which now face the designer but which would never have been posed in those former times. Therefore, this literature review will aim to take in a wide cross section of all the available literature on aspects of metal on metal articulation. The literature review was primarily undertaken when the project commenced in 1996. Additional work and product developments that have taken place in the interim 1996 to 2000 are described in the discussion in chapter 10.

2.2 A Historical Review of Metal on Metal Devices

During the last 40 years a surprisingly large number of metal on metal devices of many different designs have been used clinically. The focus of the present review will be on the McKee-Farrar and Ring which are probably the most widely known and documented of all historical metal on metal devices.

2.1.1 McKee-Farrar

As early as 1950 GK McKee in Norwich UK was concerning himself with the problems of patients undergoing arthrodesis using a long stainless steel screw (McKee, 1970; McKee, 1971; McKee, 1974; McKee 1957). Some time previous to this he had considered a number of possible designs (Figure 2.1: **Design 1**) (McKee, 1970) for hip replacements but whilst some prototypes were made they were never implanted. His adventure into metal on metal articulation began when he simply realised that it might be possible to insert a ball and socket in the mid shaft of the screw between the pelvis and femur and so allow some limited articulation (Figure 2.2: **Design 2**) (McKee, 1974). Of the 3 devices which were apparently inserted into living patients, 2 were manufactured from stainless steel and loosened within just a few months. McKee was astounded at the fact that the third device, which was made of Vitallium (a cobalt chromium alloy), showed no such signs of loosening but eventually failed mechanically at about 3 years. **Design 3** (Figure 2.3) (McKee and Watson-Farrar, 1966) followed in 1956 with the introduction of the petalled cup and small cementless Thompson stem. **Design 4** (1956-1960) incorporated the use of a flanged femoral screw along with the same petalled cup (Fig 2.4) (McKee, 1957), but in 1960 McKee then elected to use bone cement to fix both the femoral and acetabular components and **Design 5** (Figure 2.5) also incorporated a larger femoral component (a return to the Thompson), a more spherical ball, and the familiar studded cup configuration. The studs were for fixation to the cement and for ensuring an adequate and even cement mantle while the equatorial flange may have assisted cement pressurisation and added stiffness to the thin shell. The Thompson was considered unsatisfactory primarily due to poor range of motion and so by 1965, in a couple of increments, the neck had been reduced down to the final McKee-Farrar design (Fig 2.6: **Design 6**) (McKee, 1970). By 1965 McKee and Watson-Farrar had arrived at almost the final design of the McKee-Farrar product

range (Fig 2.7: **Design 7**) (McKee, 1971) when a variety of sizes of cup and stem were introduced. One final modification appears to have been made by April 1971 (McKee, 1974; August et al, 1986) where a hexagonal transverse hole was created in the neck for location of an introducer/manipulator/removal tool, interchangeability of parts of same size was allowed, and greatly reduced coefficient of friction was claimed (**Design 8**). The interchangeability was instigated in 1969 (McKee, 1982) and probably refers to a move away from "lapping-in" which is described for the early form of the device (McKee, 1966) when a head and cup would have been run together on some form of lapping machine to match them close for size and form. The reference to friction would certainly be linked to the same thing where the modification is likely to have been to increase the nominal clearance between the parts. The product range was divided into 5 models or "styles" of prosthesis in accordance with Table 2.1 (McKee, 1970).

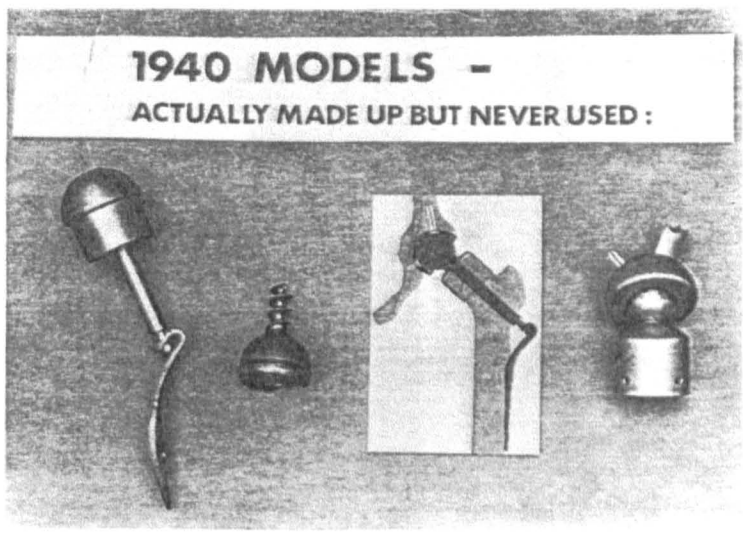

Figure 2.1: McKee Design 1
Figure shows the earliest metal on metal conceptual designs produced by McKee

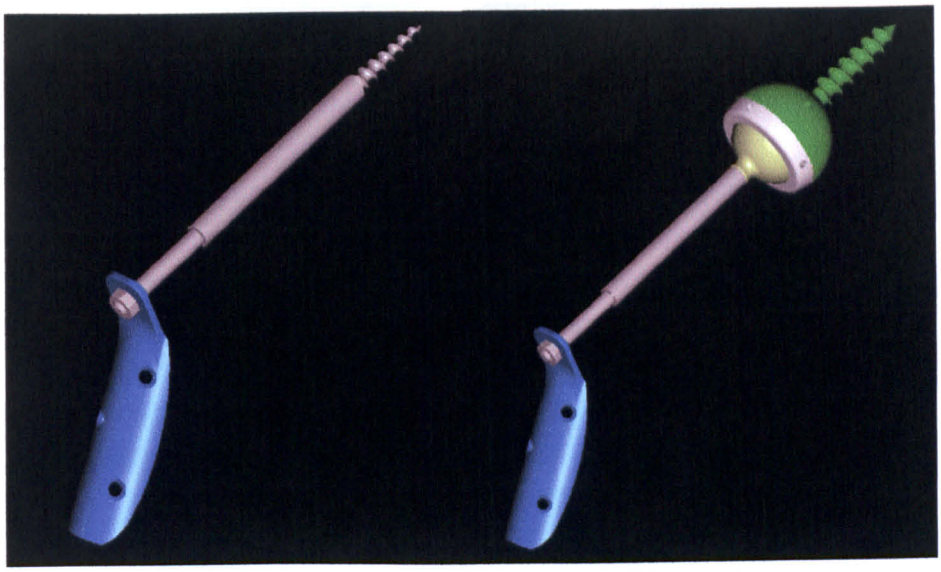

Figure 2.2: McKee Design 2

Figure shows a 3D CAD models of the earliest implanted of McKee's metal on metal designs (Right Hand Side) and how it was derived from an established lag screw implant used for arthrodesis (Left Hand Side)

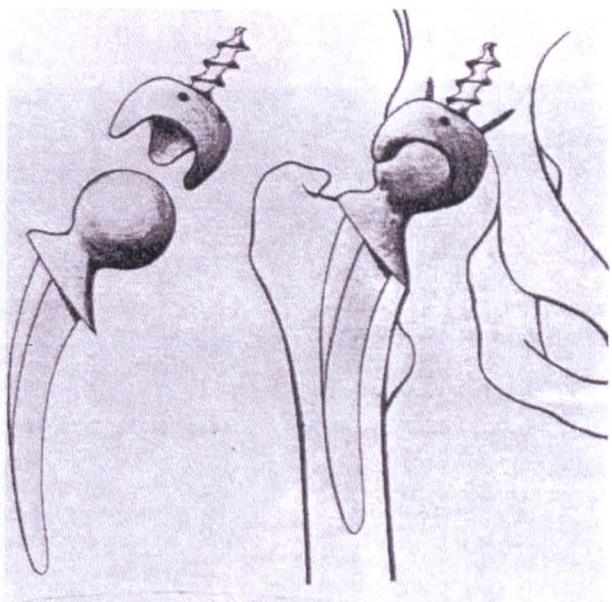

Figure 2.3: McKee Design 3

Figure shows the 1956 design concept implanted by McKee

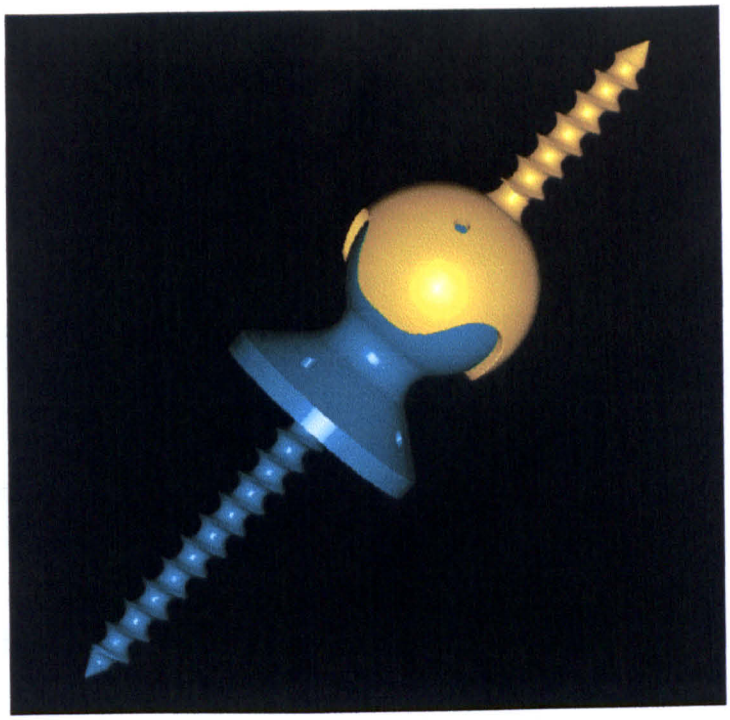

Figure 2.4: McKee Design 4
Figure shows a 3D CAD model of a design concept implanted by McKee between 1956 and 1960

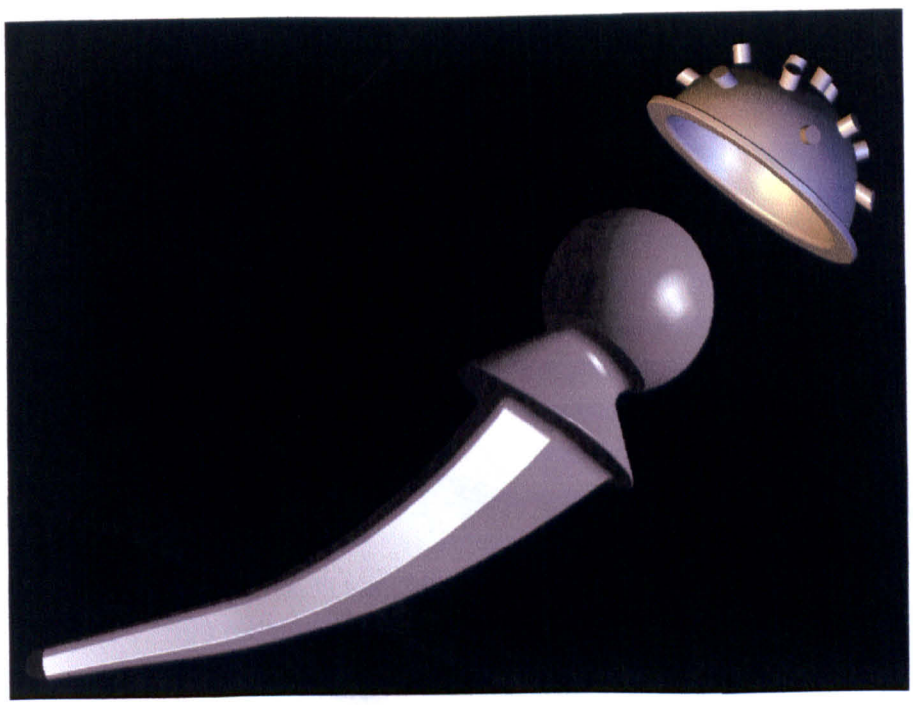

Figure 2.5: McKee Design 5
Figure shows a 3D model of the stem and the studded and flanged cup

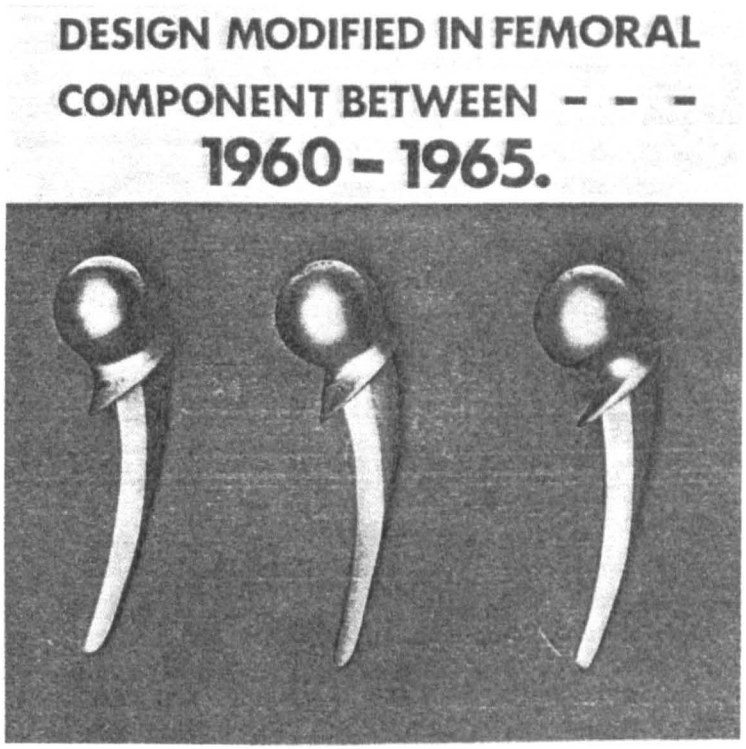

Figure 2.6: McKee Design 6

Figure shows development of the stems between 1960 and 1965. The original figure came with the caption "A Thompson prosthesis was used first after making the head spherical but this proved unsatisfactory so the under surface of the neck was burred down. Eventually a completely new redesigned femoral component was made up as the modified Thompson was not satisfactory."

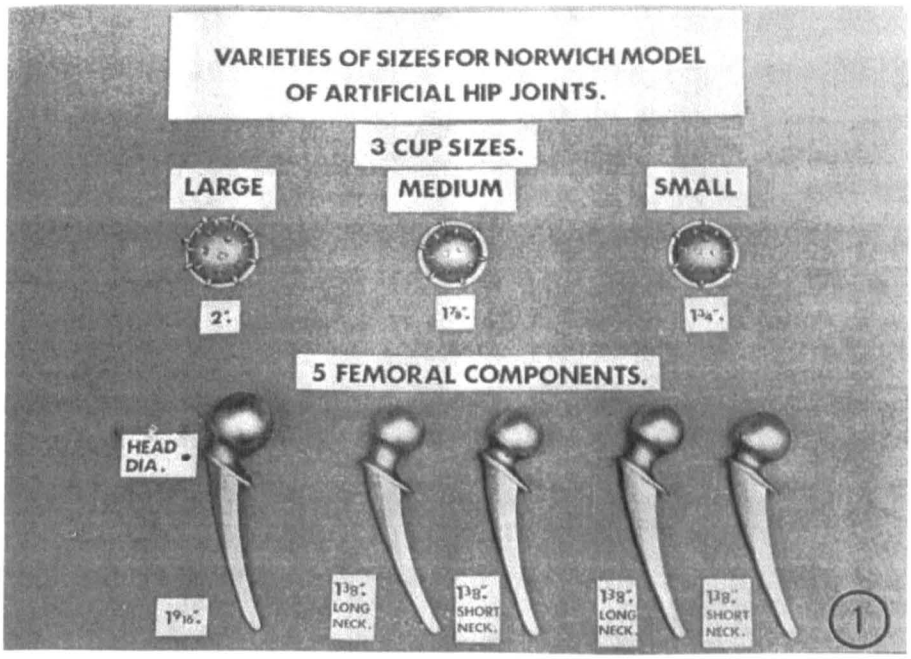

Figure 2.7: McKee Design 7

Figure shows the final product offering in a full range of sizes from 1965 which remained virtually unchanged for the next 10 years or so.

Style	Cup Size (OD)	Head Size (OD)	Neck Length
1	2"	1 9/16"	Standard
2	1 7/8"	1 3/8"	Standard
3	1 7/8"	1 3/8"	Elongated
4	1 3/4"	1 3/8"	Standard
5	1 3/4"	1 3/8"	Elongated

Table 2.1: The range of sizes for the McKee-Farrar implant

All the McKee-Farrar prostheses (with the exception of the 2 initial implants to Design 2) were made from cast cobalt chromium molybdenum alloy (McKee, 1974; McKee, 1957; McKee and Chen, 1973) broadly to ASTM F75 and called by a number of names (Vitallium, Vinertia, Alivium).

2.1.2 Ring

By 1964 the McKee-Farrar development was well in progress with the use of bone cement. At this time Peter Ring from Redhill, UK, was very interested by the metal on metal philosophy but not an advocate of the use of bone cement. He therefore elected to design his own metal on metal prosthesis which was completely cementless and for this purpose he selected a Moore's prosthesis and designed a metal cup to articulate with it. The head diameter was 1 5/8" and the material was cast cobalt chromium alloy (Ring, 1968). This prosthesis shown in Figure 2.8 (Ring, 1971) was given the designation **MkI** (Ring, 1968). However, due to range of motion problems with this design and with some fractures of the threaded stem on the cup, by 1965 Ring had evolved the **MkII** product shown in Figure 2.9 (Ring, 1971) where the 1 5/8" head was lateralized, the neck elongated and thinned, and the stem narrowed to ease insertion. The cup external geometry was changed to strengthen the stem/cup junction by creating a conical portion and increasing the thread diameter at the base (thread core tapered from 12 down to 10mm) (Ring, 1968; Ring, 1970). The head and cup were lapped together in order to produce two very close fitting parts with high surface finish (Ring, 1971). Due to a

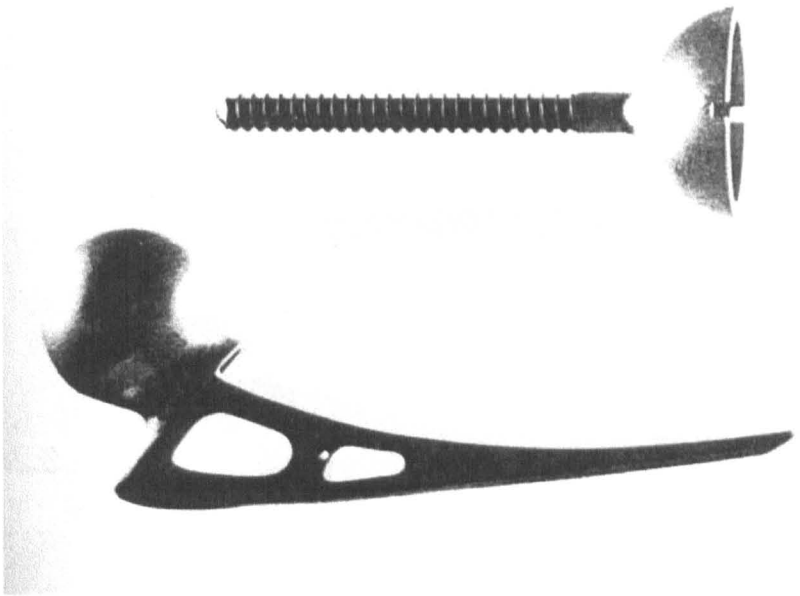

Figure 2.8: Ring MkI
Figure shows the original Ring cementless design

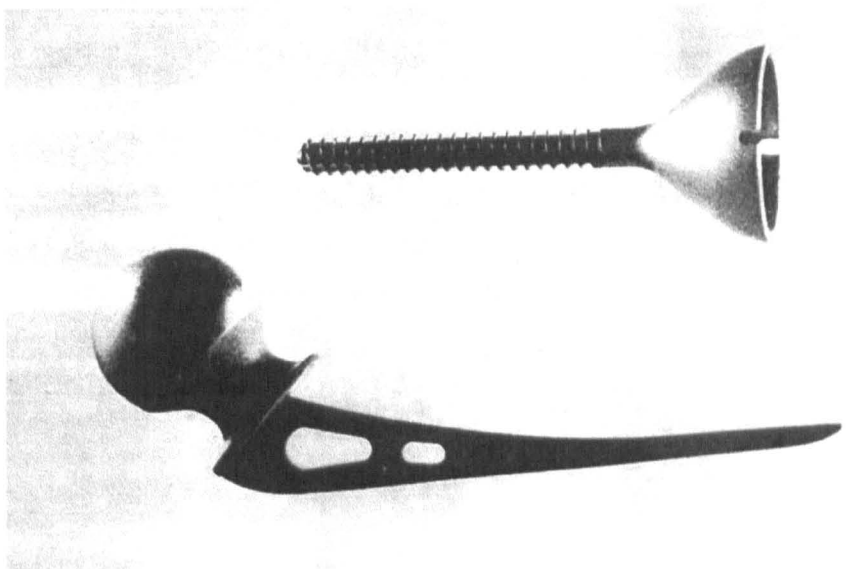

Figure 2.9: Ring MkII
Figure shows the modified design

relatively high incidence of femoral loosening with the **MkII**, in 1967 Ring created the **MkIII** as shown in Figure 2.10 (Ring, 1971) where the head was even more significantly lateralized (with respect to the stem axis) by increasing the stem/neck angle from 135 to 150° in the hope of reducing the rotational moment on the stem

(Ring, 1968) (and for this reason the **MkIII** is sometimes referred to as the valgus stem (Ring, 1983)).

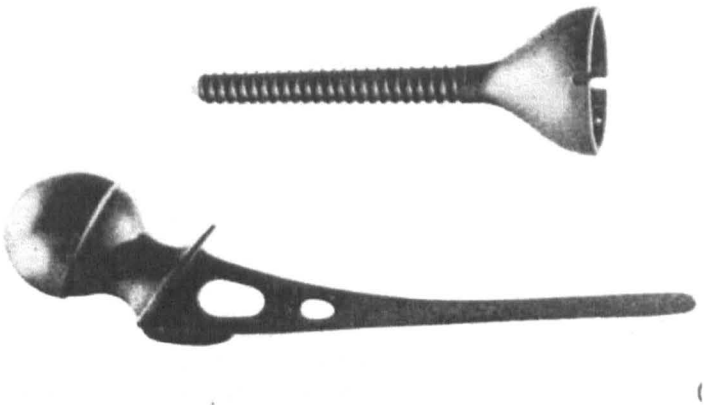

Figure 2.10: Ring MkIII
Figure shows the further modified (very lateralized head) design

This design was also lapped in until about 1969. Ring later stated that "....its use persisted for 4 years. It was found however that apart from the increase in joint loading which this configuration produces, the gait was often poor, and as a result of the medial replacement of the femur a secondary valgus of the knee resulted." (Ring, 1983). Therefore in 1971 at **MkIV** the prosthesis was further modified as shown in Figure 2.11 (Ring, 1978) whereby the neck angle reverted to 135° and a straight outer stem was used in 3 sizes. The head size remained 1 5/8".

Figure 2.11: Ring MkIV
Figure shows the final design of the Ring metal on metal articulation

Around 1969 to 1971 Ring converted from lapped in or equatorial bearing to a polar bearing configuration where a positive clearance was designed in between the articulating surfaces (Ring, 1970) and a recess was machined in the cup apex. The products might then not need to be sold in matched pairs. It is likely then that the earlier **MkIII** prostheses were of lapped in and the later ones of polar bearing type. Alongside the **MkIV**, Ring introduced a **MkV** product which was the same as the **MkIV** except that the femoral head was made from high density polyethylene as shown in Figure 2.12 (Ring, 1978; Ring, 1983). Finally, in 1980 Ring introduced the UPM metal on polyethylene product where the metal on metal cup was replaced by a polyethylene design of similar configuration but with a 32mm head, and the stem was modified somewhat as shown in Figure 2.13 (Ring, 1983). At this point it appears that the metal on metal design was abandoned.

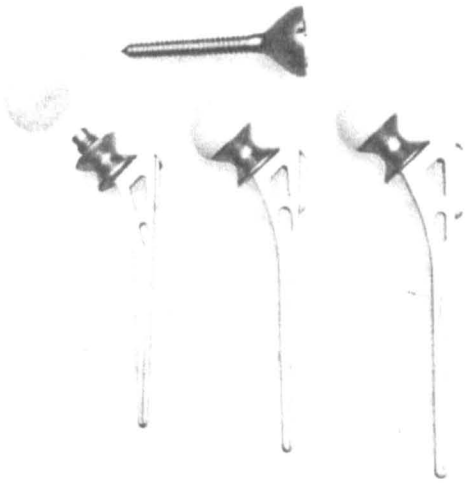

Figure 2.12: Ring MkV
Figure shows the conversion to a metal on plastic articulation

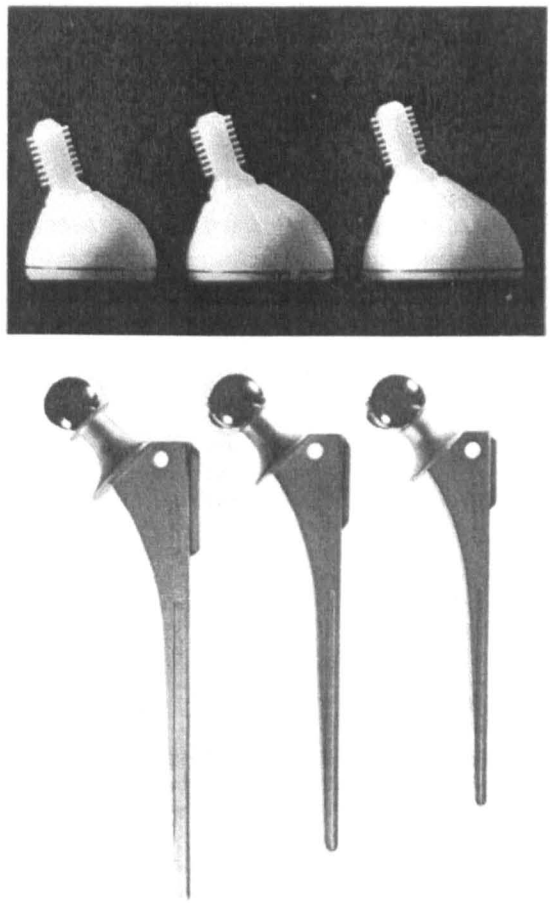

Figure 2.13: Ring UPM
Figure shows the final design of the Ring metal on plastic articulation

2.3 Design Critique of Early Devices

2.3.1 McKee-Farrar

As with the majority of devices of its day (the Charnley being perhaps the notable exception), this device suffered from a series of sub-optimal design features. First generation (Hashemi-Hejad et al, 1994) cementing technique would have been used with all the inherent problems of lack of pressurisation, possible laminations due to contamination by blood, and cement porosity. The cup would today be described as a cemented metal backed cup for which results have not generally been good (Ritter et al, 1990) and was supplied in only three external sizes to fit all acetabulae. The stem did not conform to the latest principles of sound cemented stem design which would seek to limit the stresses in the cement mantle. For instance the stem section shape presented by the Thompson style stem was seen by Crowninshield et al (1980) to create amongst the highest compressive and tensile cement stresses of any of the stem cross sections examined. By contrast, the Charnley type sections created amongst the lowest stresses. Also the Thompson stem has relatively sharp external corners which would create similarly sharp internal corners in the cement mantle leading to significant cement stress concentrations. The range of motion of this device was clearly sub optimal and impingement was a frequent occurrence (McKee, 1974). Whilst the design was improved in increments to provide a better range of motion, Wilson et al still noted that "In all hips there was a lack of full range of movement...." (Wilson et al, 1972).

2.3.2 Ring

It is clear from the literature that the design problems were with the stem all the way through. The cup design was modified only from **MkI** to **MkII** in order to cure the problem of mechanical failure (Ring, 1968). Thereafter it remained the same until replaced by the UPM in 1980. Pain, migration, and loosening all troubled the femoral component and the majority of design iterations were attempts to rectify these problems (Ring, 1983). In moving toward the "valgus" or medialized stem (or lateralized head) design of the **MkIII**, Ring was clearly unaware of the increase of joint load associated with reducing the abductor moment arm until he noted the poor performance of this

design (Ring, 1983). Today, cementless treatment of the femur is regarded as one of the most difficult areas in hip replacement and results of modern devices still struggle to match the results obtained using a modern cemented stem. For this reason, it is common practice world-wide to use a hybrid system comprising a cemented stem and cementless acetabular cup. Today it might be argued that Ring's use of an almost standard Moore type prosthesis to achieve long term stable femoral fixation was not a good idea. One is left to ponder what Ring's result would have been if he had elected to use a hybrid system. Interestingly, Ring (1978) points out that "Uncemented THA using a metal on metal prosthesis will give an excellent 5 year result in about 80% of patients, but during those 5 years symptoms that would justify revision surgery will appear in 5% of patients. These results are not dissimilar from those recorded by McKee and Chen (1973) using a cemented metal on metal prosthesis. They are inferior to those recorded by Charnley, thus suggesting that one cause of implant loosening may be the use of a metal on metal articulation.". However, it now seems reasonable to suggest that the metal on metal designs could have been significantly hindered by the use of poor prosthetic design whilst the metal on polyethylene device happened to be of a configuration which still fits with the current scientific thinking on optimum stem design.

2.4 Review of Clinical Performance of Early Devices

2.4.1 McKee-Farrar

Amongst the earliest results, McKee and Watson-Farrar (1966) reviewed 50 patients with **Design 5** prostheses after 4 years and stated a 90% success rate with 6 loosenings, most of which were explained by poor technique. The patient hip scores comprised 26% Excellent and 68% Good. McKee (1970) reviewed 3 separate series of 100 prostheses of **Design 7** in 1970 with 33, 20, and 12 months minimum follow up. In each series close to 50% were excellent and 81%, 94%, and 98% respectively were excellent or good with respect to hip score for pain, function and mobility. Revisions of 6%, 4%, and 1% had already occurred though the author had given technique or patient accident related reasons for most of these. Freeman (1970) reviewed 61 operations in 51 patients between 6 and 36 months postoperative and concluded that with 63% excellent or good with respect to pain, range of motion, and walking ability, and 2 cup

loosenings, "Undoubtedly, this type of joint replacement will be recognised for a long time as the most satisfactory method of giving a pain free stable joint". Chapchal and Muller (1970) got similar results with 70 patients followed up between none and 48 months, having satisfactory hip scores and around 3 components appearing to be loose radiographically. Wilson et al (1972) also noted great improvement in hip score from pre to post operative but had a very high infection rate of 12% and 9 loosenings out of 100 patients with 16 to 40 months follow up using **Design 7**. It should not be argued that the prosthetic design could be responsible for the high incidence of infection and so to see the true performance of the prosthesis, these should be excluded from review. The authors cite technique related issues as possible causes of loosening but also the possible effects of higher friction torque with these devices. With lapped in designs it is now understood that high friction torques could be generated. However with polar bearing prostheses as **Design 7** in this study, it is perhaps something of a convenience to suggest friction as the problem which in retrospect has never been proven to be responsible for torques of any significance in polar bearing devices.

McKee and Chen (1973) reviewed almost all the McKee-Farrar results from 1951 through to 1972 implanted in Norwich, the most interesting of which was a series of 300 of Design 6 with 34 to 84 months follow up. These represented the longer term results of the same group of 3 series reported by McKee (1970) already. Hip scores were still satisfactory with 8% having been revised. Bentley and Duthie (1973) were the first to compare the McKee-Farrar directly to the Charnley in a series of 101 McKee-Farrar (**Design 7**) and 128 Charnley with 12 to 48 months follow up. Improvements in hip score from pre to post operative were similar as were the adverse reactions though the incidence of loosening was 4 for the McKee-Farrar and none for the Charnley. Range of motion was seen to be less on the McKee-Farrar than the Charnley. The higher friction was cited as a possible reason for the early loosenings, though it might have been more appropriate to cite the suboptimal range of motion. Langenskiold and Paavilainen (1973) noted only one case of loosening out of a series of 116 hips with follow up of 1 to 61 months using **Design 7**, and almost all gave satisfactory improvement in hip score. Tillberg (1982) carried out a prospective review of 327 arthroplasties implanted between 1969 and 1972. He reported with up to 8 year follow up (on 19 arthroplasties) and showed 16% aseptic loosening. This appears high though Tillberg explained that when McKee reported 21% loose out of 100 implants at

15 years at SICOT in 1978 (equatorial bearing devices), Charnley also "admitted quite a high incidence of loosening, with figures somewhere around those given by McKee in the long run". Tillberg also showed hip scores with dramatic post operative improvement which peaked at 1 to 2 years and then began to fall away to 7 years. In contrast, Djerf and Whalstrom (1986) stated that at 5 years 90% of patients had total freedom from pain in a group of 107 McKee-Farrar (**Design 7/8**) and 70 Charnley prostheses implanted between 1976 and 1977. Indeed, there is quite unanimous agreement that the McKee-Farrar prosthesis almost always produced very satisfactory relief of pain and restoration of function. At 5 years, radiographic evidence of loosening was about 28% for McKee-Farrar and 38% for the Charnley. Clinically only 5 McKee-Farrar and 4 Charnley patients exhibited pain related to loosening. The authors concluded that "Our findings do not support the hypothesis that the metal on metal prosthesis is clinically inferior to the metal on polyethylene prosthesis". Djerf, Whalstrom and Hammerby (1986) then carried out a detailed radiographic analysis of the same series of McKee-Farrar and Charnley prostheses and found no significant difference in loosening rates between them. August, Aldam, and Pynsent (1986) carried out a survivorship study of 657 McKee-Farrar prostheses implanted at Norwich between 1965 and 1973. They presented a survivorship curve showing about 84% survival at 14 years but then dropping very rapidly to around 30% at 20 years. Visuri (1987) reported about 65% surviving at 14 years from a series of 511 implanted between 1967 and 1973. He calculated a mean annual failure rate of 2.3% which he cites as higher than for the majority of metal on polyethylene designs. Zaoussis and Patikas (1989) reported on 143 McKee-Farrar prostheses implanted between 1966 and 1974 with 12 to 20 years follow up. They concluded that mechanical loosening of 17% "...reflect the rates usually reported in very early series with unsophisticated methods". Finally, Jacobsson and Djerf (1996) reported in a 20 year follow up of the McKee-Farrar compared to the Charnley, that Harris hip score was comparable at around 40, as was survivorship, so that while the McKee-Farrar showed slightly higher survivability there was no statistical significance. Radiographically around 35% of 21 McKee-Farrar and 13 Charnley prostheses available at 20 years were loose. It is interesting to note that while the results in terms of loosening are greater than might be expected from a well designed prosthesis, it appears that wherever the McKee-Farrar is compared directly to the Charnley, there is little to choose between them in terms of both initial and long term performance.

2.4.2 Ring

Ring first published his results in 1968 (Ring, 1968) with a retrospective review of 158 hips in 128 patients of designs **MkI** (about 25 implants) and **MkII** and with 6 to 48 months follow up. According to his own hip score system looking at pain, range of motion, and stability (associated with patient's ability to ambulate) 52.5% were excellent, 42.5% good, and 4% fair, with none in the poor category. Ring states that 18% of patients had pain on weightbearing though "Complaints of pain became less and less common as the months passed.". There were no dislocations and at this point no major loosenings, though one mechanical failure was the herald of a fundamental flaw with the **MkI** design. By 1970 Ring was able to add to the experience so far by way of an update to his series (Ring, 1970). He was able to report on his latest **MkIII** (valgus) design standard with 100 implants over a maximum of 2 years. The results of his first 2 designs appeared to have remained OK with the **MkII** series having 58% excellent, 32% good, 1.5% fair, and 9% poor (excluding 6 deaths) with 2 to 5 year follow up. However, the 13 poor results included 11 stem loosenings which was the start of Ring's quest to solve the femoral stem loosening problems. Therefore the **MkIII** shows 75% excellent, 19% good, 4% fair, and only 2% poor (1 infection and 1 myositic ossificans) with maximum 2 year follow up. By 1973 Ring (Ring, 1973) could report on the results of 1045 hips in 887 patients with **MkI, II,** and **III** prostheses (the latter being of polar bearing design). His 1 to 5 year results of 542 **MkIII** prostheses show 75% excellent, 18% good, 3% fair, and 4% poor. This latter figure includes 2.2% for loosening which again was predominantly the femoral stem, and not surprisingly given the poor stem design. In 1978, Ring (Ring, 1978) published his 5 to 14 year results which give now some feel for the long term survival of the prosthesis. For the **MkI** and **II** results of 160 implants with 11 to 14 years follow up showed 34% excellent, 22% good, 6% fair, and 38% poor. For the **MkIII** prosthesis with 432 implants at 6 to 11 years follow up 65% were excellent, 20% good, 5% fair, and 10% poor. For the **MkIV** and **V** prostheses, 76% are excellent, 18% good, 4% fair, and 2% poor out of 872 implants with 1 to 6 years follow up. Ring makes the statement that of the implants in all the series requiring further surgical treatment, these were "....mainly for interface pain.". There is probably a link between pain and loosening in the long term and therefore it is probable that most revisions were for loosening. Most recently Andrew et al (1985) presented a

5 to 12 year review of 179 sequential Ring prostheses **MkIV** (except for 9 assumed to be **MkIII**) in 116 patients, where 154 hips were available for follow up review. By Rings hip score system there were 13% excellent, 36% good, 18% fair, and 25% poor (8% could not be classified). The authors also used the Harris hip score where 51 were between 0 and 60 points, 20 between 60 and 70, 20 between 70 and 80, 28 between 80 and 90, and 23 between 90 and 100, and the Charnley modification of the d'Aubigne and Postel hip score where the bulk of hips fell in the range 3 to 6 for pain and walking and between 3 to 5 for range of motion. A radiographic assessment showed a relatively high proportion of loosening and also a very high incidence of calcar resorption where 48 hips showed none, 44 up to 5mm, 31 between 5 and 10mm, 24 greater than 10mm, and the remaining 7 were pseudarthrosis or revisions to cemented stems. Again, none of the stem problems were surprising given the design and it could be argued that the stem performance should not detract from a relatively trouble free metal on metal articulation.

2.5 Review of Clinical Performance of Modern Designs

At the time of preparing this literature review in 1996 a number of companies are marketing metal on metal devices though most of these belong to the Sulzer group of companies (Allopro and Protek) and are marketing effectively the same product known as the Metasul. Also, Corin Medical have marketed the McMinn surface replacement, pioneered by a surgeon, Mr D McMinn, in Birmingham, UK. The McMinn product is currently supplied only for cementless acetabular use and is HA coated while the head fits over the neck of femur and can be used with cement. The Metasul product however comes in a variety of acetabular configurations for cemented and cementless use. Most of the Metasul designs incorporate a metal on metal insert fixed into a polyethylene bed. This may be cemented directly into the acetabulum with (known as the PERMALOCK) or without a metal mesh backing (stainless steel) "Sulmesh". When the metal mesh backing is titanium then the cup is for cementless use. Alternatively the polyethylene may be snapped into a variety of cementless metal shells in the same way as for metal on polyethylene designs. According to Weber (1992) who used the PERMALOCK prosthesis cemented into the acetabulum, the decision on cemented or cementless is still best left for the future since we currently have too little data to be conclusive either way.

However he is quite clear that today we are in a good position to claim that metal on metal offers a very realistic hope of a hip replacement without the current high incidence of late aseptic loosening. Again, Weber (1995) presents the results of 110 Metasul cemented cups with Sulmesh backing and polyethylene filling, between 1988 and 1992 with 1 to 4.5 year follow up. He explained that 10 were excluded from the study because of unsatisfactory results due to non metal on metal related issues, but that the rest were 98% excellent or good according to a Harris Hip Score. The other 2% were satisfactory. These results whilst early are very encouraging with none of the early loosening problems of the historical designs. Whilst the Metasul product has been available for around 8 years now, and according to Rolland (1995) about 20,000 have been implanted, there is currently a dearth of published literature. What literature is available however remains positive. The outcomes for more recent clinical developments are described in the discussion section of this chapter.

2.6 In Vitro and Theoretical Studies

There have been relatively few in-vitro analyses carried out to demonstrate the tribological behaviour of metal on metal bearing couples, and virtually nothing to support the initial clinical use of these devices. The literature provides a few papers which retrospectively analyse the wear, and friction performance amongst other things and these may be broken down into broadly 3 categories.

2.6.1 Simulator Studies

Walker and Erkman (1972) carried out simple pin on plate tests with CoCr couples and using different lubricants including water, Ringers solution, natural synovial fluid, and fluid from a joint with hip replacement. Synovial fluid gave the lowest friction though there was no significant difference between the different synovial fluids. Additives within the fluid were postulated to act as boundary lubricants and were probably physically or chemically adsorbed onto the surfaces. If pin on plate tests could be used as an indicator of hip joint performance, the encouraging outcome here was that synovial fluid appeared to be a reasonably good lubricant and that hip disease did not appear to lessen its lubricating efficiency.

Weber (1992) stated that prior to clinical use of the Metsul, Sulzer tested prototypes in a Stanmore hip simulator and carried out Charnley type pendulum testing. He stated that the wear and friction behaviour was significantly better than for previous metal on metal prostheses after retrieval. Streicher (1995) confirmed the use of the Stanmore hip simulator and added that Sulzer carried out 15 simulator tests on the single station machine prior to starting the clinical trial. After some experience with the Muller metal on metal from 1965 to 1967, Muller (1995) joined with Sulzer between 1987 and 1990 to be part of the Metasul development. He explained that the optimum clearance for the Metasul product was 0.15mm and indicated that friction measurements demonstrated that not only was the new generation of products superior to the older products, but that the friction was about the same as that seen on a 32mm metal on polyethylene device. He indicated debris generation of about 4 million particles per year against 1 billion for metal on polyethylene. Unsworth and Hall (1995) indicated that tests on a McKee-Farrar demonstrated a mixed lubrication regime at the normal environment within the hip demonstrated by a falling Stribeck curve. They inferred that neither metal on metal nor metal on polyethylene combinations could ever achieve full fluid film lubrication within the human environment. However we already know that the McKee-Farrar geometry was less than optimum and Jin, Dowson, and Fisher (1997) have shown that conditions of geometry do exist which would allow a very thin full fluid film to exist for metal on metal bearings within the human environment.

Recently Medley et al (1995) and Chan et al (1996) made a more concerted effort to determine the optimum geometrical conditions for lowest wear using a PM-MED hip simulator. Medley et al (1995) tested forged cobalt chromium alloy ASTM F799 (now ASTM F1537) and a commercial grade material at various nominal head diameters. They plotted weight loss against cycles and for the first time it was possible to see that an initially high wear rate could reduce to virtually nothing in an optimally designed pairing. The F799 material was very much better in terms of total wear than was the commercial alloy. Chan et al (1996) tested the wear on cast alloy ASTM F75 which was the material used for the historic product. These consistently showed wear rates higher than for F799 indicating perhaps that the wrought alloy was inherently a better material for metal on metal applications.

2.6.2 Retrieval Analysis

Amongst the earliest workers in the area of analysis of the wear surfaces of retrieved metal on metal prostheses was Walker (Walker and Gold, 1971; Walker and Erkman, 1972; Walker, Salvati and Hotzler, 1974) who examined a number of features and came up with some interesting findings and recommendations. In the earliest paper (Walker and Gold, 1971) a number of retrieved McKee-Farrar components were assessed with regard to friction and friction torque. It was suggested that whilst a lapped in type of bearing may in theory be fine and may in a number of instances perform satisfactorily, nevertheless in a number of cases it was likely that slight out of sphericity errors on either component could lead to a situation of "equatorial bearing" where, as the angle from the cup pole to the contact area increased so the friction torque rose very rapidly. Walker and Gold also calculated the theoretical friction coefficient for the tribological situation at 0.08 for the CoCr couple thus indicating a reasonable boundary lubricated regime. Initial estimates of scratch width (1-5μm) and depth (1μm) were made. As a result of this work it appeared that at least one manufacturer revised the manufacturing technique and from then on produced polar bearing prostheses and with a polar dimple in the cup. Walker and Erkman (1972), carried out an analysis of a McKee-Farrar specimen and established the presence of pit like flaws within the wear area probably caused by a fatigue type wear phenomenon as is often associated with rolling element bearings. Walker, Salvati, and Hotzler (1974) used a McKee-Farrar retrieved after 4 years implantation to establish and examine the wear areas. They identified 3 wear types: Type 1 was initial scratched surface; Type 2 was Type 1 with smoothed out scratches; and Type 3 was Type 2 with fatigue pits. They estimated a wear depth of about 0.001mm and total wear volume of around $5mm^3$ during its service life and so for the first time some estimation of the volume of wear debris released into the body was made. These figures should be compared with around 0.1 to 0.2mm per year for polyethylene bearing systems. Since Walker and Gold (1971) had already predicted the size of debris at 0.001mm and less it was possible for the first time to get some feel for the number of wear particles likely to be released into the human system. McCalden et al (1995) analysed the surfaces of 28 retrieved McKee-Farrar joints with average 15.5 years implantation and identified 4 types of wear pattern, and quantified the surface

finish which each might typically exhibit. Their conclusion was that even after such long periods in service the wear volume would be small by comparison with metal on polyethylene components. Semlitsch, Striecher, and Weber (1989) reviewed retrieved Mueller and Huggler metal on metal devices with average of 10 years in service and reported around 25±12μm for Mueller cups and 20±10μm for heads and 42±27μm for Huggler cups and 38±10μm for heads. These were shown to be well below what would have been seen for a metal on polyethylene system and equated to between 4.5 and 8μm per year respectively for the Mueller and the Huggler prostheses.

Whilst the effects of these quantities of debris are still debated it is true to say that patients with long term implants of this type survived with no adverse reaction and apparently with very little or no osteolysis. Nevertheless, with current techniques it may be possible to lessen the debris load still further and this can only be beneficial to the human system.

2.6.3 Theoretical Studies

Jin, Dowson, and Fisher (1997) demonstrated in a theoretical analysis of Hertzian contact and hydrodynamic lubrication phenomena that for a metal on metal pairing, given that the radial clearance could be made small enough and the surface finish and geometry of the components accurate enough, full fluid film lubrication was possible within the constraints of the environment of the human body. They were also able to show that for metal on polyethylene combinations this was not theoretically possible. Furthermore, in their analysis they demonstrated that as diametral clearance was reduced, the thickness of fluid film which it was possible to develop increased. Considering the achievable surface finish on the metal on metal surfaces, it was possible that a design could achieve full fluid film lubrication at least some of the time by optimising the diametral clearance. If it could be claimed that increasing fluid film layer equated to lower bearing wear, then it could be shown that as diametral clearance reduced then theoretical wear should also be reduced.

2.7 Discussion

The first requirement was to discover how these metal on metal devices performed by comparison to their contemporary implants and this should be considered in both short and long term.

In the short term, the results in terms of hip score and patient satisfaction were very good and certainly comparable with the Charnley. It was clearly demonstrated that the goals of freedom from pain, restoration of function, ease of implantation, and for the most part restoration of anatomy were achieved with these historical devices. The Ring it must be said suffered some problems with pain and the **MkIII** certainly did not restore favourable gait to all patients, and the McKee-Farrar was criticised for its poor range of motion. Nevertheless, the short term results were generally fine.

Considering the long term results of the Charnley, 10 year aseptic loosening rates varied widely depending on the definition of loosening. Revision rates with 10 year follow up were reported between 1.6% (Charnley and Cupic, 1973) and 46% (Almby and Hierton, 1982). It was not surprising that good results have been achieved by Charnley when it is considered that the prosthetic stem would still be considered to be consistent for the most part with the latest cemented stem philosophy. For the Exeter, the most appropriate data is that which was generated with the first series of polished stems between 1970 and 1975, Fowler et al (1988) showed that out of 426 implants at 13.4 years follow up, 5.5% (1.64% of stems and 3.9% of cups) were aseptically loose. Once again a very interesting difference is that some of these stems were implanted with cement pressurisation which appeared to make a significant difference to loosening rates even between the Exeter stems themselves. The matt Exeter followed and then a reversion to polished with a stronger stainless steel to reduce the relatively high incidence of stem fractures, and Malchau and Herberts (1996) show that for the former at 12 years 16.9% (10% at 10 years) of 2734 prostheses had loosened aseptically and been revised while for the latter the figure was 3.5% of 7587 prostheses at 8 years.

Similar aseptic loosening figures for the McKee-Farrar of the same era are 4% at up to 4 years (Bentley and Duthie, 1973), 11.6% at up to 8 years (Tillberg, 1982), 17% at

15.5yrs (Zaoussis and Patikas, 1989). These seem about equivalent to the matt Exeter while the polished appears considerably better. However, it should be stressed, that even if direct comparison of these studies was permissible, it is hardly surprising today to find that a Charnley or an Exeter polished stem were seen to outperform both the Ring and the McKee-Farrar. After all, the Charnley, which in terms of stem design was fairly well optimised even by today's understanding, and the Exeter, which is now one of the most popular cemented stems, are regarded as the "gold standard" prosthetic designs. In contrast, the Ring, basically a Moore stem, and the McKee-Farrar, a cemented metal backed cup and a Thompson stem demonstrated by finite element analysis to cause some of the highest cement stresses of any stem design, would never be used as part of a modern total hip replacement.

Nevertheless, surely the most compelling study must be one which set out to compare such devices and fortunately Jacobsson and Djerf (1996) compared the McKee-Farrar with the Charnley and found statistically no significant difference in performance at 20 years follow up. This is remarkable given the previous discussion of product design issues. It is important to note that the McKee-Farrar series presented by these authors would be the latest design standard (**Design 8**) and would include only polar bearing prostheses. Whilst not wanting to give the metal on metal designs an unfair advantage it is proper to compare only those prostheses which are believed to be optimum and to exclude those with known deficiencies.

Furthermore, on comparison the 1 to 5 year data for the historical and the modern designs it was clear to see that there was a significant improvement in performance of the latter which may be an early indicator of long term success. There may be a number of reasons for this which have been shown from retrospective in vitro studies and theoretical analysis. The sphericity, the clearance, the finish, and the material type may all be significant contributors in improving the wear performance, though it may be simply that the modern design of stem and cup was the reason for this improvement.

Amongst the criticisms of metal on metal joints over the years has been the perception of increased friction over metal on polyethylene articulations. Considering McKee-Farrar prostheses prior to 1971, it appears that these were all of the "lapped-in" type where as Walker and Gold (1971) point out, there was the chance to develop "equatorial

bearing" and potentially very high friction torque. It was interesting to note that on the survivorship curve shown by August, Aldam, and Pynsent (1986) the step change in the curve at about 14 years would represent around the year 1970 which is when Walker and Gold (1971) and McKee (1982) indicate that the design was changed to ensure only "polar bearing" contact. McKee (1974) alludes to such a change by April 1971 where parts were made interchangeable and had a "....greatly reduced coefficient of friction". Like the McKee-Farrar, around 1969 the Ring prosthesis moved away from a lapped in to a "polar bearing" design. Could it be possible that if lapping in led to very small or negative clearance between the parts, then some components could effectively start to grip, due to the closeness of the angles of contact to the friction angle, with consequential large increase in friction torque? If this torque were high enough and for enough cycles then it is conceivable that this could have been a contributory factor in component loosening.

However, since the lapped in designs were abandoned there was no evidence at all that friction was substantially higher for bedded in prostheses tested under a more realistic lubrication regime. Indeed Muller (1995) has stated that he found metal on metal friction about the same as for a 32mm metal on polyethylene articulation.

The toxicity of the debris released from these devices has been a further criticism and whilst this material is known to be toxic, there was over the long period of time in which the devices were implanted, no statistically significant incidence of illness or disease such as cancer which could be attributed to the presence of the device.

The conclusion appears to be that from the literature there is no evidence of problems with metal on metal articulations which would always make them inferior to metal or ceramic on polyethylene. On the contrary, there remain some reasons to believe that the low volumes of debris released by these metal on metal devices allows a prosthesis to remain firmly fixed due to the absence of osteolysis.

This being the case, and since current design, manufacturing, and research technology hold out the possibility of developing metal on metal articulations with even lower wear, there is good reason to be confident that a research programme can be carefully designed and carried out which will arrive at optimum operating conditions for

minimum friction and wear of metal on metal articulations. Such articulations properly embodied in a total hip system design could make a significant contribution to the important goal of long term prosthetic survival.

CHAPTER 3

Research Hypothesis

3.1 Research Hypothesis

From early clinical studies reported in the literature there is an indication that cobalt chromium alloy metal on metal articulations of the hip can be configured so as to reduce the volumetric wear levels and the consequent potential for osteolysis in comparison with metal on polyethylene articulations in artificial hip prostheses.

It is postulated that the wear performance of such metal on metal articulations is dependent upon both contact mechanics and lubrication conditions which in turn are influenced by head diameter, diametral clearance, and composition of the alloy used.

The aim of this research is to investigate the effect of diametral clearance, head diameter, and carbon content on the wear of metal on metal artificial hip prostheses.

3.2 Research Objectives

3.2.1 Diametral Clearance Objective

To investigate the effects on wear of a 28mm spherical metal on metal articulation of the variation of diametral clearance between the male and female components.

3.2.2 Material Composition Objective

To investigate the effects on wear of a 28mm spherical metal on metal articulation of the variation of carbon content of a wrought cobalt chromium molybdenum alloy.

3.2.3 Head Diameter Objective

To investigate the effects on wear of a spherical metal on metal articulation of the variation of nominal articulation diameter.

3.2.4 Clinical Product Objective

To investigate the effects on wear of a spherical metal on metal articulation of the hip of incorporating the optimised design features established through the previous chapters into a clinically useful product.

3.3 Structure of Thesis

Chapter 4 applies the theoretical analysis found in the literature to the specific articulation geometry envisaged in order to establish a practical range of design variables for investigation through hip simulation. Chapter 5 describes the materials and experimental methods used in the study. Chapter 6 investigates the effect on wear of the variation of diametral clearance for 28mm articulations, whilst Chapter 7 investigates the effects of specific material composition for the cobalt chromium alloy. Chapter 8 then investigates the effect on wear of both 22mm and 35mm head diameter. Finally the long term wear performance of a clinically usable design of joint replacement articulation incorporating the design features established in the preceding chapters is investigated.

CHAPTER 4

Theoretical Analysis and Design of Articulating Geometry

4.1 Introduction

Physical testing can be slow and expensive, and so in any proposed study it is prudent to gather as much information as possible to enable the most informed decision to be taken on the scope of any required physical testing. Theoretical analysis and mathematical modelling are very useful screening tools as a precursor to physical testing. In the area of metal on metal articulations both Walker and Gold (1971) and Jin, Dowson, and Fisher (1997) have provided theoretical analyses which offer some assistance in the design of a practical study using a hip simulator.

These two theoretical analyses were applied in this chapter in order to derive the parameters to be used in the design of the bearings to be investigated in the subsequent physical testing.

4.2 The Influence of Geometrical Errors (Walker and Gold)

Starting with an assumption of perfectly spherical socket of radius Rs and imperfectly spherical ball of effective radius Rb (ie instantaneous radius at any point on the surface), the relative geometry can be shown as in figure 4.1.

Then, the base clearance e between the pole of socket and ball (cup and head) is given by the expression:-

$e=(\Delta^2+2\Delta Rs)^{½} -\Delta$ where Δ=Rb-Rs (radial interference)

The relationship between e and Δ is then demonstrated from table 4.1 and from figure 4.2.

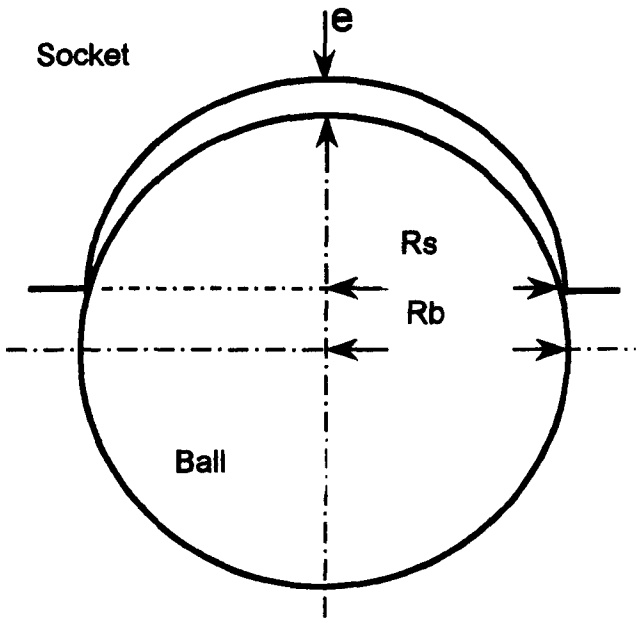

Figure 4.1: Relationship of spherical socket and ball
Figure shows the relationship when the ball is fractionally larger than the socket as could be the case due to imperfections of sphericity.
Reproduced from Walker and Gold (1971)

Δ (mm)	e (mm) Rs=11mm	e (mm) Rs=14mm	e (mm) Rs=17.5mm
0.001	0.147	0.166	0.187
0.01	0.459	0.519	0.582
0.02	0.644	0.729	0.817
0.05	1.000	1.134	1.274

Table 4.1: Base Clearance 'e' between Ball and Socket against values of Radial Interference Δ where Effective Diameter of the Ball exceeds that of the Socket

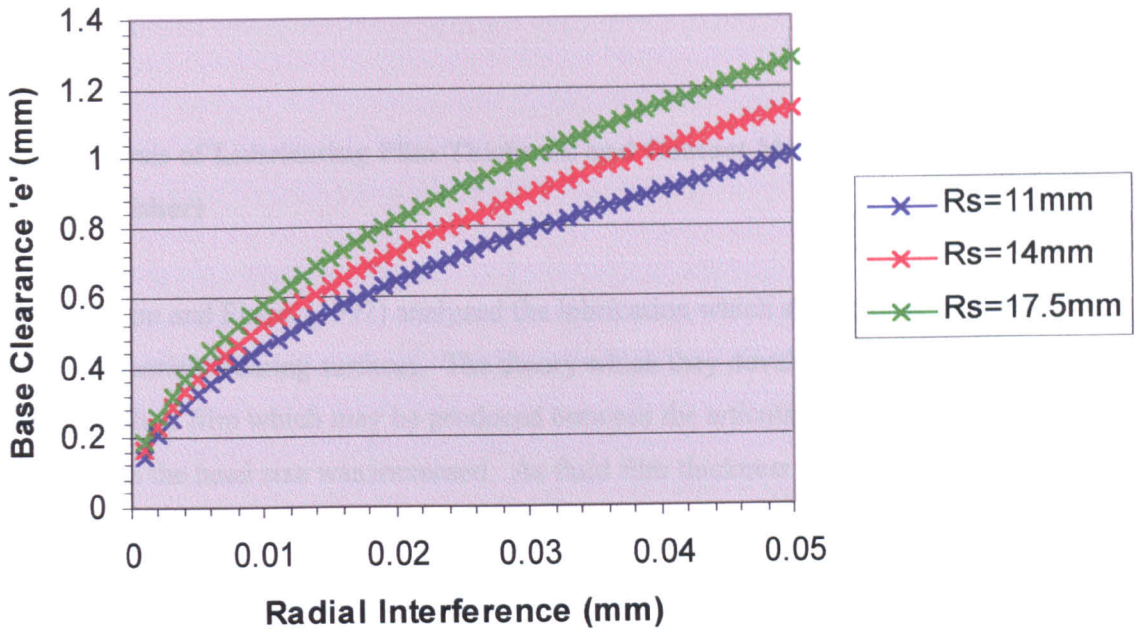

Figure 4.2: Base Clearance 'e' between Ball and Socket against values of Radial Interference where Effective Diameter of the Ball exceeds that of the Socket Figure shows the relationship when the ball is fractionally larger than the socket as could be the case due to imperfections of sphericity. Reproduced from Walker and Gold (1971)

From these data it was clear to see that for only a very small value of interference between head and cup, a relatively large gap could develop between the poles which are supposed to remain in contact. Any gap between poles would result in load transmission between head and cup through an equatorial contact zone which could lead to seizing if the angle of contact was less than the friction angle for the materials. Since typical manufacturing errors were likely to lead to accuracy of sphericity of only around 0.005mm per bearing surface, in order to ensure that the equatorial bearing situation would not arise, the minimum diametral clearance required between the physical parts during test would be predicted at about 0.01mm to ensure that a polar gap would not develop.

Therefore the mathematical analysis was able to provide useful data as to the order of minimum diametral clearance likely to give the desired articulation in the practical tests.

4.3 Analysis of Lubricating Film Thickness and Contact Mechanics (Jin, Dowson, and Fisher)

Jin, Dowson and Fisher (1997) analyzed the lubrication which should exist between mating spherical bearing surfaces. The theory which they developed suggested that the potential fluid film which may be produced between the articulating surfaces would increase as the head size was increased. As fluid film thickness is increased, the lubrication regime tends towards full fluid film so that the contact and therefore wear, between the articulating surfaces should be reduced. The authors developed a set of equations which could be used to calculate the film thickness and therefore the lubrication regime for a given set of circumstances, based on the arrangement shown.

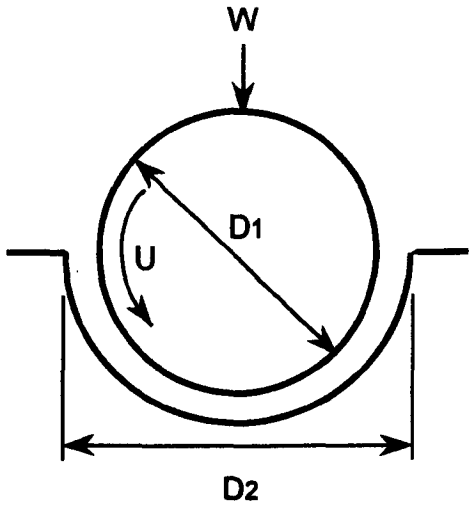

In fact, the equations developed were based on established theory of a ball on a flat plate as below and so in order to allow the equations to be relevant to the ball and socket arrangement of interest, an "equivalent radius" R was established as some function of the individual ball and socket radii.

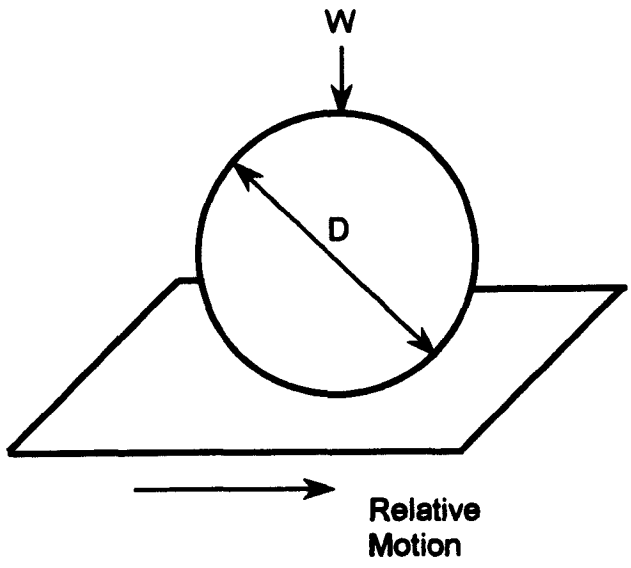

This equivalent radius could then be used as the radius of the theoretical ball on flat plane. In the following representation of the analysis the radius is replaced with diameter in all cases. It was noted by the authors that the accuracy of using a ball on flat configuration to represent a ball in socket configuration holds only when the ratio of contact half width (half width of contact patch between ball and socket formed under load) to the femoral head radius (contact width to head diameter) is very small, at less than around 0.25 (or 0.125 comparing the contact half width to the head nominal diameter).

The primary, defining, equation calculated the fluid film thickness from a given set of input characteristics and is given here in terms of diameter rather than radius of the bearing surfaces.

$$h_{min}=1.64D\left(\frac{\eta u}{E'D}\right)^{0.65}\left(\frac{w}{E'D^2}\right)^{-0.21}$$

From this and a knowledge of the roughness of the bearing surfaces a value λ, representing an indication of the applicable lubrication regime is derived from:-

$$\lambda=h_{min}/Ra$$

$\lambda<1$: Boundary Lubrication

$1<\lambda<3$: Mixed lubrication

$\lambda>3$: Fluid Film Lubrication

From Hertzian contact theory, the contact half width "a" is represented by:-

$$a=(3wD/4E')^{1/3}$$

These equations apply where :-

$$D=D_1D_2/(D_2-D_1)$$

$$E'=2[(1-\nu_1^2)/E_1+(1-\nu_2^2)/E_2]^{-1}$$

$$R_a=(R_{a1}^2+R_{a2}^2)^{0.5}$$

Finally, Timoshenko and Goodier have shown that the peak pressure within the contact zone is 1.5 times the mean pressure across the contact and is given by:-

$$q_o=3w/2\pi a^2$$

All of the above equations apply where:-

hmin = minimum film thickness

a = contact half width or radius of circular contact area

D = equivalent diameter

D_1 = head diameter

D_2 = cup diameter

η = lubricant viscosity

u = entraining velocity (half the actual relative motion between head and cup)

E' = equivalent elastic modulus

q_o = peak pressure at centre of contact

w = applied load

R_a = combined surface roughness

R_{a1} = head surface roughness

R_{a2} = cup surface roughness

E_1 = head modulus of elasticity

E_2 = cup modulus of elasticity

ν_1 = head Poisson's ratio

ν_2 = cup Poisson's ratio

For the analysis here, cobalt chromium alloy is assumed and therefore the constants for the analysis are defined as:-

w =2000N

E_1 =230GPa

E_2 =230GPa

ν_1 =0.3

ν_2 =0.3

u = a value in m/s calculated from 123°/s, and a function of head size

η =0.005Pa s

R_{a1} =0.02μm

R_{a2} =0.02μm

By varying head and cup diameter and diametral clearance between head and cup the graph of Figure 4.3a was created to represent the relationship between these variables and the predicted film thickness. Then using the data on surface finish Figure 4.3b was created to show the relationship to lambda ratio and therefore to lubrication regime.

Considering Hertzian contacts it was now possible to plot the contact half width against the same nominal diameter and diametral clearance data, and this is shown in Figure 4.4a. The peak pressure within the Hertzian contact zone for such systems is a simple function of the size of the Hertzian contact area and will therefore also be dependent upon the nominal diameter and diametral clearance. Figure 4.4b was constructed to demonstrate the relationship.

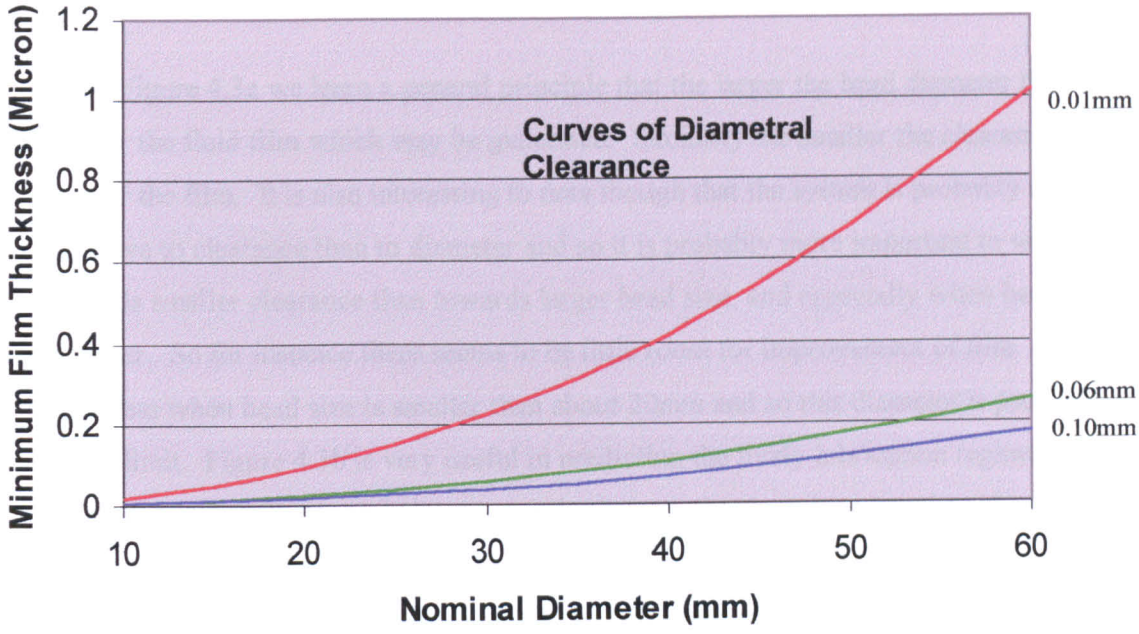

Figure 4.3a: Relationship Between Predicted Film Thickness, Nominal Bearing Diameter, and Diametral Clearance

Figure shows curves of diametral clearance on axes of nominal diameter and predicted film thickness for a cobalt chromium alloy metal on metal spherical articulation.

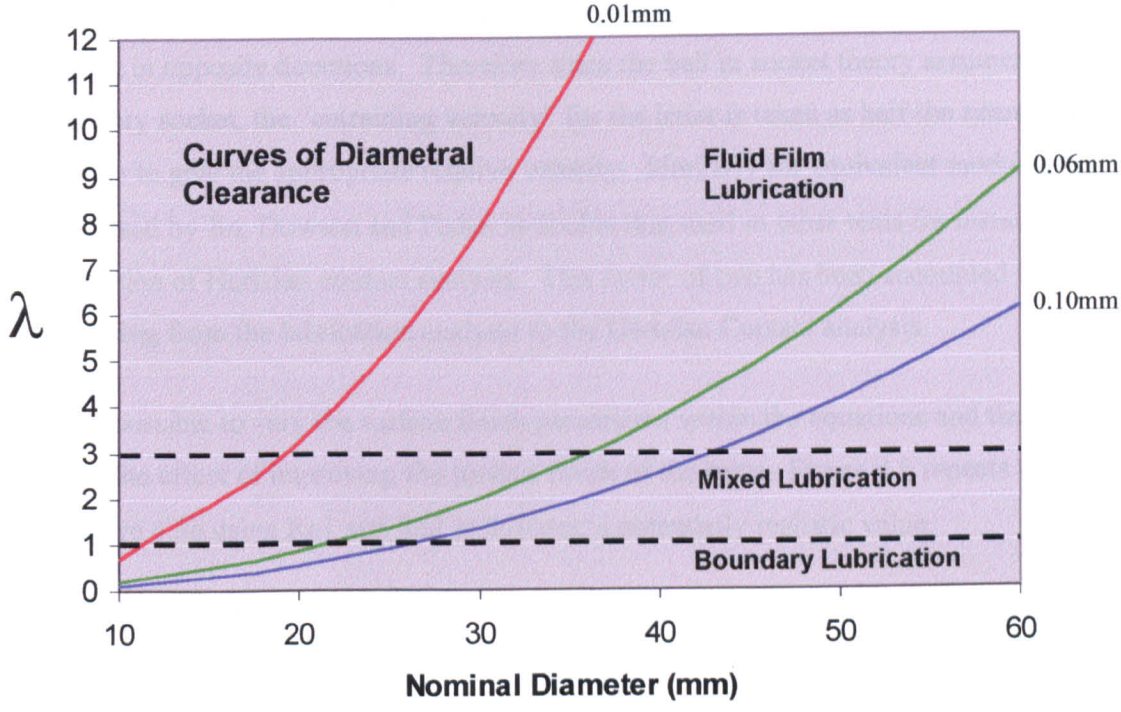

Figure 4.3b: Relationship Between Predicted Lubrication Regime, Nominal Bearing Diameter, and Diametral Clearance

Figure shows curves of diametral clearance on axes of nominal diameter and lambda ratio for a cobalt chromium alloy metal on metal spherical articulation.

From Figure 4.3a we learn a general principle that the larger the head diameter the thicker the fluid film which may be generated. Similarly the smaller the clearance the thicker the film. It is also interesting to note though that the system is probably more sensitive to clearance than to diameter and so it is probably more important to work towards smaller clearance than towards larger head size, and especially when head size is larger. So for instance there seems to be little room for improvement of film thickness when head size is smaller than about 20mm and so this diameter is probably a lower limit. Figure 4.3b is very useful in predicting the likely lubrication regime for a given nominal diameter and clearance and reiterates that in order to get into the mixed regime with a practical diametral clearance the lower limit of head size would be no less than 20mm. It also demonstrates the difficulty in obtaining a design which is within the full fluid film region. It shows also how desirable a very small clearance of the order of 0.01mm would be, and how undesirable clearances greater than about 0.10mm would be.

It should be noted that the ball on plate theory assumes that the plate and ball are both moving in opposite directions. Therefore since the ball in socket theory assumes a stationary socket, the "entraining velocity" for the latter is taken as half the actual head velocity to give the appropriate relative velocity. Similarly for equivalent modulus the value used by Jin, Dowson and Fisher is double that used in other texts for instance in calculation of Hertzian contact analysis. This factor of two has been accounted for in translating from the lubrication analysis to the Hertzian Contact analysis.

It was possible to vary the surface finish parameters within the equations and thus to assess the effect of improving the surface finish of the parts. Figure 4.5 repeats the data of Figure 4.3b using Ra1 and Ra2 at 0.01μm, a potentially realistic value.

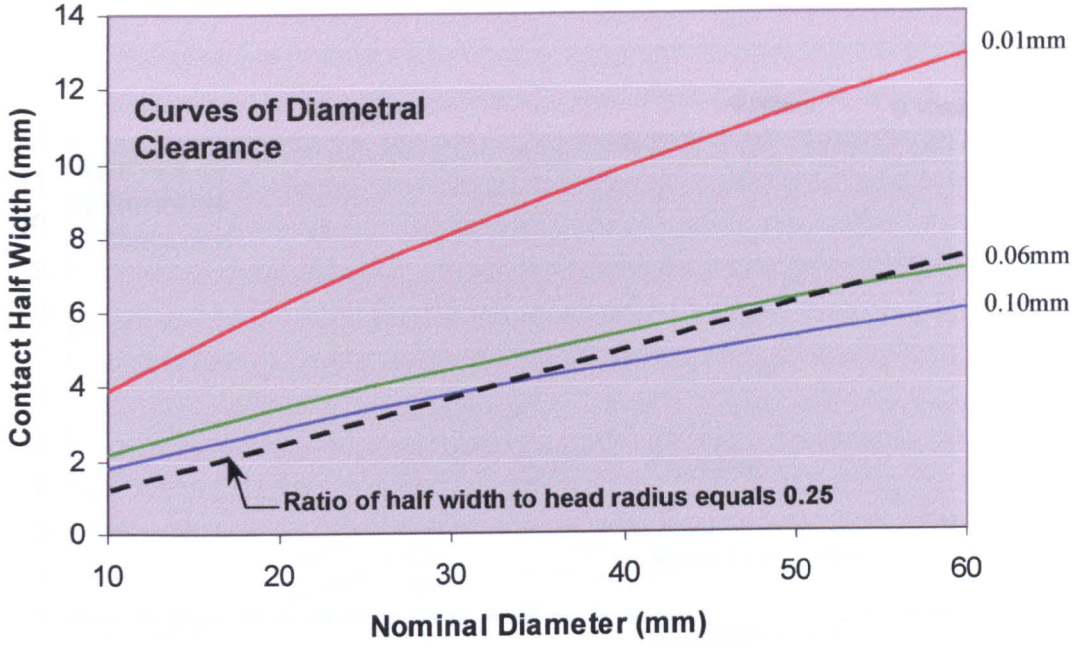

Figure 4.4a: Relationship Between Contact Half Width, Nominal Bearing Diameter, and Diametral Clearance

Figure shows curves of diametral clearance on axes of nominal diameter and Hertzian contact half width for a cobalt chromium alloy metal on metal spherical articulation.

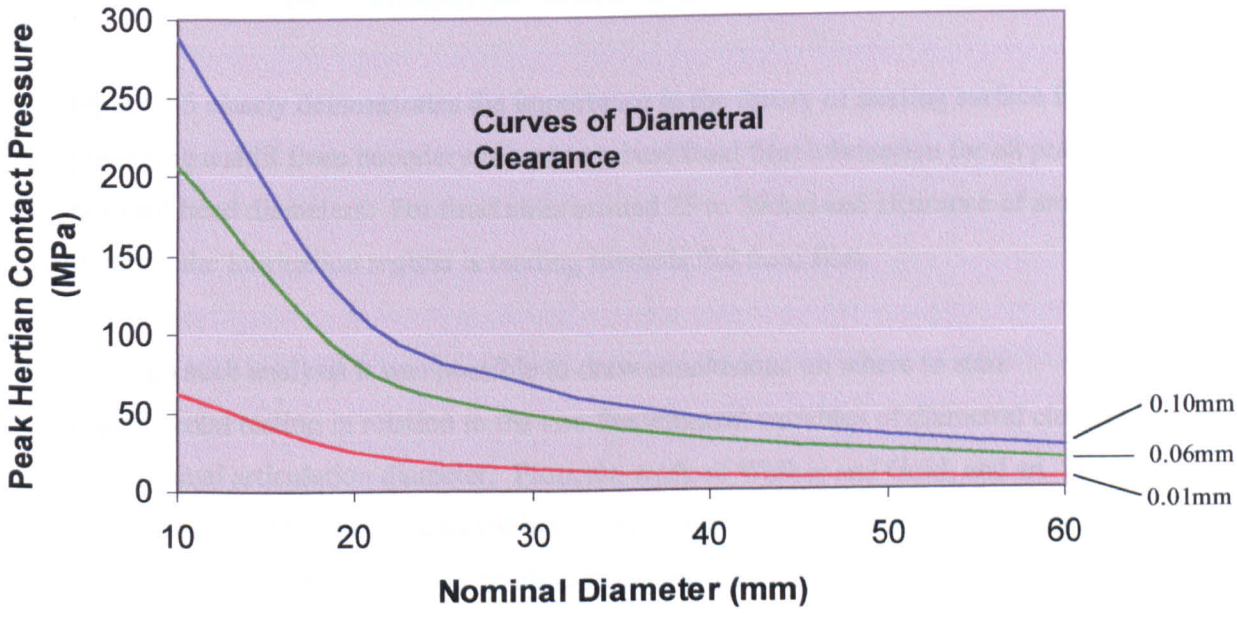

Figure 4.4b: Relationship Between Peak Pressure, Nominal Bearing Diameter, and Diametral Clearance

Figure shows curves of diametral clearance on axes of nominal diameter and peak pressure within the Hertzian contact zone for a cobalt chromium alloy metal on metal spherical articulation.

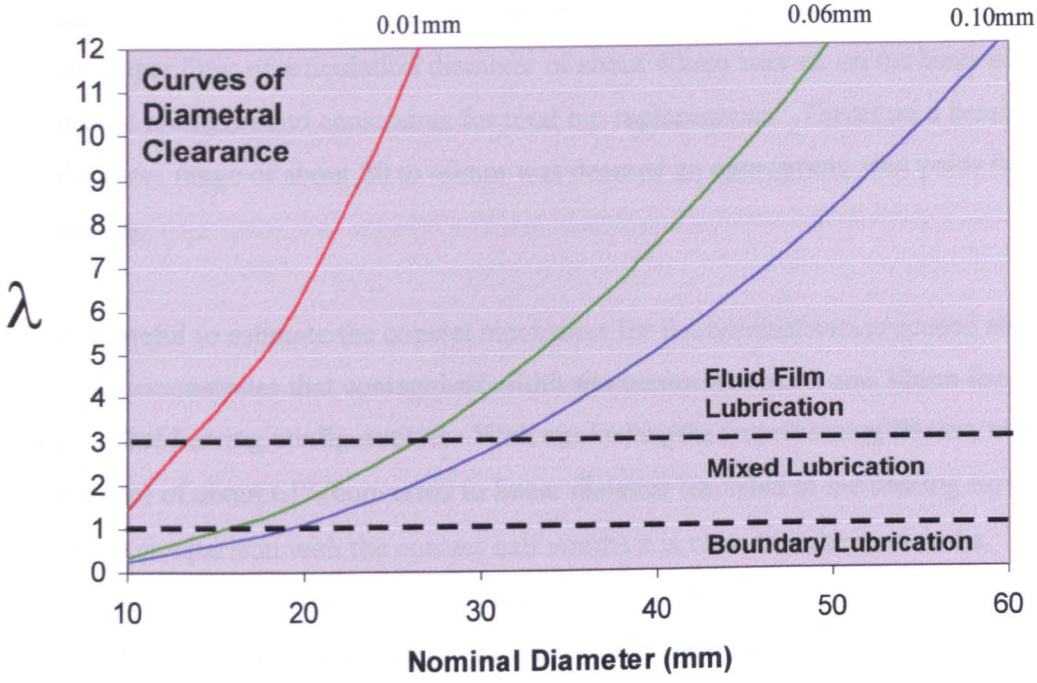

Figure 4.5: Replication of Figure 4.3b but with Better Surface Finish
Figure shows curves of diametral clearance on axes of nominal diameter and lambda ratio for a cobalt chromium alloy metal on metal spherical articulation.

Figure 4.5 clearly demonstrates the importance in the theory of starting surface finish in predicting a shift from boundary/mixed to mixed/fluid film lubrication for all practical nominal head diameters. For head sizes around 25 to 30mm and clearance of around 0.06mm the lubrication regime is tending towards full fluid film.

Through such analysis it was possible to draw conclusions on where to start experimental testing in relation to the two fundamental variables of diametral clearance and nominal articulation diameter. From the work of Walker and Gold, and an understanding of the likely achievable accuracy of spherical surfaces, a lower limit of diametral clearance would be set to about 0.01mm. From the work of Jin, Dowson, and Fisher it was decided that a clearance above 0.10mm would be less likely to be successful in terms of wear. Furthermore a range from 0.01mm to 0.10mm was thought to have a reasonable probability of showing some differentiation in wear performance and was a practical range from a manufacturing point of view. This range of clearance

was therefore deemed an appropriate start point for testing. From the work of Jin, Dowson, and Fisher, a bearing diameter of 20mm was taken as a reasonable minimum capable of showing a range of lubrication regimes over a range of diametral clearance. An upper limit of articulation diameter of about 40mm was set on the basis of practical design configuration constraints for total hip replacements. Therefore a bearing diameter range of about 20 to 40mm was deemed an appropriate start point for practical testing.

It is useful to estimate the contact mechanics for the articulations proposed and Figure 4.4a demonstrates that contact half width sits between about 3 and 10mm for all practical bearing configurations. With stroke lengths (representing flexion/extension of the hip) of about 61° (converted to linear distance travelled at the bearing surfaces for direct comparison with the contact half width) it is clear that the model of a continuously rotating sphere on a plate is close to the limits of applicability as the stroke length is not significantly greater than the width of contact. This may limit formation of the predicted fluid film. Further, from the line of half width to nominal radius ratio of 0.25 it is clear that most of the articulations considered lie outside of the applicability of the equations. Clearly this casts some doubt over the absolute accuracy of the analysis but as a predictor of relative changes the analysis remains of some value.

Finally, from Figure 4.4b any attempt to limit the peak pressure again points to a minimum nominal diameter of not less than 20mm. Above about 20mm the stress level is relatively insensitive to both diameter and clearance. It should also be noted that the analysis applies only to perfectly spherical virgin parts and clearly cannot apply to worn surfaces which would not remain spherical due to the removal of material unevenly over the bearing surfaces.

CHAPTER 5

Materials, Equipment, and Methods

5.1 Introduction

This chapter comprises a general description and discussion of the materials and equipment used to perform the testing and of the test methods employed. Some relevant information in these areas is provided within the other chapters but the present chapter forms a complete description and discussion in these areas.

5.2 Materials

The materials used within the testing program were exclusively composed of cobalt chromium alloy wrought bar meeting the requirements of ASTM F799 (now ASTM F1537). Materials from 2 different suppliers were used. These suppliers were as given in Table 5.1.

Teledyne Allvac	**Heymark Metals**
Allvac Limited Atlas House Attercliffe Road Sheffield S4 7UY UK The material itself was supplied out of the US by:- Allvac 2020 Ashcraft Avenue Monroe North Carolina 28111-5020 USA	Heymark Metals Limited Unit 4 Becklands Close Bar Lane Industrial Estate Boroughbridge North Yorkshire YO51 9NR UK

Table 5.1
List of material suppliers used in the study

The aim of the study was to have all materials within two distinct groupings as similar as possible. The two groupings were high carbon and low carbon materials. The designation of a low carbon material was that the carbon content remain within the requirements of ASTM F1537 but be no greater than 0.07% whilst for the high carbon material the designation was as for low carbon except that the carbon content be no lower than 0.18%.

Table 5.2 details all the materials used in the testing and the particular test. The fine detail for each material is given within the specific chapter describing the test in which it was used.

One typical method of production of such materials is to vacuum melt and electro slag re melt to achieve an ingot of the correct size and chemical composition. Typical ingot diameter would be around 400mm. The ingot, heated to something in excess of 1100°C, is then press forged down to a diameter of closer to 100mm. The forging process takes place in a number of steps between which the ingot is reheated back to the forging temperature. Once forged to the required size, the ingot is rolled from the forging temperature through a series of shaped rollers down to the required diameter of perhaps 30 to 50mm. During the rolling process the material is cooling and is not reheated. It is this "warm working" which achieves the specification mechanical properties as the material is mechanically worked through while cooling and much of the skill in producing the material lies in making use of the time and temperature relationship which exists through this rolling process. The bars are immediately straightened and then centreless ground. Inspection of the surfaces for flaws completes the manufacturing cycle and the final step is to measure the mechanical properties of test pieces cut from the bar. Betteridge (1982) has provided further information on the processing of wrought cobalt chromium alloys.

Material Designation	Carbon Content Designation	Test	Used to Make	Supplier
CF52	Low	28mm Diametral Clearance	Heads	Teledyne Allvac
55E11514	Low	28mm Diametral Clearance and 28mm Carbon Content	Cups	Heymark Metals
VN87	High	28mm Carbon Content, 35mm Diametral Clearance, and Final Design	Heads and Cups	Teledyne Allvac
VM12	High	28mm Carbon Content	Heads	Teledyne Allvac
VN07	High	28mm Carbon Content and 22mm Diametral Clearance	Heads and Cups	Teledyne Allvac
EG68	Low	28mm Carbon Content	Heads	Teledyne Allvac
ED96	Low	28mm Carbon Content and 35mm Diametral Clearance	Heads and Cups	Teledyne Allvac
CJ53	Low	28mm Carbon Content	Heads	Teledyne Allvac
EC75	Low	22mm Diametral Clearance	Heads	Teledyne Allvac
EJ13	Low	Final Design	Heads	Teledyne Allvac

Table 5.2
List of materials used in the study

5.3 Equipment

The equipment used in the study was documented and described in the following sections.

5.3.1 Microfinishing Machine

Ernst Thielenhaus GmbH (42285 Wuppertal, Germany) have been developing expertise in manufacture of equipment for the production of parts with super accurate dimensions

and super fine finish for around 100 years. All the metal on metal samples produced in the study were made using the Thielenhaus "microfinishing" process. Figure 5.1 shows the Type KF50F2 (No 1.1.002453) machine on which all the parts except the cup inserts for the final design test were microfinished.

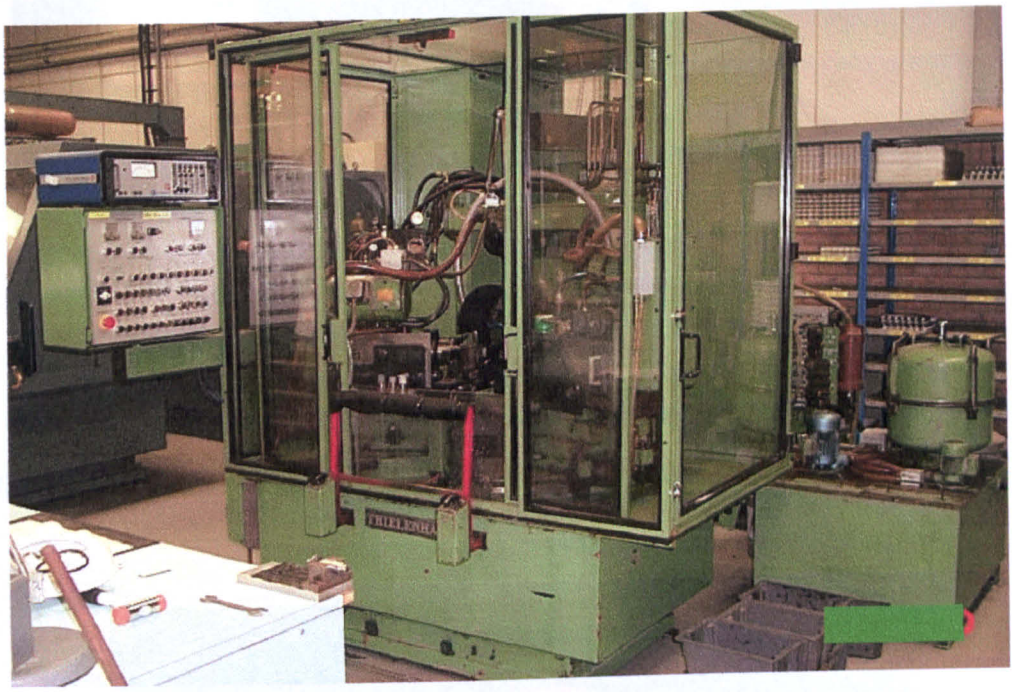

Figure 5.1: Thielenhaus Type KF50F2 (No 1.1.002453) Microfinishing Machine

The final design cup inserts were microfinished on a machine equipped with additional axis motion options to facilitate entry of the microfinishing stones into the cup form. Figure 5.2 shows a more modern machine equipped with such functionality which is used in the routine production of inserts of the final design.

The Thielenhaus microfinishing process for producing spherical bearing surfaces works on the very simple principle that any section in a single plane through a spherical surface will be circular in form. Therefore if a circle may be brought into contact with a surface such that the circle makes full contact with the surface at any location on the surface then that surface by definition must be spherical. Figure 5.3 shows such a section through a sphere.

Figure 5.2: Thielenhaus Microfinishing Machine Suitable for Microfinishing the Cup Inserts

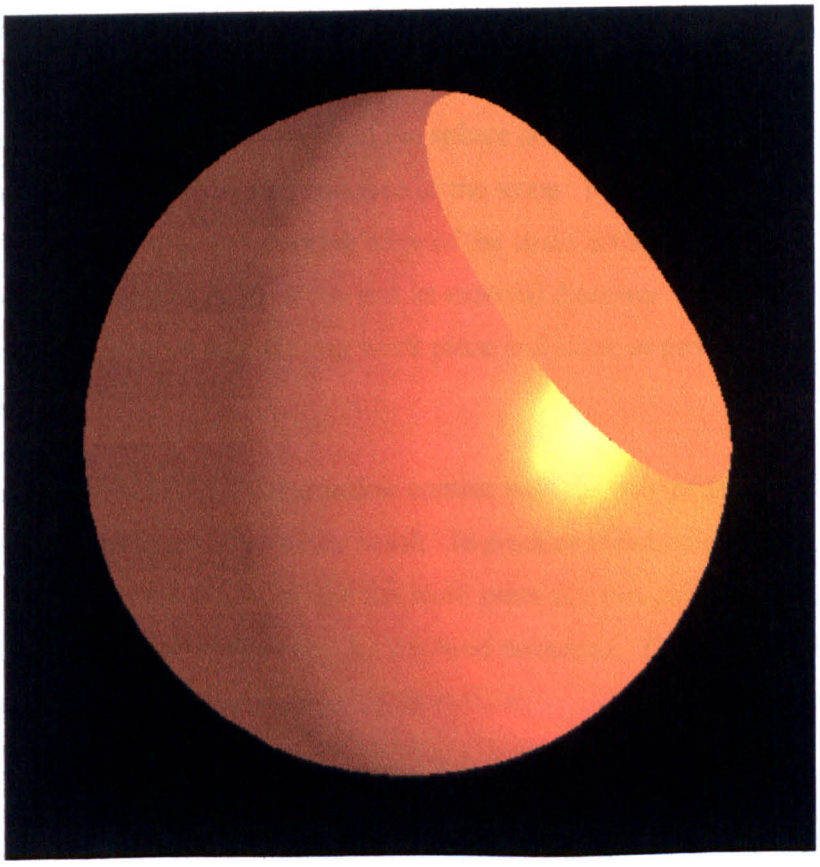

Figure 5.3: Plane Section through a Sphere
Figure shows that any plane section through a sphere is circular in form.

By rotating a roughly spherical (concave or convex) component on some chosen axis, and bringing into contact with that surface a microfinishing stone of cylindrical form (external or internal) which is also rotating on its own axis of symmetry, it is possible for the circular contact made between the rough sphere and the stone to cause the roughly spherical workpiece to become perfectly spherical (but of smaller diameter). The axis of the cylindrical stone must intersect the axis of rotation of the work piece and will generally be inclined at about 45° to it. The principle is that the combined rotations ensure that the stone (circular edge) makes contact with every part of the work piece surface and so eventually through a process of wear every part of the work piece surface will form part of a circle of contact with the stone. The work piece will therefore be inherently spherical. For example in the case of a femoral head (convex spherical surface) consider a single point on the edge of the stone formed by the intersection of the front face and internal diameter of the stone. Consider this point on the edge rotating about the axis of symmetry of the stone. Now consider that instead of the head rotating, that the stone also rotates about the axis of rotation of the femoral head whilst the head remains stationary (i.e. all motion is relative to the head). The surface formed by the locus of the point on the stone edge as it moves due to both rotations is a sphere (or a portion of a sphere). The diameter of the sphere is directly related to the distance from the centre of the sphere to the front face of the stone. For a cup, exactly the same argument applies except that the working edge of the stone is that formed by the intersection of the front face of the stone and its external diameter. Figure 5.4 shows the Thielenhaus machine set up with cup work piece and stone in position during microfinishing.

However it is important that the stone makes contact with the pole of the spherical work piece otherwise a polar pip will certainly result. In practice the circular line of contact theoretically made between the stone and the work piece is a circular band of contact in order to ensure that the pole is straddled by the band thickness. The stone must also be large enough to overlap the edge of the bearing surface.

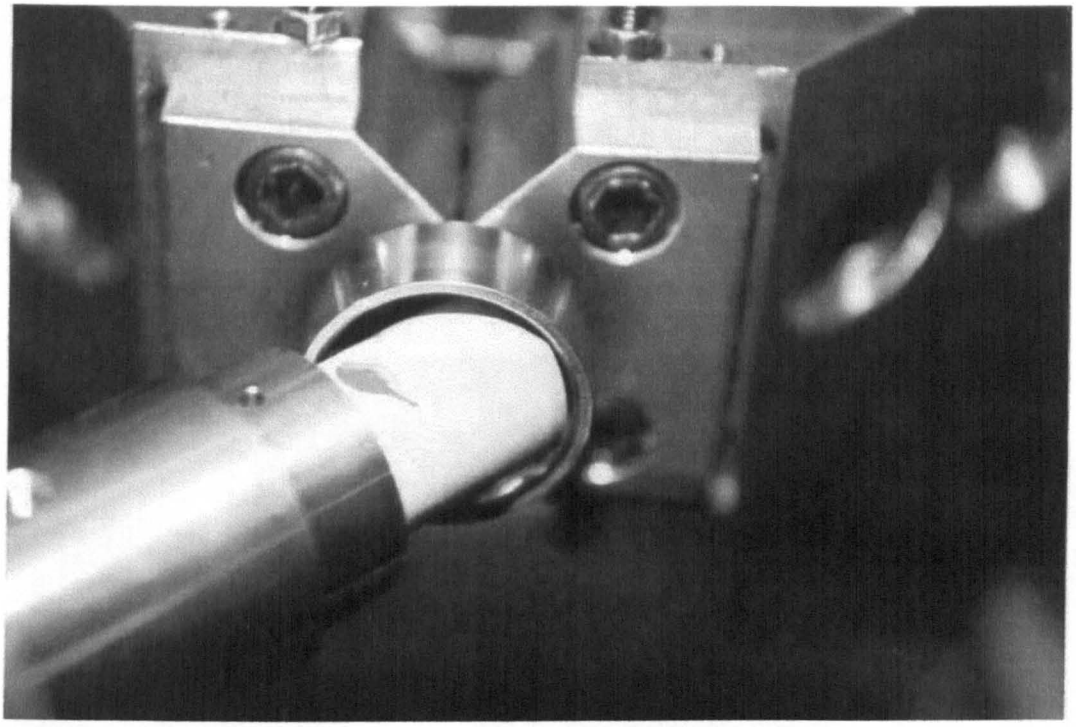

Figure 5.4: Microfinishing a Cup

Figure shows the relationship of the cup work piece and the stone during microfinishing. Note that the working edge of the stone is the external corner and note the angle of about 45° between the axes of the cup and the stone.

Consider the case of a cup, and consider that as microfinishing progresses, the stone is feeding forward along its axis of rotation as material is being removed from the cup surface. At each location of the stone, a cup of particular diameter is created. If the stone feeds further the cup diameter increases. By this means, the diameter of both heads and cups is controlled. There is one potential problem with reduction of a head diameter and two with growth of a cup diameter. Since the stone is being fed in along its own axis of rotation there is a danger that if fed in too far the pole of the work piece will cease to be covered by the stone and a pip may then result. For cups, a further danger exists that, as the stone is fed in, the edge of the stone designed to overlap the edge of the bearing surface may no longer overlap. The portion of the bearing surface no longer covered by the stone will then not grow along with the rest and give the effect of a constricted cup mouth which may then foul on the mating head during articulation. Similarly, it is possible to create a cup form with bearing surface extending to more than a hemisphere but once again there exists the danger that the cup mouth diameter will be smaller than the spherical diameter.

In order to be able to create spherical surfaces of precise diameter the use of in process measurement is achieved by means of contacting calliper arms linked to an electronic gauging unit. This calliper arm arrangement can be seen in figure 5.5. The arms move forward along the work piece axis and make contact with the head or cup on a portion of exposed spherical surface. By carefully pre setting the required size, the gauge will indicate when the calliper arms are registering the pre set diameter.

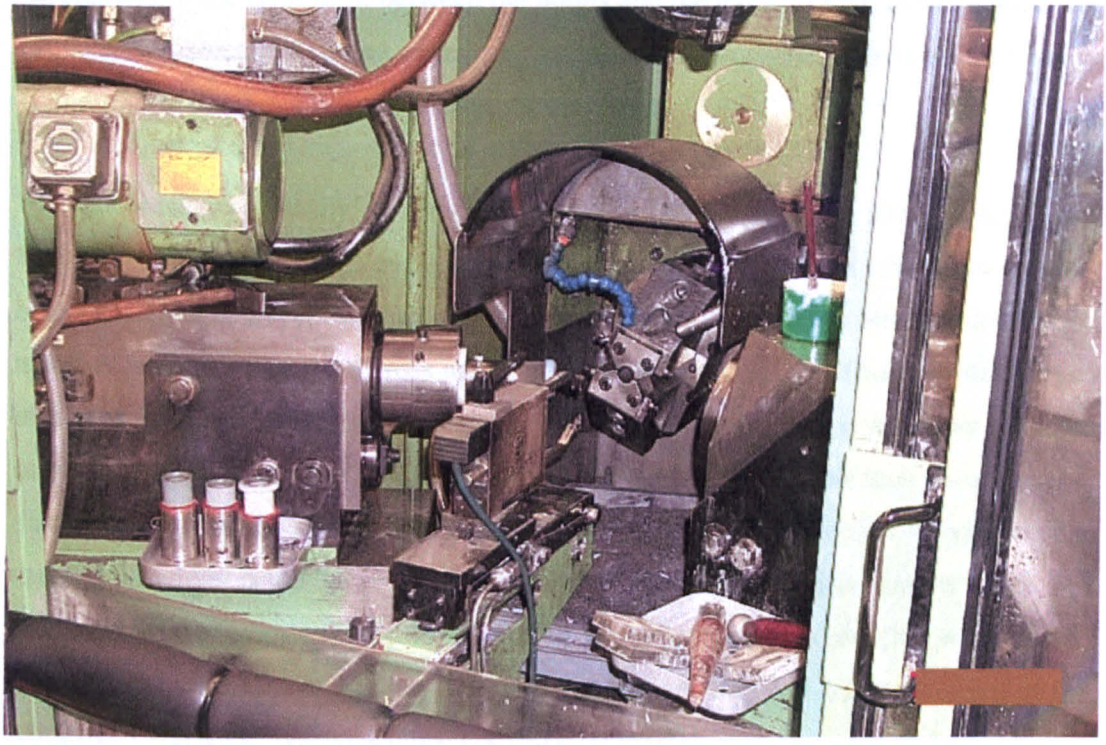

Figure 5.5: Arrangement of In Process Measurement Calliper Arms
Figure shows the Thielenhaus machine with work holding jaws, microfinishing spindle, and in process measurement calliper arms.

5.3.2 Co-ordinate Measuring Machine

Co-ordinate Measuring Machines or CMM's were developed in the early 1980's as computer technology become more cheaply available through personal computers. The principle is extremely simple. A reading is taken by triggering a mechanical probe (recent advances are enabling non contact methods of taking readings from surfaces). Typically a probe consists of a ruby sphere of appropriate size (say 2mm diameter) captured on the end of a thin metal shank. The act of bringing the probe into contact with a surface triggers the probe and at that point a reading is taken and stored in the

machine's computer. The reading is simply the x, y, and z co-ordinate values from some 0,0,0 reference point. If a series of points are taken, scattered over a surface, mathematical analysis within the machine's computer enables the attributes of the surface to be measured. For example by taking 3 points on a surface, a circle may be fitted to the points with a single calculated diameter. With four points it is possible to calculate the circle which best fits the points, along with its centre point position, and an assessment in the error in fit between the points and the circle. Other obvious measures are length, diameter of sphere, cone, etc. Further, measures of error in terms of flatness, roundness, and sphericity are possible.

The machines are typically composed of a granite surface table with sliding frame. The frame is composed of 2 legs and a connecting cross member. This frame slides on air bearings in one of the co-ordinate directions. Mounted on the cross member is a second member which slides on the cross member, again on air bearings. This provides motion in one of the other co-ordinate directions. Finally, a third member is generally mounted on the second member, again sliding by means of air bearings in the final co-ordinate direction. This final direction is typically vertical (z). Mounted on the bottom end of this third member is the trigger probe. Each of the slides has motion sensors which measure sliding distance to enable the machine to keep track of where the probe centre resides within the 3 co-ordinate system space envelope. Figure 5.6 shows a view of the Mitutoyo (Warwick, Warwickshire, UK) BH305 manual machine used in the study whilst Figure 5.7 shows a close up of the trigger probe and the master calibration ball.

The measurement steps for a typical spherical bearing surface was as follows using the **"GEOPAK"** software supplied with the machine.

i. Secure the calibration master ball into one of the threaded holes in the granite table and ensure it is thoroughly cleaned.

ii. With the **GEOPAK** software loaded and running type **DP** to **Define** the **Probe**.

iii. Select the option to measure the master ball and choose 5 points.

Figure 5.6: Mitutoyo CMM model BH305

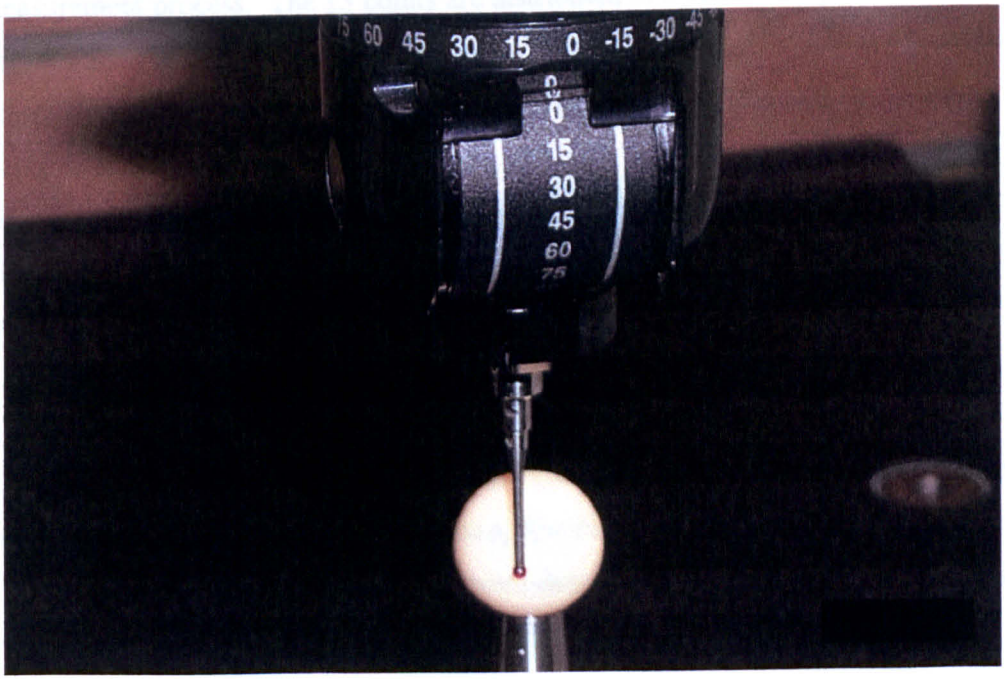

Figure 5.7: CMM Trigger Probe and Ceramic Calibration Master Ball

iv. Carefully contact the ceramic ball with the ruby tipped probe 5 times with 4 equally spaced equatorial points and 1 polar point. The machine will automatically store the probe size data based on an assumption of the actual master ball size stored within its computer.

v. As a check the master ball may be measured to verify that the machine calculates the correct size for it by typing SP to measure a **SPHERE** and using function **F5** to select 5 points. Again carefully contact the ceramic ball with the ruby tipped probe 5 times with 4 equally spaced equatorial points and 1 polar point. The machine will automatically calculate the diameter of the master ball, its centre position in relation to the 0,0,0 point, and the error in sphericity. The size should be within about 1 micron of the calibrated master ball diameter and the sphericity within about 2 microns.

vi. Heads or cups may now be measured in exactly the same way but by selecting 13 points using function **F5** within the **SPHERE** command **SP**. All surfaces to be measured must be cleaned and the components secured against movement during the measurement process. The 13 points are distributed in 3 bands of 4 points at levels between the equator and the pole and with a final polar point. The key is to get the greatest spread of points over the surface as evenly as possible.

vii. The calculated measurements including those for the master ball are recorded through use of the machine's printer through the **PRINT RESULTS** command **PR**.

5.3.3 Profilometer

Surface finish of male and female bearing surfaces was measured using a Surfanalyzer 5000 (Mahr Federal Products, Providence, Rhode Island, USA) as shown in figure 5.8. The measurement method and settings were determined as follows but with detailed description of each step presented in Appendix E.

i. Decide whether calibration of the machine is required and choose metric (μm) or English units (μin) (**"System 2"** under the Configure menu).

ii. Choose filter type (**"Filters"** under the Setup menu).
Standard ANSI RC, ANSI RC P/C, 50% Gaussian P/C.

iii. Choose roughness and waviness cutoff filter lengths (**"Filters"** under the Setup menu).
0.003"or 0.080 mm, 0.010" or 0.25 mm, 0.030" or 0.80 mm, 0.100" or 2.50 mm. If a longer cutoff length is needed, changing the drive speed to 0.1"/s or 2.5 mm/s will increase the cutoff lengths by a factor of ten.

iv. Choose traverse mode and drive speed (**"Traverse/Range"** under the Setup menu)
Modes: 5 cutoff, Traverse Length, Stop-to-Stop.
Drive speed: Use 0.01"/s or 0.25 mm/s for most cases. Using 0.1"/s or 2.5 mm/s will increase the cutoff filters by a factor of ten.

v. Determine if curve adjusting skid is needed

vi. Choose stylus/probe tip
High Resolution, Groove Bottom, Transverse Chisel Tip

vii. Choose waveform display (**"Waveform Displays"** under the Configure menu)
Filtered Roughness, Leveled Profile, Filtered Waviness, Unleveled Profile

viii. Choose parameters to be printed out (**"Parameters 1"** or **"Parameters 2"** under the Setup menu)
e.g. Ra, Rt, Rz, etc

ix. Choose x-axis and y-axis (i.e. graduation) scales you expect to use for printout (**"Graduation Scales"** under the Configure menu)

x. Input correct sample and operator identification for the trace printout (**"Report Printout"** under the Configure menu).
Use this Report Header for descriptions that will not change with a group of traces (e.g. lab request number, type of parts, etc.). The file name can be used to identify the specific sample and trace.

xi. Level the sample, optimize the probe range/sensitivity, close the levelling window, and run the trace using the **START** button on the main screen and the **START** button on the next screen.

Check the number of roughness features within a cutoff filter length and change if necessary. Check the horizontal and vertical graduation scales and change if necessary. If any changes are made, the trace must be rerun using the **START** button.

xii. Save the trace by going to "Load/Save" under the Setup menu.
Use the file name box to uniquely identify the part, the area and the direction traced (Note: There can be no spaces in the file name). When the file name is entered and the trace saved, print the trace using the **PRINTER** button on the main screen

Figure 5.9 shows a typical trace with the settings selection, the trace, and the results.

5.3.4 Balance

Weight measurements were done using a Sartorius balance (Sartorius AG, Goettingen Germany) model number MC210S having a resolution of 0.01 mg and a capacity of 210g as shown in figure 5.10. It was because of the limited capacity that the cup used in the majority of the tests (Figure 6.1a and Figure B6.1b) had a central weight reduction hole in the spigot. By this means the weight of cup sample was limited to 128g.

5.3.5 Hip Simulator

The hip simulator used for all the wear tests within the study was a 12 station MMED from MATCO (Rosebank Drive, LaCanada, California 91011, USA) model EW12. The machine consists of a Servo hydraulic Test Platform (STP) capable of applying force and mechanical rotation to 12 wear test samples simultaneously. Figure 5.11 shows a typical view of the machine. The force is variable between 0 and 5kN per station. The computer or Command System Controller (CSC) controls the force applied to the specimens while collecting and storing the test data. Up to 10 million cycles are

allowed per test. The simulator is capable of applying a number of force curves though in the present study the Paul (1967) curve with a maximum load of 2000N per station was used exclusively with a frequency of 1.1Hz. The sample tested within each station was bathed in serum, as described later, by using special fixtures which both located the test pieces and allowed for retention of the fluid. Figures 5.12 a and b show a typical station during a test by photograph and CAD representation.

The two defining elements of the simulator are the methods of loading and of moving the samples. Loading was applied through the hydraulic rams, one per station, vertically downwards. In this study the head was attached to the hydraulic ram and so the configuration was the inverse of the in vivo situation (upside down). Therefore during the test in this simulator the force vector remained constant with respect to the head. Figure 5.13 shows the Paul cycle used.

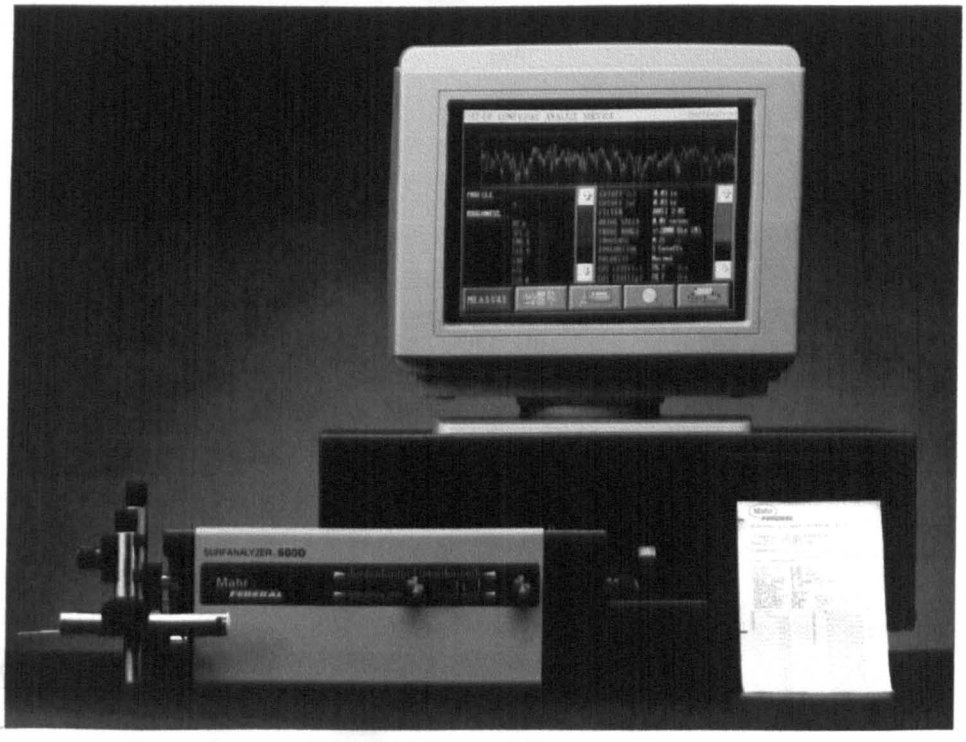

Figure 5.8: Surfanalyzer 5000 profilometer

FEDERAL®

SURFANALYZER 5000 07/15/96 14:13

SAVED AS: (MC100-B)

Company: JJPI

Part: MOM6 INNER SURF. PRE TEST

Operator: MARIE LUNN

TEST CONDITIONS...

CUTOFF (r)	0.080 mm
CUTOFF (w)	0.80 mm
FILTER	50% Gaussian P/C
DRIVE SPEED	0.25 mm/sec
PROBE RANGE	+/-12.5 Um (H)
PROBE RATIO	1:1
EVALUATION	0.56 mm
TRAVERSE	5 Cutoffs
POLARITY	Normal
HORIZ GRAD	0.05 mm/div
VERT SCALE	+/-0.25 Um

HORIZ GRAD	0.05 mm/div
VERT SCALE	+/-0.25 Um
	(0.05 Um/div)

1 div = 1 cm

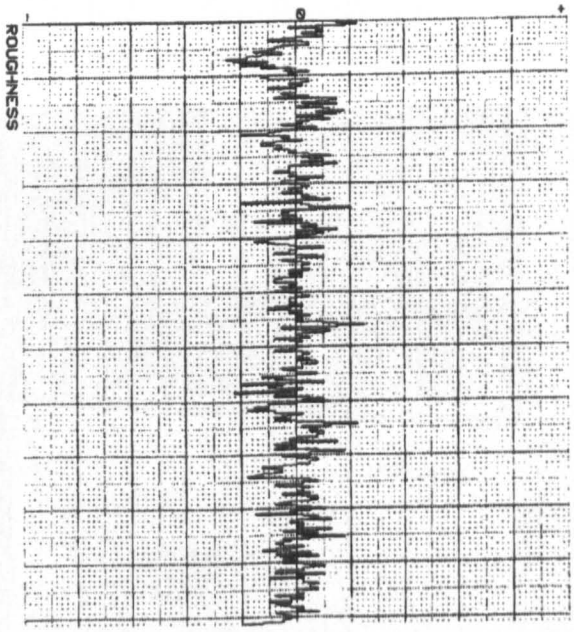

PARAMETER RESULTS...

ROUGHNESS...

Ra	0.014	Um
Rq	0.018	Um
Rz	0.096	Um
Rt	0.12	Um
Rp	0.06	Um
S	11.3	Um
Rsk	0.00	

Figure 5.9: Typical Printout from The Surfanalyzer

Figure shows the input, and output information for the measurement of a metal on metal cup bearing surface. The figure is not to scale.

Figure 5.10: Sartorius balance model MC210S

Figure 5.11: MMED EW12 Hip Simulator

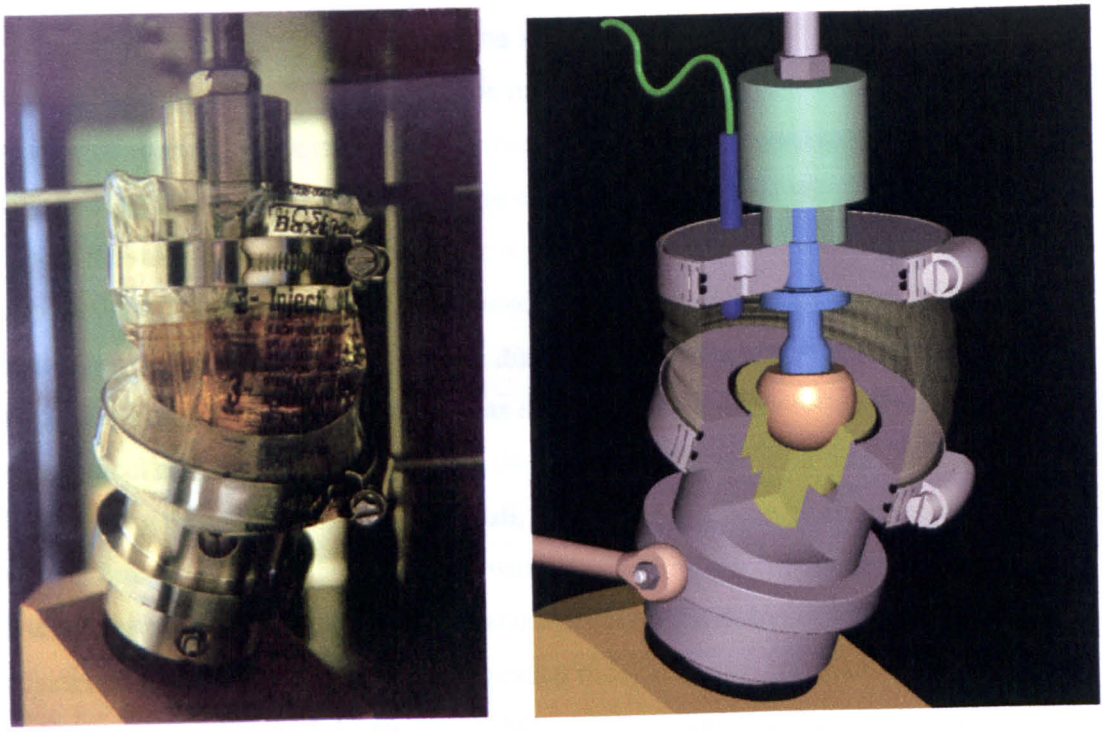

Figure 5.12: MMED EW12 Hip Simulator Station

The arrangement of a single station during a test showing test fixtures and fluid retention. 5.12a (left) shows a photograph of a station during test whilst 5.12b (right) shows a cutaway CAD model of a station clearly showing the internal arrangement.

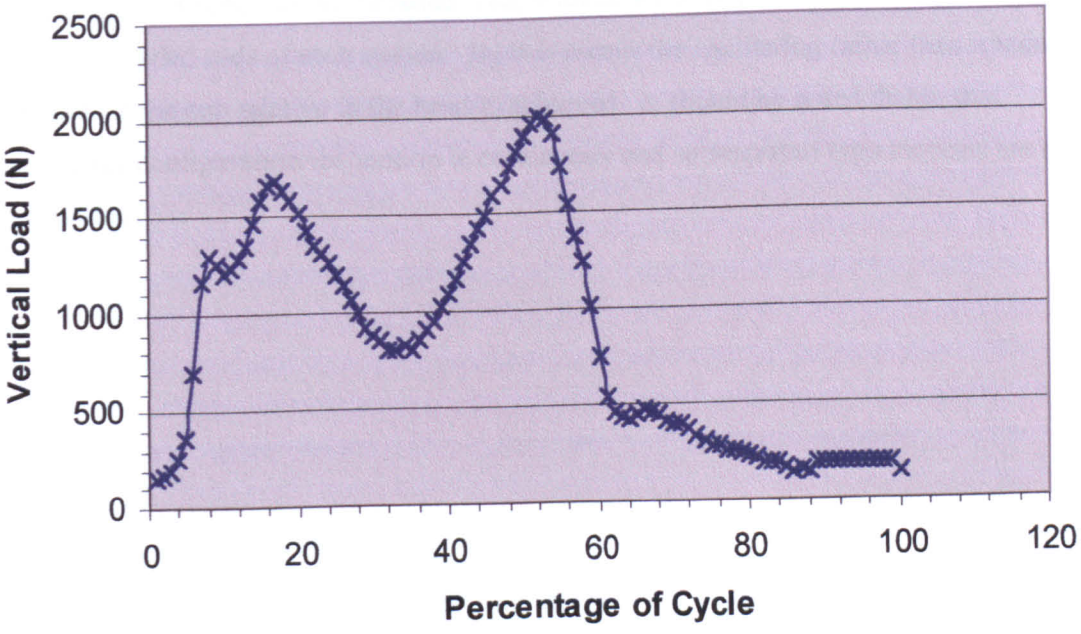

Figure 5.13: Paul walking Cycle

The figure shows the form of the Paul walking cycle used in the study at a peak load of 2000N.

Considering the rotational motions of the simulator, Medley et al (1997) have thoroughly studied the kinematics of the machine and it simply remains to provide a review of some of the design features which achieved the oscillating cup motion. Figure 5.14 shows a CAD representation of the side view of a typical station set up where the main drive for each station was provided directly below the axis of load application of the hydraulic ram. Mounted on this axis of rotation was a drive block with a top surface inclined at 23°. At a distance of 35.6mm from the main drive axis, measured along the inclined surface, was a bearing mounted threaded shaft perpendicular to the inclined face. The distance from the inclined face of the drive block, along the axis of the threaded shaft, to the intersection with the main drive axis was 83.8mm. Onto this threaded shaft was mounted the test cup holding fixture. During the process of aligning the cup and head samples, it was necessary by adjustment of the test fixtures on the threaded rods, to ensure coincidence between head and cup centres. Figure 5.15 shows a CAD representation of a pair of stations to show their relative relationship and the linkage between them. A single station simulator arranged as above would not produce the appropriate relative motion between head and cup. Therefore in the hip simulator each pair of stations is fixed rigidly together by means of a tie rod mounted on bearings at each end and connected to the outside of the test fixtures attached to the threaded rods, with connection pivot point being on the axes of the threaded rods of each station. By this means the oscillating rather than rotational motion of the cup relative to the head is achieved. It should be noted that in this simulator configuration the motion is continuous and so stop/start type motions are not simulated.

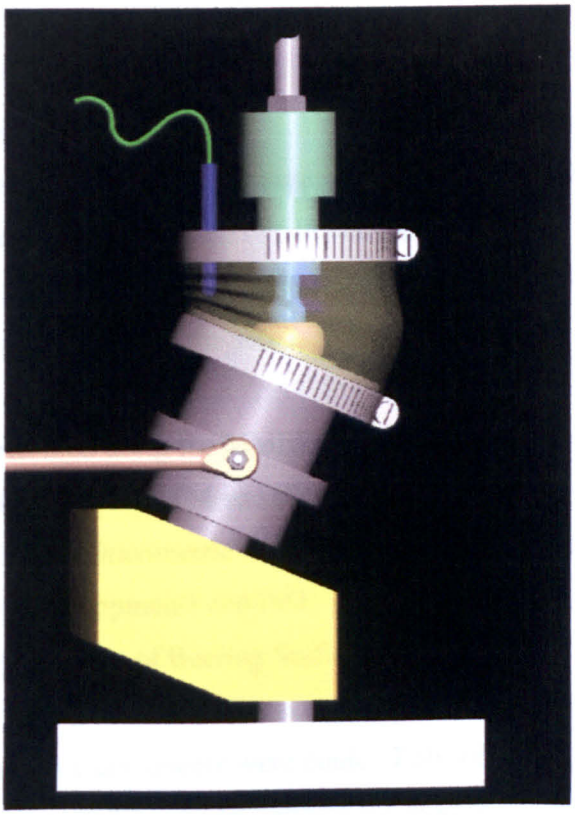

Figure 5.14: MMED EW12 Hip Simulator Station Side View
Figure shows a CAD representation of the side view of a station during test. The geometrical orientation of the parts is clear and the temperature probe can be seen inserted through the lid.

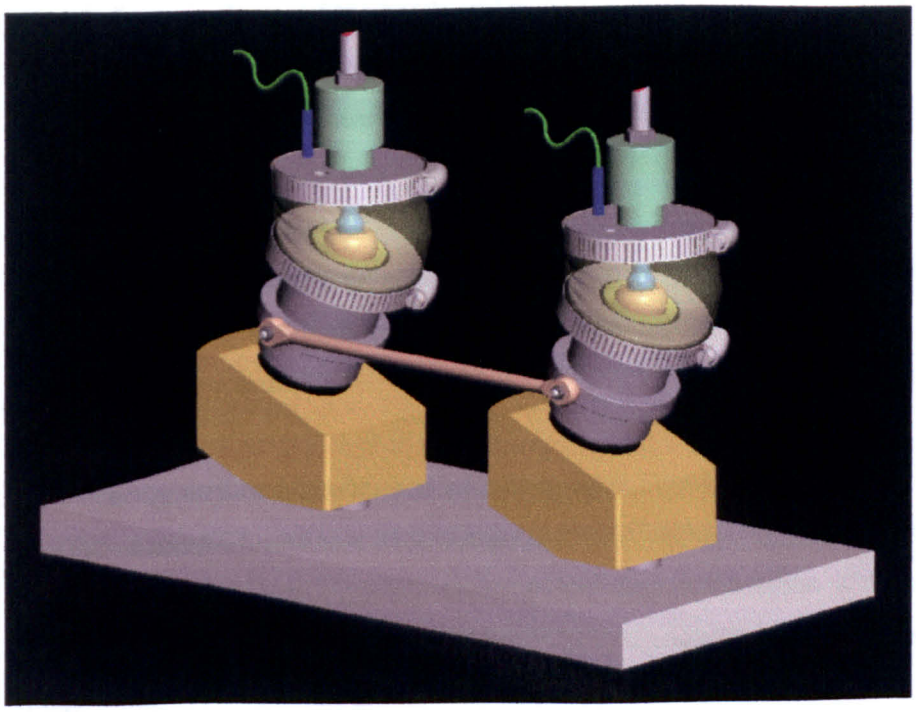

Figure 5.15: MMED EW12 Hip Simulator Station Pair Diagrammatic
Figure shows the arrangement of a pair of stations during a test.

5.4 Methods

The test method including cleaning, hip simulator cycling, and measuring is outlined. Cleaning the specimens was of particular importance due to the necessity on the one hand to remove as much of the build up of adhered calcium phosphate films from the lubricant (Chan et al, 1996) as possible, and on the other hand to ensure that metallic surface layers were not removed in the process.

Wear testing was performed using the MMED EW12 station hip simulator using a methodology based largely on ASTM and ISO guidance documents for simulator wear testing (ASTM: Guide for Gravimetric Wear Assessment of Prosthetic Hip Designs in Simulator Devices (in development) and ISO: ISO/TR 9326 Guide to Laboratory Evaluation of Change of Form of Bearing Surfaces of Hip Joint Prostheses as well as ISO/TR 9325 Guide to Hip Joint Simulators). A number of notable deviations and additions to these guidance documents were made. Reference to figures 5.12, 5.14, and B5.15 a, b, and c may be useful in understanding the assembly of the hip simulator station as discussed below:-

i. The surface roughness of the heads and cups was measured in two locations on the articulating surface using a profilometer equipped with a curve adjusting skid. Traces were taken near the pole in orthogonal directions for the heads and about 5mm from the pole in a radial direction for the cups. Cups were tilted as required to aid measurement. Appropriate traverse length was determined using the five cut-off method (see section on Profilometer and Appendix E) and Guassian filtering and highest resolution possible were used. Ra, Rp, Ry, Rv, and Rsk were measured.

ii. The bearing surface diameter and sphericity were measured on a Mitutoyo BH305 manual Co-ordinate Measuring Machine (CMM). Typically, using the Sphere (SP) command, 13 points were taken in four radial tracks of 3 points each and with each track spaced about 90° from the previous, followed by a final polar point.

iii. Sample weights were measured to ±0.00001g using a Sartorius balance making 3 measurements for each in rotation. Cups were always placed with bearing surface down in the same orientation on the weighing pan. The final value of weight was the mean of the three measured values.

iv. For the cups for all tests except the final design test, special stainless steel fixtures were used to locate them on the simulator. The fixtures were attached to the simulator via a screw thread and the cups located into a close fitting socket and were secured with a set screw against the flat on the cup spigot. Care was taken to ensure that the cups could be aligned and realigned in identical orientation whenever they were assembled onto the simulator. For the final design test the cups (inserts) were assembled via a friction locking taper to titanium shells. These shells were potted into the simulator fixtures such that the cut out notch on each shell lined up with the front to back axis of each station (that is perpendicular to the tie rod joining each pair of stations). URALITE 3177 polyurethane (HB Fuller Company, St. Paul, Minnesota, USA) was used to secure these to the stainless steel simulator fixtures. The inside surface of each shell was protected during the potting process to ensure that no potting media was deposited onto it Using the cut out notch as a guide, the three screw holes in the bottom of each shell were set to the left hand side. An alignment mark was made on each cup. This alignment mark was set to the front of the front to back axis of each station. For the heads, consistent alignment was achieved in a similar manner, with the heads mounted onto special rod fixtures which were in turn mounted into the hip simulator.

Taper surfaces of rods and shells were cleaned by scrubbing with a soft nylon brush and a solution of 1 scoop of Terg-a-zyme (Alconox Inc., 9 East 40th Street New York, New York State, USA) to 1 litre of warm water. These were then thoroughly rinsed and dried using compressed air.

v. Wear was measured on the basis of cumulative head and cup weight loss, which was obtained using the following formula:-

Net weight loss = (Initial insert weight+Initial head weight)-(Interval insert weight +Interval head weight)

vi. Where control samples were used as part of a test, these were assembled in the same way as the simulator samples to replicate any effects of the assembly process on the sample masses. For the final design test, each sample was subjected to a compressive load of 2000N to ensure parts were firmly together. These were then immersed in bovine serum for the duration of the test interval. All subsequent disassembly, cleaning, and weighing procedures were identical for control and tested samples.

vii. Cleaning of components was carried out as follows:-

During and after cleaning, powder free gloves were worn when handling the parts.

During intra test cleaning (ie not done during pre test cleaning) serum residue was removed by rinsing in water. All samples were kept immersed in individual containers of distilled water. Samples were soaked in a solution of 40% v/v glacial acetic acid, 40% v/v nitric acid, and 20% v/v distilled water for 10 minutes. Each sample was in turn removed from the solution, rinsed in tap water, wiped with a Texwipe® (Texwipe Wipers Natural 4"x4", Engineered Fabrics™ for Critical Environments, The Texwipe® Company, Upper Saddle River, New Jersey 07458, USA) and returned to its individual container of fresh distilled water. Where serum film was not removed the process was repeated once more only.

Samples were wiped with a soapy Texwipe®, using a fresh wipe for each and then returned to individual plastic containers and immersed in a solution of Terg-a-zyme (1 scoop) and warm water (1 litre) ensuring that no air was trapped in the concave/internal parts of each sample.

The parts were then sonicated for 30 minutes, rinsed with distilled water, sonicated for 10 minutes in distilled water, rinsed in distilled water, sonicated for

3 further minutes, and once again rinsed in distilled water. A dry nitrogen jet was used to dry each sample before soaking in isopropyl alcohol for a minimum of five minutes and thoroughly drying again with the nitrogen jet. Finally a vacuum desiccator was used for 30 minutes to fully dry the samples making certain that all internal surfaces were exposed to the vacuum.

Test fixtures were cleaned by soaking in a solution of Terg-a-zyme (1 scoop) and warm water (0.5 litre) for 30 minutes followed by scrubbing with a nylon bristled brush as necessary to remove serum residue, rinsed, and air dried. Alternatively the laboratory dishwasher was allowed for the metallic parts provided that parts were placed so that they could not touch during the wash cycle.

viii. Samples were weighed using a Sartorius balance as described in iii. above.

ix. The hip simulator was set up for the tests as follows:-

The cups were aligned in the fixtures as described earlier, and checking that the sample numbers matched with the station numbers were as the predetermined listing. For the tests other than the final design, an O ring was employed to seal around the top outside diameter of the cup. It was permissible to use a small amount of K-Y jelly to lubricate this during the assembly process. Where the set screw was required, this was tightened. The rubber sleeves used to retain the fluid around each sample were now installed using hose clamps to fix to bottom fixture. The femoral heads were press fitted onto the rods aligning the laser marked "C" with the flat on the rod. A second hose clamp was fitted to the sleeve top end but not tightened. The lids were assembled to the rods, aligning the flat surface on the rod with the set screw in the lid and the set screw was then tightened. The rods were then mounted into the upper part of each simulator station, ensuring full insertion of the rods and checking that the correct head is fitted to each station. The lid set screw was positioned to the back and with the anti-rotation arm pushed against the left rear column at each station, the rod set screws were tightened.

The power up sequence for the simulator was initiated in the following way. First the computer was switched on. When the computer display showed the MMED operating screen then the main power to the simulator could be switched on. Finally, the hydraulic pump could be switched on.

The hydraulic rams or pistons were lowered by entering a small negative load value to the simulator via the computer. A value of –200 to –250 N (F5 and enter value) was usual. Due to internal friction it was permissible to lower pistons manually if they did not respond to the input load. Once the pistons were down, each sleeve was stretched around the lid so that it extended over the top surface of the lid evenly, and such that there was still a little slack on the most extended side. The second hose clamp was slid into place over the lid outside diameter and sleeve and tightened to form a solid leak tight joint. Through a small hole in each lid, a quantity of 75ml of fresh filter sterilized bovine serum with preservatives (see xii. below) was added to each station. Through a further hole a temperature probe was added to measure fluid temperature, and the filling hole was plugged.

With a –20N load applied to each station through the computer, the rotational motor was switched on. Alignment of components was checked by observing the motion of the horizontal anti-rotation arms. If the total vertical travel of any arm exceeded 12mm through a full rotation, the motor was turned off and height of the rotating block adjusted. This adjustment was carried out by loosening the clamping screw and then rotating the large central screw under the fixture. Generally 1-2 turns would be considered sufficient to try again. Prior to switching the motor back on the clamping screw was re-tightened. This adjustment was repeated until all stations were properly aligned.

x. The simulator test protocol was as follows:-

The loading curve filename was entered at the computer (CTRL F3 and Curve). For a standard test , the "phip756.dat" curve was used, which simulates the walking cycle for a 77kg individual. A test number of "1" was entered (F2 and Test No) along with the beginning and end cycle numbers, a standard wear test

being from 0 to 2 million cycles. With –150N applied, the rotational motor was once again switched on. The test was started by entering the start command (SHIFT F2 and Start). During the initial cycles of any test it was important to ensure that none of the fixtures worked loose. If any looseness was observed the rotation motor was stopped, the samples realigned as the above procedure, and the clamping screw firmly re tightened prior to restarting the test. If the test was to be run unattended then at the end of each attended period a note was made of the cycle count and machine hours in case of a power interruption during the unattended period. Should any unusual event occur during a test, the information was recorded in a notebook, including station number, date, time, cycle count, and a description of the event. During an uneventful test it was also considered good practice to record daily progress notes by simply stating the date, time, cycle count, and that the test is running without problems.

xi. The tests were conducted with the samples bathed in 75ml of bovine serum. The serum was supplied by Hyclone (Logan, Utah, USA). It was filter sterilized by passing through a 0.2μm filter to remove any unwanted bacteria, crystals and particles of larger size than the filter size. Sodium azide at 0.2% w/v EDTA at and 20 mM were used as preservatives to prolong the life of the serum. These were added to the serum each time a new bottle was thawed and opened as follows.

Distilled water (500ml) was measured out and poured into a glass container. EDTA (37.2 g) was weighed out and added to the distilled water. Sodium azide (10g) was weighed out and added to the solution (Always wear goggles, lab coat or apron, and chemical-resistant gloves when weighing and mixing sodium azide.). With a magnetic stirrer in the container, the solution was stirred thoroughly by placing on a stirrer/hot plate using only very low heat and stirring motion until all powder substance was completely dissolved. Each time a fresh bottle (500 ml) of serum was thawed, 50 ml of this solution was added as preservative. The final concentration of sodium azide and EDTA was approximately 0.2%w/v and 20 mM, respectively (The final sodium azide concentration was 0.2% weight (g)/volume (ml). There were 10 g in 500 ml in the preservative solution which was then diluted 10:1 with the serum. The

EDTA concentration was expressed as millimolar (mM). A 1 molar solution contains 1 mole (or 1 molecular weight)/litre. The molecular weight of the EDTA disodium salt dihydrate used in the tests was 372.24 g. There were 37.2 g in 500 ml of preservative solution, which was then diluted 10:1 with the serum giving 20 millimoles/litre).

As far as possible, each individual test was carried out using serum from the same lot in order to eliminate one possible source of variation. When a new lot had to be used, the composition was matched as closely as possible to the previous lot and all stations were changed to the new lot. Since the analysis of the serum provided calcium and phosphate levels, great care was taken in selecting lots of serum which recorded minimum values for these substances

xii. Serum changes were set to occur at the earlier of, the weighing interval or intervals of 250,000 to 300,000 cycles, with the exact number of cycles being recorded. A siphon was used to remove exhausted serum, being careful to run distilled water through the siphon tube to clean it between stations, in order to prevent cross contamination. The serum was collected in individual plastic bottles labelled with head, cup, and station numbers as well as cycle interval, and stored at -20°C for later analysis. Each station was refilled with 75ml of fresh filter sterilized bovine serum with preservatives prior to restarting the test.

xiii. Weight measurement of the heads and cups was set to be done at approximately 50,000; 100,000; 250,000; 500,000; 1,000,000; 1,500,000; and 2,000,000 cycles. Longer tests such as the final design test were planned to have further measurements at intervals of about 500,000 cycles. The exact cycle number at which each measurement was made was recorded.

The serum was removed from each chamber as described in xii. above, and heads, lids and trunnion rods removed ensuring that the heads remained wetted by storing in individual containers of distilled water. Next the sleeves, hose clamps, and set screw were removed. Using compressed air, the cups were removed from their fixtures. The cups were then cleaned and dried, and weighed using the procedures of viii. and iii. above respectively. The

articulating surfaces of heads and cups were examined visually and any observed changes recorded.

The upper and lower fixtures on each station were cleaned thoroughly with a small amount of detergent and a soft nylon brush. The detergent was removed by repeated rinsing. The fixtures were finally dried with an air jet, swabbed with alcohol, and re dried with the air jet.

The fluid retaining sleeves were discarded at periodic intervals and replaced with new to reduce the chance of a station failure through fluid leakage. The test cups and heads and all fixtures were reassembled to each station as described in x. above including immersion of parts in serum.

Finally, with the rotational motor on and -200N applied, the test was restarted by pressing SHIFT F2.

xiv. At the end of the test the following procedure was followed:-

The rotational motor was turned off and the pistons raised. The final cycle number was recorded. Each station was disassembled and the components cleaned using the procedure outlined in viii above.

The components were cleaned and dried, and then weighed as described in iii. above. Surface roughness was determined using profilometry as described in i. above and size measured as described in ii. above before returning the samples to their original containers for storage.

5.5 Summary

Within this chapter the key elements of materials, equipment, and methods have been discussed. Particular reference has been made to the cobalt chromium alloy materials selected for the study and their source of supply, the microfinishing technology used to create the spherical bearing surfaces, the hip simulator used to carry out the wear

testing, and the analysis equipment used to measure and otherwise interrogate the bearings such as CMM, surface finish tester, and balance.

I was personally responsible for the whole metal on metal development within my company from 1994. My own understanding of the materials used in the study was restricted to the mechanical properties and compositions rather than a detailed knowledge of the metallurgy. The manufacture of the bearing surfaces was done by skilled operators within the New Milton (Johnson and Johnson Professional Products, Stem Lane, New Milton, Hampshire, UK, now transferred to DePuy International Ltd a Johnson and Johnson Company, Leeds, West Yorkshire, UK) facility but I personally developed a significant expertise in the microfinishing process and especially the theory of the way the process is effected. The wear testing was carried out at the Raynham facility (Mary Beth Schmidt, Johnson and Johnson Professional Inc., Raynham, Massachusetts, USA) by Applied Research scientists and technicians. I performed all the analysis and interpretation of the raw data generated in the tests which, through the iterative process of research and development, led to the specification and design of the subsequent tests and ultimately the design and test of the final optimised clinical product. To ensure I understood the simulation process, I spent some time assisting with one of the tests including disassembly of the samples from the simulator, cleaning and weighing of the samples, and re-assembly to the simulator. Surface finish and weight measurements were carried out almost exclusively in the Raynham facility whilst CMM measurements were performed exclusively by myself in New Milton.

CHAPTER 6

Investigation of the Effect of Diametral Clearance on Wear for a 28mm Articulation in a Hip Simulator Test

6.1 Introduction

The theory proposed by Jin, Dowson, and Fisher (1997) and discussed in chapter 4 of this thesis suggested that for a given diameter of metal on metal articulation, operating within a suitable lubricating fluid, the potential for fluid film lubrication to develop between the articulating surfaces increases as the clearance between the surfaces is reduced. As the lubrication regime for the articulation tends towards full fluid film, the contact and, therefore, wear between the articulating surfaces should be reduced due to increasing quality of separation between the surfaces. The following study was therefore carried out to investigate experimentally the relationship between diametral clearance and metal on metal wear for a 28mm diameter head configuration in direct comparison to the theoretical analysis.

6.2 Method

A 12 station MMED hip simulator as described in detail in chapter 4 was used. Samples of 28mm nominal diameter head and cup test pieces covering a range of diametral clearance were tested to about 2 million cycles in bovine serum using the loading curve described by Paul (1967) at a maximum load of 2000N and a frequency of 1.1Hz. The mass of the samples was measured at intervals throughout the test using a balance capable of measuring to 5 decimal places of a gramme. In order to cover the widest possible spectrum of diametral clearance, it was decided to include at one end of the spectrum some negative clearance samples (head larger than the cup) to replicate the effects of the so called "equatorial bearing" designs of the earliest (pre 1970) historical products, and at the other end a clearance of around 0.3mm being the largest clearance felt to be of practical interest and about the value used for metal on polyethylene articulations. This range also embraced the clearance value for a later (post 1970) "polar bearing" historical device, typically of around 0.1mm.

6.3 Materials

For the purposes of this test it was considered that the standard cobalt chromium alloy material used in the manufacture of femoral heads by Johnson and Johnson Orthopaedics would be acceptable for use in metal on metal articulations. This test did not evaluate the material type but focused on the variation of diametral clearance, where all other variables were held as constant as possible. The questions regarding the variation of material type are investigated in chapter 7 of the thesis. Table 6.1 details the relevant information relating to the materials used. All materials were cobalt chromium alloy wrought bar to ASTM F799 (Now ASTM F1537).

6.4 Test Pieces

Twelve samples were prepared for use in the 12 station hip simulator. Due to the expertise in making heads, and the inexperience with the manufacture of cups, the required diametral clearance values were achieved by making the cups as close to 28mm as possible and measuring them. Once an accurate measurement of the cups was obtained, the heads were made to match with the required clearance. It was done in this order because control of head diameter was much better than that for the cups. The polished spherical bearing surfaces were achieved using a special purpose Thielenhaus (Type: KF50F2; No 1.1.002453) microfinishing machine which utilized cylindrical tubular shaped stones for the metal removal process. The machine was equipped with an in process gauging system to enable femoral head diameter to be measured whilst machining with the stage 1 roughing stone. For the subsequent 3 stages up to and including the final polishing stone, control of diameter was only possible indirectly by setting a time limit for the contact of each stone with the workpiece.

	Heads	Cups
Material Designation	CF52 (5760A)	55E11514 (WO5704)
Material Supplier	Teledyne Allvac	Heymark Metals Ltd
Bar Diameter	28.6mm	40mm
Composition (%wt)		
C	.050	.037
S	.0005	.003
Mn	.55	.67
Si	.68	.02
Cr	27.48	27.41
Mo	5.74	6.02
Co	Balance	Balance
Fe	.19	.24
Ni	.07	.12
N	.1885	.22
P		.005
Condition	As rolled	Hot forged, Peeled
Surface	Centreless ground	
Hardness (HRc)	41	
Grain size[1]	ASTM 10 or finer	Less than ASTM 10
Test Pieces		
UTS (MPa)	1343/1327	1313
.2% Yield (MPa)	1046/1048	939
El%	18.8/17.4	29.4 (4xD)
RA%	16.5/15.0	26.5
Hardness (HRc)	42	41.5

[1] ASTM E112, 1996

Table 6.1

Material details for the 28mm variable diametral clearance wear test samples.

Figure 6.1a shows a sectioned assembly of the head and cup. The test pieces were solid in form as described in the cup drawing E02931 part number 655580 (Figure B6.1b). The mating femoral head was a standard 12/14 taper +0 design (Johnson and Johnson Orthopaedics Product Code HO2011-28), except with specially controlled head diameter.

The detailed dimensions of the cup test pieces were determined firstly so that they fitted properly into the test fixture and secondly to maintain the sample mass below a certain critical value such that a more sensitive balance could be used. The need for lowest sample mass was met by use of a hollowed cylindrical spigot at the base of the test cups.

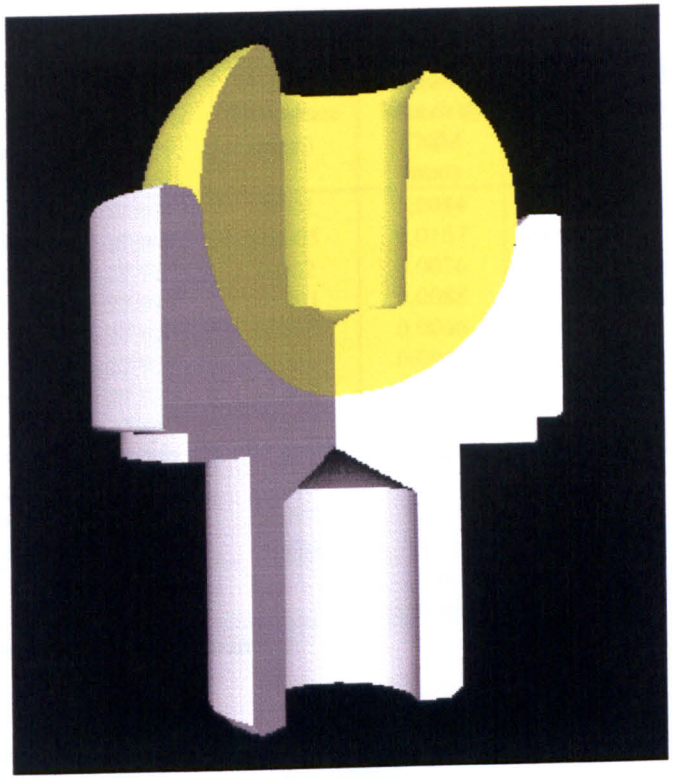

Figure 6.1a: Hip Simulator Test Pieces

Three dimensional cut away model of the hip simulator metal on metal test sample pairings. Note that in the simulator the head would be exactly as illustrated but the cup would be rotated by 22.5° about the head centre.

The complete range of components used are detailed in Table 6.2 along with dimensions of the articulating surfaces. Note the relatively large difference between the CMM and micrometer readings for MH006 and MH011. These are discussed in detail later but are thought to indicate an error in the CMM rather than the micrometer values.

6.5 Pre Test Surface Finish

To complete the pretest geometrical data, a range of surface finish measurements were taken on the heads and cups as Table B6.3. For the heads, two traces were taken, both near the pole and in orthogonal directions. For the cups, again 2 traces were taken per cup at about 5mm from the pole and directly towards the equator.

Head Sample	Head Diameter Micrometer (mm)	Head Diameter CMM (mm)	Diameter Difference (mm)	Head Sphericity CMM (mm)	Cup Sample	Bore Diameter CMM (mm)	Bore Sphericity CMM (mm)
MH005	27.910	27.911	0.001	0.0084	MC005	28.074	0.0051
MH006	27.914	27.909	-0.005	0.0167	MC006	27.955	0.0034
MH007	27.915	27.917	0.002	0.0036	MC007	27.965	0.0039
MH008	27.918	27.917	-0.001	0.0088	MC008	27.836	0.0110
MH009	27.922	27.923	0.001	0.0066	MC009	27.874	0.0015
MH010	27.926	27.929	0.003	0.0067	MC010	27.957	0.0037
MH011	27.930	27.921	-0.009	0.0118	MC011	28.004	0.0030
MH012	27.934	27.937	0.003	0.0068	MC012	28.073	0.0050
MH013	27.939	27.940	0.001	0.0086	MC013	28.047	0.0039
MH014	27.943	27.943	0.000	0.0077	MC014	28.121	0.0029
MH015	27.947	27.948	0.001	0.0084	MC015	28.036	0.0032
MH016	27.948	27.947	-0.001	0.0090	MC016	28.270	0.0038
Master Ball*		Not Available		Not Available	Master Ball*	19.976	0.0029

*Master ball calibrated at 19.9776mm diameter

Table 6.2

Geometrical details of the articulating surfaces for the 28mm variable diametral clearance wear test samples

6.6 Pairing of Test Pieces

The components were matched to give a range of diametral clearance as shown in Table 6.4. It should be noted that within the capability of the processing, between zero and 0.174mm the samples were spaced as close to 0.020mm apart as possible. It should also be noted that because of the discrepancy between some of the pretest head diameters measured on the CMM and with a simple micrometer, as will be discussed in detail later, it was decided that the micrometer measurement was more reliable and so the micrometer size was used to calculate the clearance.

The components were marked so that the same orientation of head and cup could be maintained throughout the test regardless of the number of times they were separated for measurement of wear.

Sample Head	Sample Cup	Diametral Clearance (mm)
MH005	MC008	-0.074
MH006	MC009	-0.040
MH014	MC010	0.014
MH009	MC006	0.033
MH007	MC007	0.050
MH011	MC011	0.074
MH013	MC015	0.097
MH010	MC013	0.121
MH012	MC012	0.139
MH008	MC005	0.156
MH015	MC014	0.174
MH016	MC016	0.322

Table 6.4
Sample heads and cups matched to give required variation of diametral clearance.

6.7 Results

The test was run for 2028204 cycles of the hip simulator in accordance with the test method described previously. Measurements of wear were made as weight loss using the balance at 0; 20,000; 53,110; 107,325; 284,975; 605,010; 1,157,280; 1,609,800 and 2,028,204 cycles. At each interval, prior to weighing, the samples were cleaned by a specially developed process as described fully in chapter 5 and which was aimed at removing any adhered substances on the one hand but not removing any metallic substrate material on the other. It should be noted that during the first simulator testing, including that described in this chapter, the cleaning technique was not fully developed and therefore was not quite as efficient in removal of the adhered surface films as was the case for subsequent testing when the final cleaning procedure was adopted. Chapter 5 describes these cleaning procedures in more detail.

The wear data is summarized in Table B8.5 and total wear is presented in Figures 6.2 and 6.3 as a function of diametral clearance and number of cycles. Figure 6.2 shows the wear curve for each individual sample. It is possible to make out the negative clearance samples which failed completely after only about 20,000 cycles. Note that these samples exhibited the highest wear rate during these first 20,000 cycles. It is also evident that each individual wear curve is composed of two distinct regions: an initial high wear region up to about 500,000 cycles followed by a substantially reduced and relatively

constant wear rate for the rest of the test cycles. The figure also shows that the amount of wear was dependent upon the diametral clearance, and more particularly that the variation in overall wear between the samples was established predominantly during the first 500,000 cycles, after which the wear rates for all surviving samples appear to be about equal. Figures 6.3 show the individual wear curves of Figure 6.2 but three dimensionally which improves the visibility of the data. Figures 6.3a and b are the same except that in Figure 6.3b the negative clearance samples are not represented, the X axis scale is linear, and the Y axis scale has been converted to mm^3. The important message given by Figures 6.3 is that there is clearly a range of diametral clearance within which wear is reduced.

The steady state fluid temperature was measured for each sample pair, except for those with negative clearance, throughout the course of the test and results are shown in Table B6.6 and in Figure 6.4. Each curve in Figure 6.4 is for a constant number of cycles with points on the curve for each sample. It was considered to be important to take the temperatures only after the simulator had done sufficient cycles to have established a reasonable steady state condition. Therefore for each curve, the number of hours operation of the simulator before taking the measurement was recorded.

The post test surface finish results are as shown in Table B6.7. For the heads, two traces were taken, both near the pole and in orthogonal directions. For the cups, again 2 traces were taken per cup at about 5mm from the pole and directly towards the equator. Amongst the data presented in Tables B6.3 and B6.7 perhaps the most important point to note is that all the samples (cups and heads) met the manufacturing requirement for surface finish of 0.05μm Ra both pre and post test with the exception of one post test value of 0.066μm (MH014). In fact, the mean Ra values pre and post test were respectively 0.009μm for heads and 0.014μm for cups, and 0.017μm for heads and 0.012μm for cups.

After completion of the test, all the samples were re-measured using the same CMM as for pre test measurement and the relevant data is presented in Table 6.8. The important data from Table 6.8 are the sphericity values which were, with the exception of MH008

(0.0054mm) and MC008 (0.0143), all within the manufacturing requirement of 0.005mm. Indeed, when considering the pre test roundness values from Table 6.2 it is noted that several of the sphericity values exceeded the manufacturing limit. However, for these measurements, the master ball was either showing relatively high asphericity (cups) or else was not measured, casting some doubt on the accuracy of the pre test sphericity values. Retrospectively it is believed that all these parts were within the 0.005mm limit.

Table 6.9 allows comparison of the diameters of the head and cup samples both pre and post test. For most of the pre and post test measurements, the diameters were within the accuracy of the CMM itself. However MH008, MH015, and MH016 appeared to show a net increase in diameter which may be consistent with wear from the head surface. Also MC008 appeared to have increased in diameter by 0.016mm. The important point to note is that the final diametral clearance values are reasonably close to the starting values in all cases.

It is not unusual for laboratory tests to have certain problems during their execution, particularly where these are carried out over the space of a number of weeks as with hip simulator testing. Table 6.10 details some of the problems which occurred during the course of the test. Where a fluid leak occurred during a test interval showing an unusual increase in wear it has been considered that this increase in wear was a test error phenomenon as opposed to being a real effect. For instance for sample MH012/MC012 (0.139 clearance) in the last interval the wear curve of Figure 6.2 demonstrated a sudden and pronounced increase. Since this was the same interval in which the fluid was lost completely then it was correct to assume that the real wear during this interval would have been the same as calculated by extrapolating the previous two intervals for instance.

Head Sample	Final Head Diameter CMM (mm)	Final Head Sphericity CMM (mm)	Cup Sample	Final Bore Diameter CMM (mm)	Final Bore Sphericity CMM (mm)	Starting Diametral Clearance (mm)
MH005	27.911	0.0030	MC008	27.852	0.0143	-0.074
MH006	27.913	0.0027	MC009	27.871	0.0042	-0.040
MH014	27.943	0.0026	MC010	27.957	0.0014	0.014
MH009	27.923	0.0022	MC006	27.953	0.0015	0.033
MH007	27.917	0.0018	MC007	27.967	0.0042	0.050
MH011	27.930	0.0022	MC011	28.004	0.0030	0.074
MH013	27.941	0.0036	MC015	28.033	0.0028	0.097
MH010	27.926	0.0049	MC013	28.048	0.0023	0.121
MH012	27.935	0.0044	MC012	28.073	0.0010	0.139
MH008	27.922	0.0054	MC005	28.071	0.0023	0.156
MH015	27.950	0.0047	MC014	28.120	0.0027	0.174
MH016	27.957	0.0139	MC016	28.267	0.0034	0.322
Master Ball*	19.976	0.0002	Master Ball*	19.977	0.0019	

*Master ball calibrated at 19.9776mm diameter

Table 6.8

The data of Table 6.2 repeated after completion of the wear test is presented.

Head Sample	Head Diameter (mm)		Reduction in Head Diameter (mm)	Cup Sample	Bore Diameter (mm)		Increase in Bore Diameter (mm)	Diametral Clearance (mm)	
	Initial	Final			Initial	Final		Initial	Final
MH005	27.910	27.911	-0.001	MC008	27.836	27.852	0.016	-0.074	-0.059
MH006	27.914	27.913	0.001	MC009	27.874	27.871	-0.003	-0.040	-0.042
MH014	27.943	27.943	0.000	MC010	27.957	27.957	0.000	0.014	0.014
MH009	27.922	27.923	-0.001	MC006	27.955	27.953	-0.002	0.033	0.030
MH007	27.915	27.917	-0.002	MC007	27.965	27.967	0.002	0.050	0.050
MH011	27.930	27.930	0.000	MC011	28.004	28.004	0.000	0.074	0.074
MH013	27.939	27.941	-0.002	MC015	28.036	28.033	-0.003	0.097	0.092
MH010	27.926	27.926	0.000	MC013	28.047	28.048	0.001	0.121	0.122
MH012	27.934	27.935	-0.001	MC012	28.073	28.073	0.000	0.139	0.138
MH008	27.918	27.922	-0.004	MC005	28.074	28.071	-0.003	0.156	0.149
MH015	27.947	27.950	-0.003	MC014	28.121	28.120	-0.001	0.174	0.170
MH016	27.948	27.957	-0.009	MC016	28.270	28.267	-0.003	0.322	0.310

Table 6.9

Comparison of the articulating surface geometry's pre and post testing

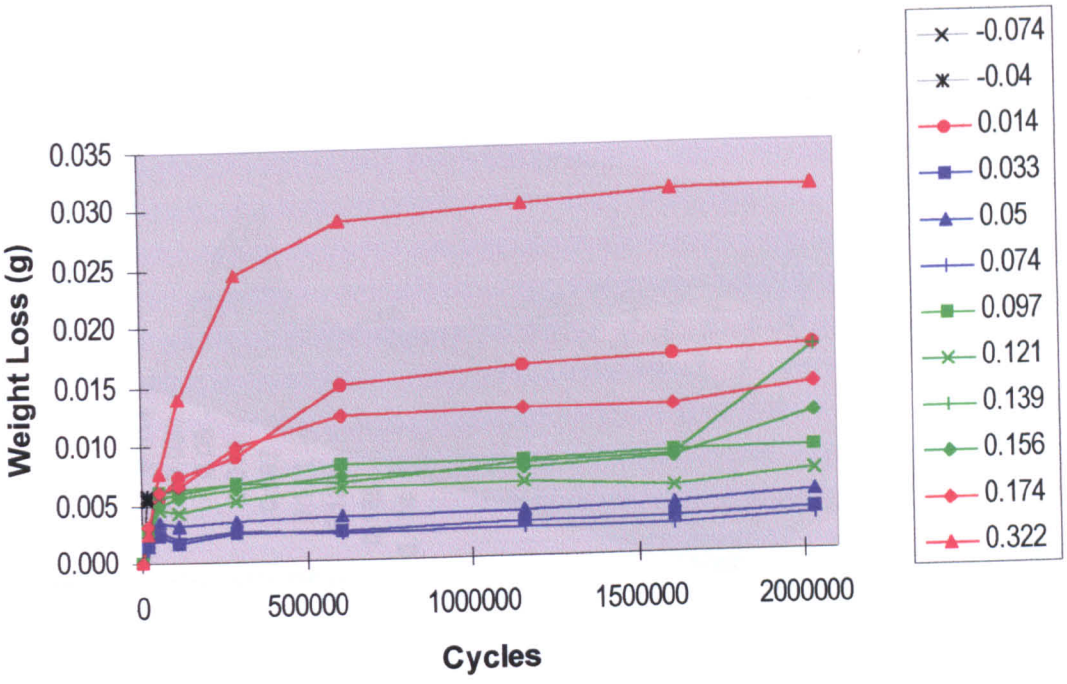

Figure 6.2: Total Wear for 28mm Samples

Figure shows weight loss against number of cycles of the hip simulator for the 12 samples having variation of clearance between head and cup.

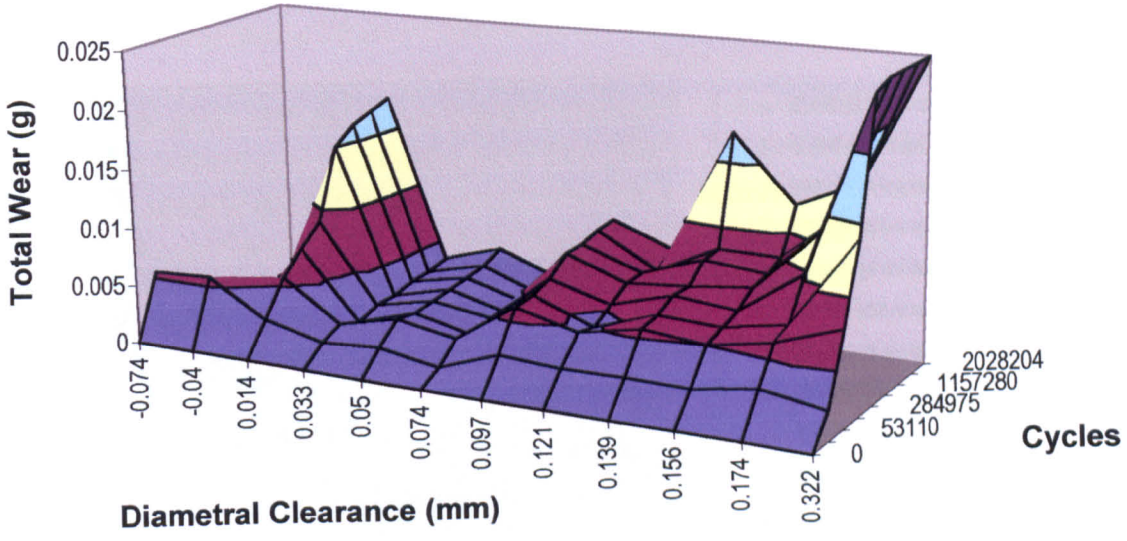

Figure 6.3a: 3 Dimensional Total wear Plot

Figure shows weight loss against number of cycles of the hip simulator for the 12 samples having variation of clearance between head and cup in a three dimensional format which clearly illustrates the lowest wear samples.

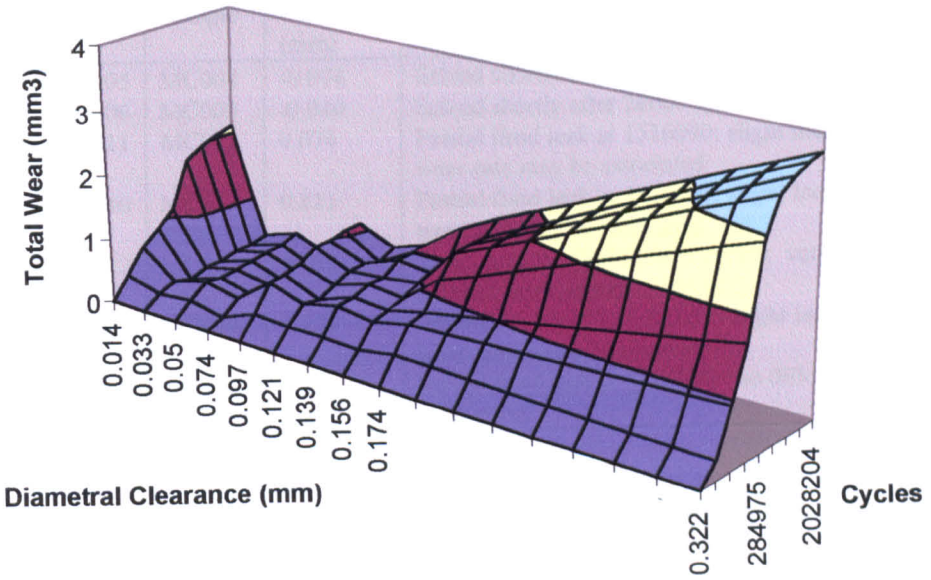

Figure 6.3b: 3 Dimensional Total Wear Plot

Figure shows weight loss against number of cycles of the hip simulator for the 10 samples having variation of positive clearance between head and cup in a three dimensional format which clearly illustrates the lowest wear samples. The X axis is shown to a linear scale.

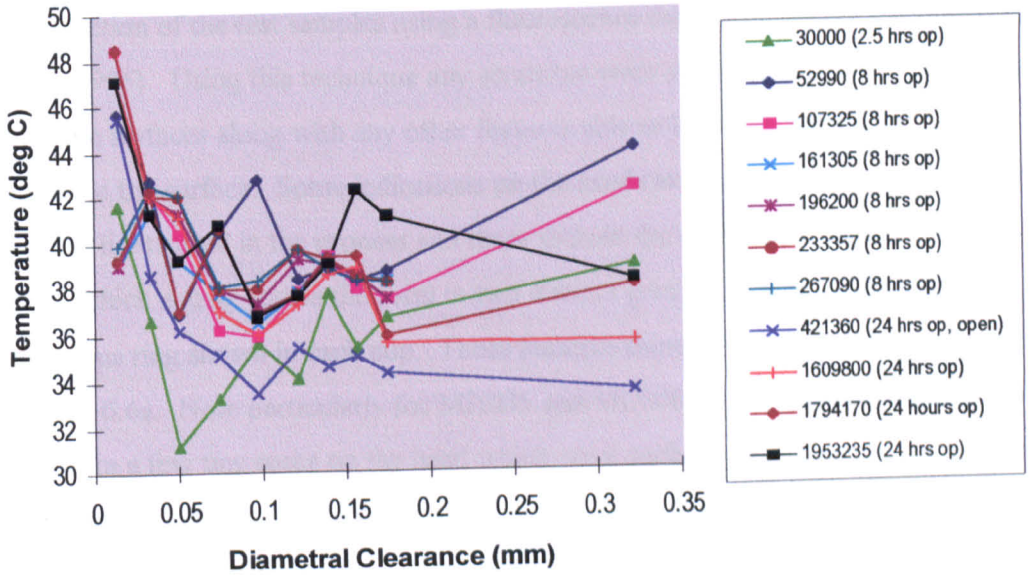

Figure 6.4: Effect of Diametral Clearance on Temperature.

Each curve represents the temperature profile for all samples at a particular number of cycles through the test. The legend indicates the particular number of cycles and for how long the simulator had continuously run prior to taking the temperatures. It was considered that these times were long enough to ensure steady state temperatures were recorded.

Head Sample	Cup Sample	Diametral Clearance (mm)	Test Information
MH005	MC008	-0.074	Seized shortly after 20000 cycles: testing stopped
MH006	MC009	-0.040	Seized shortly after 20000 cycles: testing stopped
MH011	MC011	0.074	Partial fluid leak at 1516090: slight increase in wear rate may be associated
MH010	MC013	0.121	Partial fluid leak at 1516090: slight increase in wear rate may be associated
MH012	MC012	0.139	Total fluid loss at 1850075 cycles: very significant increase in wear rate
MH015	MC014	0.174	Partial fluid leak at 1696650: slight increase in wear rate may be associated
MH016	MC016	0.322	Partial fluid leak at 1516090: no difference to wear curve

Table 6.10
Problems encountered during the simulator wear test.

Table 6.11 details the visual information gleaned from a visual inspection of the head and cup wear surfaces. Of particular note was that for the negative clearance test pieces, equatorial bearing had been achieved by virtue of the fact that both head and cup were unmarked at or near the pole. All the wear was limited to a narrow band close to the equator. Figures 6.5 and 6.6 show respectively the head and cup surfaces looking directly on the pole (represented by location of axis of symmetry on the bearing surface) of a selection of the test samples using a fluorescence marker technique developed by Ward (1996). Using this technique any scratches were shown up clearly on the shiny reflective surfaces along with any other features able to hold the fluorescent material applied to the surface. Some indications on the heads and cups were due to reflections from the lights used in the process and these include the eight thick, straight, short dashes which zigzag across the form in two distinct groups, as well as the bright continuous ring shown in each cup. These features showed up most clearly in Figure 6.5a and 6.6a. Note particularly for MH005 and MC008 (-0.074 mm clearance), that apart from a few tiny spots on the head which were surface contaminants, and one spiral microfinishing mark at 4 o'clock on the cup it was clear that the surfaces were virgin. Note also that on heads Figures 6.5c to f and cups 6.6d and e, a deposit on the surfaces has been left after the cleaning process which should not be confused with wear of the surface.

Figures 6.5b and 6.6b show respectively the head and cup surfaces looking directly on the pole of MH014 and MC010 (0.014 mm clearance). The wear markings were present over the pole area but were much more prominent near to the equator on both head and cup. This was consistent with the very small positive clearance. For the rest of the test pieces, the wear scratches were more pronounced generally toward the pole.

6 8 Discussion

Given the good roundness values obtained post test (Figure 6.8) it is likely that the pre test values (Figure 6.2) are unreliable, particularly for the heads. This may be due to the CMM not being calibrated correctly against the master ball or perhaps dirt on the probe tip. This conclusion is also supported by the fact that the microfinishing process inherently produces parts of high roundness. Further, it is not likely that the simulator testing would improve the roundness of the articulating surfaces since material would be removed from the surfaces in local areas. The true pre test roundness of the heads is probably much closer to the post test values.

The general closeness of the pre and post test diameters from Table 6.9 indicates that these values were accurate (MH016 being the possible exception). However, had the CMM pre test head diameters been used, then four heads would have shown distinct differences between pre and post test values rather than just one. This supports the decision to consider the micrometer head diameter as more reliable in this case and therefore use it as the diameter for subsequent analysis such as calculation of diametral clearances. Whilst the CMM is a three dimensional check of geometry and also should yield information about form, nevertheless it is suspicious for the micrometer value to be different to the CMM value. Furthermore, since the two negative clearance samples left the majority of the bearing surfaces completely unworn, then the post test measurement should have been identical to the pre test measurement. Since the post test measurements were repeated to ensure that they were indeed repeatable, then they are believed to be the most accurate. Therefore in reality it is believed that for the -0.074mm sample, the true diametral clearance for the test was -0.059mm (Table 6.9).

Head Sample	Diametral Clearance (mm)	Description of Surface Appearance
MH005	-0.074	No pole marks, wide band of marks sharply differentiated at base less at pole edge. Wear band looks like half figure of eight.
MH006	-0.040	As above.
MH014	0.014	Wear marks extend close to base with sharp cut off. Figures of eight evident. Light scratches evident all over pole area.
MH009	0.033	As above but wear marks slightly lighter.
MH007	0.050	Light scratching on dome. Narrow band where surface dulled about 45° from pole. A few light scratches near to base.
MH011	0.074	Light scratching at pole with sudden finish at about 22°. Band of very little scratching then giving way to dulled band at about 45° from pole and about 180° of circumference. Finally wide band of light figure of eight scratches ending sharply near base.
MH013	0.097	Light circular pole scratching then at 45° a dulled band all round. Virtually no further scratching closer to pole.
MH010	0.121	As above.
MH012	0.139	Light scratching at pole. Very deep scratching in narrow dulled band at about 30° from pole. Some light fig of eight scratches towards base at one side only.
MH008	0.156	As above but without the deep scratches.
MH015	0.174	As above but without the deep scratches.
MH016	0.322	Light pole scratching and narrow but very distinct dull band all round at about 30°. Some reasonably deep scratching south of dull band in second band around 180° at about 80°.
Cup Sample	Diametral Clearance (mm)	Description of Surface Appearance
MC008	-0.074	Bore completely unmarked except very narrow band at equator.
MC009	-0.040	Ditto with Thielenhaus marks and dark ring in pole.
MC010	0.014	Light scratching over entire surface up to equator but with very lightest shiniest patch right at pole about 10mm diameter.
MC006	0.033	Light scratching over entire surface but densest at 45° and fading slightly towards equator and pole.
MC007	0.050	Light to medium scratching from pole to about 2-4mm short of equator with densest scratching at about 30° fading out to equator.
MC011	0.074	Light scratching from pole to 45° and then virtually nothing to equator where some scratches on 1mm band at rim are apparent.
MC015	0.097	As above but dulled band from equator and about 5-7mm wide.
MC013	0.121	Scratching from pole to rim but fading substantially after 45° from pole.
MC012	0.139	Generally light scratching over entire surface with superposed narrow band of heavy scratching and dulled area at about 45° from pole.
MC005	0.156	Pole dull with a few superposed deep scratches. Fairly agressive scratches over rest of surface apart from 1 patch from 45° out to the equator and about 180° around circumference where surface looks unworn.
MC014	0.174	Fairly aggressive scratches over surface apart from 1 patch from 45° out to the equator and about 90° around circumference where surface looks unworn.
MC016	0.322	Fairly dense but light scratching from pole to 45° then changing in form to short deep scratches running more circumferential up to the equator. One small patch from 45° to the equator and about 90° circumferentially appears to be unworn except for a group of short but deep scratches.

Table 6.11

Information from a post test visual inspection of the wear test heads and cups

Fig 6.5a: MH005 (-.074)

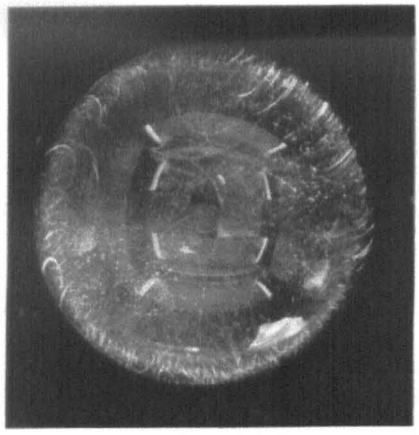

Fig 6.5b: MH014 (0.014)

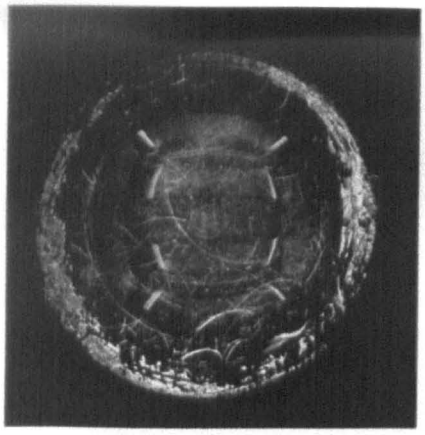

Fig 6.5c: MH007 (0.050)

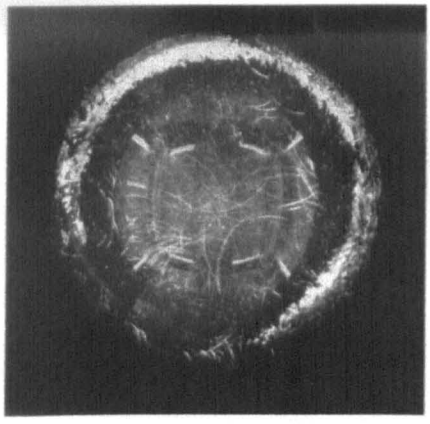

Fig 6.5d: MH011 (0.074)

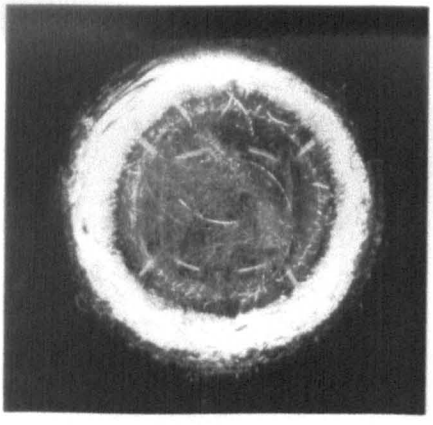

Fig 6.5e: MH010 (0.121)

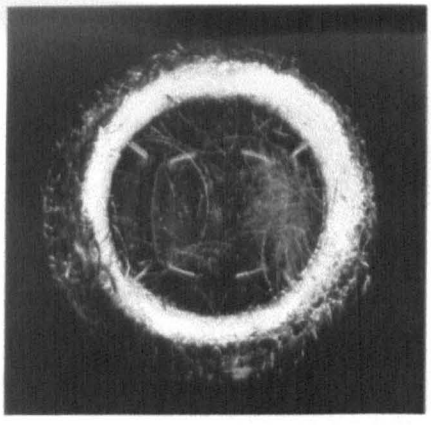

Fig 6.5f: MH016 (0.322)

Figure 6.5: Fluorescing Photographs of Sample Heads

Figure shows a photograph for a selection of the sample heads taken looking directly on the pole. The fluorescence technique allows the condition of the articulating surface to be shown clearly. Heads are identified by head number and diametral clearance.

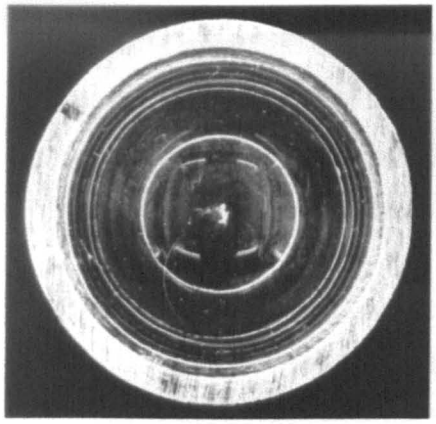

Fig 6.6a: MC008 (-.074)

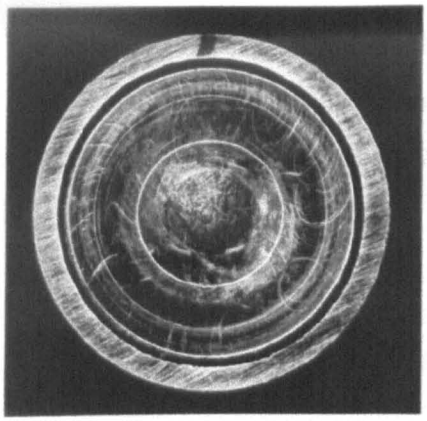

Fig 6.6b: MC010 (0.014)

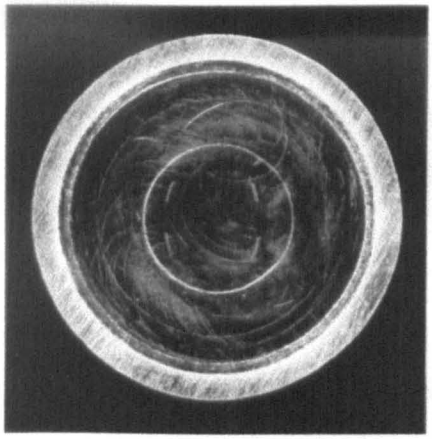

Fig 6.6c: MC007 (0.050)

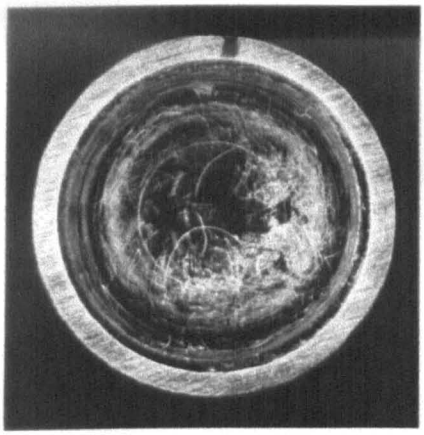

Fig 6.6d: MC011 (0.074)

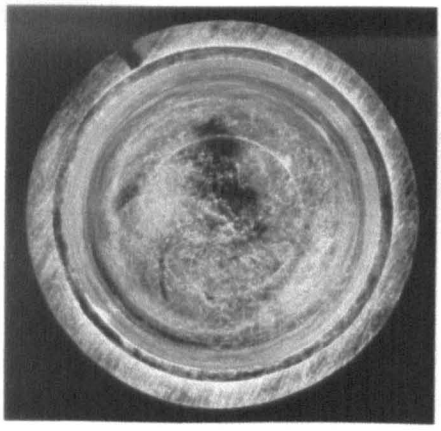

Fig 6.6e: MC013 (0.121)

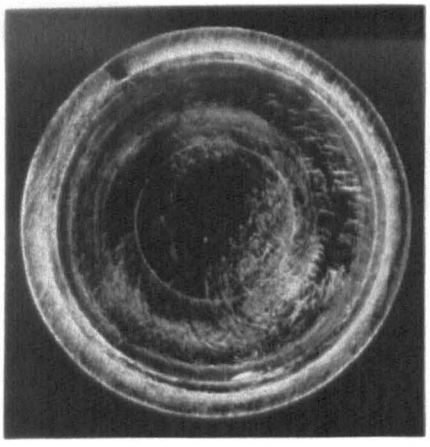

Fig 6.6f: MC016 (0.322)

Figure 6.6: Fluorescing Photographs of Sample Cups

Figure shows a photograph for a selection of the sample cups taken looking directly on the pole. The fluorescence technique allows the condition of the articulating surface to be shown clearly. Cups are identified by cup number and diametral clearance.

The out of roundness error for the cup from this pairing (MC008) also appeared to be large at 0.0143mm (Table 6.8). However, neither the poor roundness nor the lower true negative clearance were believed to change in any way the conclusions which could be drawn from this or any of the sample pairings.

Regarding the surface finish of the parts, in general the visual appearance of the cups was not so good as for the heads. This was because manufacture of cups was new to the company and no reasonable method was available to apply a final polishing operation with for instance a soft cotton mop as was the practice with heads. Hence, on very careful examination it was sometimes possible to see fine superficial Thielenhaus marks spiraling from the equator towards the pole. This may be the reason for the pre test mean cup Ra value being 64% greater than for the heads (Table B6.3). Nevertheless, all pre test Ra values were well within the requirement of N2 or 0.05μm, the highest being 0.03μm for cup MC010.

The visual appearance of the articulating surfaces after the testing (except for the negative clearance samples) was of numerous scratches, some fine and some more pronounced, superimposed on a still shiny surface. It was noted during the testing that this scratched appearance was produced within the first few thousand cycles and once established did not really change. With respect to surface finish (Tables B6.3 and B6.7), the post test Ra values were only about 20% higher than the pretest values. For the heads, all the measures of finish except Rsk showed an increase, which in the case of Rp, Ry, and Rv, was substantial. Since these parameters are measures of maximum values found within the sampling length whereas Ra represents an average for the sample length, then the conclusion is that there exist on the surface relatively few deeper scratches which, whilst not influencing the Ra value due to their sparseness, have an effect on the other parameters since there are sufficient of these to occur at least once within a given sampling length.

The presence of these fewer deeper scratches along with more numerous finer scratches explains the overall visual impression of a scratched surface. It is important to note

though, that such a "scratched" surface impression can be generated by simply taking virgin metal on metal pairs and articulating them under no load by for example spinning the head in the cup. Whilst cobalt chromium alloy is extremely tough and quite hard, a polished surface of such material is marked very easily. Therefore a scratched appearance does not necessarily imply a notable physical difference when compared to a polished appearance on a virgin surface.

These markings in themselves are obviously not a cause of increased wear, since articulating pairs having such scratched appearance at say 1 million cycles, have a significantly lower wear rate than virgin samples starting a test. Indeed, it may be that such networks of scratches on the surface enhance the fluid retaining capacity of the joint and therefore lead directly to lower wear. The idea of manufacturing articulating surfaces with such scratches on is interesting from two viewpoints: firstly it would probably reduce manufacturing costs; and secondly could provide head and cup combinations with reduced overall wear.

Since the scratches were seen to appear within just a few thousand cycles, but reduction of wear rate was typically at about 500,000 cycles, then the creation of an initially scratched surface cannot be the complete answer for the "bedding in" of the articulations. However if one considers that a scratch in cobalt chromium is generally created by the displacement of material rather than its removal, such that a subsurface valley is formed bounded on either side by raised lips as described by Minakawa et al (1997), then subsequent articulations of the surfaces are likely to result in the wearing away of the raised lips. Ultimately this would lead to a scratch comprising just a valley superimposed onto the original surface. It may be that the creation of a surface where the majority of the scratches were of the latter form would take of the order of 500,000 cycles by which time the bedding in phenomenon has occurred and the bearing is beginning to exhibit lower wear. The creation of such a surface in the workshop rather than in the human body may offer some real advantage therefore.

If the bedded in surfaces did consist of such a network of modified scratches then it would be reasonable to expect the post test values of Rsk to be of greater negative value than the pre test values. In fact, and even ignoring the 11.220 figure from MC010,

Tables B6.3 and B6.7 indicate nothing conclusive with similar negative values for pre and post test.

Considering the visual appearance of the samples, a number of observations could be made and discussed. Firstly, it was clear that the negative clearance samples had left significant areas of bearing surface still virgin due to no contact occurring over these regions (Figure 6.5a and 6.6a). Where contact had occurred, this took the form of a narrow annular band on the cup adjacent to the lead in chamfer where very high wear had clearly occurred. For the head, more of the surface had articulated with the cup surface due to the nature of operation of the simulator and the contact geometry. On the head the wear band was constructed of clearly visible half figures of eight (not shown in Figure 6.5a since they were near the equator). This pattern is expected due to the motion of the hip simulator as described by Ramamurti et al (1996).

For the other samples the general impression was that these appeared quite similar, with similar scratch patterns visible from the pole towards the equator on both heads and cups. Some differences were noted however and particularly the fact that cup samples around the lower wear region (MC007, MC011, MC015) appeared to have less scratching beyond about 45° to the pole. Due to the nature of the motion of the simulator it is anticipated that any wear pattern on the heads and cups would be symmetrical about the polar axis and this is borne out visually from Figures 6.5 and 6.6. This symmetry occurred about the cup polar axis even though the polar axis of the cup was inclined on the simulator at 23° to the polar axis of the head. For reasons not entirely clear, the 0.156 (MC005), 0.174 (MC014), and 0.322 (MC016) cups exhibited an unworn area between 45 and 90° from the pole, and between 90 and 180° around the circumference. This may be attributed to a departure of the actual hip simulator performance from true anatomical performance, due to the way the load pattern of the Paul loading cycle is synchronized to the motion, or indeed to the geometrical roundness errors inherent within the pairs of samples.

For the 0.014mm clearance sample head MH014 (Figure 6.5b) there was evidence of head wear taking place from the pole right up past the equator. Well defined figure of

eight markings were clearly evident with a sharply defined cutoff at the edge of contact between the mating surfaces (theoretically 23° beyond the equator). This demonstrates that for this low clearance sample, wear is taking place over most of the articulating surface. This is confirmed by noting that wear scratches were evident over all the cup (MC010) surface. Even with the 0.033mm clearance sample head MH009, the wear pattern was the same but a little lighter beyond the equator. Other samples exhibited some figure of eight wear marks in this region between the equator and the base of the head but all very light compared to MH014.

A band of clearance was defined for a 28mm head within which a metal on metal articulation should exhibit the lowest wear. The reducing wear trend which was exhibited as diametral clearance was decreased from 0.322mm is supported by the lubrication theory proposed by Jin, Dowson and Fisher (1997). However, with further reductions in clearance below the "low wear" band, the reversal of the wear trend represented a departure from the theory. This was thought to be due to geometrical errors which are inevitable with any manufactured part but not present in a theoretical model. Where small clearances approach the order of the cumulative geometrical errors, contacts may develop much closer to the equator, as seen for the small clearance sample MC010/MH014 as described above, and the possibility of a simulated local negative clearance exists. This was first predicted by Walker and Gold (1971) in about 1969 in a study of the geometry of the so called "Equatorial Bearing" or "Lapped In" devices. The authors describe a situation where if a male and female bearing surface are exactly the same size there is no clearance between them. If roundness is perfect this may be a suitable situation. However if geometrical errors of roundness exist it is possible that as relative rotation between the parts occurs, the articulating surfaces may tend to become wedged together and either jam completely or rub and wear excessively and exhibit relatively high friction torque.

It may be therefore that there is a practical lower limit of clearance which would only be lowered further by improvements in bearing sphericity brought about by improved manufacturing techniques. The current lower limit appears to be at around 0.030mm.

It was possible to simulate the effects of so called "Equatorial Bearing" devices such as the pre 1970 McKee-Farrar and Ring prostheses on a hip simulator by having a negative or very low clearance. In this case the negative clearance samples reached about 20,000 cycles, exhibiting the highest wear rate, before seizing completely.

The generally low level of volumetric wear for these metal on metal articulations (0.384 to 3.76mm^3) was in contrast to the much higher mean levels for metal on polyethylene articulations of 19.6mg (20.8mm^3 assuming ρ=940kg/m^3 for UHMWPE) found by Schmidt and Hamilton (1996) under similar test conditions using a calcium stearate free vacuum sterilized material.

It was also noticeable that with the lower clearance samples, head and cup wear results were similar, whilst with increased clearance the head wear was dominant. An explanation for this may be that as clearance increases, the initial conformity between the articulating surfaces is reduced and therefore more wear has to take place in order to produce mating surfaces of the required conformity. Since the head is the convex surface, more material may be worn away from this than from the cup during the bedding in process. Furthermore, due to the set up in the hip simulator, the load is always applied through the same small contact region of the head. The loaded contact region of the cup, in contrast, moves around over a relatively large proportion of the cup surface during each simulator cycle. Therefore, cup wear would be likely to be spread over a larger area than for the head.

Considering wear volume, clearly the volumetric wear which had taken place was detected relatively easily by measurement of mass loss. The CMM procedure however was less efficient in detecting any kind of loss of material from the head or cup surfaces. The CMM method was probably accurate to within only $\pm$1 or 2μm on measurement of diameter. Considering a typical wear from the 0.05mm clearance sample MH007/MC007 of 0.0051g, this represents a total wear volume of 0.612mm^3. Considering the contact region to be 25° either side of the pole then this equates to a total surface wear area of 522mm^2 (407mm^2 for the cup and 115mm^2 for the head). Therefore the total linear wear is estimated at 0.0007mm for the cup and 0.003mm for the head (see details of the derivations and calculations in Appendix C1) . Clearly this

represents a very small amount of wear and possibly too little to be detected by the CMM in terms of change in form of the spherical surface. Clearly it would be easier to detect change in form of the head than the cup since the head appears to have the highest linear wear. This finding is in agreement with the fact that the size and form of the post test samples are not significantly changed from the pre test data.

An alternative method of theoretical calculation of linear penetration from known volumetric wear is presented in Appendix C2 where it was assumed that the mating spheres simply overlapped or intersected until the volume of intersection was the same as the measured wear volume. Then the linear penetration and, very usefully, the radius of the conforming contact patch were calculable.

The most interesting approach to this analysis was to estimate from the actual data for 28mm head diameter, the radius of conforming contact at which the wear rate changed from the higher to the lower value. For the 0.05mm diametral clearance sample (MH007/MC007), this step change occurred at about 107000 cycles when the total volume was 0.0032g or 0.384mm^3. From the theory, for this sample configuration the volumetric wear value would have occurred at a linear penetration of 4.29μm, and a radius of contact patch of 7.279mm. It is assumed that the radius of conforming contact patch at which wear rate switches from the higher "bedding in" wear rate to the lower steady state value, may be a function of head diameter but remains constant with changing diametral clearance. That being so, at the extremes of diametral clearance tested in the 28mm series, the volume of wear at that radius of contact could be estimated. Further, by means of testing this assumption, the sample having the largest clearance (MH016/MC016 having diametral clearance of 0.322mm) was assessed in the same way. Stabilization of the wear curve is estimated to have taken place at 605000 cycles where the wear volume was 0.0289g or 3.468mm^3. Again, from the theory, for this sample configuration the volumetric wear value would have pertained at a linear penetration of 32.9μm, and a radius of contact patch of 7.8mm. Similarly when the 0.174mm clearance sample is taken (MH015/MC014), where stabilization of the wear curve is again seen to occur at about 605000 cycles, the penetration is 15.68μm and the radius to the edge of the conforming contact patch is about 7.44mm. These results

clearly demonstrate the strength of the assumption that the point at which the wear curve stabilizes to a steady state lower wear rate is consistent with the radius of conforming contact reaching a value of between 7.2 and 7.8mm. Theoretically then it would have been possible using these equations and having run just 1 sample of a given head diameter and specific diametral clearance on the hip simulator, to predict the curves for any other diametral clearance.

Considering a simple case with constant head diameter of 28mm and diametral clearances of 0.014, 0.06, and 0.322mm, the theoretical values for the radius of conforming contact patch and wear volume, for each case, are presented in Table C2.1 up to a conforming contact radius of about 7.2mm. Figure 6.7 then shows the same data graphically. From the graph, the sensitivity to wear volume of the starting or basic diametral clearance was very evident. For a large starting or basic diametral clearance, such as 0.322, the volume of wear to reach a steady state lower wear rate is about 5.5 times that for the 0.06mm clearance and about 22 times that for a 0.014mm clearance.

Furthermore it was noted from the wear curves of Figure 6.2 that once steady state wear conditions had pertained in any of the samples, the value of the wear rate was about equal regardless of initial clearance. Therefore, it was concluded that if some manufacturing technique could be applied to the head or cup components (or both) in order to achieve an intimately conforming contact patch of radius around 7 to 7.5mm (for 28mm diameter components) then it may be possible to avoid a great deal of the wear seen on current entirely spherical starting geometry designs. Furthermore, it was noted that since the steady state wear curves of Figure 6.2 had about the same value of wear rate, it may be concluded that the actual starting or basic diametral clearance is not so important and may be made towards the larger end of the spectrum, if this would facilitate ease of manufacture, without impairing wear performance. Such a design of bearing might give the theoretical performance of a bearing with extremely low clearance well below the current practical limits, even when the normal current levels of geometrical errors are present . In the series of test samples reported here, there was no discernible difference in final wear rate for samples ranging from 0.014 to 0.322mm diametral clearance.

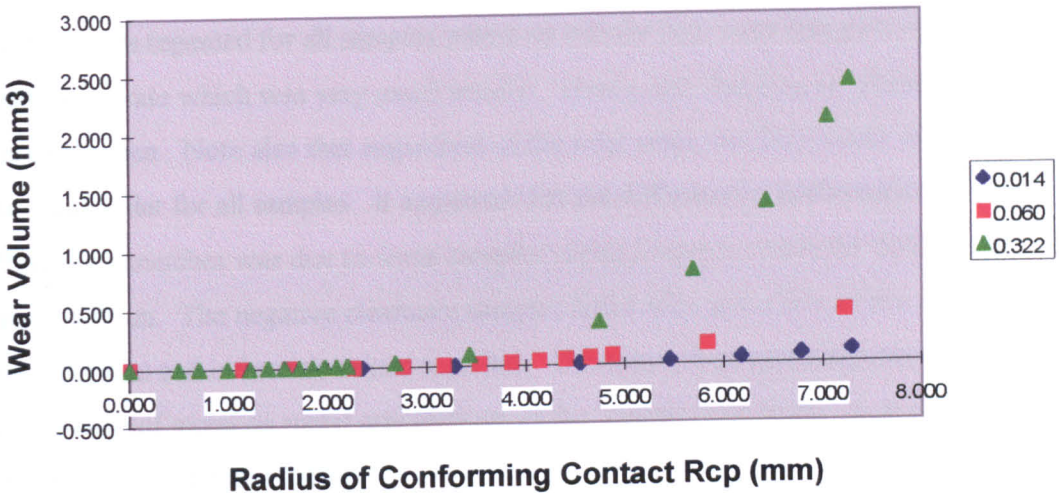

Figure 6.7: Wear Volume Against Contact Radius

Values of wear volume (V) plotted against radius of conforming contact patch (Rcp) for theoretical 28mm head diameter with diametral clearance of 0.014, 0.060, and 0.322mm.

Finally, it is also interesting to note that the theoretical total linear penetrations (at 2 million cycles) consistent with the measured volumetric wear for the various samples ranged from 5.52μm (0.05mm diametral clearance), through 17μm (0.174mm diametral clearance), to 34.4μm (0.322mm diametral clearance).

There was little to conclude from the temperature data except that the samples were maintained at around body temperature throughout the test, though it did appear that temperature increased slightly with the smallest clearances of 0.033mm and below. Perhaps this indicated slightly higher friction for these samples since it may be assumed that friction generally produces heat which would be expected to raise the temperature level of the fluid. However, at this point there was not sufficient distinction between the samples to make serious conclusions based on the temperature data. Furthermore, it could have been that the simulator itself produced heating effects during the test which may have affected certain test stations and therefore samples more than others. The important conclusion to be reached from the temperature data is that it remained reasonably stable throughout the test for all samples at a level of about 38°C.

For the wear data however there were a number of important conclusions which could be reached. The typical wear curve reported by Medley et al (1995 and 1996) and Chan et al (1996) was repeated for all samples where an initially high wear rate gave way to a steady state rate which was very much smaller. Hence, the "bedding in" phenomenon was easily seen. Note also that regardless of the total wear, the final steady state wear rate was similar for all samples. It appeared that the difference in performance between different mismatches was due to some samples taking longer to reach the final steady state condition. The negative clearance samples failed after just a few cycles with very high wear rate and ultimately seized together. This may tell us something about the performance of metal on metal articulations of the "equatorial bearing" type which were implanted up until about 1970.

The samples were segregated into low, medium, and high wear groups according to the total wear at the end of the test but due consideration being taken for higher wear due to fluid leakage from the station with sample at 0.139mm clearance. Considering that this would have worn during the last interval, at the same rate as the previous two or three intervals, then it could be argued that this would have represented a medium wear sample. Fig 6.8 takes the "low" wear samples and shows the curves with expanded vertical axis, enabling the steady state wear rate to be seen more easily and indicating some distinction between the curves in terms of performance. However, at this level of wear it was not easy to separate experimental error and expected variation from true trends. The conclusion here is that there was no significant difference between these samples, at least at the 2 million cycle level.

Regarding the bedding in phenomenon, it could be postulated that this could be due to a combination of three factors which together improve the lubrication regime and or the wear resistance of the material. Firstly, it is possible that the network of surface scratches, once the raised lips have been worn away, create a better lubrication environment for the articulation. Secondly, the articulation under load may work harden the contact regions of one or both surfaces and therefore result in a more wear resistant couple. Thirdly, the very slight change in form which takes place as a result of the loss of material in the first 500,000 cycles produces a geometrical situation where an improved lubrication regime may pertain. If this phenomenon could be more properly

understood then a further step reduction in metal on metal wear couples could be possible.

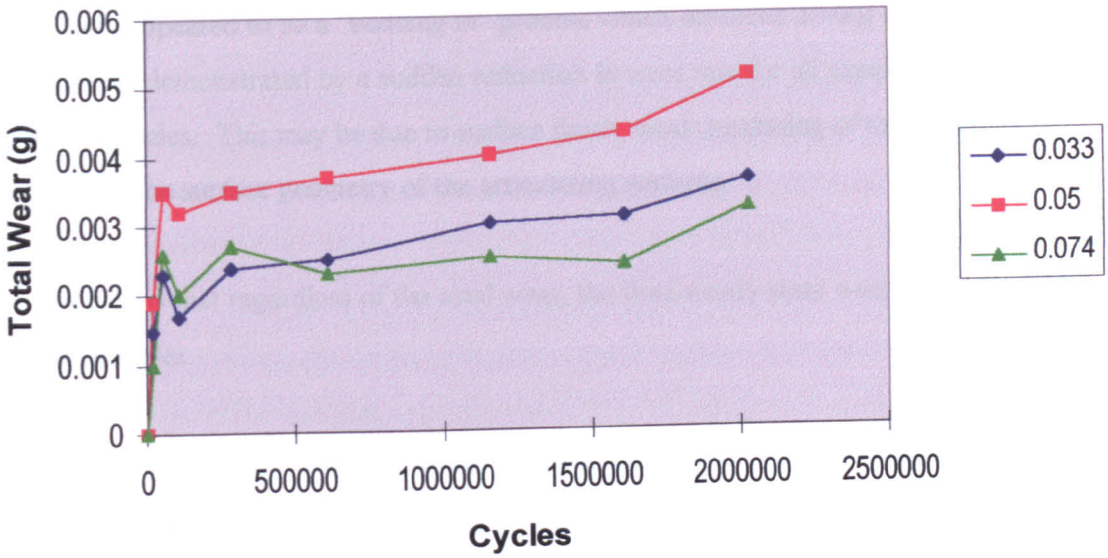

Figure 6.8: Replication of the "Low Wear" Samples of Figure 6.2.
In order to see on a larger vertical scale how the lowest wear samples performed, these are shown in isolation.

The performance of the samples through the test was demonstrated very clearly using a 3D plot as Figure 6.3. Here the "valley" created by the low wear samples flanked by the higher wear samples gave some initial indication of the preferred band of operating clearance which should be aimed at in a metal on metal design and points therefore to the required tightness of manufacturing tolerance.

6.9 Conclusions

a. There may be a practical lower limit of diametral clearance which would only be lowered further by improvements in bearing sphericity brought about by improved manufacturing techniques. The current lower limit appears to be at around 0.030mm.

b. There appeared to be a "bedding in" process which occurred during the wear test which was demonstrated by a sudden reduction in wear rate for all samples after about 500,000 cycles. This may be due to surface finish, work hardening of the materials, or change of the surface geometry of the articulating surfaces.

c. Note also that regardless of the total wear, the final steady state wear rate was similar for all samples.

d. A band of clearance was defined for a 28mm head within which a metal on metal articulation appeared to exhibit the lowest wear.

e. It was possible to simulate the effects of so called "Equatorial Bearing" devices such as the pre 1970 McKee-Farrar and Ring prostheses on a hip simulator by having a negative or very low clearance.

f. The generally low level of volumetric wear for these metal on metal articulations (0.384 to 3.76mm^3) was in contrast to the much higher mean levels for metal on ultra high molecular weight polyethylene articulations of 20.8mm^3 found under similar test conditions.

g. The linear wear estimate for a sample in the low wear region of diametral clearance is 0.0007mm for the cup and 0.0030mm for the head calculated by a simple technique (Appendix C1), and around 5.52μm when calculated by a more complex technique (Appendix C2).

h. At the end of the "bedding in" phase of wear, the radius of conforming contact patch is calculated at between about 7.2 and 7.8mm for all samples. This provides useful

information for assessing the optimum non spherical starting geometry which might be used in order to produce bearing pairs which would eliminate initial wear phase.

i. The volume of wear during the "bedding in" phase was estimated for the largest clearance tested at 5.5 times that for a .06mm clearance and 22 times that for a 0.014mm clearance.

j. Since the steady state wear rate for all samples was around the same, then this indicates that in producing a non spherical starting geometry, the basic spherical diametral clearance is not important from a wear point of view and could be made quite large for manufacturing purposes without affecting the wear performance of the bearing.

k. Temperature effects due to friction within the articulation were observed to be just sufficient to raise the fluid temperature to around 38°C which was acceptable for the test.

CHAPTER 7

Investigation of the Effect of Material Composition on Wear in a Hip Simulator Test

7.1 Introduction

Chapter 6 of this thesis demonstrated that for a given articulation diameter, in this case 28mm, the diametral clearance could be selected so that wear volume during simulator testing was effectively minimized. However, this testing had so far ignored the possible effects on wear performance of variation of articulation diameter or of the composition of the material. Having established a diametral clearance which should yield a minimized volumetric wear during testing, it was possible to hold that clearance as a constant and vary the type of material in order to assess whether any particular combination of materials was preferred.

Schmidt et al (1996) had presented data from unidirectional pin on disc testing which appeared to demonstrate that the best combination of materials was a high carbon against high carbon content cobalt chromium alloy. High carbon was considered to be above say 0.18% where the normal alloys contained about 0.05% and were therefore designated as low carbon. It should be stated that both high and low carbon materials tested conformed with the requirements of ASTM F1537 (formerly ASTM F799) which allows up to 0.35% carbon. Figure 7.1 replicates the results shown by Schmidt et al (1996) and clearly demonstrates a great contrast between the performances of these alloys when paired like against like.

The following study was therefore carried out to investigate experimentally the effect on wear of combining heads and cups of different carbon contents using 28mm nominal diameter bearing couples. The aim was to determine whether the results obtained by Schmidt et al (1996) on the simple pin on disc apparatus could be replicated using a hip simulator. The use of the hip simulator would increase the cost and length of the experiment but was considered to be superior to pin on disc testing. This superiority was assumed in that the tribological environment created using the hip simulator would

almost certainly be closer to that of a metal on metal device in vivo than a pin on disc machine due to the geometry of the hip simulator specimens being almost identical to a clinical metal on metal device. Furthermore, as an extension of the work of Schmidt et al (1996) it was proposed to test a further hypothesis that high carbon against low carbon content materials might also perform well.

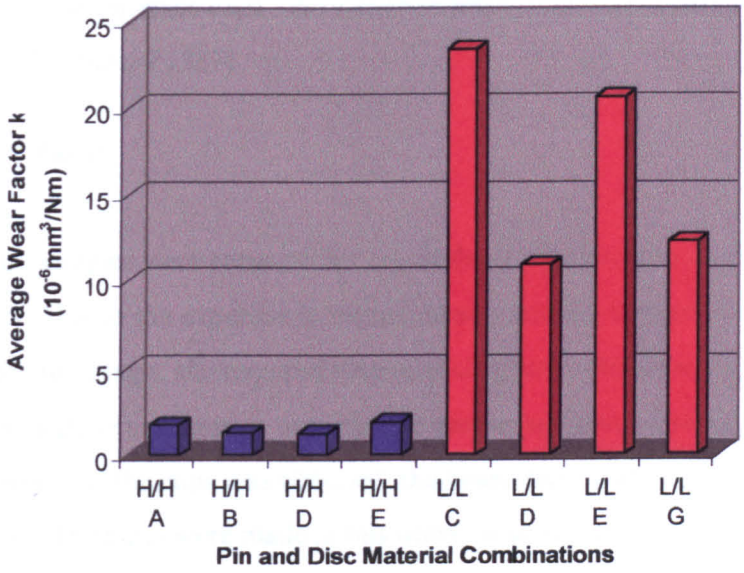

Figure 7.1: Pin on Disc Test Results

Test results for metal on metal pin on disc testing as presented by Schmidt et al (1996) as evidence that metal on metal spherical bearing pairings should be designed and manufactured using high against high carbon materials. Materials A to G represent CoCrMo alloys from different manufacturers. H/H represents high carbon content (0.20-0.30%) and L/L low carbon content (0.05-0.08%) combinations. Material A is cast and B to G are hot rolled.

7.2 Method

A 12 station MMED hip simulator as described in detail in chapter 5 was used. Samples of 28mm nominal diameter head and cup test pieces were selected to have diametral clearance as close to 50μm as possible. The test samples were manufactured in different combinations of high and low carbon cobalt chromium alloy which were tested to about 2 million cycles in bovine serum using the loading curve described by Paul (1967) at a maximum load of 2000N and a frequency of 1.1Hz. The mass of the samples was measured at intervals throughout the test using a balance capable of measuring to 10^{-5} gramme.

7.3 Materials

For the purposes of this test it was considered that the standard cobalt chromium alloy material used in the manufacture of femoral heads by Johnson and Johnson Orthopaedics would be acceptable for use as the low carbon material to be tested. The high carbon material was acquired specially for the testing. Table 7.1 details the relevant information relating to the materials used. All materials were cobalt chromium alloy wrought bar to ASTM F799 (now F1537)

7.4 Test Pieces

Thirty six samples were prepared for use in three separate tests on the 12 station hip simulator. Due to the expertise in making heads, and the inexperience with the manufacture of cups, the required diametral clearance values were achieved by making the cups as close to 28mm as possible and measuring them. Once an accurate measurement of the cups was obtained, the heads were made to match with the required clearance. The parts were made in this order because control of head diameter was much better than that for the cups. The polished spherical bearing surfaces were achieved using a special purpose Thielenhaus (Type: KF50F2; No 1.1.002453) microfinishing machine which utilized cylindrical tubular shaped stones for the metal removal process. The machine was equipped with an in process gauging system to enable femoral head diameter to be measured whilst machining with the stage 1 roughing stone. For the subsequent 3 stages up to and including the final polishing stone, control of diameter was only possible indirectly by setting a time limit for the contact of each stone with the workpiece.

Fig 6.1a shows a sectioned assembly of the head and cup. The test pieces were solid in form as described in the cup drawing E02931 part number 655580 (Figure B6.1b). The mating femoral head was a standard 12/14 taper +0 design (Johnson and Johnson

Material Designation	VN87	VM12	VN07	EG68 (9017A)	ED96	CJ53 (6376A)	55E11514 (WO5704)
Used to Make	Heads and Cups	Heads	Heads and Cups	Heads	Cups	Heads	Cups
Material Designation on Carbon Content	High	High	High	Low	Low	Low	Low
Material Supplier	Teledyne Allvac	Teledyne Allvac	Teledyne Allvac	Teledyne Allvac	Teledyne Allvac	Teledyne Allvac	Heymark Metals Ltd
Bar Diameter	43mm	28.6mm	43.2mm	28.6mm	44.5mm	28.6mm	40mm
Composition	(%wt)						
C	.197	.223	.235	.05	.055	.055	.037
S		.0004	.0006		.0006	.0004	.003
Mn	.73	.90	.55	.53	.62	.63	.67
Si	.09	.65	.73	.58	.68	.67	.02
Cr	26.99	27.56	27.66	27.66	27.74	27.47	27.41
Mo	5.55	5.69	5.70	5.71	5.76	5.64	6.02
Co	Balance	Balance	Balance	Balance	Balance	Balance	Balance
Ti		.01	.01				
Fe	.12	.17	.18	.38	.28	.16	.24
Ni	.49	.39	.02	.31	.01	.03	.12
N	.0962	.177	.177	.18	.178	.165	.22
P		.001	.001				.005
W		.01	.01				
Condtion	As rolled	As rolled	1135°C, 30 mins, WQ	As rolled	As rolled	As rolled	Hot Forged, Peeled
Surface	Centre--less ground	Centre--less ground	Centre--less ground	Centre--less ground	Centre--less ground	Centre--less ground	
Hardness (HRc)	43/45	N/A	34/41		39	39	
Grain Size[1]	Avg ASTM 10	N/A	Avg ASTM 8	Avg ASTM 12.5	Avg ASTM 10	Avg ASTM 10	Less than ASTM 10
Test Pieces							
UTS (MPa)	1221/1260	1339/1332	1301/1278	1349/1358	1278/1287	1324/1356	1313
0.2% Yield (MPa)	907/963	1049/1046	815/798	1047/1045	841/838	1041/1044	939
El%	17.5/17.2	11.4/10.5	20/19.4	21.2/21.9	38.6/29.6	18/22	29.4 (4xD)
RA%	11.9/13.1	10.2/10.1	16.8	18.8	24.1	16.7/20.2	26.5
Hardness (HRc)	42	45	40	42	39	44	41.5

[1] ASTM E112, 1996

Table 7.1

Material details for the 28mm variable carbon content wear test samples.

Orthopaedics Product Code HO2011-28), except with specially controlled head diameter.

The detailed dimensions of the cup test pieces were determined firstly so that they fitted properly into the test fixture and secondly to maintain the sample mass below a certain critical value such that a more sensitive balance could be used. The need for lowest sample mass was met by use of a hollowed cylindrical spigot at the base of the test cups shown in Figure 6.1a.

The complete range of components used are detailed in Table 7.2 along with the materials and the dimensions of the articulating surfaces. Thirty six test samples were manufactured for test because it was felt that this number would be required in order to have any chance of showing a statistical difference between the performance of these samples. Therefore three simulator runs would be required in order to yield 36 test results. This number would also allow for a small number of samples which would not reach the end of the test.

All the components were marked so that the same orientation of head and cup could be maintained throughout the test regardless of the number of times they were separated for measurement of wear.

7.5 Pre Test Surface Finish

The pre test surface finish data is not shown for these parts as it was considered to be similar to the data shown in chapter 6, with typical Ra values around 0.01μm.

7.6 Results

The tests 1, 2, and 3 were run for 2036820, 2020822, and 2000410 cycles of the hip simulator respectively in accordance with the test method described previously. Measurements of wear were made as weight loss using the balance at suitable intervals throughout the test and as shown in Table B7.3a, b, and c. At each interval, prior to

Head/Cup Sample Number MH/MC and Carbon Content H/C	Material Carbon Content and Designation		Head Measurement CMM (mm)		Bore Measurement CMM (mm)		Diametral Clearance (mm)	Test Run No.
	Head	Cup	Diameter	Sphericity	Diameter	Sphericity		
17 H/H	VM12	VN07	27.930[2]	N/A	27.979	0.0083	0.049	1
18 H/H	VM12	VN07	27.939[2]	N/A	27.987	0.0059	0.048	1
19 H/L	VM12	55E11514	27.939[2]	N/A	27.990	0.0023	0.051	1
20 H/L	VM12	55E11514	27.944[2]	N/A	27.997	0.0035	0.053	1
21 H/H	VN07	VN07	27.935[2]	N/A	27.988	0.0024	0.053	1
22 H/H	VN07	VN07	27.938[2]	N/A	27.992	0.0041	0.054	1
23 H/L	VN07	55E11514	27.938[2]	N/A	27.988	0.0063	0.050	1
24 H/L	VN07	55E11514	27.959[2]	N/A	28.014	0.0046	0.055	1
25 L/H	CJ53	VN07	27.936[2]	N/A	27.986	0.0045	0.050	1
26 L/H	CJ53	VN07	27.937[2]	N/A	27.988	0.0023	0.051	1
27 L/L	CJ53	55E11514	27.943[2]	N/A	27.998	0.0030	0.055	1
28 L/L	CJ53	55E11514	27.996[2]	N/A	28.051	0.0027	0.055	1
Master Ball[1]			N/A	N/A	N/A	N/A		
60 L/H	EG68	VN87	28.028	0.0032	28.077	0.0017	0.049	2
61 L/H	EG68	VN87	27.989	0.0033	28.042	0.0027	0.053	2
62 L/H	EG68	VN87	28.006	0.0031	28.053	0.0023	0.047	2
63 L/H	EG68	VN87	28.038	0.0026	28.086	0.0053	0.048	2
64 L/H	EG68	VN87	28.010	0.0023	28.060	0.0022	0.050	3
65 L/H	EG68	VN87	28.024	0.0020	28.075	0.0020	0.051	3
66 L/H	EG68	VN87	28.077	0.0024	28.129	0.0041	0.052	3
67 L/H	EG68	VN87	28.054	0.0019	28.101	0.0034	0.047	3
68 H/H	VN87	VN87	28.026	0.0032	28.071	0.0033	0.045	2
69 H/H	VN87	VN87	28.019	0.0035	28.069	0.0030	0.050	2
70 H/H	VN87	VN87	28.040	0.0065	28.092	0.0042	0.052	2
71 H/H	VN87	VN87	28.032	0.0030	28.081	0.0047	0.049	2
72 H/H	VN87	VN87	28.025	0.0028	28.071	0.0041	0.046	3
73 H/H	VN87	VN87	28.021	0.0025	28.069	0.0046	0.048	3
74 H/H	VN87	VN87	28.004	0.0015	28.052	0.0020	0.048	3
75 H/H	VN87	VN87	28.042	0.0070	28.087	0.0048	0.045	N/A[3]
76 L/L	EG68	ED96	28.102	0.0045	28.148	0.0023	0.046	2
77 L/L	EG68	ED96	28.026	0.0012	28.076	0.0032	0.050	2
78 L/L	EG68	ED96	28.060	0.0025	28.109	0.0012	0.049	3
79 L/L	EG68	ED96	28.375	0.0037	28.420	0.0044	0.045	3
80 H/L	VN87	ED96	28.223	0.0013	28.270	0.0048	0.047	2
81 H/L	VN87	ED96	28.107	0.0055	28.154	0.0048	0.047	2
82 H/L	VN87	ED96	28.226	0.0023	28.270	0.0049	0.044	3
83 H/L	VN87	ED96	28.124	0.0017	28.171	0.0048	0.047	3
84 H/L	VN87	ED96	28.061	0.0041	28.105	0.0020	0.044	3
Master Ball[1]			19.976	0.0005	N/A	N/A		

[1]Master ball calibrated at 19.9776mm diameter
[2]Measured with micrometer and not CMM
[3]Not Tested

Table 7.2

Material and geometrical bearing surface details of the test piece samples for the 28mm variable carbon content wear test samples including detail of simulator run number.

weighing, the samples were cleaned by a specially developed process as described fully in chapter 5 and which was aimed at removing any adhered substances on the one hand but not removing any metallic substrate material on the other.

The wear data is summarized in Tables B7.3a, b, and c and total wear presented in Figures 7.2a, b, and c. Figures 7.2 show the wear curve for each individual sample but Figures 7.3a, b, and c show as bar charts the final wear results at the end of each test (note that sample MH/MC079 was left out of Figures 7.3 since it was considered to be a rogue sample with high wear attributed to a test error). Figures 7.3d, e, and f show the sum total of wear at the end of the tests when all test pieces were added according to material type, with 7.3f being the final situation when the 3 optimum clearance specimens of Chapter 6 were added in to the low/low carbon content group (MH009/MC006, MH/MC007, MH/MC011). These samples had wear curves as shown in Figure 6.8. Since the tests all concluded within ±1% of the same number of cycles it was considered acceptable to directly compare the final wear numbers for all three tests without significant error. The data for Figures 7.3 is shown in tables B7.4a, b, c, d, e and f where Appendix C3 details the method for performing the statistical calculations according to Greer (1988).

Note that in Figures 7.2, the bedding in phenomenon, where initially high wear gives way to a much lower steady state wear was visible, albeit somewhat less distinctly in test 1 (Figure 7.2a).

After completion of the tests, the samples were re-measured using the same CMM as for the pre-test measurements and the relevant data is presented in Table 7.5. Table 7.6 compares pre and post test diameters and clearances for each sample.

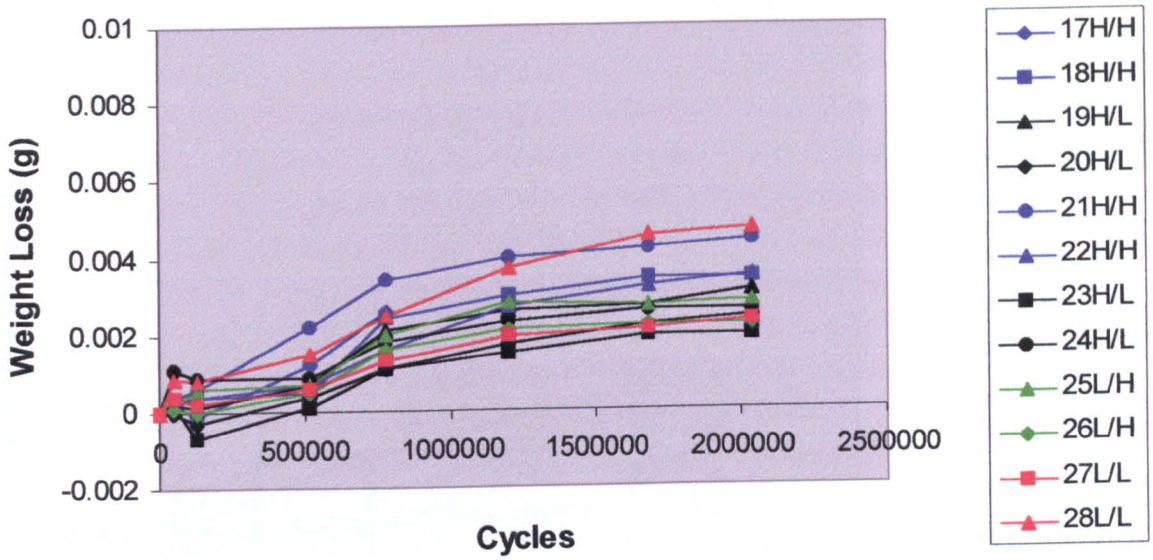

Figure 7.2a: Total Wear for 28mm Variable Carbon Content Samples (Test 1)
Figure shows weight loss against number of cycles of the hip simulator for the 28mm variable carbon content wear test samples for the first of three such tests.

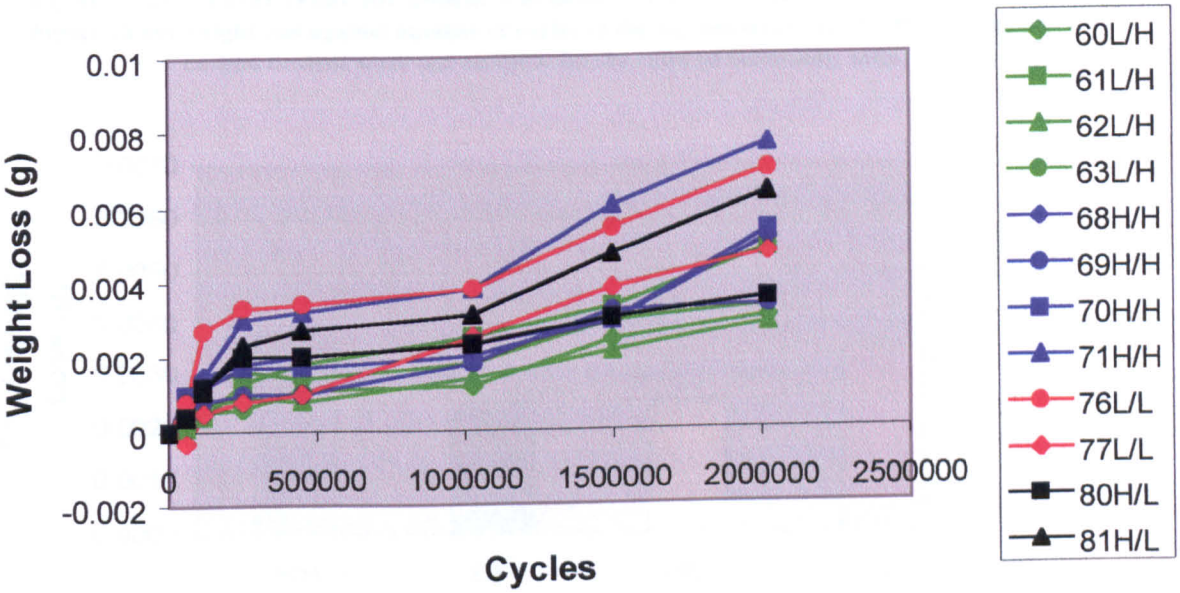

Figure 7.2b: Total Wear for 28mm Variable Carbon Content Samples (Test 2)
Figure shows weight loss against number of cycles of the hip simulator for the 28mm variable carbon content wear test samples for the second of three such tests.

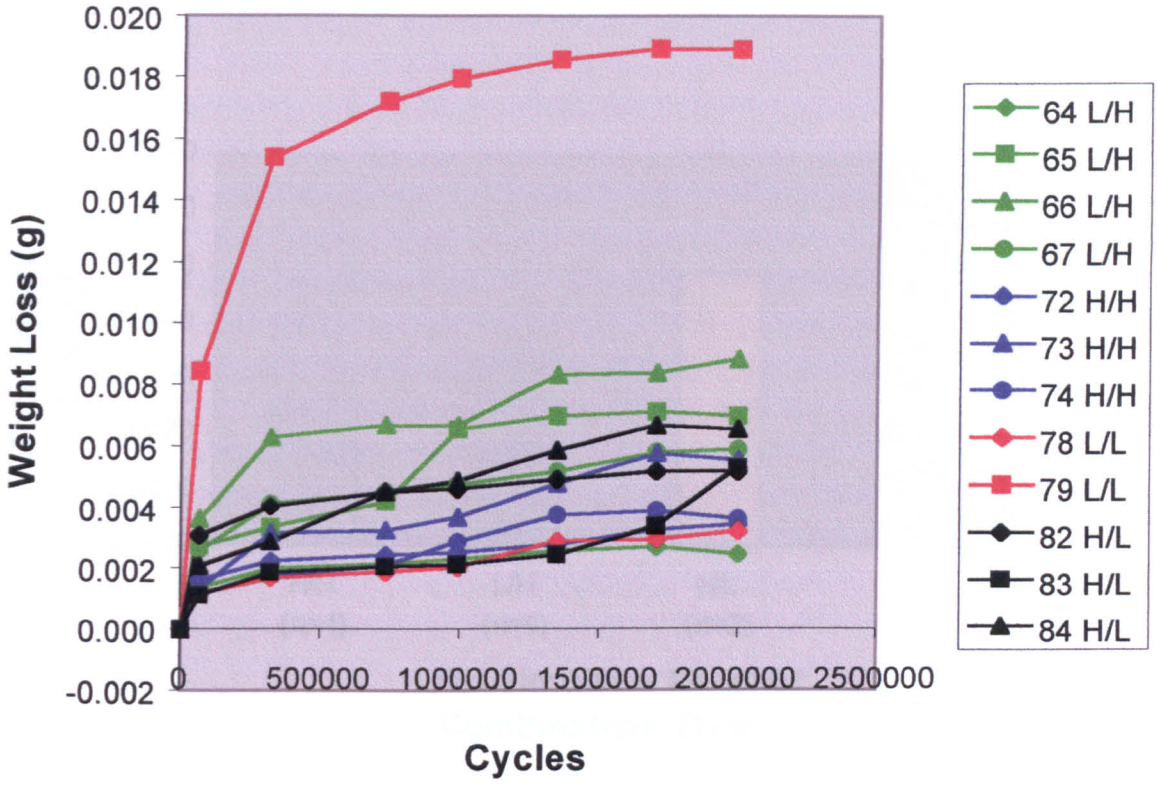

Figure 7.2c: Total Wear for 28mm Variable Carbon Content Samples (Test 3)
Figure shows weight loss against number of cycles of the hip simulator for the 28mm variable carbon content wear test samples for the third of three such tests.

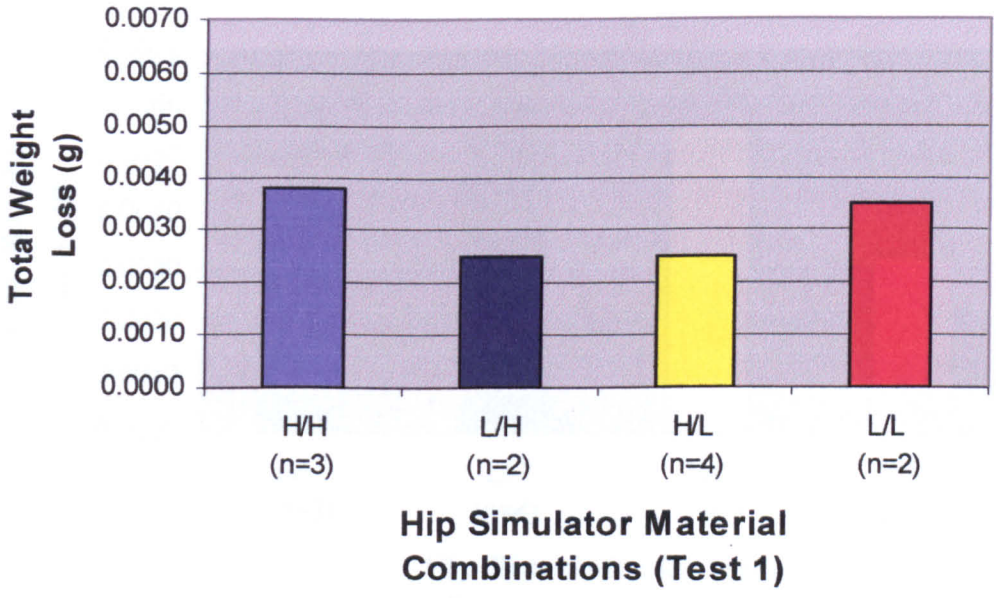

Figure 7.3a: Total Wear at 2 Million Cycles for 28mm Variable Carbon Content Samples (Test 1)
Figure shows weight loss at about 2 million cycles of the hip simulator for the 28mm variable carbon content wear test samples for the first of three such tests.

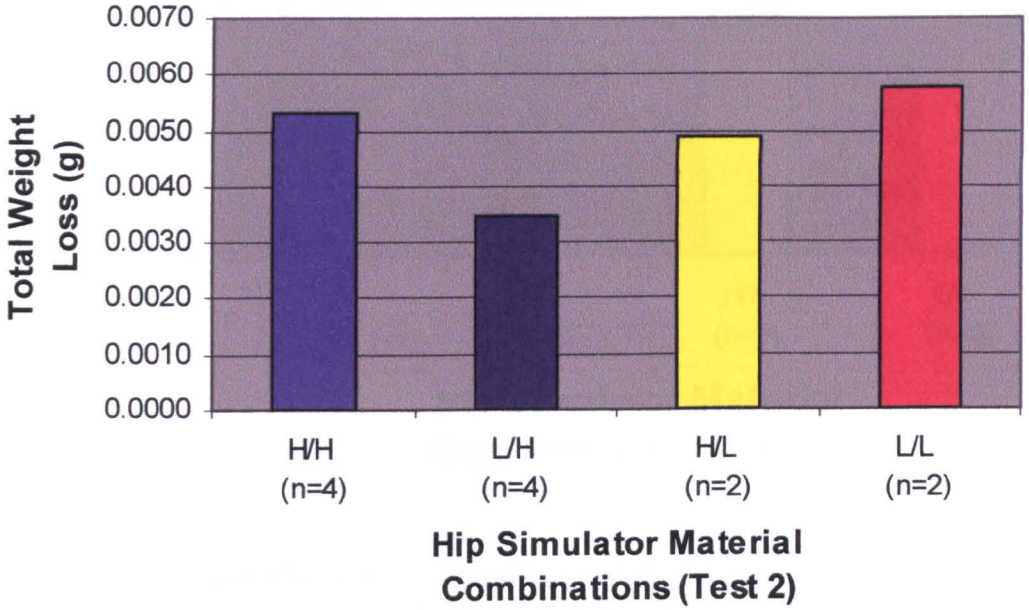

Figure 7.3b: Total Wear at 2 Million Cycles for 28mm Variable Carbon Content Samples (Test 2)

Figure shows weight loss at about 2 million cycles of the hip simulator for the 28mm variable carbon content wear test samples for the second of three such tests.

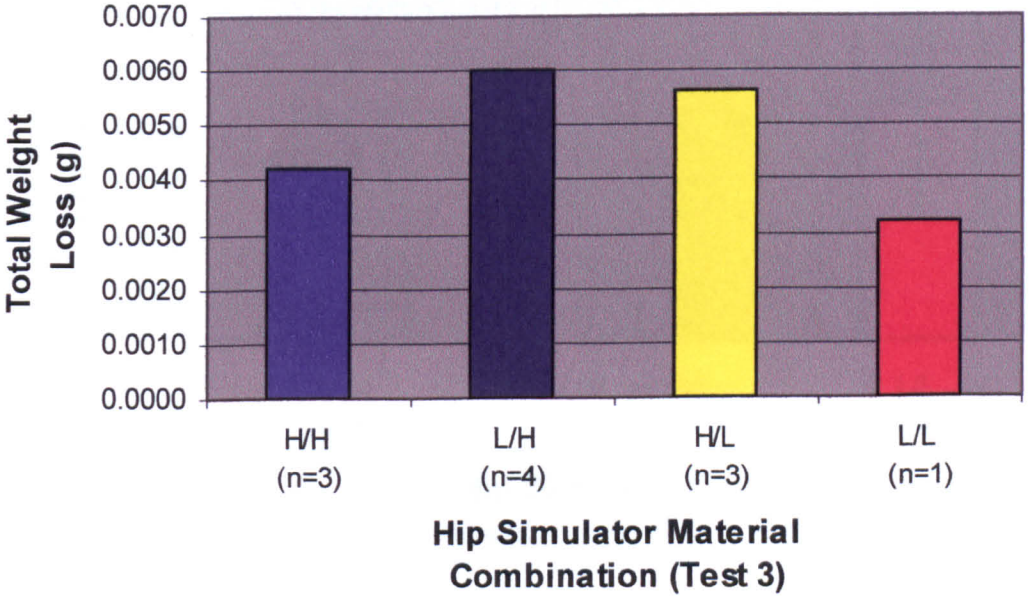

Figure 7.3c: Total Wear at 2 Million Cycles for 28mm Variable Carbon Content Samples (Test 3)

Figure shows weight loss at about 2 million cycles of the hip simulator for the 28mm variable carbon content wear test samples for the third of three such tests.

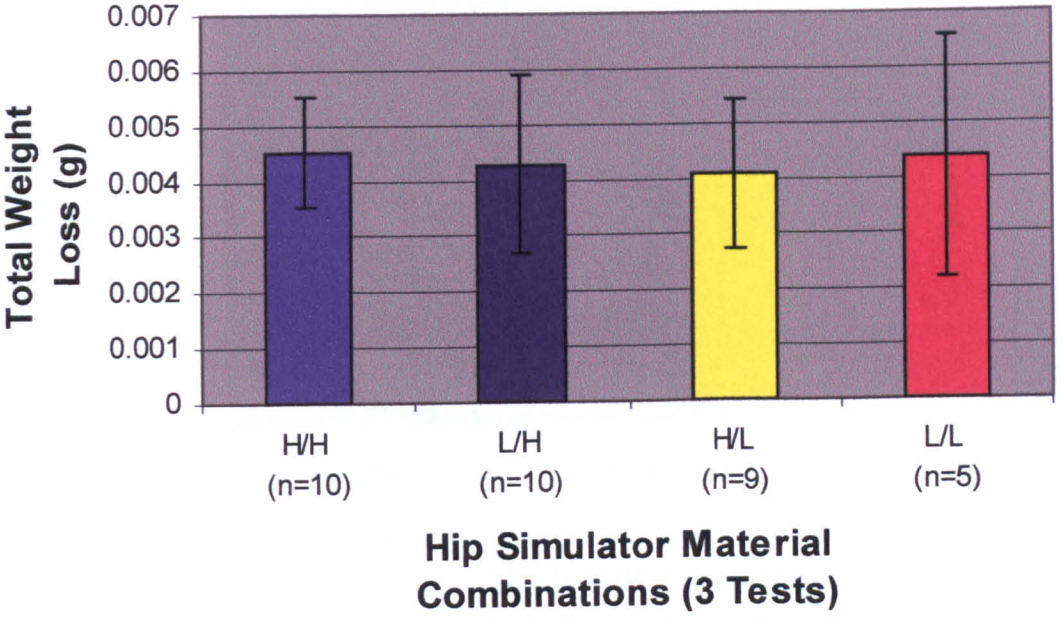

Figure 7.3d: Total Wear at 2 Million Cycles for 28mm Variable Carbon Content Samples (Sum of 3 Tests)

Figure shows weight loss at about 2 million cycles of the hip simulator for the 28mm variable carbon content wear test samples for the sum of all the three tests. The error bars represent the 95% confidence levels for the population means (Appendix C3).

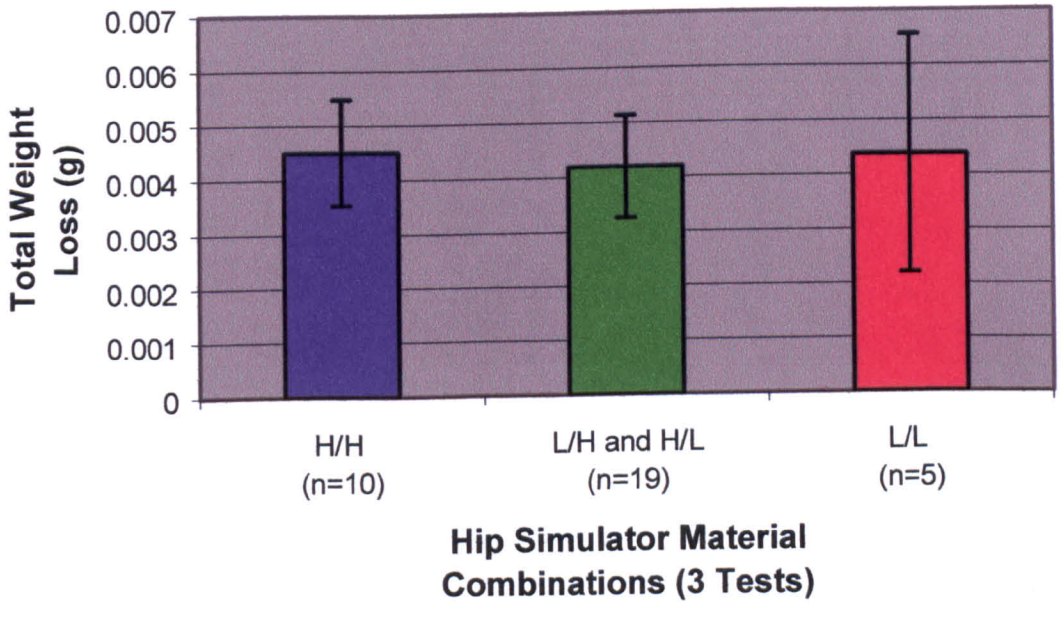

Figure 7.3e: Total Wear at 2 Million Cycles for 28mm Variable Carbon Content Samples (Sum of 3 Tests)

Figure shows weight loss at about 2 million cycles of the hip simulator for the 28mm variable carbon content wear test samples for the sum of all the three tests, and where the High/Low and Low/High combinations have been added directly. The error bars represent the 95% confidence levels for the population means (Appendix C3).

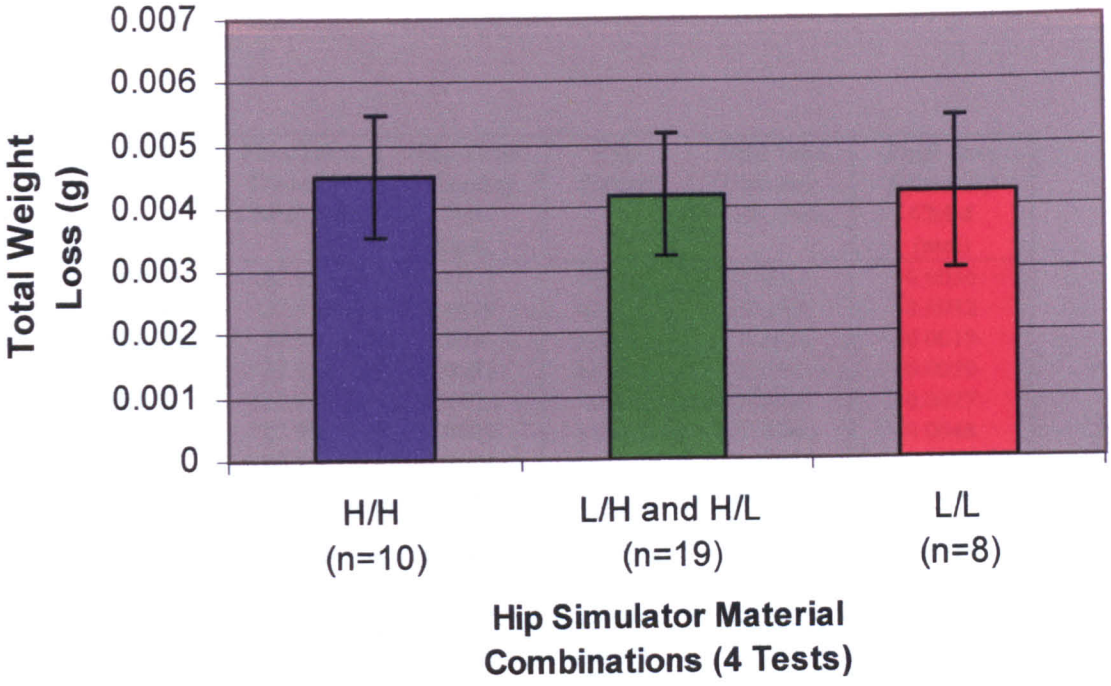

Figure 7.3f: Total Wear at 2 Million Cycles for 28mm Variable Carbon Content Samples (Sum of 4 Tests including Fig 6.8)

Figure shows weight loss at about 2 million cycles of the hip simulator for the 28mm variable carbon content wear test samples for the sum of all the three tests including the addition of the three samples of Figure 6.8 (Low/Low specimens), and where the High/Low and Low/High combinations have been added directly. The error bars represent the 95% confidence levels for the population means (Appendix C3).

Head Sample	Final Head Diameter CMM (mm)	Final Head Sphericity CMM (mm)	Cup Sample	Final Bore Diameter CMM (mm)	Final Bore Sphericity CMM (mm)
MH017	27.938	0.0072	MC017	27.987	0.0036
MH018	27.952	0.0029	MC018	27.988	0.0032
MH019	27.953	0.0043	MC019	27.989	0.0019
MH020	27.958	0.0022	MC020	27.994	0.0029
MH021	27.949	0..0023	MC021	27.985	0.0027
MH022	27.952	0.0029	MC022	27.994	0.0048
MH023	27.953	0.0024	MC023	27.984	0.0024
MH024	27.973	0.0013	MC024	28.012	0.0027
MH025	27.947	0.0024	MC025	Missing	-
MH026	27.951	0.0009	MC026	27.984	0.0037
MH027	27.956	0.0020	MC027	27.997	0.0031
MH028	28.007	0.0028	MC028	28.049	0.0032
Master Ball*	19.977	0.0016	Master Ball*	19.977	0.0016
MH060	28.031	0.0021	MC060	28.074	0.0027
MH061	27.994	0.0019	MC061	28.038	0.0033
MH062	28.009	0.0025	MC062	28.046	0.0017
MH063	28.043	0.0017	MC063	28.082	0.0046
MH064	28.015	0.0020	MC064	28.056	0.0049
MH065	28.032	0.0027	MC065	28.071	0.0028
MH066	28.084	0.0018	MC066	28.130	0.0016
MH067	28.058	0.0036	MC067	28.096	0.0016
MH068	28.028	0.0039	MC068	28.068	0.0034
MH069	28.022	0.0031	MC069	28.064	0.0028
MH070	28.047	0.0041	MC070	28.089	0.0022
MH071	28.036	0.0034	MC071	28.080	0.0043
Master Ball*	19.978	0.0009	Master Ball*	19.977	0.0022
MH072	28.028	0.0034	MC072	28.067	0.0023
MH073	28.024	0.0028	MC073	28.068	0.0021
MH074	28.006	0.0029	MC074	28.043	0.0043
MH076	28.107	0.0021	MC076	28.154	0.0025
MH077	28.029	0.0036	MC077	28.088	0.0033
MH078	28.064	0.0034	MC078	28.120	0.0023
MH079	28.382	0.0040	MC079	28.416	0.0064
MH080	28.227	0.0012	MC080	28.276	0.0056
MH081	28.111	0.0027	MC081	28.155	0.0051
MH082	28.227	0.0038	MC082	28.276	0.0028
MH083	28.126	0.0022	MC083	28.179	0.0048
MH084	28.062	0.0044	MC084	28.108	0.0044
Master Ball*	19.978	0.0009	Master Ball*	19.978	0.0009
			MC075**	28.088	0.0031

*Master ball calibrated at 19.9776mm diameter

**MC075 not used

Table 7.5

The geometry data of Table 7.2 repeated after completion of the wear test is presented.

Head Sample	Head Diameter (mm)		Reduction in Head Diameter (mm)	Cup Sample	Bore Diameter (mm)		Increase in Bore Diameter (mm)	Diametral Clearance (mm)	
	Initial	Final			Initial	Final		Initial	Final
MH017	27.930	27.938	-0.008	MC017	27.979	27.987	0.008	0.049	0.049
MH018	27.939	27.952	-0.013	MC018	27.987	27.988	0.001	0.048	0.036
MH019	27.939	27.953	-0.014	MC019	27.990	27.989	-0.001	0.051	0.036
MH020	27.944	27.958	-0.014	MC020	27.997	27.994	-0.003	0.053	0.036
MH021	27.935	27.949	-0.014	MC021	27.988	27.985	-0.003	0.053	0.036
MH022	27.938	27.952	-0.014	MC022	27.992	27.994	0.002	0.054	0.042
MH023	27.938	27.953	-0.015	MC023	27.988	27.984	-0.004	0.050	0.031
MH024	27.959	27.973	-0.014	MC024	28.014	28.012	-0.002	0.055	0.039
MH025	27.936	27.947	-0.011	MC025	27.986	Missing	-	0.050	N/A
MH026	27.937	27.951	-0.014	MC026	27.988	27.984	-0.004	0.051	0.033
MH027	27.943	27.956	-0.013	MC027	27.998	27.997	-0.001	0.055	0.041
MH028	27.996	28.007	-0.011	MC028	28.051	28.049	-0.002	0.055	0.042
MH060	28.028	28.031	-0.003	MC060	28.077	28.074	-0.003	0.049	0.043
MH061	27.989	27.994	-0.005	MC061	28.042	28.038	-0.004	0.053	0.044
MH062	28.006	28.009	-0.003	MC062	28.053	28.046	-0.007	0.047	0.037
MH063	28.038	28.043	-0.005	MC063	28.086	28.082	-0.004	0.048	0.039
MH064	28.010	28.015	-0.005	MC064	28.060	28.056	-0.004	0.050	0.041
MH065	28.024	28.032	-0.008	MC065	28.075	28.071	-0.004	0.051	0.039
MH066	28.077	28.084	-0.007	MC066	28.129	28.130	0.001	0.052	0.046
MH067	28.054	28.058	-0.004	MC067	28.101	28.096	-0.005	0.047	0.038
MH068	28.026	28.028	-0.002	MC068	28.071	28.068	-0.003	0.045	0.040
MH069	28.019	28.022	-0.003	MC069	28.069	28.064	-0.005	0.050	0.042
MH070	28.040	28.047	-0.007	MC070	28.092	28.089	-0.003	0.052	0.042
MH071	28.032	28.036	-0.004	MC071	28.081	28.080	-0.001	0.049	0.044
MH072	28.025	28.028	-0.003	MC072	28.071	28.067	-0.004	0.046	0.039
MH073	28.021	28.024	-0.003	MC073	28.069	28.068	-0.001	0.048	0.044
MH074	28.004	28.006	-0.002	MC074	28.052	28.043	-0.009	0.048	0.037
				MC075*	28.087	28.088	0.001	0.045	
MH076	28.102	28.107	-0.005	MC076	28.148	28.154	0.006	0.046	0.047
MH077	28.026	28.029	-0.003	MC077	28.076	28.088	0.012	0.050	0.059
MH078	28.060	28.064	-0.004	MC078	28.109	28.120	0.011	0.049	0.056
MH079	28.375	28.382	-0.007	MC079	28.420	28.416	-0.004	0.045	0.034
MH080	28.223	28.227	-0.004	MC080	28.270	28.276	0.006	0.047	0.049
MH081	28.107	28.111	-0.004	MC081	28.154	28.155	0.001	0.047	0.044
MH082	28.226	28.227	-0.001	MC082	28.270	28.276	0.006	0.044	0.049
MH083	28.124	28.126	-0.002	MC083	28.171	28.179	0.008	0.047	0.053
MH084	28.061	28.062	-0.001	MC084	28.105	28.108	0.003	0.044	0.046

MC075 Not used

Table 7.6

Comparison of articulating surface geometry's pre and post testing.

As with the testing in Chapter 6, there were some problems with the execution of the tests. Table 7.7 details some of the problems which occurred during the course of the tests.

Sample Number	Test Information
MH/MC017	Sample lost after about 780450 cycles due to fluid retaining sleeve failure and consequent dry running
MH/MC023	Simulator trunnion rod loosened after about 513710 cycles and metallic debris was evident in the fluid. No apparent effect on wear performance of sample
MH/MC064	Cleaning protocol deviated in that no acid cleaning was performed on this sample. No apparent effect on wear performance of sample
MH/MC074	Cleaning protocol deviated in that no acid cleaning was performed on this sample. No apparent effect on wear performance of sample

Table 7.7
Problems encountered during the simulator wear tests.

Tables 7.8a and b detail the information gathered from a visual analysis of the post test surfaces. Figures 7.4 and 7.5 show respectively a selection of the head and cup surfaces looking directly on the pole utilizing the fluorescence marker technique developed by Ward (1996). Some indications on the heads and cups were due to reflections from the lights used in the process and these include the eight thick, straight, short dashes which zigzag across the form in two distinct groups, as well as the bright continuous ring shown in each cup.

Typical indications on couples which reached the end of the test with no failure of apparatus were light scratching superposed onto a still polished surface. Some apparently deeper scratches were generally evident though in much fewer numbers than the light "scouring" scratches. These phenomena are typical and expected from such a wear process where it is believed that particles are being removed from the surfaces and are likely then to make contact with other areas of surface and produce scratches consistent with the relative motions taking place under test conditions. Occasional dents in the surface of the heads are expected as a function of the many handling processes taking place during the test and perhaps more particularly after the testing was completed. From experience with these materials (even though they are relatively hard) the polished surfaces are damaged very easily by contact with other hard surfaces. It is

Head Sample	Description of Surface Appearance
MH017	Surface appears uniformly scoured over whole surface except for a band at the bottom edge about 1-5mm wide which appears to be closer to virgin surface. At one side of head the scoured surface has a quite well defined edge. Scouring is mostly light and in all directions giving the impression of a circular pattern. Superimposed are slightly deeper scratches running north to south. Markings consistent with dry running.
MH018	Surface appears almost perfect with addition of a few small light almost circular scratches concentrated from pole to equator. A very few figure of 8 scratches present lower than equator. One small deeper dent noted.
MH019	Surface appears almost perfect with addition of a few small light almost circular scratches concentrated from pole to equator. A very few figure of 8 scratches present lower than equator. One small deeper dent noted.
MH020	Surface appears almost perfect with addition of a few small almost circular scratches concentrated from pole to equator. Scratches a little deeper than MH019
MH021	Surface appears almost perfect with addition of a few small almost circular scratches concentrated from pole to equator. A very few figure of 8 scratches present lower than equator. Scratches a little deeper than MH019
MH022	From about 20 to about 40 degrees from pole markings are much denser if not much deeper than on the other cups. There appears to be a series of annular striations formed by small circular scratch marks. Rest of surface including pole appears almost unmarked
MH023	Surface appears almost perfect with addition of a few small light almost circular scratches concentrated from pole to equator. Three small deeper dents noted.
MH024	Many pronounced and long curling scratches superposed onto a mirror surface between about 15 and 60 degrees from equator. Scratch ends reach almost to equator
MH025	Much more prolific scratching than previous heads though non very deep. Many small light and slightly deeper scratches overlapping all over head down to about 60 degrees from equator giving generally dulled appearance. A very few figure of 8 scratches present lower than equator.
MH026	Shows signs of full figure of 8 scratch pattern around about 120 degrees circumferentially which reach down to about 4mm from the base. The top of the figure of 8 is clear as a well defined edge where the scratch pattern ends at about 40 degrees from the pole. Above this and towards the equator the scratch pattern is of many light scratches overlapping to give a dull effect but fading towards the pole which appears relatively unworn
MH027	Similar to MH026 but with only the top half of the figure of 8 defined and that not as distinct. The pole region appeared more scratched
MH028	Some evidence of film build up on this part around pole and a distinct pattern of more pronounced scratches at about 40 degrees from the pole. These appear again to be the top ends of the figure of 8 scratches but where only about a third of the 8 is present except in 2 regions where a very few were present lower than the equator down to about 5mm from the base of the head and were very light past the equator

Table 7.8a

Information from a post test visual inspection of the wear test heads MH017 to MH028

Head Sample	Description of Surface Appearance
MH060	Overall very few marks at all. Some scratches dispersed around the pole and to about 30 degrees from pole. Around about 120 degrees circumferentially some bottom halves of figure of 8 scratches visible reaching to within about 3mm of the base of the head but very light
MH061	Extremely light scratching visible to head out from pole to about 30 degrees. Some traces of adhered film, and a few very local and small but deeper marks
MH062	Similar to MH061 but with more scratches and deeper. More adhered film evident. More deeper scratches or dents possibly not consistent with the simulator.
MH063	Some adhered film evident. Polar scratch marks light and typical. Strong figure of 8 marks evident around about 90 degrees circumferentially and extending from about 20 degrees above the equator to within about 3mm of the base
MH064	Very light typical scratches. Evidence of 3 circumferential parallel scratches just above equator not consistent with hip simulator. At least 1 quite long and very deep dent type scratch north to south straddling the equator
MH065	Some light adhered film evident over pole. Typical and very light scratching mostly around polar region
MH066	Some light adhered film evident over pole. Typical and very light scratching mostly around polar region
MH067	Some light adhered film evident over pole. Typical and very light scratching mostly around polar region. Evidence of figure of 8 scratching over a circumerential band of about 45 degrees and extending from about 20 degrees above the equator to about 4mm from the head base
MH068	Some light adhered film evident over pole. Typical and very light scratching mostly around polar region
MH069	Some light adhered film evident over pole. Typical and very light scratching mostly around polar region
MH070	Some light adhered film evident over pole. Typical and very light scratching mostly around polar region
MH071	Some light adhered film evident over pole and stronger band above equator. Typical and very light scratching mostly around polar region

Table 7.8b

Information from a post test visual inspection of the wear test heads MH060 to MH071

not envisaged that these dents have affected the wear results to any large extent and none of the components showed such proliferation of these features as to lead to removal from the test. Heads MH073, MH074, and MH075 bear this out with evidence of indentations but with reasonable wear performance. Similarly there were a number of instances of figure of eight markings running from pole to base of heads and often with quite sharp cut off line circumferentially. This indicates some contact with the edge of the cup bearing surface at its mouth and whilst not apparently generally affecting the wear performance (compare heads MH077, MH078, MH080, MH081, and MH082 which showed generally very light scratching, with heads MH026 and MH063 where figure of eight markings were present and it seems evident that high wear does not always accompany such markings) of the couples this should be investigated further.

Head Sample	Description of Surface Appearance
MH072	Very few scratches and these generally around the pole. Relatively large number of dents also around pole
MH073	Very few scratches and these generally around the pole. Relatively large number of dents also around pole. Strange pattern or group of round indentations on one side towards pole. Some evidence of imperfections in the original microfinished surface at equator for about 45 degrees circumferentially
MH074	Very few scratches and these generally around the pole. Relatively large number of dents also around pole
MH076	Very few scratches and these generally around the pole. More than usual amount of adhered surface film present circumferentially at about 30 degrees to equator
MH077	Very few scratches and these generally around the pole
MH078	Very few scratches and these generally around the pole
MH079	Polar marks normal and relatively light. Extensive, full, and very pronounced figure of 8 marks from just above equator to about 2mm from base of head all way round
MH080	Very few scratches and these generally around the pole
MH081	Very few scratches and these generally around the pole
MH082	Very few scratches and these generally around the pole
MH083	Very few scratches and these generally around the pole. Relatively large number of dents also around pole
MH084	Very few scratches and these generally around the pole

Table 7.8c

Information from a post test visual inspection of the wear test heads MH072 to MH084

Indeed, it has been established that sample 079 was a rogue sample and it clearly showed evidence of strong figure of eight markings. It is suggested that these markings occurred when the edge of the cup bearing surface contacts the head surface during articulation which should not occur. It may then be that there was some geometrical attributes or errors on the bearing couples showing the figure of eight markings that could be identified and avoided in future. It seems then that visual appearance may occasionally be an indicator of some malfunction of a test or of high wear for some other reason but that generally the visual appearance can appear similar when wear results are quite different (compare MH065 in Fig 7.4d with MH072 in Fig 7.4e where wear is 0.0069g and 0.0034g respectively) and alternately the appearance can vary whilst the wear performance is comparable (compare MH019 in Fig 7.4a with MH026 in Fig 7.4b where wear is 0.0031g and 0.0022g respectively). What was very clear from the visual analysis was that samples which were lost due to dry running were quite different from samples which reached the end of the test with no such problems.

Cup Sample	Description of Surface Appearance
MC017	Entire surface scoured from pole to equator. Scratches are relatively deep with a couple of very deep ones. Scratches appear to run in all directions. This is very consistent with dry running and sample loss.
MC018	Surface generally still mirror polished but with superposed medium depth scratches mostly located between 22.5 degrees of the equator and the pole and circular in form.
MC019	Surface generally still mirror polished but with a greater profusion of medium depth circular form scratches than MC018 from pole to equator.
MC020	Surface generally still mirror polished but with superposed light to medium depth scratches mostly located between 15 degrees of the equator and the pole and circular in form.
MC021	Surface generally still mirror polished but with superposed light to medium depth scratches located over whole surface and circular in form. Evidence of polishing wear on the large outside diameter of the test piece all the way round and at level of interface with test fixture. Some wear of cup could be attributed to this.
MC022	Light scratches cover most of surface but are least prevalent at pole. Single deep straight scratch having the appearance of being a manufacturing defect evident running towards the equator starting at about 45 degrees from pole.
MC023	Circular light scratches over most of surface, which remains mirror like. Fewer scratches at pole. One complete circular scratch of about 10mm diameter and having centre about 30 degrees from pole evident.
MC024	Surface generally still mirror polished but with superposed light to medium depth scratches mostly located between 15 degrees of the equator and the pole and circular in form. Three very deep dents visible roughly equispaced on a circumferential line about 45 degrees from pole.
MC025	Missing
MC026	Surface generally still mirror polished but with superposed medium depth scratches mostly located between 22.5 degrees of the equator and the pole and circular in form. Then a clear band at the equator and about 3mm wide is evident. The band is clearly demarked at its lower edge where all the scratches within the band which run radially abruptly end. This could be evidence of some malfunction.
MC027	The mirror polished surface is still evident though largely dulled by a high density of light depth scratched from pole to within about 15 degrees of the equator.
MC028	The mirror polished surface is still evident though largely dulled by a high density of light depth scratched from pole to within about 15 degrees of the equator.

Table 7.8d

Information from a post test visual inspection of the wear test cups MC017 to MC028

Cup Sample	Description of Surface Appearance
MC060	Polished surface still evident with only very light scratches and relatively few from pole to about 30 degrees from equator and virtually nothing closer to the equator.
MC061	As above but with a few more pronounced scratches.
MC062	As above.
MC063	As MC061 but with some dullness of the surface up to about 40 degrees from pole but excluding a small polar area about 5mm in diameter which is mirror polished and free of both dullness and almost any scratches.
MC064	As MC061 but non scratched region towards equator appears dull.
MC065	Very light depth scratches and relatively few except one very pronounced circular scratch about 10mm in diameter and centred at about 5mm from the pole. General dullness over almost entire surface.
MC066	Scratching is almost entirely constrained between about 10 and 40 degrees from the pole. Scratching is generally light and scratched area is also dull. Non scratched area is mirror polished. One deep circular scratch about 7mm diameter and centred about 5mm from the pole is evident.
MC067	As M060 but with some dullness also but only in scratched area and again a clear polar spot is present about 5mm diameter.
MC068	As above.
MC069	As above.
MC070	As MC065 but with dullness constrained to scratched area only.
MC071	Scratching is almost entirely constrained between about 10 and 40 degrees from the pole. Scratching is generally light and scratched area is also dull. Non scratched area is mirror polished.

Table 7.8e

Information from a post test visual inspection of the wear test cups MC060 to MC071

Cup Sample	Description of Surface Appearance
MC072	Surface remains mirror polished but with superposed medium depth circular form scratches between about 10 and 50 degrees from the pole. General dullness also present on this portion of surface though the rest including the pole remains almost virgin.
MC073	As MC072 except scratches reach to about 70 degrees.
MC074	Polished surface still evident with only very light scratches and relatively few from pole to about 40 degrees from equator and virtually nothing closer to the equator.
MC076	As MC072
MC077	Surface remains mirror polished but with superposed medium depth circular form scratches between about 10 and 50 degrees from the pole. Very fine Thielenhaus marks evident on unscratched surface towards pole indicating that this is virgin surface.
MC078	Medium depth and density scratches between pole and about 45 degrees.
MC079	Scratching is almost entirely constrained between about 10 and 50 degrees from the pole. Scratching is generally light. Non scratched area is mirror polished. One deep circular scratch about 10mm diameter and centered about 5mm from the pole is evident.
MC080	As above.
MC081	As above but with no deep circular scratch.
MC082	As above.
MC083	As MC072 but with very small (about 1mm) circular dull spot at the pole..
MC084	As MC078.

Table 7.8f

Information from a post test visual inspection of the wear test cups MC072 to MC084

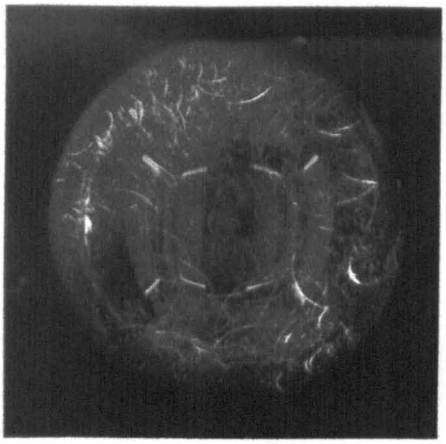

Fig 7.4a: MH019

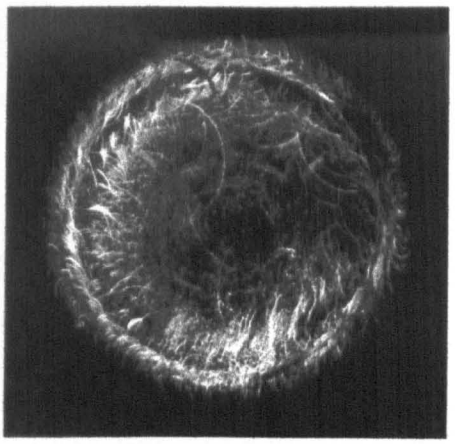

Fig 7.4b: MH026

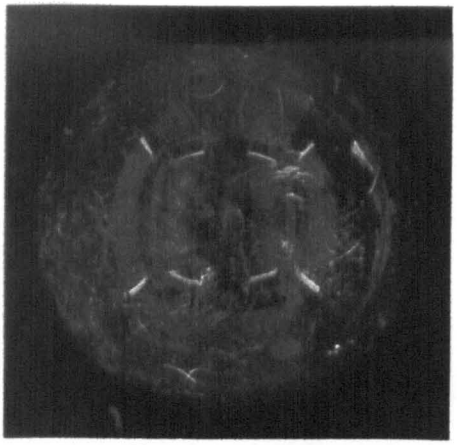

Fig 7.4c: MH060

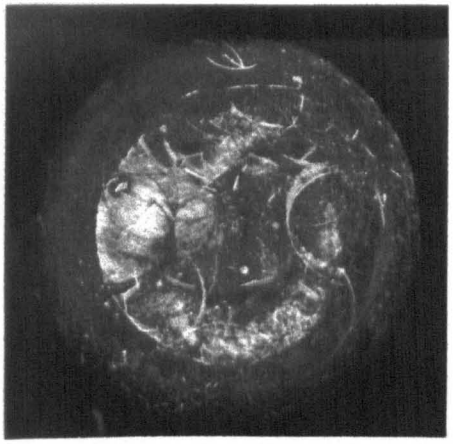

Fig 7.4d: MH065

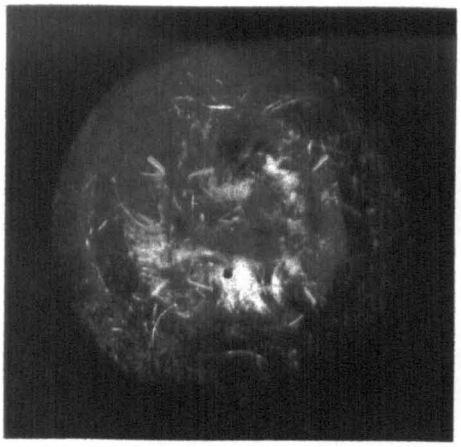

Fig 7.4e: MH072

Fig 7.4f: MH078

Figure 7.4: Fluorescing Photographs of Sample Heads

Figure shows a photograph for a selection of the sample heads taken looking directly on the pole. The fluorescence technique allows the condition of the articulating surface to be shown clearly. Heads are identified by head number.

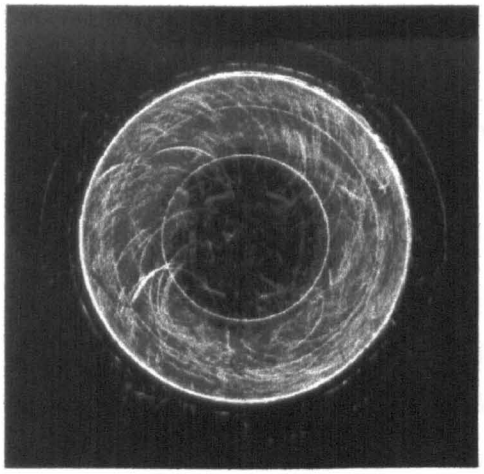

Fig 7.5a: MC019

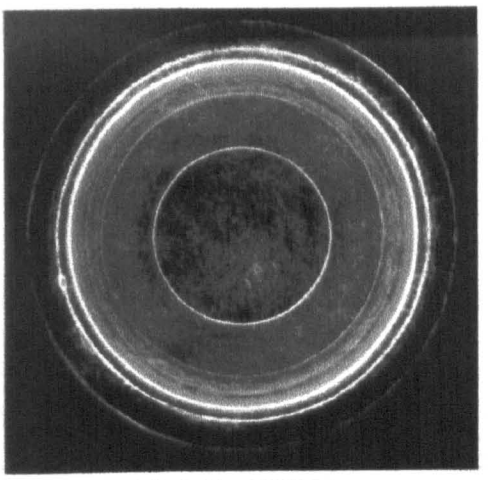

Fig 7.5b: MC026

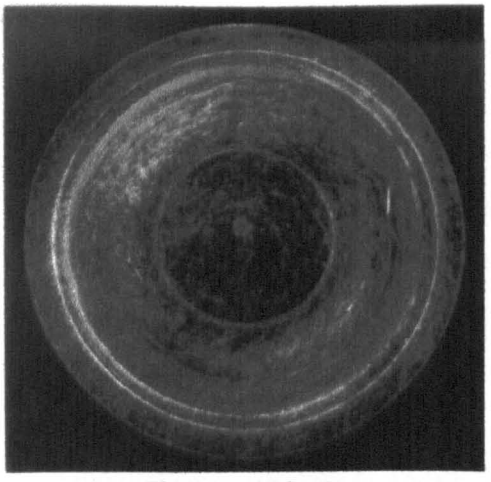

Fig 7.5c: MC060

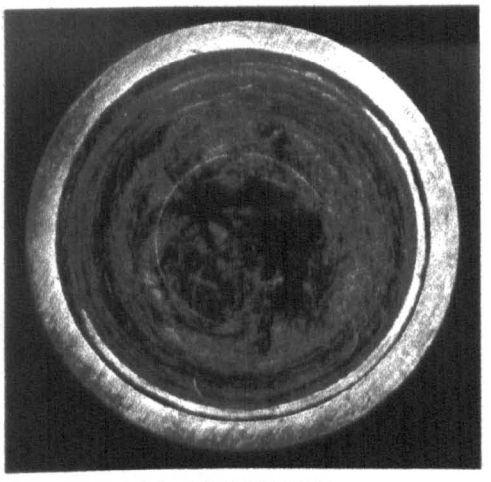

Fig 7.5d: MC065

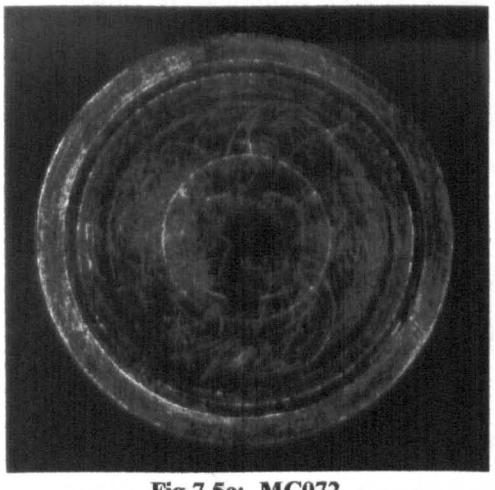

Fig 7.5e: MC072

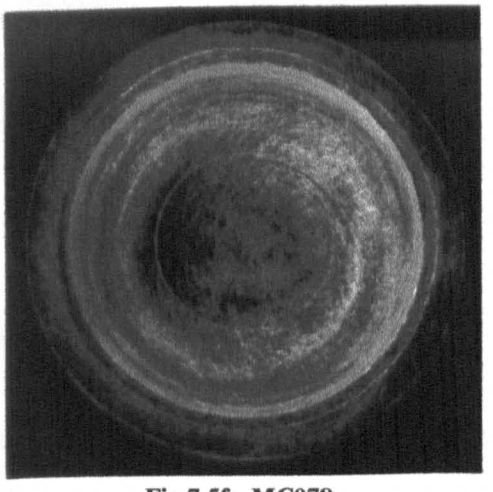

Fig 7.5f: MC078

Figure 7.5: Fluorescing Photographs of Sample Cups

Figure shows a photograph for a selection of the sample cups taken looking directly on the pole. The fluorescence technique allows the condition of the articulating surface to be shown clearly. Cups are identified by cup number.

7.7 Discussion

The starting point for this chapter was the work of Schmidt et al (1996) which suggested that carbon content was very important in reduced bearing wear. The suggestion was that both bearing components should be made from high carbon material in order to minimize wear. The basis for this suggestion was pin on disc testing of high against high and low against low carbon combinations. The tests in this chapter utilized a hip simulator to about two million cycles in order to test the suggestion of Schmidt et al (1996) under in vitro conditions more closely akin to the true anatomical conditions pertaining within the human hip joint. Figures 7.2 clearly show that the wear curves for all three tests followed the general pattern established in chapter 6 where an initial bedding in period of high wear rate yields, within about 200,000 cycles, to a more steady state lower wear rate. Typical wear figures for the optimum clearance couples of chapter 6 of about 0.003g after 2 million cycles were matched by the results of the three tests of this chapter (which were carried out with clearance within the optimum band established in chapter 6), thus providing some confidence in the consistency and repeatability of the test method.

Geometrically, the data of Tables 7.2 (pre-test) and 7.6 (post test) indicate that bearing diametral clearances were typically close to the value of 0.050mm aimed at as a result of the findings of chapter 6. It was interesting to note that of all the couples tested and which completed the number of cycles required with no test problems, only one couple (MH/MC079) stood out from the rest due to its unusually high wear. Comparing the starting geometry of this couple it is also evident that it stood out from the others in terms of its nominal diameter, being about 28.40 rather than about 28.08. The consequence of this nominal oversizing did not become apparent until it was noted that the unusually high wear of this bearing couple was accompanied by very pronounced figure of eight markings as described in Table 7.8c. It seems clear that where these marks were full figures of eight with the bottom of the eight within about 3mm of the base of the head then the lip of the cup at the edge of the bearing surface was making contact with the head. This situation should not normally occur and where it was seen to occur it is inferred that additional wear over and above the normal polar wear must have occurred. When considering the severity and completeness of these markings it was

noted that heads MH026, MH027, MH063, and MH067 also exhibited figure of eight markings which might be deemed to have had a significant effect on the bearing wear figure of Tables B7.3. However, review of the performance of these samples compared with the rest demonstrated no evidence of higher wear associated with the presence of the figure of eight features. Indeed, quite low wear resulted from all these samples except 067 and there were numerous samples without the figure of eight markings with wear comparable to or higher than 067. So, rather than providing an explanation as to why some wear results were higher than others except in the case of sample 079, the figure of eight markings show evidence of some previously unseen phenomena which should be understood. Clearly it was not the design intent for the edge of the cup to contact the femoral head and therefore an understanding of how it has occurred and how to prevent it may be useful for future metal on metal designs.

To establish that the edge of the cup bearing surface adjacent to the chamfer had been the feature which had caused the figure of eight marks on the head, it was necessary to show by calculation that with the cup and head positioned in the simulator, the edge of the cup bearing surface would reach the most extreme extents of head figure of eight markings. The angular alignment of the parts within the simulator was a 23° rotation of the head in the cup from a starting point of both head and cup axes of symmetry being in line. Measurements of the cup showed that the centre of the bearing surface was 0.755mm below the front face of the cup and the lead in chamfer was 1mm deep. Thus the edge of the bearing surface was 0.245mm below its centre (or equator). Considering the head and cup bearing surfaces to be concentric (ignoring clearance) the 23° rotation would take the edge of the cup bearing surface some 5.47mm along the axis of the head towards its base. Considering that the initial contact would have been 0.245mm below the head centre, the final extreme contact would have been 5.225mm from head centre measured along the head axis towards the base. Measurements of the head indicated an overall height of 24.33mm and therefore the dimension from base to equator was 10.13mm. With a base to bearing surface chamfer of 3.19mm, the dimension from equator to extent of bearing surface was 6.94mm. Deducting from this the 5.225mm extent of marking left a distance from edge of head bearing surface to extreme edge of marking of 1.72mm. This figure was exactly confirmed by direct measurement on the head. This confirmed that the bold figure of eight markings on the head were caused by

direct contact with the lip of the cup (the edge created where the lead in chamfer intersected the bearing surface).

A similar analysis performed on the sample confirmed that the other end of the figure of eight marking nearest to the pole of the head was also caused by the same contact with the lip of the cup. Adding the 0.245 and 5.47mm dimensions to the 10.13mm dimension and subtracting the 3.19mm chamfer length dimension gave a calculated dimension from edge of bearing surface to far end of figure of eight markings of 12.66mm. This was demonstrated to be correct by measurement on the head.

Having established that contact was made during articulation between the edge of the cup bearing surface and the head, leading to excessive wear of the couple through the test, a reason for this occurrence was required. As discussed already the nominal diameter of the components of bearing 079 was about 0.3mm larger than the rest of bearings in the test. The theory of chapter 4 would not suggest a variation of performance due to this diameter difference but it was felt that perhaps the manufacturing process had created some deviation from acceptable form around the edge of the bearing surface of the cup when the diameter was pushed out by an extra 0.3mm. To investigate this possibility, cup MC079 (diameter 28.420mm) was compared with MC073 (diameter 28.069) on the CMM where the latter had achieved a reasonable performance in the test and importantly without any figure of eight scratches in evidence. The test made measurements of bore diameter parallel to the cup front face and spaced about the spherical bore centre (negative distances represented diameters below the spherical centre and closer to the pole of the bore). The diameters and sphericity values (9 point CMM circles) were plotted in table 7.9 along with a theoretical calculation of diameter at that level in relation to spherical centre and calculated from the known spherical diameter.

Figure 7.6 shows the data of Table 7.9 plotted with cup axis horizontal. It was easy to see the chamfer on the actual cup form to the right hand side and that the theoretical and actual forms matched closely over the spherical region. The crucial point to note however was that in creating the larger bore of MC079, the spherical bore surface had grown to possibly a full hemisphere as it truncated the pre machined chamfer, whereas

the smaller bore of MC073 had remained clearly less than a hemisphere. It was considered important to have a bearing surface somewhat less than a full hemisphere to prevent any chance for cone clutching or for a bearing surface of more than a full hemisphere to be created. From figure 7.6 the correct geometry is shown by MC073 where the chamfer intersected the spherical portion below the spherical centre.

Needless to say couple 079 were discounted from the analysis but note was taken of the need to have less than a full hemispherical bearing surface in any future metal on metal designs.

Given the results of the study as performed, and from Figs 7.3f particularly, it was clear that in contrast to the results obtained for simple pin on disc testing by Schmidt et al (1996) where high carbon against high carbon combinations performed considerably better than low against low carbon, no difference of statistical significance was noted between any combinations in the present testing. Whilst in principle the mean wear data for high against high and low against low combinations was higher than for high against low combinations, the error bars indicate clearly the lack of significance in the results.

The outcome of this testing was not considered to be altogether surprising however. It is well known that pin on disc or pin on plate testing with uniaxial motion is no more than a simple material screening test where the tribology of the natural joint is not reflected at all accurately. Further, from chapter 4 of this thesis it was shown that if geometrical, dynamic, and lubricating fluid characteristics were correctly chosen then full fluid film lubrication was potentially possible for a 28mm articulation and a mixed lubrication regime would certainly have been achieved. That being the case, one would expect that as the lubrication regime tended towards full fluid film, the sensitivity of the test to variations of materials used to manufacture the bearings would be diminished. When a condition of full fluid film was achieved, there would be no sensitivity at all to the bearing surface materials. Therefore it was concluded that one of the reasons for the difference in result between the simple pin on disc testing and the full hip simulator testing was that the latter achieved a lubrication regime much closer to full fluid film.

Level (mm)	Diameter for MC079 (mm)	Sphericity for MC079 (mm)	Theoretical Diameter for MC079 (mm)	Diameter for MC073 (mm)	Sphericity for MC073 (mm)	Theoretical Diameter for MC073 (mm)
0.50	28.864	0.0054	28.759	28.759	0.0038	28.051
0.40	28.720	0.0032	28.568	28.568	0.0026	28.057
0.30	28.608	0.0055	28.415	28.415	0.0045	28.062
0.20	28.524	0.0049	28.295	28.295	0.0053	28.066
0.15	28.490	0.0058	28.243	28.243	0.0050	28.067
0.10	28.464	0.0018	28.203	28.203	0.0041	28.068
0.05	28.441	0.0050	28.164	28.164	0.0042	28.068
0	28.424	0.0045	28.135	28.135	0.0035	28.069
-0.05	28.412	0.0046	28.108	28.108	0.0044	28.068
-0.10	28.407	0.0042	28.089	28.089	0.0013	28.068
-0.15	28.404	0.0052	28.071	28.071	0.0037	28.067
-0.20	28.403	0.0062	28.063	28.063	0.0038	28.066
-0.25	28.401	0.0048				28.064
-0.30	28.398	0.0034	28.055	28.055	0.0074	28.062
-0.35	28.396	0.0021				28.060
-0.40	28.394	0.0030	28.053	28.053	0.0033	28.057
-0.45	28.390	0.0030				28.054
-0.50	28.387	0.0026	28.047	28.047	0.0054	28.051
-0.60	28.379	0.0042	28.04	28.040	0.0064	28.043
-0.70	28.369	0.0036	28.029	28.029	0.0072	28.034
-0.80	28.357	0.0055	28.019	28.019	0.0043	28.023
-0.90	28.346	0.0031	28.005	28.005	0.0036	28.011
-1.00	28.332	0.0061	27.992	27.992	0.0063	27.997

Table 7.9

Actual and theoretical points on the bearing surface and lead in chamfer of cups MC073 and MC079.

Now, whilst the testing in this chapter was carried out to compare the effects of variation of carbon content of the material, due to the claims made by Schmidt et al (1996), no relationship has been established between carbon content (high or low) and hardness. As a result of the findings of this chapter it became of interest to establish whether hardness could be shown to have any influence on wear performance. Two comparisons which could be investigated to some degree from the data generated were wear against mean hardness and wear against hardness difference between the articulating elements. Table 7.10 indicates the materials used in this study, and their carbon contents along with the bulk hardness values from the material certification (taken from tables 6.1 and 7.1).

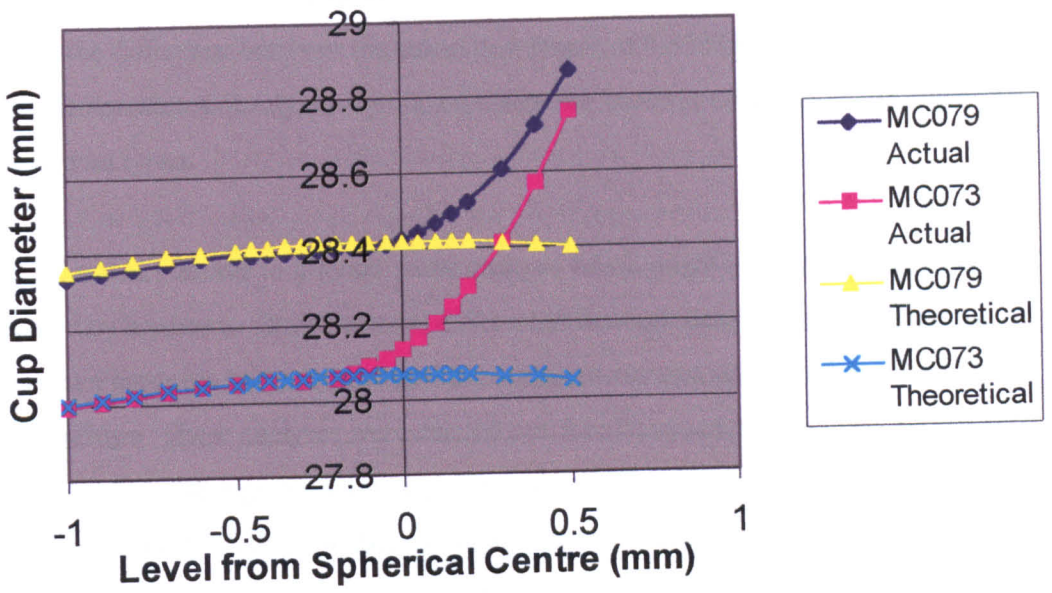

Figure 7.6: Cup form Plots Near Bearing Surface Edge

Figure shows actual and theoretical form plots for cups MC073 and MC079 from CMM data of table 7.9 with cup axis of revolution shown horizontal. The cup lead in chamfer is clearly visible and should intersect the spherical form below the spherical centre at the zero level as shown on MC073.

Material Designation	Carbon Content	Test Piece Hardness (HRc)
VN87	High	42
VM12	High	45
VN07	High	40
EG68	Low	42
ED96	Low	39
CJ53	Low	44
55E11514	Low	41.5
CF52	Low	42

Table 7.10

Hardness data for the materials used for the carbon content variation test.

From these data it was possible to calculate mean hardness for the high and the low carbon material groups and plot as a bar chart showing the 95% confidence limits for the population mean using the analysis of Appendix C (the means and 95% confidence limits were 42.333±4.623 HRc for high and 41.700 ±2.057 HRc for low carbon content). This was shown in Figure 7.7. It was clear from this graph that there was a 95%

certainty that the maximum hardness difference between high and low carbon content materials of the types used in this work was 7.3 HRc but more likely the difference would be the difference between the calculated means of 0.633 HRc. Moreover this analysis demonstrates clearly no significant difference in terms of hardness value between these material types.

However, it was possible to attempt some analysis which might indicate how wear could be affected by hardness. Both hardness differential between head and cup samples as well as mean hardness for each head and cup sample were compared with wear for the sample pairings. These analyses were carried out for all the samples and also for discrete groupings such as the high/high, low/high (including high/low) or low/low pairings. Table 7.11a provides all the raw data for such analysis. Tables 7.11b through e then provide the mean data which was shown in figures 7.8a through h.

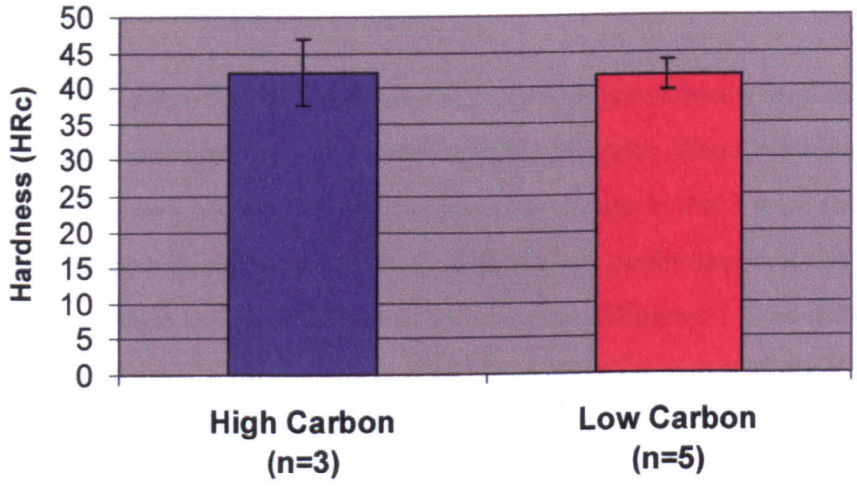

Figure 7.7: Mean Material Hardness for High and Low Carbon Content Materials Used in the Carbon Content Variation Study

Figure shows the estimate of population means for high and low carbon cobalt chromium alloy materials of chapters 6 and 7. The error bars represent the 95% confidence levels for the population means (Appendix C3).

It would appear from these data that whilst there was no clear relationship evident between hardness and wear, a tendency towards reducing wear with increasing hardness difference or with increasing mean head/cup hardness existed. This trend was seen to some degree in all the figures 7.8 with the exception of 7.8e which was seen to turn up sharply in wear between hardness differentials of 2.5 and 3. However note that when

sample sizes were as small as 1, 2, or even 3 (as in this case), then it was to be expected that certain data would go against the general trend. It was also noted that whilst the mean wear data was plotted, the scatter of the individual data points within each grouping was often quite substantial. It was therefore concluded that whilst some general trend towards reduction in wear with increase of either hardness difference or mean hardness between head and cup existed, the range of both hardness difference and of mean hardness was considered too small to be of real significance. The data does however suggest that combinations should be tested which provide a greater range (around 10 Rockwell points) and with sufficient sample sizes to more fully investigate the effect of hardness. Additionally, whilst this study compared the samples on the basis of a certification hardness value taken on behalf of each bulk material batch on a sample from the batch, it may be prudent, to improve the quality of such discussion, to take a hardness measurement directly on each component and repeat the comparisons of tables 7.11 and figures 7.8 after establishing whether the samples made from the same material have consistently similar hardness.

From Table 7.1 where the available material properties are shown, it was notable that all materials except one were from the same supplier, Teledyne Allvac, with the other being supplied by Heymark Metals Ltd. All the low carbon cups in test 1 were manufactured using material from this latter supplier. Considering the performance of this material against that supplied by Teledyne Allvac by reference to Figures 7.2 did not indicate any substantial difference. Likewise it was noted from table 7.1 that of all the Teledyne Allvac materials, for some unexplained reason the high carbon alloy VN07 was apparently heat treated differently to the rest during manufacture of the bar by the material supplier. Again by reference to the performance of samples where this alloy was utilized compared to those where it was not in the first test, there appears to be no

Head/Cup Sample Number MH/MC and Carbon Content H/C	Head/Cup Hardness Difference (HRc)	Head/Cup Mean Hardness	Wear for High/High Samples (g)	Wear for High/Low and Low/High Samples (g)	Wear for Low/Low Samples (g)
18 H/H	5	42.5	0.0034		
21H/H	0	40	0.0044		
22 H/H	0	40	0.0035		
68 H/H	0	42	0.0051		
69 H/H	0	42	0.0033		
70 H/H	0	42	0.0053		
71 H/H	0	42	0.0076		
72 H/H	0	42	0.0034		
73 H/H	0	42	0.0055		
74 H/H	0	42	0.0036		
19 H/L	3.5	43		0.0031	
20 H/L	3.5	43		0.0024	
23 H/L	-1.5	40.5		0.0019	
24 H/L	-1.5	40.5		0.0026	
25 L/H	4	42		0.0028	
26 L/H	4	42		0.0022	
60 L/H	0	42		0.0030	
61 L/H	0	42		0.0048	
62 L/H	0	42		0.0028	
63 L/H	0	42		0.0033	
64 L/H	0	42		0.0025	
65 L/H	0	42		0.0069	
66 L/H	0	42		0.0088	
67 L/H	0	42		0.0059	
80 H/L	3	40.5		0.0035	
81 H/L	3	40.5		0.0063	
82 H/L	3	40.5		0.0051	
83 H/L	3	40.5		0.0053	
84 H/L	3	40.5		0.0065	
9/6 L/L	0.5	41.5			0.0036
07 L/L	0.5	41.5			0.0051
11 L/L	0.5	41.5			0.0032
27 L/L	2.5	42.5			0.0023
28 L/L	2.5	42.5			0.0047
76 L/L	3	40.5			0.0069
77 L/L	3	40.5			0.0047
78 L/L	3	40.5			0.0032

Table 7.11a

Hardness data for the materials used for the carbon content variation test. Note that mean hardness values are rounded down to nearest whole or half Rockwell.

Material Type	Hardness Difference (Cup-Head) (HRc)	Mean Wear (g)	Number of Samples N	Mean Hardness (HRc)	Mean Wear (g)	Number of Samples n
Mixed	-1.5	0.00225	2	40.0	0.00395	2
Mixed	0.0	0.00469	17	40.5	0.00460	10
Mixed	2.5	0.00350	2	42.0	0.00479	15
Mixed	3.0	0.00519	8	42.5	0.00347	3
Mixed	3.5	0.00275	2	43.0	0.00275	2
Mixed	4	0.00250	2			
Mixed	5	0.00340	1			

Table 7.11b

Mean wear versus hardness data for all materials used for the carbon content variation test. Note that mean hardness values are rounded down to nearest whole or half Rockwell.

Material Type	Hardness Difference (Cup-Head) (HRc)	Mean Wear (g)	Number of Samples N	Mean Hardness (HRc)	Mean Wear (g)	Number of Samples n
High/High	5	0.00340	1	40.0	0.00395	2
High/High	0	0.00463	9	42.0	0.00483	7
High/High				42.5	0.00340	1

Table 7.11c

Mean wear versus mean hardness data for the high/high carbon materials used for the carbon content variation test. Note that mean hardness values are rounded down to nearest whole or half Rockwell.

Material Type	Hardness Difference (Cup-Head) (HRc)	Mean Wear (g)	Number of Samples N	Mean Hardness (HRc)	Mean Wear (g)	Number of Samples n
Low/Low	0.5	0.00397	3	40.5	0.00493	3
Low/Low	2.5	0.00350	2	41.5	0.00397	3
Low/Low	3.0	0.00493	3	42.5	0.00350	2

Table 7.11d

Mean wear versus mean hardness data for the low/low materials used for the carbon content variation test. Note that mean hardness values are rounded down to nearest whole or half Rockwell.

Material Type	Hardness Difference (Cup-Head) (HRc)	Mean Wear (g)	Number of Samples N	Mean Hardness (HRc)	Mean Wear (g)	Number of Samples n
H/L & L/H	-1.5	0.00225	2	40.5	0.00446	7
H/L & L/H	0.0	0.00475	8	42.0	0.00430	10
H/L & L/H	3.0	0.00534	5	43.0	0.00275	2
H/L & L/H	3.5	0.00275	2			
H/L & L/H	4.0	0.00250	2			

Table 7.11e

Mean wear versus mean hardness data for the high/low and low/high materials used for the carbon content variation test. Note that mean hardness values are rounded down to nearest whole or half Rockwell.

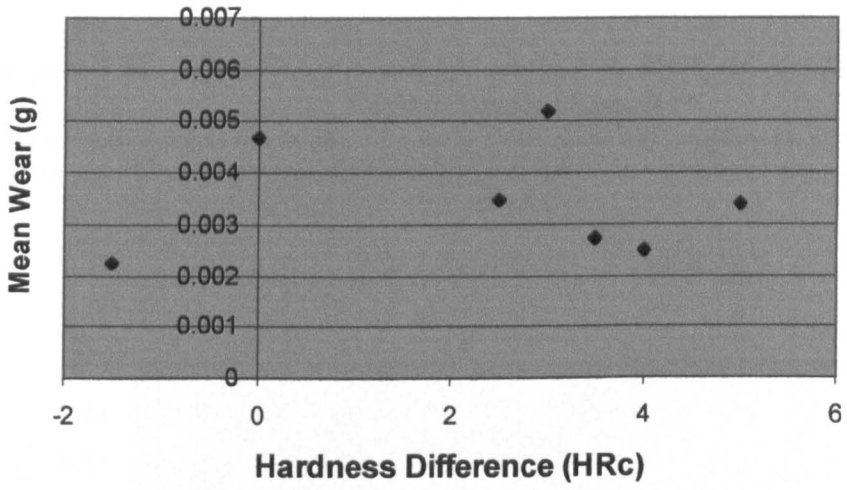

Figure 7.8a: Mean Wear Against Sample Hardness Difference for 28mm Variable Carbon Content Samples

Figure shows weight loss at about 2 million cycles of the hip simulator for the 28mm variable carbon content wear test samples plotted against difference in hardness between cup and head for all 34 samples.

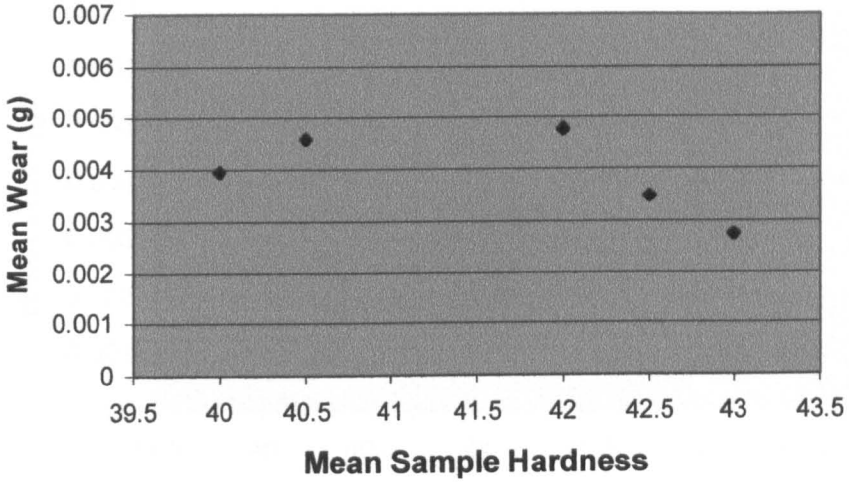

Figure 7.8b: Mean Wear Against Mean Sample Hardness for 28mm Variable Carbon Content Samples

Figure shows weight loss at about 2 million cycles of the hip simulator for the 28mm variable carbon content wear test samples plotted against the mean hardness of cup and head for all 34 samples.

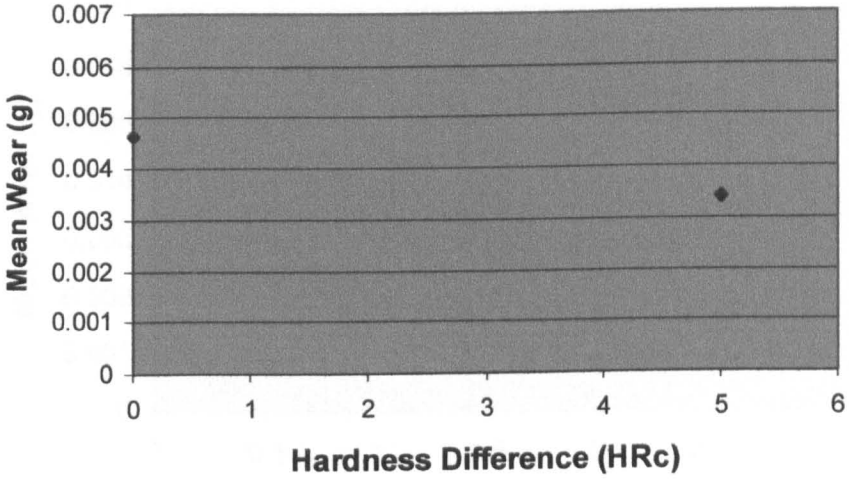

Figure 7.8c: Mean Wear Against Sample Hardness Difference for 28mm Variable Carbon Content High/High Samples

Figure shows weight loss at about 2 million cycles of the hip simulator for the 28mm variable carbon content wear test samples plotted against difference in hardness between cup and head for all 10 high/high carbon content samples.

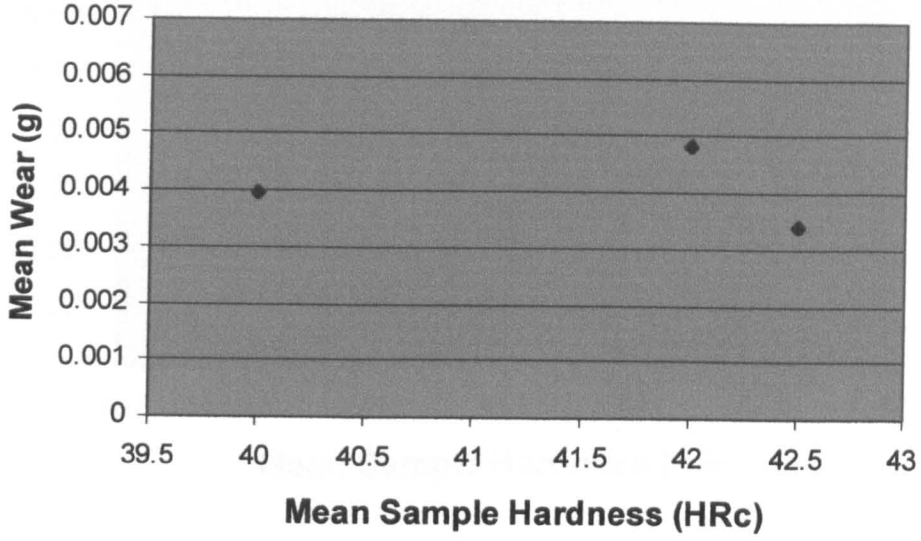

Figure 7.8d: Mean Wear Against Mean Sample Hardness for 28mm Variable Carbon Content High/High Samples

Figure shows weight loss at about 2 million cycles of the hip simulator for the 28mm variable carbon content wear test samples plotted against the mean hardness of cup and head for all 10 high/high carbon content samples.

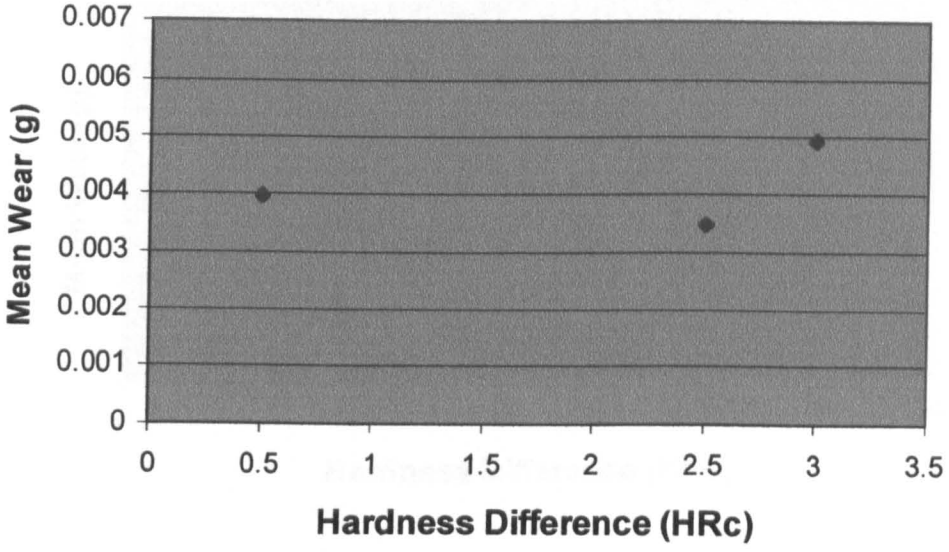

Figure 7.8e: Mean Wear Against Sample Hardness Difference for 28mm Variable Carbon Content Low/Low Samples

Figure shows weight loss at about 2 million cycles of the hip simulator for the 28mm variable carbon content wear test samples plotted against difference in hardness between cup and head for all 8 low/low carbon content samples which includes the three optimum clearance samples from chapter 6.

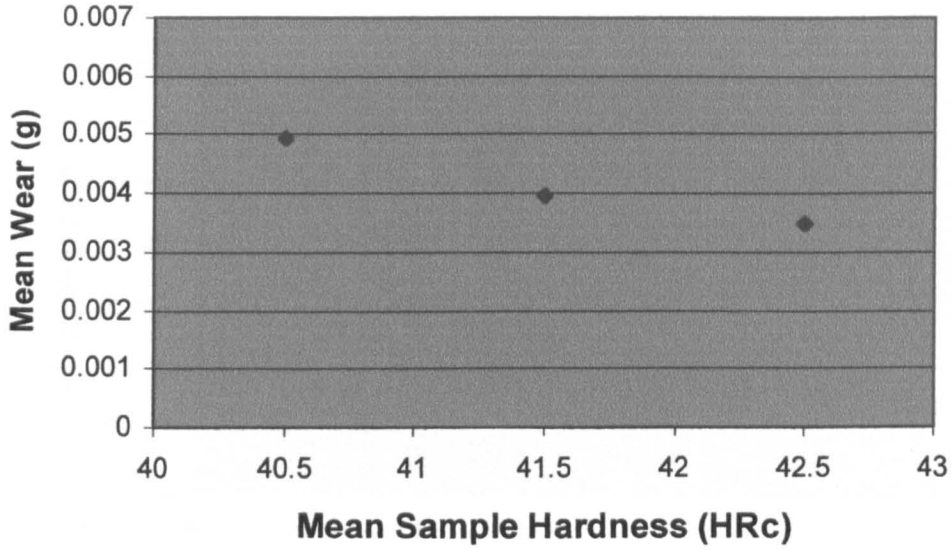

Figure 7.8f: Mean Wear Against Mean Sample Hardness for 28mm Variable Carbon Content Low/Low Samples

Figure shows weight loss at about 2 million cycles of the hip simulator for the 28mm variable carbon content wear test samples plotted against the mean hardness of cup and head for all 8 low/low carbon content samples which includes the three optimum clearance samples from chapter 6.

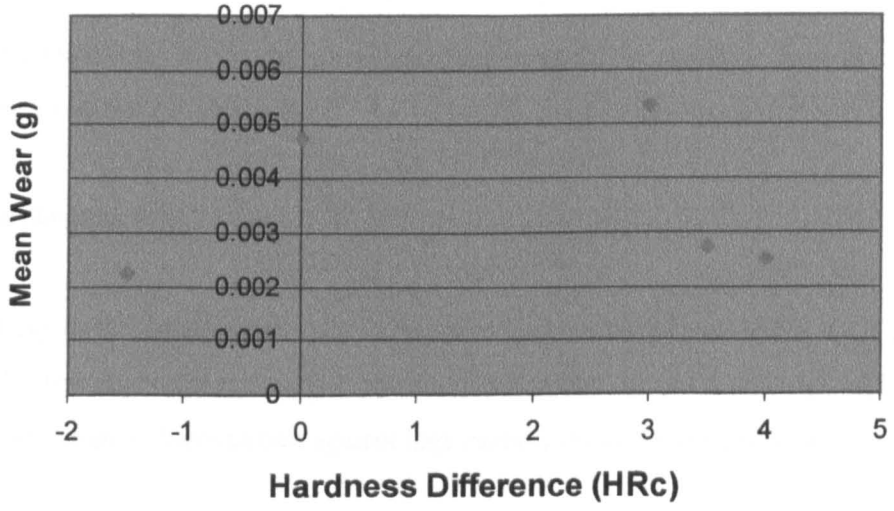

Figure 7.8g: Mean Wear Against Sample Hardness Difference for 28mm Variable Carbon Content High/Low and Low/High Samples

Figure shows weight loss at about 2 million cycles of the hip simulator for the 28mm variable carbon content wear test samples plotted against difference in hardness between cup and head for all 19 high/low and low/high carbon content samples.

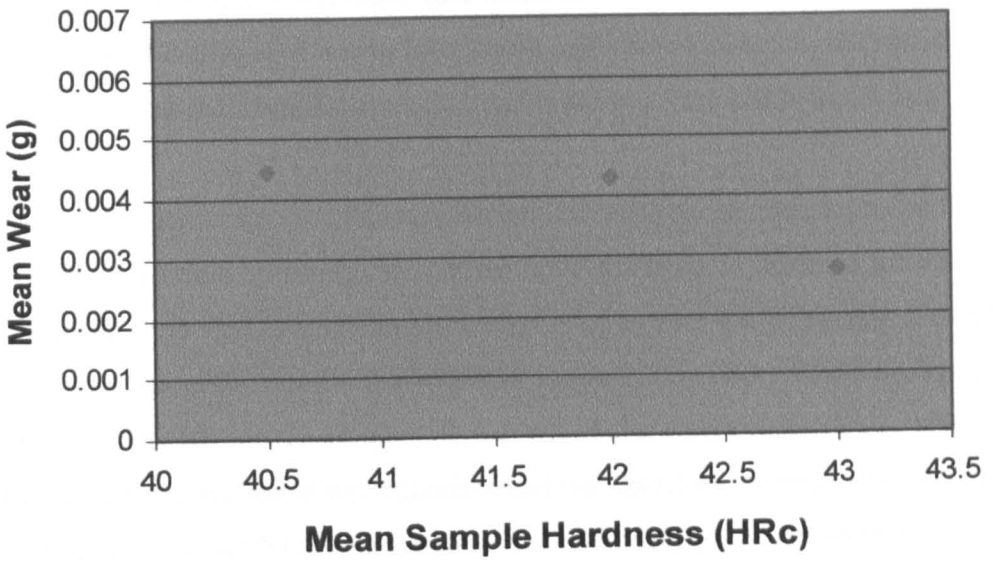

Figure 7.8h: Mean Wear Against Mean Sample Hardness for 28mm Variable Carbon Content High/Low and Low/High Samples

Figure shows weight loss at about 2 million cycles of the hip simulator for the 28mm variable carbon content wear test samples plotted against the mean hardness of cup and head for all 19 high/low and low high carbon content samples.

clear differentiation. It was therefore determined that all the materials were in a fit condition to be used in the study.

7.8 Conclusions

a. Contrary to the data presented by Schmidt et al (1996) as shown in Fig 7.1, the findings of this study did not support the claim that metal on metal articulations of the hip should comprise high carbon against high carbon cobalt chromium alloy.

b. Testing materials using simple uniaxial pin on plate or disc apparatus is not likely to yield results comparable with those for the same materials tested on a more anatomical apparatus such as a hip simulator.

c. Using a hip simulator it was found that whilst the lowest mean total wear was for combinations of high against low or low against high carbon materials, the statistical findings were that there was no significant difference at a 95% confidence level.

d. One of the reasons for the difference in result between the simple pin on disc testing and the full hip simulator testing was that the latter was likely to achieve a lubrication regime much closer to full fluid film. If the theory of chapter 4 and the tests of chapter 6 yielded an optimum clearance within which to design a 28mm hip articulation, and given that the couples tested in this chapter were designed that way, then it is likely that the lubrication regime applicable was optimized and that therefore the articulations became less sensitive to the subtleties of material choice. Much bigger variations in material may be needed to demonstrate any measurable reductions in bearing wear.

e. A general though not clear trend towards reduced wear with increase of either hardness difference or mean hardness between cup and head was noted. It was recommended that a further study should purposely test samples of hardness range of at least 10 HRc and in sufficient numbers to investigate this further.

f. Investigation of the test failure of couple 079 showed the need to have less than a full hemispherical bearing surface in any future metal on metal designs.

CHAPTER 8

Investigation of the Effect of Head Diameter on Wear in a Hip Simulator Test

8.1 Introduction

In the previous two chapters the optimum diametral clearance for a 28mm metal on metal bearing and the effect on bearing performance of variations in carbon content of the material were investigated. This chapter presents the studies of the influence of different nominal diameters on wear under similar test conditions using the same hip simulator as for the previous tests. It was decided to test bearings as small as 22mm and as large as 35mm nominal diameter.

8.2 Method

A 12 station MMED hip simulator as described in detail in chapter 5 was used. Samples of 22mm and 35mm nominal diameter head and cup test pieces covering a range of diametral clearance were tested to about 2 million cycles in bovine serum using the loading curve described by Paul (1967) at a maximum load of 2000N and a frequency of 1.1Hz. The mass of the samples was measured at intervals throughout the test using a balance capable of measuring to 10^{-5} gram.

These samples were directly compared to the 28mm nominal diameter samples described in the previous chapters.

8.3 Materials

The materials to be used for this test were selected as the high carbon and low carbon cobalt chromium molybdenum alloys as used in the testing of chapter 7. The low carbon material was used for the femoral heads and was the standard material used by Johnson and Johnson for manufacture of standard femoral heads. The high carbon material was used for the cup components and was sourced from the same supplier as the low carbon

material. Table 8.1 details the relevant information relating to the materials used. All materials were cobalt chromium alloy wrought bar to ASTM F799 (Now ASTM F1537).

Material Designation	EC75	VN07	ED96	VN87
Used to Make	22mm Heads	22mm Cups	35mm Heads	35mm Cups
Material Designation on Carbon Content	Low	High	Low	High
Material Supplier	Teledyne Allvac	Teledyne Allvac	Teledyne Allvac	Teledyne Allvac
Bar Diameter	28.6mm	43.2mm	44.5mm	43mm
Composition	(%wt)			
C	.053	.235	.055	.197
S	.0004	.0006	.0006	
Mn	.94	.55	.62	.73
Si	.68	.73	.68	.09
Cr	27.70	27.66	27.74	26.99
Mo	5.73	5.70	5.76	5.55
Co	Balance	Balance	Balance	Balance
Ti		.01		
Fe	.23	.18	.28	.12
Ni	.01	.02	.01	.49
N	.1650	.177	.178	.0962
P		.001		
W		.01		
Condition	As rolled	1135°C, 30 mins, WQ	As rolled	As rolled
Surface	Centreless ground	Centreless ground	Centreless ground	Centreless ground
Hardness (HRc)	41/48	34/41	39	43/45
Grain size[1]	Avg ASTM 10	Avg ASTM 8	Avg ASTM 10	Avg ASTM 10
Test Pieces				
UTS (MPa)	1218/1208	1301/1278	1278/1287	1221/1260
0.2% Yield (MPa)	969	815/798	841/838	907/963
El%	13.9/14.0	20/19.4	38.6/29.6	17.5/17.2
RA%	13.7/14.8	16.8	24.1	11.9/13.1
Hardness (HRc)	42	40	39	42

[1] ASTM E112, 1996

Table 8.1

Material details for the 22 and 35mm variable diametral clearance wear test samples.

8.4 Test Pieces

Twelve samples of each diameter were prepared for use in the 12 station hip simulator. Due to the expertise in making heads, and the inexperience with the manufacture of cups, the required diametral clearance values were achieved by making the cups as close to 22 or 35mm as possible and measuring them. Once an accurate measurement of the cups was obtained, the heads were made to match with the required clearance. The reason for this order of manufacture was that control of head diameter was much better than that for the cups. The polished spherical bearing surfaces were achieved using a special purpose Thielenhaus (Type: KF50F2; No 1.1.002453) microfinishing machine which utilized cylindrical tubular shaped stones for the metal removal process. The machine was equipped with an in process gauging system to enable femoral head diameter to be measured whilst machining with the stage 1 roughing stone. For the subsequent 3 stages up to and including the final polishing stone, control of diameter was only possible indirectly by setting a time limit for the contact of each stone with the workpiece.

Fig 6.1a shows a sectioned assembly of the head and cup. The test pieces were solid in form as described in the cup drawing E02931 part number 655579 for 22mm and 655710 for 35mm (Figure B7.1b). The mating femoral head for the 22mm articulations was a standard 10/12 taper +0 design (Johnson and Johnson Orthopaedics Product Code 85-3811), except with specially controlled diameter. The mating femoral head for the 35mm articulations was based on a 12/14 35mm head part number 617472 and drawing number 02701, again with specially controlled diameter.

The detailed dimensions of the cup test pieces were determined firstly so that they fitted properly into the test fixture and secondly to maintain the sample mass below a certain critical value such that a more sensitive balance could be used. The need for lowest sample mass was met by use of a hollowed cylindrical spigot at the base of the test cups shown in Figure 6.1a.

The complete range of components used are detailed in Table 8.2 along with dimensions of the articulating surfaces. Two simulator runs were used with 12 22mm samples in one run and the 12 35mm samples in the other. For each nominal size the 12 samples were

manufactured with different diametral clearance ranging from 0.010 to 0.160mm. This would allow some assessment of optimum clearance at particular nominal diameter for comparison with the results of chapter 6. All components were marked so that the same orientation of head and cup could be maintained throughout the test regardless of the number of times they were separated for measurement of wear. A control sample was used in the 35mm test to ensure that the test method was not influencing the results. This couple was subjected to the cleaning and weighing protocol but was not wear tested.

8.5 Pre Test Surface Finish

The pre test surface finish data is not shown for these parts as it was considered to be similar to the data shown in chapter 6, with typical Ra values around 0.01μm.

8.6 Pairing of Test Pieces

The components were matched as shown in table 8.2 to give a range of diametral clearance. It was not considered to be necessary to test the extremes of clearance considered in chapter 6. It was felt that the tests carried out on 28mm negative and very large clearances had provided the required understanding of the effect on wear of such articulating conditions even if diameter were changed. Therefore the range of clearance was limited to between 0.010 and 0.150mm theoretically (except the control sample which had a diametral clearance of 0.162mm). The actual clearances were within a maximum error of 0.003mm on the 22mm samples (0.050mm clearance was actually 0.047mm) and 0.005mm on the 35mm samples (0.040mm clearance was actually 0.035mm, 0.050mm clearance was actually 0.045mm, and 0.120mm clearance was actually 0.115mm). The components were marked so that the same orientation of head and cup could be maintained throughout the test regardless of the number of times they were separated for measurement of wear.

Head/Cup Sample Number MH/MC and Carbon Content H/C	Head Diameter CMM or Micrometer* (mm)	Head Sphericity CMM (mm)	Bore Diameter CMM (mm)	Bore Sphericity CMM (mm)	Diametral Clearance (mm)
29 L/H	21.932*	N/A	21.943	0.0034	0.011
30 L/H	21.986*	N/A	22.005	0.0019	0.019
31 L/H	21.976*	N/A	22.005	0.0034	0.029
32 L/H	21.964*	N/A	22.006	0.0039	0.042
33 L/H	21.973*	N/A	22.020	0.0017	0.047
34 L/H	22.020*	N/A	22.079	0.0037	0.059
35 L/H	22.031*	N/A	22.100	0.0023	0.069
36 L/H	21.898*	N/A	21.976	0.0043	0.078
37 L/H	21.899*	N/A	21.990	0.0022	0.091
38 L/H	21.934*	N/A	22.034	0.0012	0.100
39 L/H	21.964*	N/A	22.086	0.0046	0.122
40 L/H	22.021*	N/A	22.169	0.0011	0.148
Master Ball[1]	Not Available	Not Available	19.977	0.0019	
44 L/H	34.984	0.0016	34.995	0.0024	0.011
45 L/H	34.981	0.0019	35.000	0.0026	0.019
46 L/H	34.981	0.0026	35.010	0.0018	0.029
47 L/H	34.976	0.0021	35.011	0.0029	0.035
48 L/H	35.005	0.0020	35.050	0.0028	0.045
49 L/H	35.001	0.0025	35.057	0.0029	0.056
50 L/H	35.004	0.0031	35.074	0.0026	0.070
51 L/H	35.005	0.0028	35.080	0.0021	0.075
52 L/H	35.011	0.0021	35.097	0.0026	0.086
53 L/H	35.005	0.0031	35.103	0.0025	0.098
54 L/H	35.016	0.0023	35.131	0.0028	0.115
55 L/H	34.996	0.0019	35.143	0.0025	0.147
56 L/H[2] Control	34.989	0.0016	35.151	0.0009	0.162
57 L/H	34.990	0.0025	35.153	0.0018	Not used
58 L/H	35.012	0.0029	35.163	0.0028	Not used
Master Ball[1]	19.977	0.0011	19.977	0.0011	

[1]Master ball calibrated at 19.9776mm diameter
[2] Control sample weighed and cleaned but not wear tested
N/A is Not Available

Table 8.2
Geometrical details of the articulating surfaces for the 22 and 35mm variable diametral clearance wear test samples

8.7 Results

The tests for 22 and 35mm diameters were run for 2076464 and 2022343 cycles respectively of the hip simulator in accordance with the test method described previously. Measurements of wear were made as weight loss using the balance at suitable intervals throughout each test and as shown in Table B8.3a and b. At each

interval, prior to weighing, the samples were cleaned by a specially developed process as described fully in chapter 5 and which was aimed at removing any adhered substances on the one hand but not removing any metallic substrate material on the other.

The wear data is summarized in Table B8.3a and b and total wear is presented in Figures 8.1, 8.2, and 8.3 as a function of diametral clearance and number of cycles. The figures show the wear curve for each individual sample for 22 and 35mm samples where both 8.2 and 8.3 show the 35mm samples but the scale of Figure 8.3 is the same as that of Figure 8.1 to allow direct comparison of 22 and 35mm sample data.

The 22 and 35mm tests were subject to some problems relating to their execution, as detailed in Table 8.4. These technical problems either ended the specimens suitability to continue and further testing ceased, or was not deemed to prevent the specimen continuing. In this latter case, when comparing the wear rate during the interval in which the problem occurred, it is clear that the instance of the problem has had some effect on the sample performance. In the case of sample MH/MC038, the very clear high wear rate between 1027502 and 1509464 cycles is clearly higher than the rate for the previous or following interval and should be explained by the fluid leak. It was interesting to note that in the following interval the wear rate had returned to a level very close to the mean wear rate for most samples in the "steady state" region of the wear curve. It may therefore be reasonable to assume that had the fluid leak not have occurred, the final performance of this sample would have been very similar to that of sample MH/MC037. There remained however two samples which exhibited unexpected increases in wear rate for which there remained no known cause. Sample MH/MC032 between 1116825 and 1471677 cycles, where once again the interval following exhibited a wear rate more resembling the general "steady state" value. Similarly, sample MH/MC031 exhibited a very high rate in the last test interval but in this case the end of the test precluded being able to say whether the next interval rate would be lower again. Enough testing experience had been gained to this point to believe that metal on metal samples in a hip simulator did not exhibit sudden changes in wear rate without some external influence such as a test error. Therefore, whilst nothing was noted with regard to test errors for samples MH/MC031 and MH/MC032, it was assumed that something must have gone wrong with the test which lead to the sudden increase in wear.

For the 35mm samples, MH/MC044 and 054 were mixed up for 418 cycles. This created one couple MH044/MC054 having a clearance of 0.147mm and another MH054/MC044 having a negative clearance of –0.021mm. from the experience of negative clearance samples in chapter 7 which seized after 20000 cycles, 418 was probably not sufficient to cause such catastrophic consequences. The components were remeasured at 719819 cycles and demonstrated wear of 0.0011g for MH/MC044 and 0.00036g for MH/MC054. Such wear over such a small number of cycles is rather high considering that the wear for the entire previous interval (498418 to 719401) was 0.00071g and 0.0092g respectively. Couple 054 appears from Figure 9.2 to be a very high wear sample anyway, with the additional wear due to the error not having a particularly marked impact on the form of the curve. Conversely, couple 044 did show a wear rate during the interval 719401 to 857600 which was noticeably higher than that of the intervals on either side. However, within the overall 2 million cycle test, it was adjudged that the incident had not significantly change the final outcome for either couple. However, sample MH/MC050 did exhibit a quite marked change in wear rate during the interval 719401 to 857600, due to a broken tie rod which allowed the cup to spin on the head, which was adjudged to have an effect on the overall outcome of the test for that sample (a simple estimate of 17% higher wear than if the failure had not occurred). Note that for the 22mm samples shown in Figure 8.1, the initially higher wear rate (bedding in) leading to a final "steady state" lower wear rate was clearly in evidence whilst for the 35mm samples this form of curve was much less distinct where initially very low wear gave way to a higher rate between 1 and 1.5 million cycles, which itself gave way to a lower "steady state" wear rate beyond 1.5 million cycles. This form was akin to that exhibited by the variable carbon content samples of Figure 7.2a.

After completion of the tests, all the samples were re-measured using the same CMM as for pre test measurements and the results are presented in Table 8.5. Table 8.6 compares pre and post test diameters and clearances for each sample.

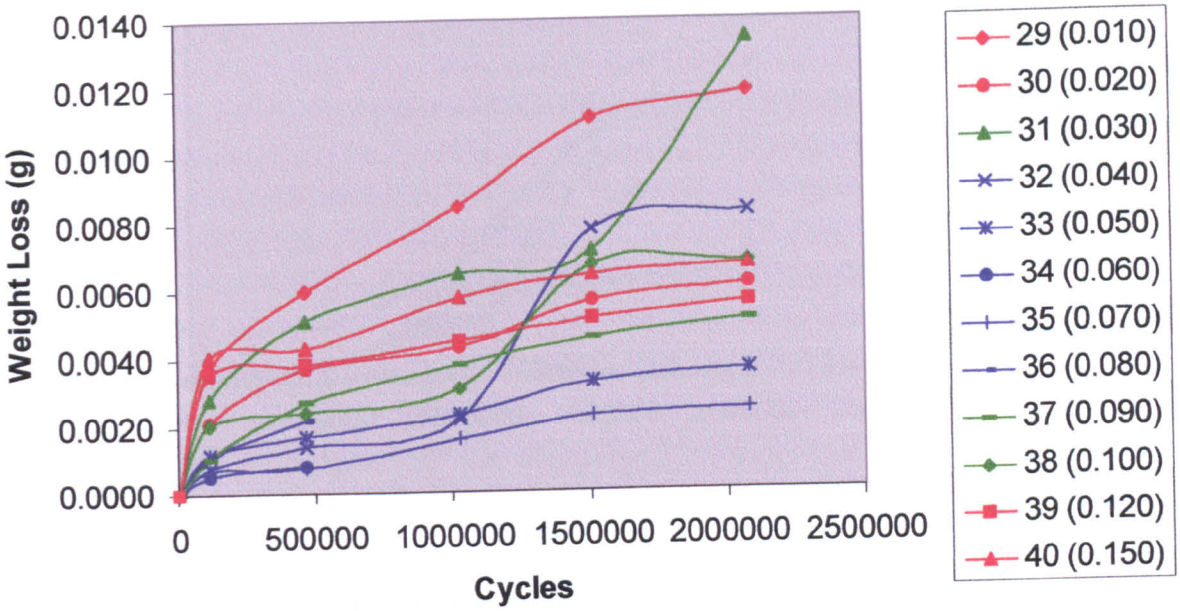

Figure 8.1: Total Wear at 2 Million Cycles for 22mm Samples

Figure shows weight loss against number of cycles of the hip simulator for the 22mm variable diametral clearance wear test samples.

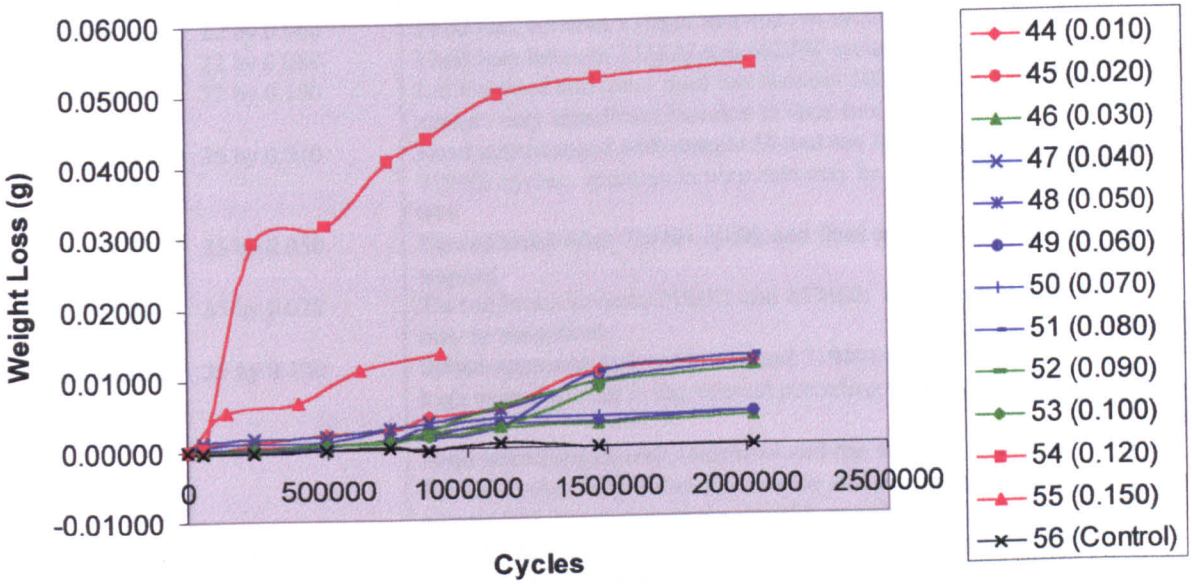

Figure 8.2: Total Wear at 2 Million Cycles for 35mm Samples

Figure shows weight loss against number of cycles of the hip simulator for the 35mm variable diametral clearance wear test samples.

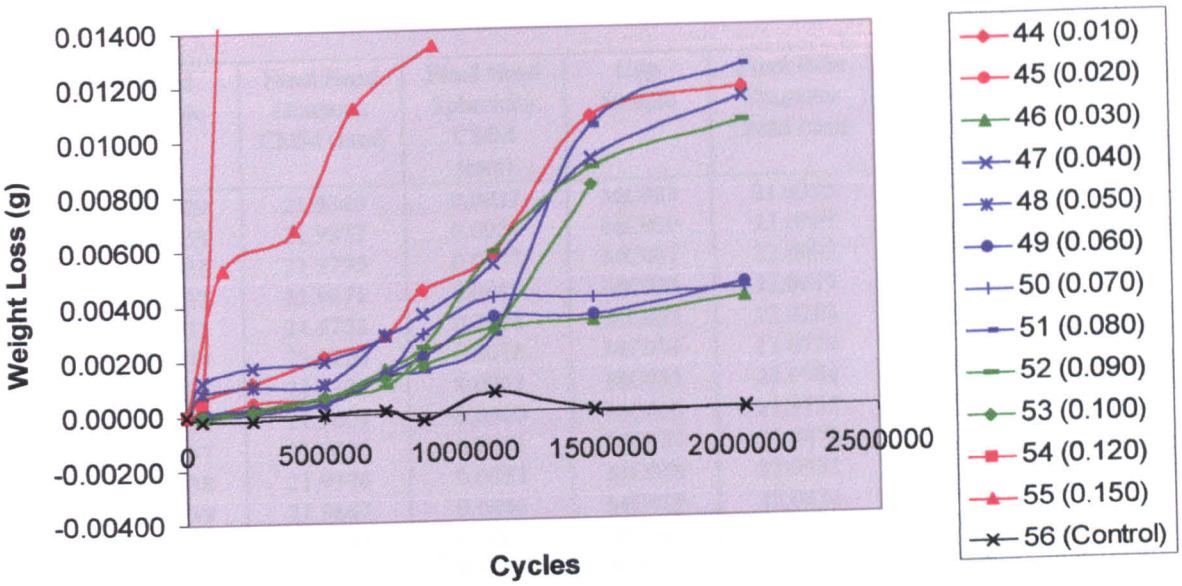

Figure 8.3: Replication of Figure 9.2

Figure shows weight loss against number of cycles of the hip simulator for the 35mm variable diametral clearance wear test samples as Figure 8.2 but with same scale as Figure 8.2 for easier direct comparison.

Sample Number	Head Size and Diametral Clearance (mm)	Test Information
MH/MC034	22 by 0.060	Fluid leak between 113825 and 462794 cycles: testing stopped
MH/MC036	22 by 0.080	Fluid leak between 113825 and 462794 cycles: testing stopped
MH/MC038	22 by 0.100	Lid loosened and some fluid lost between 1027502 and 1509464 cycles: very significant increase in wear rate
MH/MC044	35 by 0.010	Head interchanged with sample 54 and run for 418 cycles after 719401 cycles: increase in wear rate may be associated for sample 044
MH/MC048	35 by 0.050	Tie rod broke after 719401 cycles and fluid was lost: testing stopped
MH/MC050	35 by 0.070	Tie rod broke between 719401 and 857600: increase in wear rate may be associated
MH/MC054	35 by 0.120	Serum appeared dark at 237128 and 719401 measurements: very high wear occurred in the interval preceding these measurements. Head interchanged with sample 44 and run for 418 cycles after 719401 cycles: slight increase in wear rate may be associated for sample 044 though not obviously with sample 54
MH/MC055	35 by 0.150	Sample ran for only 1 million cycles separately to the remaining samples. Test stopped for timing purposes rather than failure.

Table 8.4

Problems encountered during the simulator wear test.

Head Sample	Final Head Diameter CMM (mm)	Final Head Sphericity CMM (mm)	Cup Sample	Final Bore Diameter CMM (mm)	Final Bore Sphericity CMM (mm)
MH029	21.9345	0.0027	MC029	21.9395	0.0025
MH030	21.9877	0.0023	MC030	22.0007	0.0019
MH031	21.9795	0.0037	MC031	22.0003	0.0021
MH032	21.9671	0.0019	MC032	22.0019	0.0021
MH033	21.9753	0.0024	MC033	22.0203	0.0022
MH034	22.0220	0.0018	MC034	22.0724	0.0047
MH035	22.0328	0.0053	MC035	22.0980	0.0017
MH036	21.9004	0.0040	MC036	21.9735	0.0041
MH037	21.9020	0.0034	MC037	21.9870	0.0025
MH038	21.9376	0.0053	MC038	22.0331	0.0017
MH039	21.9667	0.0046	MC039	22.0834	0.0029
MH040	22.0244	0.0062	MC040	22.1647	0.0069
Master Ball[1]	19.9826	0.0005	Master Ball[1]	19.9825	0.0002
MH044	34.9846	0.0020	MC044	34.9923	0.0020
MH045	34.9798	0.0023	MC045	34.9955	0.0027
MH046	34.9833	0.0020	MC046	35.0099	0.0022
MH047	34.9769	0.0029	MC047	35.0071	0.0060
MH048	35.0065	0.0038	MC048	35.0499	0.0034
MH049	35.0014	0.0039	MC049	35.0578	0.0017
MH050	35.0039	0.0036	MC050	35.0717	0.0029
MH051	35.0058	0.0044	MC051	35.0750	0.0018
MH052	35.0117	0.0064	MC052	35.0953	0.0020
MH053	35.0064	0.0125	MC053	35.1003	0.0052
MH054	35.0202	0.0143	MC054	35.1275	0.0018
MH055	34.9979	0.0095	MC055	35.1459	0.0026
MH056[2]	34.9888	0.0020	MC056[2]	35.1485	0.0029
Master Ball[1]	19.9825	0.00014	Master Ball[1]	19.9826	0.0003

[1]Master ball calibrated at 19.9823mm diameter
[2]Control sample not wear tested

Table 8.5

The geometry data of Table 9.2 repeated after completion of the wear test is presented.

Head Sample	Head Diameter (mm)		Reduction in Head Diameter (mm)	Cup Sample	Bore Diameter (mm)		Increase in Bore Diameter (mm)	Diametral Clearance (mm)	
	Initial	Final			Initial	Final		Initial	Final
MH029	21.932[1]	21.9345	-0.0025	MC029	21.943	21.9395	-0.0035	0.011	0.005
MH030	21.986[1]	21.9877	-0.0017	MC030	22.005	22.0007	-0.0043	0.019	0.013
MH031	21.976[1]	21.9795	-0.0035	MC031	22.005	22.0003	-0.0047	0.029	0.021
MH032	21.964[1]	21.9671	-0.0031	MC032	22.006	22.0019	-0.0041	0.042	0.035
MH033	21.973[1]	21.9753	-0.0023	MC033	22.020	22.0203	0.0003	0.047	0.045
MH034	22.020[1]	22.0220	0.0020	MC034	22.079	22.0724	-0.0066	0.059	0.050
MH035	22.031[1]	22.0328	-0.0018	MC035	22.100	22.0980	-0.0020	0.069	0.065
MH036	21.898[1]	21.9004	-0.0024	MC036	21.976	21.9735	-0.0025	0.078	0.073
MH037	21.899[1]	21.9020	-0.0030	MC037	21.990	21.9870	-0.0030	0.091	0.085
MH038	21.934[1]	21.9376	-0.0036	MC038	22.034	22.0331	-0.0009	0.100	0.096
MH039	21.964[1]	21.9667	-0.0027	MC039	22.086	22.0834	-0.0026	0.122	0.117
MH040	22.021[1]	22.0244	-0.0034	MC040	22.169	22.1647	-0.0043	0.148	0.140
MH044	34.984	34.9846	-0.0006	MC044	34.995	34.9923	-0.0027	0.011	0.007
MH045	34.981	34.9798	0.0012	MC045	35.000	34.9955	-0.0045	0.019	0.016
MH046	34.981	34.9833	0.0023	MC046	35.010	35.0099	-0.0001	0.029	0.027
MH047	34.976	34.9769	-0.0009	MC047	35.011	35.0071	-0.0039	0.035	0.030
MH048	35.005	35.0065	-0.0015	MC048	35.050	35.0499	-0.0001	0.045	0.043
MH049	35.001	35.0014	-0.0004	MC049	35.057	35.0578	0.0008	0.056	0.056
MH050	35.004	35.0039	0.0001	MC050	35.074	35.0717	-0.0023	0.070	0.068
MH051	35.005	35.0058	-0.0008	MC051	35.080	35.0750	-0.0050	0.075	0.069
MH052	35.011	35.0117	-0.0007	MC052	35.097	35.0953	-0.0017	0.086	0.084
MH053	35.005	35.0064	-0.0014	MC053	35.103	35.1003	-0.0027	0.098	0.094
MH054	35.016	35.0202	-0.0042	MC054	35.131	35.1275	-0.0035	0.115	0.107
MH055	34.996	34.9979	0.0019	MC055	35.143	35.1459	0.0029	0.147	0.148
MH056[2]	34.989	34.9888	0.0002	MC056[2]	35.151	35.1485	-0.0025	0.162	0.160

[1]Micrometer values only
[2]Control sample not wear tested

Table 8.6

Comparison of articulating surface geometry's pre and post testing.

Table 8.7 details the visual information gleaned from a visual inspection of the head and cup wear surfaces. Figures 8.4 and 8.5 show respectively the head and cup surfaces looking directly on the pole (represented by location of axis of symmetry on the bearing surface) of a selection of the test samples using a fluorescence marker technique developed by Ward (1996). Using this technique any scratches were shown up clearly on the shiny reflective surfaces along with any other features able to hold the fluorescent material applied to the surface. Some indications on the heads and cups were due to reflections from the lights used in the process and these include the eight thick, straight, short dashes which zigzag across the form in two distinct groups, as well as the bright

continuous ring shown in each cup. These features showed up most clearly in Figure 8.4c and 8.5f.

Head Sample	Diametral Clearance (mm)	Description of Surface Appearance
MH029	0.011	Surface generally remains mirror polished but covered in light scratches concentrated between 3mm below and about 6mm above the equator. These tend to be figure of 8 markings but generally missing the bottom loop. Towards the pole are fewer but more circular light scratches.
MH030	0.019	Surface appears as above except that some areas are covered with a thin milky film and there are a about 20 circular dents obviously created after testing due to the presence of raised lips around their perimeter. These latter marks must have been damage sustained subsequent to completion of testing.
MH031	0.029	Surface appears as above except that the scratches are fewer and concentrated above the equator with almost no scratches below, and with no surface damage.
MH032	0.042	As above
MH033	0.047	As above but with markings generally even more polar, only very slight evidence of milky film towards pole, and a few small dents.
MH034	0.059	Surface exhibits very heavy scratching from equator to within about a 3mm radius of the pole. Very few marks below the equator.
MH035	0.069	Scratching of surface is extremely light but milky deposit much more dense and concentrated in a 5mm band just above the equator and about 180 degrees around it.
MH036	0.078	Surface exhibits very heavy scratching from equator to within about a 3mm radius of the pole. Very few marks below the equator.
MH037	0.091	Extremely light scratching around the polar region and almost nothing elsewhere.
MH038	0.100	Light scratching of mirror polished surface only and concentrated in polar region. Some evidence of milky film also at pole.
MH039	0.122	Light scratching of mirror polished surface only and concentrated in polar region.
MH040	0.148	Relatively heavy scratching of mirror polished surface concentrated in polar region. Evidence of dense milky film in a 5mm band below the pole and extending about 180 degrees around the equator.

Table 8.7a

Information from a post test visual inspection of the 22mm wear test heads MH029 to MH040

Head Sample	Diametral Clearance (mm)	Description of Surface Appearance
MH044	0.011	Surface generally remains mirror polished but covered with light scratches, some extending almost to the edge of the bearing surface. Evidence of a thin milky film towards the pole.
MH045	0.019	Surface exhibits very heavy scratching from below the equator to the pole.
MH046	0.029	Virgin surface broken by just a few scratches of a heavier nature than usual on these sample. No scratches apparent below the equator.
MH047	0.035	Polished surface is broken only by a 5mm band of light but dense scratches at about 45 degrees from the pole and all the way round.
MH048	0.045	Evidence of extremely heavy scratching above the equator and heavy black deposits.
MH049	0.056	Extremely light scratching and concentrated around the pole. A few areas exhibiting the milky film.
MH050	0.070	Light scratching dispersed over much of the surface along with some areas of deposits above the equator. At least one linear dent consistent with damage done off the simulator either during or after the test.
MH051	0.075	Very minor and scattered scratching of polished surface with all scratches being above the equator.
MH052	0.086	Very minor and scattered scratching of polished surface with all scratches being above the equator. Some evidence of light deposits also above equator.
MH053	0.098	Surface extensively and heavily scratched from pole almost down to the edge of the bearing surface.
MH054	0.115	Heavy scratching all over the surface but with full figure of 8 scratches equi-spaced 8mm either side of the equator.
MH055	0.147	Heavy scratching concentrated at the pole along with some light figure of 8 scratching equi-spaced 8mm either side of the equator and over about 90 degrees around the equator
MH056 Control	0.162	Surface appears undamaged apart from a few light scratches and a few small dents.

Table 8.7b

Information from a post test visual inspection of the 35mm wear test heads MH044 to MH056

Cup Sample	Diametral Clearance (mm)	Description of Surface Appearance
MC029	0.011	Surface well covered with light to medium circular scratches from pole to equator. Milky film deposited over some areas of the surface.
MC030	0.019	Many light to medium circular scratches around the equator and extending to about a 5mm radius from the pole. The pole appears to have almost no scratches at all.
MC031	0.029	Surface well covered with light to medium circular scratches from pole to equator. Very light milky film deposited over some of the surface.
MC032	0.042	Surface well covered with light to medium circular scratches from pole to equator.
MC033	0.047	Surface well covered with light circular scratches from pole to equator.
MC034	0.059	Very heavy scratching all around circumferentially and out to the equator except for the polar region which remains relatively unscratched. Scratched areas also associated with milky deposit.
MC035	0.069	Light scratching present over most of bearing surface.
MC036	0.078	Heavy scratching evident over entire surface.
MC037	0.091	Light scratching present over most of bearing surface.
MC038	0.100	Light scratching accompanied by a very thin milky film present over most of bearing surface.
MC039	0.122	Fairly dense but light scratches over surface from pole to within about 3mm of equator
MC040	0.148	Fairly dense but light scratches over surface from pole to within about 3mm of equator along with some film deposits.

Table 8.7c

Information from a post test visual inspection of the 22mm wear test cups MC029 to MC040

Cup Sample	Diametral Clearance (mm)	Description of Surface Appearance
MC044	0.011	Scratches evident right out to the equator and medium severity though relatively sparse.
MC045	0.019	Very deep scratches over entire surface and quite dense.
MC046	0.029	Relatively few but medium severity scratches mostly within polar region.
MC047	0.035	Quite heavy and dense scratching located in a 12mm band centred at 45 degrees from the pole. Very few scratches at pole or towards equator.
MC048	0.045	Very heavy scratches and black deposits over most of surface but less around the equator.
MC049	0.056	Very light sparse scratching over surface and hardly any towards the equator.
MC050	0.070	Light but dense scratching over entire polar region up to about 45 degrees from pole but very few any closer to the equator.
MC051	0.075	Medium severity and dense scratching over entire polar region up to about 45 degrees from pole but very few any closer to the equator.
MC052	0.086	Very few medium severity scratches at pole.
MC053	0.098	Very heavy scratches and black deposits over entire surface.
MC054	0.115	Many medium severity scratches within polar region.
MC055	0.147	Many light scratches within polar region.
MC056 Control	0.162	Surface appears completely unscratched.

Table 8.7d

Information from a post test visual inspection of the 35mm wear test cups MC044 to MC056

As with the visual condition of heads reported from previous chapters, typical indications on couples which reached the end of the test with no failure of apparatus were light scratching superposed onto a still polished surface. Some apparently deeper scratches were generally evident though in much fewer numbers than the light "scouring" scratches. These phenomena are typical and expected from such a wear process where it is believed that particles are being removed from the surfaces and are likely then to make contact with other areas of surface and produce scratches consistent with the relative motions taking place under test conditions. Occasional dents in the surface of the heads are expected as a function of the many handling processes taking place during the test and perhaps more particularly after the testing was completed. From experience with these materials (even though they are relatively hard) the polished surfaces are damaged very easily by contact with other hard surfaces. It is not envisaged that these dents have affected the wear results to any large extent and none of the components showed such proliferation of these features as to lead to removal from the test. Only heads 054 and 055 showed any evidence of the figure of eight markings seen in previous tests and these

were only quite minor in the case of MH055. These markings, running from base to pole, indicate some contact with the edge of the cup bearing surface at its mouth were quite pronounced on MH054. Examination of mating cup MC054 showed no evidence of wear close to the rim as which is as expected for a couple with diametral clearance of 0.120mm. However it was noted from Table 8.4 that during the test, and for a brief period of 418 cycles, head 054 was accidentally coupled with MC044 creating a couple having a negative diametral clearance (-0.021mm). Examination of MC044 clearly showed the wear markings at the edge of the bearing surface consistent with the figure of eight markings on MH054. If the couple had been allowed to run for a longer period of time it is considered likely that it would have suffered the same fate as that of the negative clearance couples of chapter 6: catastrophic failure due to seizing. In fact the period of running was not sufficient, it would appear, to affect the wear performance of this couple or the alternate couple MH044/MC054 which ran for the same number of cycles with a positive clearance of 0.147mm.

From the visual analysis, as with previous tests in chapters 6 and 7, it was possible to make some crude judgement about the performance of the couples based on final visual appearance. For instance it has been shown above that certain markings such as figure of eight were generally only present when there was some geometrical or clearance problem with the test pieces. Complete failure of the parts for instance by dry running was always very easy to spot due to the extremely heavy nature of head and cup markings. Further, as diametral clearance increased from couple to couple there was some visual trend towards markings becoming less equatorial and more polar in concentration.

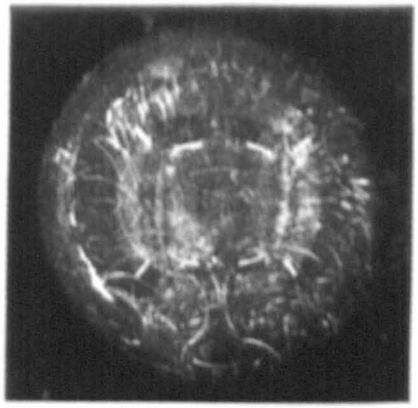

Fig 8.4a: MH029 22mm (0.011)

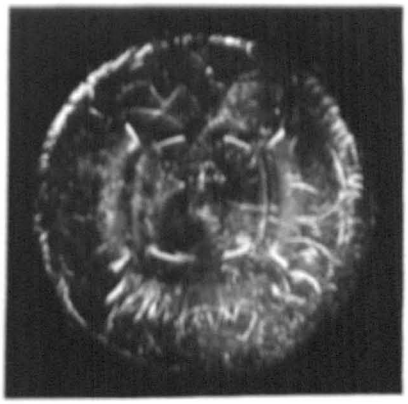

Fig 8.4b: MH046 35mm (0.029)

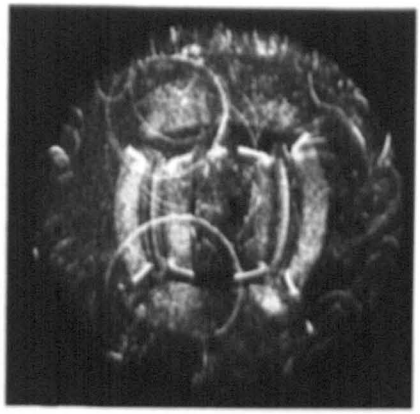

Fig 8.4c: MH033 22mm (0.047)

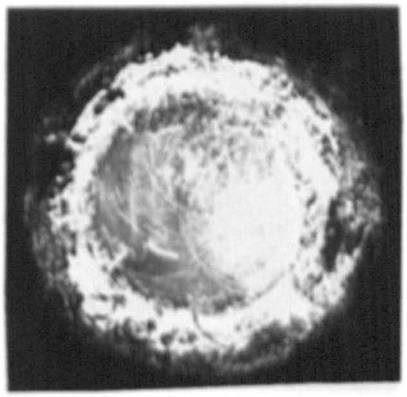

Fig 8.4d: MH048 35mm (0.045)

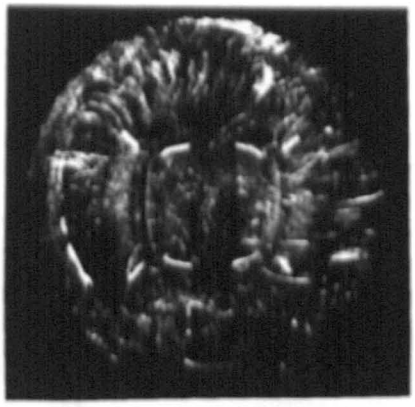

Fig 8.4e: MH036 22mm (0.78)

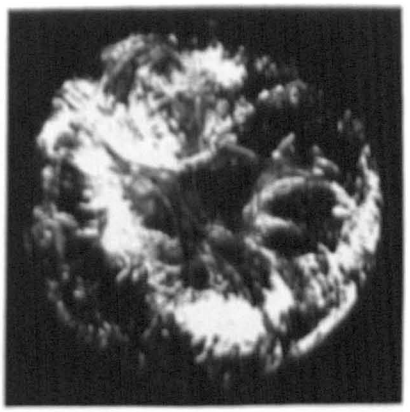

Fig 8.4f: MH055 35mm (0.147)

Figure 8.4: Fluorescing Photographs of Sample Heads

Figure shows a photograph for a selection of the sample heads taken looking directly on the pole. The fluorescence technique allows the condition of the articulating surface to be shown clearly. Heads are identified by head number and diametral clearance.

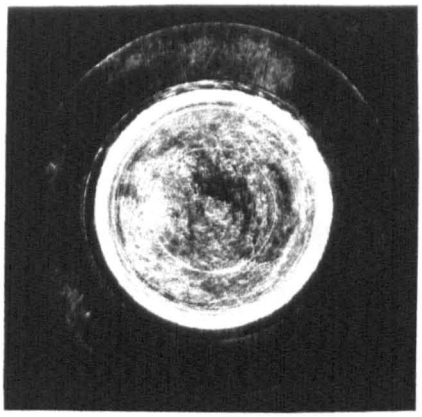

Fig 8.5a: MC029 22mm (0.011)

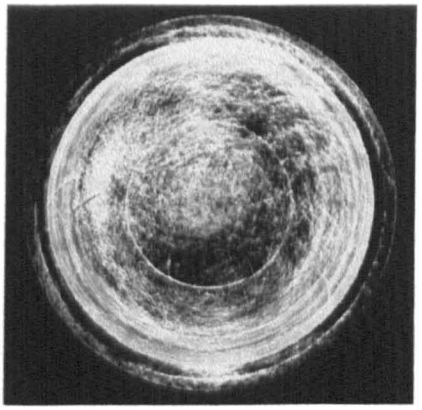

Fig 8.5b: MC046 35mm (0.029)

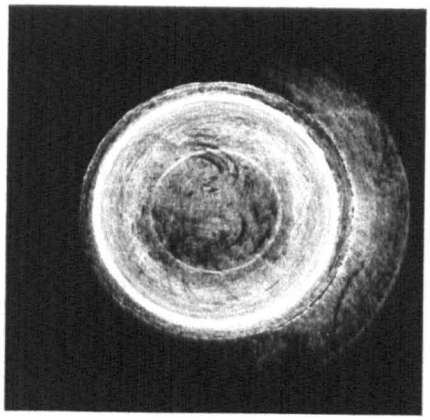

Fig 8.5c: MC033 22mm (0.047)

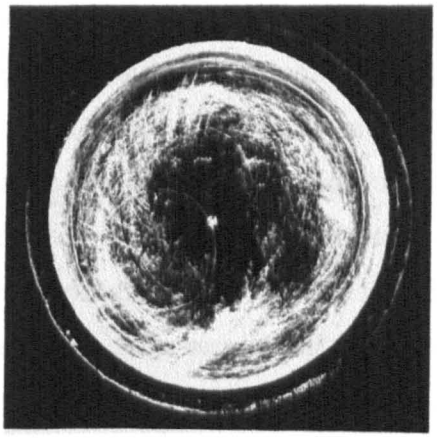

Fig 8.5d: MC048 35mm (0.045)

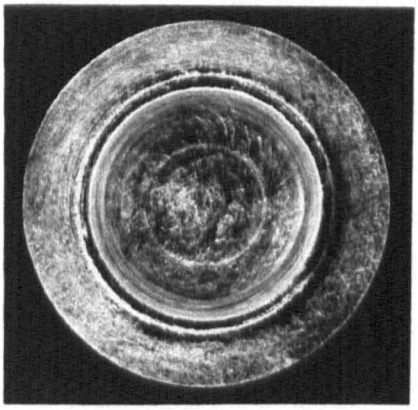

Fig 8.5e: MC036 22mm (0.078)

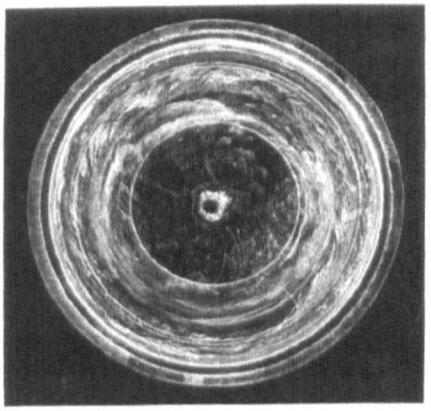

Fig 8.5f: MC055 35mm (0.147)

Figure 8.5: Fluorescing Photographs of Sample Cups

Figure shows a photograph for a selection of the sample cups taken looking directly on the pole. The fluorescence technique allows the condition of the articulating surface to be shown clearly. Cups are identified by cup number and diametral clearance.

8.8 Discussion

The biggest difference between pre and post test diameter measurements was an increase of 0.0042mm in diameter of a 35mm head and a reduction of 0.0066mm in diameter of a 22mm cup. Table 8.6 also shows that in almost every case the head size appeared to increase whilst the cup size appeared to reduce which would seem to be the opposite of what ought to occur. However, if consideration is given to the method of measuring the surface using a CMM, in the case of a head, a worn area would tend to produce a local flattening of the head which several CMM points may pick up at being part of a larger diameter than the initial surface (ie the local radius of curvature of the flattened area may be larger than that of the unworn area.). Regardless of the actual values, it is noted that changes in both size and roundness of the surfaces are extremely small and final roundness of most samples was within the design requirement of 0.005mm for virgin bearing surfaces. As a cross check from pre to post test size and form the control sample MH/MC056 had a maximum error on diameter between pre and post test results of 0.0025mm. This order of discrepancy is a reflection of the accuracy of the CMM.

From the visual evidence presented in chapter 6 compared with that of the current chapter, it was noted that for couples which successfully completed two million cycles of the simulator without significant test failures, the visual surfaces were quite similar regardless of head size within the range tested. This observation, whilst not entirely surprising illustrated that the same kind of lubrication conditions were applicable for all three head diameters. Indeed there appeared to be more sensitivity of visual indications to diametral clearance than head size for 22, 28, and 35mm samples. From the theoretical analysis of chapter 4 based on the work of Jin, Dowson, and Fisher (1997) the lubrication regime for a bearing couple of diametral clearance 0.060mm would fall within the mixed lubrication regime regardless of head size between 22 and 35mm. For diametral clearance of 0.010mm the theory predicts that the same couples would all be lubricated by a full fluid film and at a larger clearance of 0.100mm bearings with diameter less than about 25mm would be boundary whilst those above would be subject to a mixed lubrication regime. Since there is no step change in lubrication as one moves from boundary to mixed and from mixed to fluid film lubrication, then it is not surprising that the visual appearance of all samples was similar. If any difference in wear markings

should be seen, it would be between MH/MC038, 039, and 040 (22mm with diametral clearance of 0.100, 0.122, and 0.148 respectively) and MH/MC044, 045, and 046 (35mm with diametral clearance of 0.011, 0.019, and 0.029 respectively) where the former would be predicted to be boundary lubricated and the latter by full fluid film. However, no significant visual difference in appearance was noted. This possibly indicates that in practical reality, there would need to be a greater difference in diameter (say 10mm to 50mm diameter) to overcome the lack of sensitivity of the visual appearance to variation of head size.

With respect to performance, Figures 8.1 and 8.3 allow clear comparison of 22mm with 35mm. However, considering each test separately initially a number of observations were possible. Figure 8.1 shows that as with 28mm diametral clearance data of chapter 6, each sample exhibits, to a lesser or greater extent, the bedding in phenomenon described in chapter 6. Also, with the exception of couple MH/MC031, the final "steady state" wear rate approaching two million cycles is approximately the same for all samples. Thus once more it could be seen that the difference in total wear performance was established during bedding in, and once this phase was complete then the samples behaved similarly regardless of starting clearance. The colour coding on the figure is deliberate where the samples falling within the optimum clearance band for 28mm couples were coloured blue, those falling one or two increments outside the optimum band were green, and those with clearance considered to be quite suboptimal (low or high) were coloured red. Figure 8.1 clearly shows that, with a few exceptions, the samples are ordered through the test with blue being lowest, green medium, and red highest wear. For 22mm couples, a lower clearance limit of 0.030mm and an upper limit of 0.090mm would appear appropriate as it was for the 28mm samples. The mean optimum clearance would then be around 0.050 to 0.060mm. For the 35mm samples of Figure 8.3, the control couple (subjected to all the test steps except not articulated) demonstrates that the test method is not picking up spurious amounts of weight loss or gain with its 2 million cycle result being virtually zero wear. The 35mm samples did not appear to demonstrate the bedding in phase of wear so clearly demonstrated in all the previous tests. The reason for this remains unclear and especially since Chan et al (1996) showed that with a larger 45mm head size and the same simulator motion, this phase was exhibited in their test. It is also interesting to note that they used a different material

(ASTM F75) and had wear of around 0.03g at 2 million cycles which was considerably more than the testing of this chapter. Nevertheless, with respect to the other features of the wear curves, the outcome remains similar to that for 22 and 28mm samples. The order of samples through colour coding again shows that the more optimal blue couples demonstrate lowest, less optimal green higher, and the least optimal clearance red samples the highest wear. Therefore, for 35mm couples, a lower clearance limit of 0.030mm and an upper limit of 0.090mm would appear appropriate as it was for the 22 and 28mm samples.

Apart from a few samples which showed intervals of sudden high wear within an otherwise uneventful test such as MH/MC032, the only very discrepant sample was MH/MC054. Extremely high wear was measured in two separate test intervals coupled with darkening of the lubricating serum. There remains no full explanation of this event and since the next smaller and next larger clearance samples were seen to be closer to the average for the group then it has to be assumed that this was not a real phenomenon but an artifact of the test.

In order to compare the wear of the 22, 28, and 35mm diametral clearance samples more directly, mean data for samples within the range 0.030 to 0.090mm inclusive was compiled in Table 8.8 and shown in Figure 8.6. It should be understood that one difference between the three groups was that the 28mm components were made from low carbon cobalt chromium alloy whilst the 22 and 35mm components had high carbon cups articulating with low carbon heads. However, the data presented in Figure 7.3 would indicate that little real difference in wear performance would be attributed to this difference between the groups.

Cycles for 22mm	0	113825	462794	1027502	1509464	2076464			
22mm Mean Wear (g)	0.0000	0.00117	0.00211	0.00327	0.00497	0.00484			
Cycles for 28mm	0	20000	53110	107325	284975	605010	1157280	1609800	2028204
28mm Mean Wear (g)	0.0000	0.0018	0.0036	0.00328	0.00385	0.00418	0.00443	0.00463	0.0052
Cycles for 35mm	0	57415	237128	498418	719401	857600	1116825	1471677	2022343
35mm Mean Wear (g)	0.0000	0.00028	0.00052	0.00076	0.00178	0.00244	0.00413	0.00654	0.00789

For volumetric wear (mm^3) multiply the weight loss values by 120 for material density of $8331kg/m^3$

Table 8.8

22, 28, and 35mm diametral clearance variation wear test results for samples between 0.030 and 0.090mm diametral clearance inclusive. Note that the data point at 2026464 cycles for sample MH/MC031 was excluded since it exhibited an unusually high wear rate over the final interval.

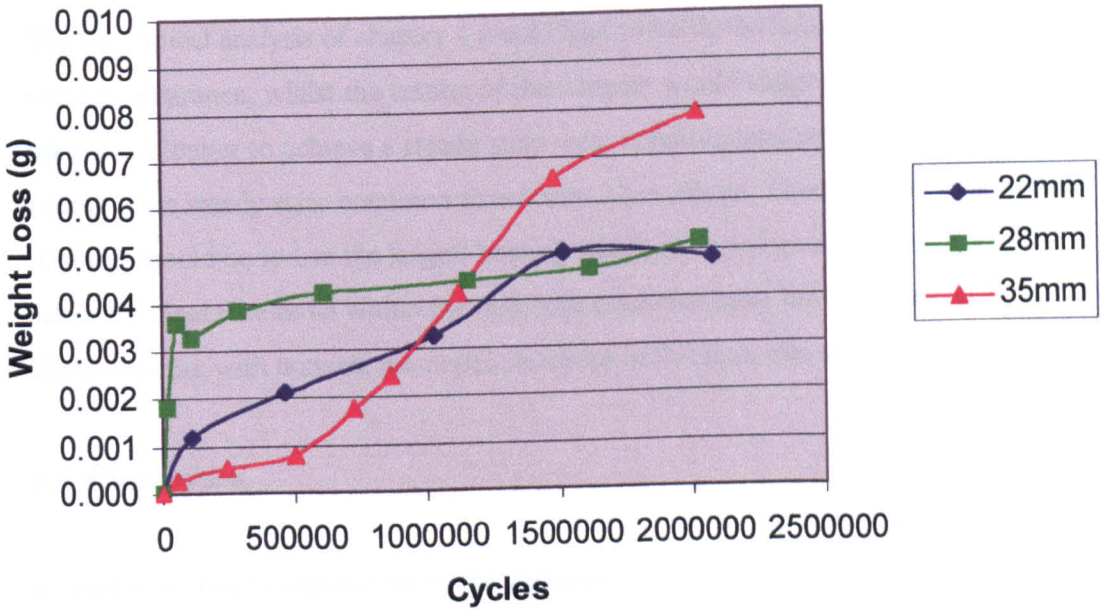

Figure 8.6: Mean Total Wear at 2 Million Cycles for 22, 28, and 35mm Samples

Figure shows mean weight loss against number of cycles of the hip simulator for the 22, 28, and 35mm variable diametral clearance wear test samples with diametral clearance between 0.03 and 0.09mm. Note that sample MH/MC031 excluded at final interval due to unusually high wear rate over final interval.

From Figure 8.6 it was clear that whilst the 28mm and 22mm samples appeared to have gone through the bedding in phase and into the steady state wear phase, the 35mm samples appeared to be exhibiting the higher wear rate associated with bedding in. Whilst at around two million cycles the wear of all three groups was similar, the figure indicates that at greater numbers of cycles a further divergence between the 22 and 28, and the 35mm couples could well have occurred. Unfortunately the test was not taken on to three million cycles to confirm this. The 22 and 28mm couples were seen from Figure 8.6 to be almost indistinguishable having similar mean wear at two million cycles and achieving a similar steady state wear rate. The 22mm samples however showed a less pronounced bedding in wear phase.

Being able to compare such wear test data for 22, 28, and 35mm couples allows a more informed choice of bearing diameter for a clinical metal on metal articulation. There are a number of clinical and commercial reasons for choosing 28mm above 22 or 35mm as well as the technical reasoning based on the data generated in this chapter along with chapter 4 and chapter 6.

The theoretical analysis of chapter 4 would lead towards the largest head size and the smallest clearance, whilst the testing of this chapter would suggest that 35mm bearings take much longer to achieve a steady state wear condition and produce more wear in reaching the steady state condition than either 22 or 28mm. Therefore the most robust solution should be to use the largest bearing which exhibited good performance and select the clearance to be within the optimum clearance band for minimum wear: a 28mm bearing with nominal diametral clearance of 0.05mm was preferred.

8.9 Conclusions

a. Post test visual examination of the surfaces of 22, 28, and 35mm couples demonstrated that all surfaces were similar in appearance. There was a greater variation in appearance with variation of diametral clearance than with head diameter.

b. The total wear for 22 and 35mm articulations after 2 million cycles on the hip simulator were similar to that for the 28mm articulations described in chapter 6.

c. The 35mm group of samples exhibited a different form of wear curve from that of the 22 and 28mm groups and at two million cycles had not achieved a steady state wear rate. This test should be continued to 3 million cycles to investigate at what point a steady state wear rate is achieved.

d. The optimum diametral clearance for 22mm and 35mm diameters was seen to be between about 0.05 and 0.06mm and was exactly as the optimum for 28mm articulations.

e. As with 28mm articulations, the test demonstrated the presence of a band of clearance within which wear could be minimized. This band was the same for 22, 28, and 35mm and lay between 0.030 and 0.090mm.

f. Based on the evidence of the testing to date there was no technical reason why a 28mm bearing with nominal diametral clearance of 0.05mm should not be taken forward to further testing with a view to development of a clinical product.

CHAPTER 9

Investigation of the Long Term Wear Performance of a Clinical Metal on Metal Product Design in a Hip Simulator Test

9.1 Introduction

Chapter 8 of this thesis demonstrated that the wear performance of 22 and 35mm metal on metal samples was similar to that of 28mm as presented in chapter 6, where all tests were performed on an MMED type hip simulator. Whilst the 35mm samples showed a poorer performance both in terms of total wear and final wear rate after a two million cycle test, there was almost nothing to choose between 22 and 28mm performance. Based on these results, whilst 35mm may have been shown to be less desirable, it would require consideration of factors other than the experimental wear results to allow a decision to be taken on which diameter to take through to a clinical product. The theory proposed by Jin, Dowson, and Fisher (1997) and discussed in chapter 4 suggested that the larger the head size for a given clearance the better the lubricating film thickness. It could be argued therefore that the 22mm diameter should be avoided and it remains unclear in that case why the 35mm samples did not perform better. However, for further factors in the decision to select one articulating diameter over the others, it was necessary to consider both clinical and commercial areas. Clinically there is thought to be some correlation between head size and dislocation rate, with smaller head sizes showing generally higher potential for dislocation as indicated for example by Courtois et al (1985). With a metal on metal design, dislocation is considered to be more serious than with a metal on polyethylene design due to the perceived greater damage likely to be done to the head bearing surface from contact with the face and rim of the metallic acetabular component. This would contraindicate the use of a 22mm diameter. From a commercial standpoint, the most commonly used head size is 28mm and could be considered the most easily accepted by the surgical community, as well as offering the opportunity to provide a single femoral head standard for both metal on metal or metal on polyethylene articulations. A 35mm diameter has the disadvantage of not easily allowing the articulation to be designed into an acetabular cup in the smaller acetabular size range (below 50mm). Sizes of acetabular cup less than 50mm are frequently

required with the most common sizes being 52 and 54, but with many product ranges offering cups down to 46, 44, and sometimes 42mm. These products are most demanded in the Asia/Pacific regions where average body size is smaller than elsewhere in the world. Product weight can also be a perceived problem with a joint replacement where a 35mm head or a larger sized 22mm acetabular cup could appear quite heavy in comparison to a surgeon's usual product.

Having considered the arguments it was decided that a product based on the 28mm articulation gave a reasonable security against dislocation, allowed acetabular cup sizes down to 48, with the possibility to introduce further sizes 46 and possibly 44 should a product prove successful through clinical investigation, and it was felt that the surgeon community would accept this as a reasonable diameter for such a device both in terms of familiarity with the size, and the weight of the head and/or cup elements. Further, a 28mm articulation had the backing of test results which demonstrated at least equivalent performance with any other head size tested and a body of theory which gave no reason to contraindicate its use.

9.2 Device Design

Laboratory testing which identifies an optimum metal on metal configuration for minimising friction and wear is of greatest value when it is possible to incorporate the features of such a configuration into a practical prosthetic design. Certainly some of the early metal on metal designs such as the McKee-Farrar (once the equatorial bearing issue was resolved) suffered from poor hip replacement design (cemented Thompson stem and cemented metal backed cup).

In the incorporation of the optimum 28mm articulation established through the foregoing chapters, into an acetabular cup design, the 5 essential goals of hip replacement had to be considered:-

Restoration of anatomy
Restoration of function
Relief of pain

Ease of implantation

Longevity

Therefore, a press fit, porous coated acetabular cup was proposed since clinical evidence points to such devices outperforming cemented acetabular devices. In this case the DePuy (Johnson and Johnson) S-ROM ZTT cup external form was used since this was considered to be a clinically proven design. This design also allows for up to 3 fixing screws to be used to fix the shell to the acetabulum should the initial press fit prove insufficient. The material for this part of the device (the Shell) was titanium alloy, where titanium is recognized as arguably the best metallic material of choice with respect to biocompatibility. In order to allow treatment of the majority of patients in the clinical investigation the shells were provided in sizes from 48 to 68mm with 2mm increments between. Sizes down to 46mm ought to be relatively easy to introduce at a later date if the investigation proved successful. To enable the use of the fixing screws and in order to allow for the use of a titanium alloy shell, the cup was necessarily to be configured in two parts. A cobalt chromium alloy insert incorporating the articulating geometry established through the foregoing chapters was therefore fitted into the titanium alloy shell. Since it was decided at an early stage of development that there was to be no polyethylene used in the design, to effect a positive lock between the shell and the insert it was decided to use the same method as used for locking modular heads onto hip stems: a taper fit. Theoretical investigation of taper angle led to a predicted optimum between 10 and 15°, and laboratory testing demonstrated the optimum value to be 10° total included angle (5° half angle). This choice of carefully controlled taper configuration was designed to allow secure fixation without loosening or relative motion whilst allowing disassembly using the appropriate instruments should that be required. Regarding corrosion between the mating taper surfaces, the clinical and experimental evidence from published papers indicated that well designed and properly assembled tapers do not suffer from corrosion of any significance even when mating surfaces of titanium alloy and cobalt chromium alloy were used. By creating a lip around the edge of the articulation surface of the insert, extra protection against dislocation was provided in the design, and as a further protection a 10° augmented insert was designed to be used in cases where the cup face was too steep as implanted. The augmented design was achieved simply by rotating the internal geometry of the standard design by 10° with

respect to the external insert geometry about an axis in the plane of the insert front face and blending the geometries together. One great benefit of using a taper lock between the parts was that the augmentation of the augmented insert could be positioned precisely where required with infinite rotational variability. The interface between the shell and insert was designed to ensure contact only between the male and female taper surfaces and so that the insert could not bottom out in the shell. The insert wall thickness varied but was generally of the order of 3mm, thus giving the possibility of greater compliance with the final design than had been the case with the semi infinite solid test pieces of the previous tests.

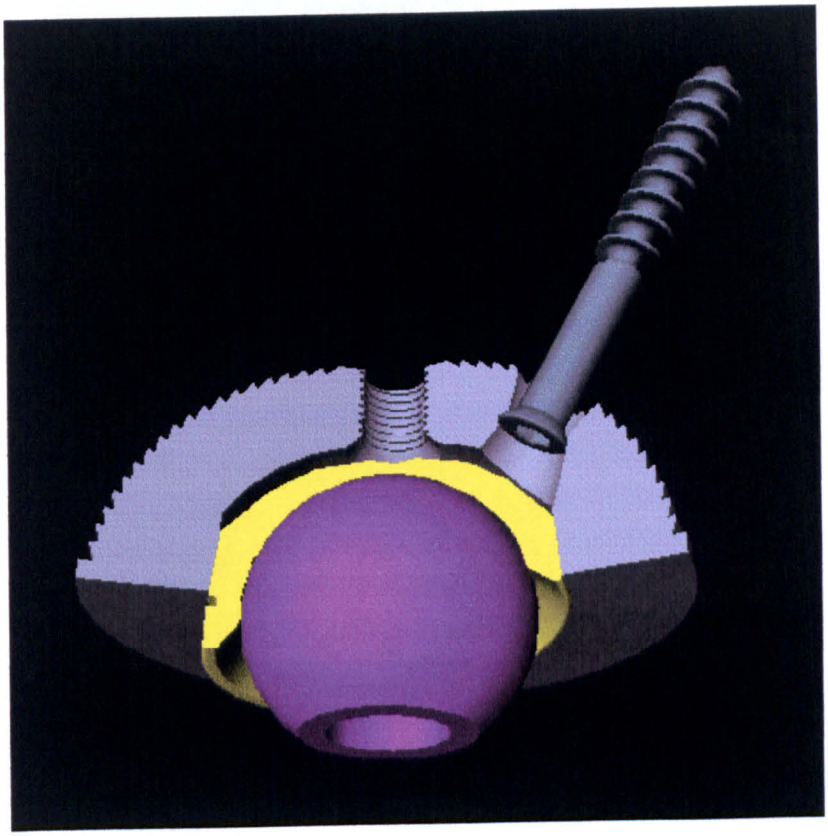

Figure 9.1: CAD Image of Metal on Metal Cup
Figure shows a partially cut away CAD model of a Metal on Metal shell, augmented insert, and femoral head.

The femoral head being an integral part of the design was carefully configured to provide a range of neck length offsets as well as embodying the all important male articulation geometry. Any stem within the company portfolio could be used with the metal on metal

device. Figure 9.1 shows a cut away view of the device showing the instance of an augmented insert and Figure 9.2 shows a photograph of the device along with typical cemented stem.

Figure 9.2: Photograph of Typical Metal on Metal Total Hip
Photograph shows a typical combination of the metal on metal cup with augmented insert coupled with a cemented TPS stem.

9.3 Method

A 12 station MMED hip simulator as described in detail in chapter 5 was used to investigate the wear performance of the clinical product in vitro. Samples of final design

metal on metal implants were selected for test utilizing the smallest acetabular cup size of 48mm. Six standard and six augmented inserts were to be tested. The titanium alloy shells were slightly different to the clinical product in that the porous coated beads were not applied to the external surface though each shell was nevertheless exposed to the sintering cycle. For purposes of holding the shells in the simulator, the shells were potted into a polyurethane resin.

The samples were tested to about 5 million cycles in bovine serum using the loading curve described by Paul (1967) at a maximum load of 2000N and a frequency of 1.1Hz. The mass of the samples was measured at intervals throughout the test using a balance capable of measuring to 10^{-5} gram.

9.4 Materials

For the purposes of this test, shells, heads, and inserts were prepared. The shells were size 48mm and selected to be manufactured from the design material Ti6Al4V to BS7252 Part 3 in accordance with the manufacturing drawing. The heads were manufactured from low carbon cobalt chromium alloy to ASTM F799 (now F1537) material, this being the standard used in the manufacture of femoral heads by Johnson and Johnson Orthopaedics. The inserts were manufactured from high carbon cobalt chromium alloy to ASTM F799 (now F1537). Table 9.1 details the relevant information relating to the materials used.

9.5 Test Pieces

Twelve samples were prepared for use in a single test on the 12 station hip simulator. The polished spherical head bearing surfaces were achieved using a special purpose Thielenhaus (Type: KF50F2; No 1.1.002453) microfinishing machine which utilized cylindrical tubular shaped stones for the metal removal process. The machine was equipped with an in process gauging system to enable femoral head diameter to be measured whilst machining with the stage 1 roughing stone. For the subsequent 3 stages up to and including the final polishing stone, control of diameter was only possible indirectly by setting a time limit for the contact of each stone with the workpiece. The

cup samples were microfinished using similar technology but by Ernst Thielenhaus manufacturers of the Thielenhaus equipment.

The test pieces were prepared to be as close as practically possible to the final implant design. The shells were of smallest size 48 and without porous coating though they were subject to the sintering cycle to replicate the material properties at the shell/insert interface. The inserts were per the final implant design with 6 standard and 6 augmented being used. The mating femoral head was a standard 12/14 taper +0 design (Johnson and Johnson Orthopaedics Product Code HO2011-28), except with specially controlled head diameter. The diametral clearance was aimed at 0.050mm.

The complete range of components used are detailed in Table 9.2 along with the materials and the dimensions of the articulating surfaces. All the components were marked so that the same orientation of head and cup could be maintained throughout the test regardless of the number of times they were separated for measurement of wear.

9.6 Pre Test Surface Finish

The pre test surface finish data is not shown for these parts as it was considered to be similar to the data shown in chapter 6, with typical Ra values around 0.01μm.

9.7 Results

The test was run for a total of 5195220 cycles of the hip simulator in accordance with the test method described previously. Measurements of wear were made as weight loss using the balance at suitable intervals throughout the test and as shown in Table B9.3. At each interval, prior to weighing, the samples were cleaned by a specially developed

Material Designation	VN87	EJ13
Used to Make	Cups	Heads
Material Designation on Carbon Content	High	Low
Material Supplier	Teledyne Allvac	Teledyne Allvac
Bar Diameter	43mm	28.6mm
Composition	(%wt)	
C	.197	.052
S		
Mn	.73	.71
Si	.09	.70
Cr	26.99	27.48
Mo	5.55	5.87
Co	Balance	Balance
Ti		
Fe	.12	.37
Ni	.49	.44
N	.0962	.177
P		
W		
Condtion	As rolled	As rolled
Surface	Centreless ground	Centreless ground
Hardness (HRc)	43/45	N/A
Grain Size[1]	Avg ASTM 10	Avg ASTM 11
Test Pieces		
UTS (MPa)	1221/1260	1320/1341
0.2% Yield (MPa)	907/963	1013/1017
El%	17.5/17.2	21.2/24.5
RA%	11.9/13.1	18.8/18.5
Hardness (HRc)	42	40.8

[1] ASTM E112, 1996

Table 9.1

Material details for the final design wear test samples.

Head/Cup Sample Number MH/MC	Shell Number MS	Insert Type	Head Diameter CMM (mm)	Head Sphericity CMM (mm)	Bore Diameter CMM (mm)	Bore Sphericity CMM (mm)	Diametral Clearance (mm)
100	MS14	Aug	27.994	0.0029	28.051	0.0044	0.057
101	MS01	Aug	27.937	0.0036	28.003	0.0027	0.066
102	MS02	Aug	28.102	0.0043	28.143	0.0064	0.041
103 Control	MS03	Aug	28.065	0.0061	28.117	0.0019	0.052
104	MS13	Aug	28.023	0.0032	28.071	0.0034	0.048
105	MS05	Aug	27.923	0.0054	27.985	0.0042	0.062
106	MS06	Aug	28.239	0.0032	28.283	0.0034	0.044
107	MS07	Std	28.025	0.0042	28.070	0.0059	0.045
108	MS08	Std	28.038	0.0034	28.090	0.0041	0.052
109	MS09	Std	27.979	0.0033	28.036	0.0046	0.057
110	MS10	Std	27.927	0.0027	27.986	0.0047	0.059
111	MS11	Std	28.075	0.0024	28.135	0.0042	0.060
112	MS12	Std	27.947	0.0033	28.006	0.0046	0.059
113Control	MS04	Std	27.932	0.0023	27.991	0.0033	0.059
Master Ball[1]			19.976	0.0012	19.976	0.0012	

[1]Master ball calibrated at 19.9776mm diameter

Table 9.2

Insert type and geometrical bearing surface details of the test piece samples for the final design wear test.

process as described fully in chapter 5 and which was aimed at removing any adhered substances on the one hand but not removing any metallic substrate material on the other. The samples were divided into 2 equal groups of 6 samples (3 standard and 3 augmented insert) and one group disassembled for weighing at regular intervals throughout the test whilst the other was not disassembled between 1149800 and 5195220 (approximately 4 million cycles). This was done so that for 6 samples the effect of 4 million cycles without disturbance in a physiological fluid under hip simulator cyclic loading conditions could be studied in relation to the behaviour of the taper fit interface and specifically its resistance to fretting and corrosion.

The wear data is summarized in Tables B9.3 and total wear presented in Figure 9.3. Figure 9.3 shows the wear curve for each individual sample but Figure 9.4 shows the mean curve for the standard and augmented insert. Note that in Figure 9.3 the bedding in phenomenon, where initially high wear gives way to a much lower steady state wear, was clearly visible. Note also that in Figure 9.4 the error bars for some data points were rather large primarily due to the small numbers (2 or 3) in the sample. The error bars for

the other data points having 5 or 6 test pieces in the sample were considered more representative of the true population. Only the latter error bars are shown in Figure 9.4.

After completion of the test, the samples were re-measured using a CMM and the relevant data is presented in Table 9.4. Table 9.5 compares pre and post test diameters and clearances for each sample.

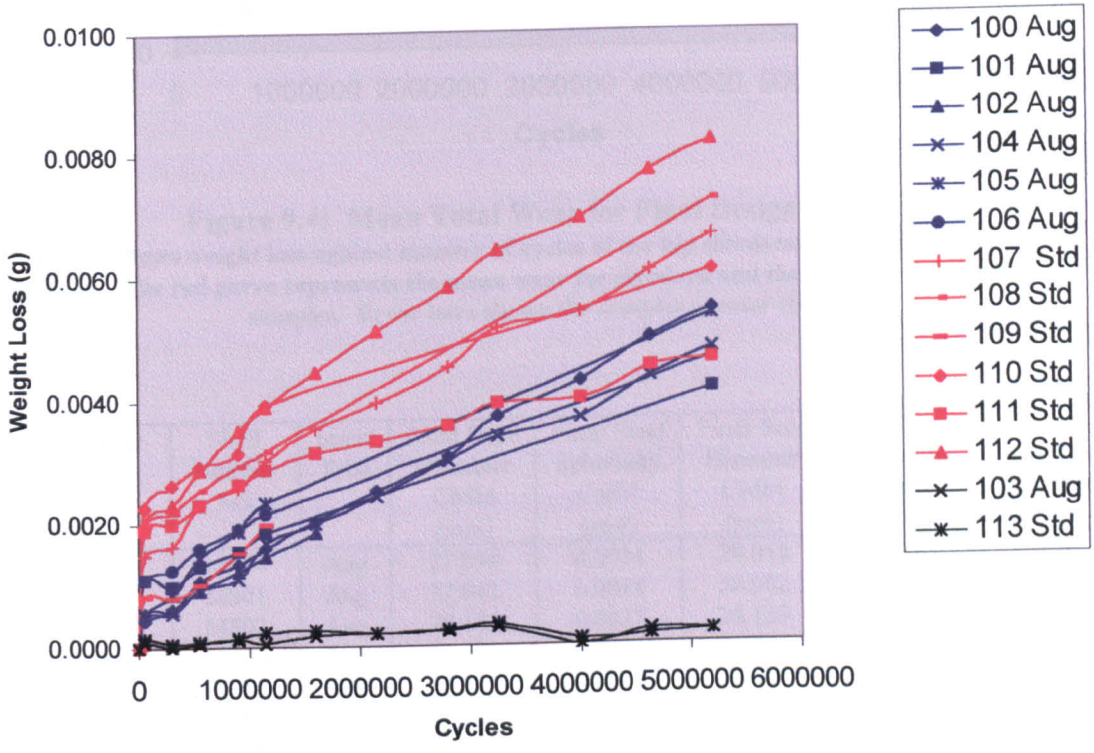

Figure 9.3: Total Wear for Final Design Samples

Figure shows weight loss against number of cycles of the hip simulator for the final design test samples. The red curves represent standard and the blue curves augmented samples. The black curves represent the control samples.

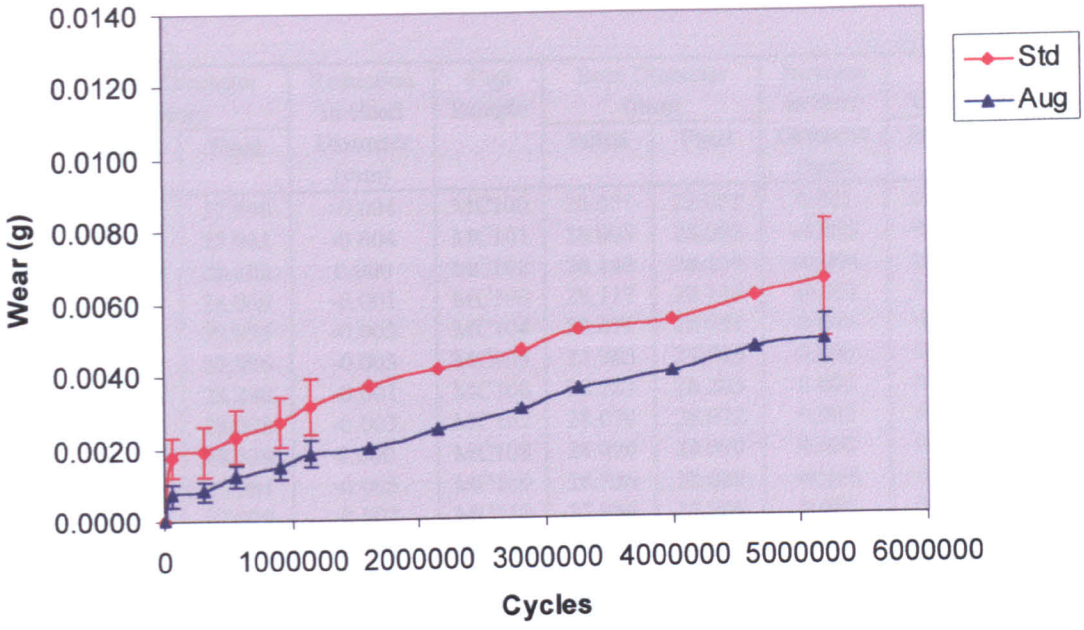

Figure 9.4: Mean Total Wear for Final Design Samples

Figure shows weight loss against number of cycles of the hip simulator for the final design test samples. The red curve represents the mean wear for standard and the blue curve for augmented samples. Error bars shown for samples greater than 4.

Head/Cup Sample Number MH/MC	Shell Number MS	Insert Type	Final Head Diameter CMM (mm)	Final Head Sphericity CMM (mm)	Final Bore Diameter CMM (mm)	Final Bore Sphericity CMM (mm)	Final Diametral Clearance (mm)
100	MS14	Aug	27.998	0.0034	28.052	0.0030	0.054
101	MS01	Aug	27.941	0.0014	28.002	0.0023	0.061
102	MS02	Aug	28.102	0.0027	28.139	0.0013	0.037
103 Control	MS03	Aug	28.066	0.0040	28.115	0.0019	0.049
104	MS13	Aug	28.025	0.0014	28.071	0.0014	0.046
105	MS05	Aug	27.926	0.0022	27.985	0.0024	0.059
106	MS06	Aug	28.240	0.0036	28.285	0.0008	0.045
107	MS07	Std	28.028	0.0033	28.072	0.0026	0.044
108	MS08	Std	28.038	0.0027	28.090	0.0042	0.052
109	MS09	Std	27.984	0.0055	28.020	0.0109	0.036
110	MS10	Std	27.929	0.0027	27.986	0.0025	0.057
111	MS11	Std	28.074	0.0029	NA[2]	NA[2]	NA[2]
112	MS12	Std	27.950	0.0049	28.006	0.003	0.056
113Control	MS04	Std	27.933	0.0018	27.993	0.0032	0.063
Master Ball[1]			19.9828	0.0013	19.9826	0.0010	

[1]Master ball calibrated at 19.9823mm diameter

[2]NA since part lost

Table 9.5

The geometry data of Table 9.2 repeated after completion of the wear test is presented.

Head Sample	Head Diameter (mm)		Reduction in Head Diameter (mm)	Cup Sample	Bore Diameter (mm)		Increase in Bore Diameter (mm)	Diametral Clearance (mm)	
	Initial	Final			Initial	Final		Initial	Final
MH100	27.994	27.998	-0.004	MC100	28.051	28.052	0.001	0.057	0.054
MH101	27.937	27.941	-0.004	MC101	28.003	28.002	-0.001	0.066	0.061
MH102	28.102	28.102	0.000	MC102	28.143	28.139	-0.004	0.041	0.037
MH103	28.065	28.066	-0.001	MC103	28.117	28.115	-0.002	0.052	0.049
MH104	28.023	28.025	-0.002	MC104	28.071	28.071	0.000	0.048	0.046
MH105	27.923	27.926	-0.003	MC105	27.985	27.985	0.000	0.062	0.059
MH106	28.239	28.240	-0.001	MC106	28.283	28.285	0.002	0.044	0.045
MH107	28.025	28.028	-0.003	MC107	28.070	28.072	0.002	0.045	0.044
MH108	28.038	28.038	0.000	MC108	28.090	28.090	0.000	0.052	0.052
MH109	27.979	27.984	-0.005	MC109	28.036	28.020	-0.016	0.057	0.036
MH110	27.927	27.929	-0.002	MC110	27.986	27.986	0.000	0.059	0.057
MH111	28.075	28.074	0.001	MC111	28.135	NA[1]	NA[1]	0.060	NA[1]
MH112	27.947	27.950	-0.003	MC112	28.006	28.006	0.000	0.059	0.056
MH113	27.932	27.933	-0.001	MC113	27.991	27.993	0.002	0.059	0.060

[1] Not available since part lost

Table 9.6

Comparison of articulating surface geometry pre and post testing.

As with the previous testing, there were some problems with the execution of the tests in this chapter. Table 9.7 details some of the problems which occurred during the course of the test. In both cases of test failure the samples were lost and could not continue the test due to the severity of damage done by the period of dry running.

Sample Number	Test Information
MH/MC102	Sample lost due to fluid leakage and dry running along with tie rod failure
MH/MC109	Sample lost due to fluid leakage and dry running along with tie rod failure

Table 9.7

Problems encountered during the simulator wear test.

Tables 9.8a and b detail the information gathered from a visual analysis of the post test surfaces. Typical indications on couples which reached the end of the test with no failure of apparatus were light scratching superposed onto a still polished surface. Some apparently deeper scratches were generally evident though in much fewer numbers than the light scratches. These phenomena were typical and expected from such a wear process where it is believed that particles are being removed from the surfaces and are

likely then to make contact with other areas of surface and produce scratches consistent with the relative motions taking place under test conditions. Occasional dents in the surface of the heads were expected as a function of the many handling processes taking place during the test and perhaps more particularly after the testing was completed It is not envisaged that these dents have affected the wear results to any large extent. Perhaps most significantly however, the wear markings on these final design samples were indistinguishable from those of the previous samples tested, which thus demonstrated that the wear mechanism of the bearing was not upset by moving from the semi infinite solid test piece geometry to the final design geometry. Two samples showed extremely heavy markings which was consistent with them having failed due to simulator breakdown during the test.

Head Sample	Description of Surface Appearance
MH100	Surface remains mirror polished but with a few generally light scratches superimposed. These are most exclusively around the polar region.
MH101	As above but scratches even less pronounced.
MH102	Extremely heavy wear from about 45 degrees from equator to the pole. This is characterized by an annular band of concentric circular scratches running parallel to the equator.
MH103	Head is almost virgin. Very light scratching or scuffing is evident probably consistent with storage than any wear processes. One small dent evident near the pole.
MH104	Greater number of curving light scratches around polar region with a series of much heavier, linear scratches all parallel, close to each other, and oriented radially.
MH105	A large number of medium depth and short curved scratches cover the region above the equator almost as if it has been randomly scoured. Below the pole the surface remains almost virgin.
MH106	As above but with some longer and more pronounced curving scratches around the pole. Some light circumferential scratches also present blow the equator and with three or so linear bands of scratches directed from base to pole ending around the equator and being light in nature.
MH107	Similar to above but with milky discoloured patch at pole to about 30 degrees from pole.
MH108	As above but with the polar scratches being deeper.
MH109	Extremely heavy wear at MH102 but with band of concentric wear circles extending from equator to the pole with a very deep polar recess complete with central pip.
MH110	As MH100
MH111	As above but with milky discoloured patch at pole about 30 degrees from pole.
MH112	Mirror polished surface as MH100 with some circular scratches at the pole and at least one relatively deep dent near the pole.
MH113	Almost virgin surface from base to pole but with very light circular scratches around polar region.

Table 9.8a

Information from a post test visual inspection of the wear test heads MH100 to MH113

Quite strangely the control sample cups MC103 and MC113 showed very fine overlapping scratches which completely obliterated the polished surface. In both cases the mating head was virtually virgin. The reason for the cup marking was unclear.

Head Sample	Description of Surface Appearance
MC100	Deep spiral scratches from just below edge of bearing surface to about 20 degrees from the pole.
MC101	As above but with one small but very heavy patch of scratching at about 45 degrees from pole and about 2mm wide by 10mm long running circumferentially.
MC102	Extremely heavy wear over almost all the bearing surface except a 1 to 2mm band around the edge of the bearing surface. There is also heavy scoring of the chamfer surface leading into the bearing surface and also to the rim of the cup.
MC103	The polished surface is completely obscured in the polar region to about50 to 60 degrees from the pole by a large number of light overlapping and curved scratches as if heavily scoured. Around the bearing surface edge the surface remains almost virgin.
MC104	Entire surface covered with quite deep heavy scratches out from pole right to edge of bearing surface.
MC105	Surface covered with relatively light scratches out from pole and stopping short of the edge of the bearing surface.
MC106	As above.
MC107	As above but with polar patch of milky discolouration extending to about 30 degrees from pole. Centre of this patch at pole is clear and virgin mirror polished surface about 5mm in diameter. Around the edge of the bearing surface a clear pattern of fine criss cross scratches is evident consistent with the microfinishing process used in manufacture. These marks are normally polished out but in this case have remained.
MC108	Surface covered with heavy scratches except a 5mm diameter patch offset slightly from pole which appears completely virgin. Milky discolouration visible offset fom pole in opposite direction and about 10mm wide by 15mm long.
MC109	Extremely heavy wear over almost all the bearing surface except a portion at one side over about 90 degrees and of maximum width of about 5mm in the centre and thinning to nothing at its ends. The wear is composed of annular rings with central pip about 20 degrees from the pole.
MC110	Mirror polished surface entirely intact with a few light to medium scratches over the surface.
MC111	Cup missing.
MC112	As MC110 but with some fine microfinishing marks still visible near to the edge of the bearing surface.
MC113	The polished surface is completely obscured in the polar region to about50 to 60 degrees from the pole by a large number of light overlapping and curved scratches as if heavily scoured. Around the bearing surface edge the surface remains almost virgin.

Table 9.8b

Information from a post test visual inspection of the wear test inserts MC100 to MC113

9.8 Discussion

As with some of the other tests, there was typically an increase in head diameter between pre and post test measurements on the CMM and a reduction in bore diameter. Once again as in chapter 8, this may have been due to the local radius of curvature changes

between new and worn surfaces as measured by the CMM rather than an actual increase of head or decrease of bore size. Apart from those components which failed during the test and were severely damaged, the largest absolute change in diameter of any component after 5 million cycles was 0.004mm. It was also notable that for the control parts which were not worn, the maximum apparent change in diameter was 0.002mm and thus represents the limits of accuracy of the CMM. The post test sphericity values for all specimens except those which failed, was below the 0.005mm allowance for pre test parts. Therefore bearing surface size and form were altered only fractionally through the 5 million cycle test.

From visual inspection of post test bearing surfaces it was clear that there was no noticeable difference between the appearance of the present samples compared with the samples tested in previous chapters and particularly chapter 7. This supports the idea that incorporating the bearing surface into a clinical prosthetic device design would not change the performance of the bearing couple. Further, it was noted that from the same visual inspection there was no noticeable difference in appearance of standard compared with augmented inserts.

With respect to wear performance it was shown, as demonstrated in Figure 9.4, that there was a significant difference between the standard and augmented test pieces. Further, since both groups of samples appeared to have the same steady state wear rate then the difference in wear performance was seen to be totally due to differences in bedding in of the 2 groups. The only explanation available is that in rotating the bearing surface of the standard insert around by 10° with respect to the external surface to create the augmented insert design, the mechanics of the design was also changed. Considering the actual differences between the two constructs as loaded into the simulator during testing, there appears to be only differences in stiffness which could reasonably be expected to produce a difference in wear performance. Practically speaking though the difference whilst apparently significant was actually quite slight and not of any great consequence clinically.

Considering the wear performance of the clinical device with that of the semi infinite solid test pieces used in previous testing, Figure 9.5 shows the data of Figure 9.4 but

with an extra wear curve representing the mean wear for the high/low and low/high carbon content samples of chapter 7 as shown in table B9.9. From the figure it was clear that the differences between the 3 curves was not of practical clinical significance. Indeed there was clearly a greater difference in performance between standard and augmented final design samples than between the final design samples and the samples of chapter 7. This demonstrates the successful incorporation of the optimum bearing surface developed using the semi infinite solid style test piece of Figure 6.1a into the clinical design as shown in Figure 9.1.

In comparison of the wear rates obtained in this test with the rates obtained using the same simulator for metal on polyethylene bearings as presented by Farrar, Schmidt, Hamilton, and Greer (1997) it was clear that the rates for the metal on metal articulation are much lower than that for either form of polyethylene as demonstrated in Figure 9.6. The metal on metal final design wear rate was 0.109 mm^3/million cycles for standard and 0.094mm^3/million cycles for augmented inserts taken between 553550 and 5195220 cycles. The equivalent figure for metal on polyethylene taken through a 2 million cycle test was 30mm^3/million cycles for a standard grade of material sterilized by gamma irradiation in air and 10mm^3/million cycles for a calcium stearate free grade of material sterilized in a vacuum packed foil pouch. The latter value demonstrated the order of improvement which has taken place in the wear performance of polyethylene bearing materials through the latter half of the 1990's.

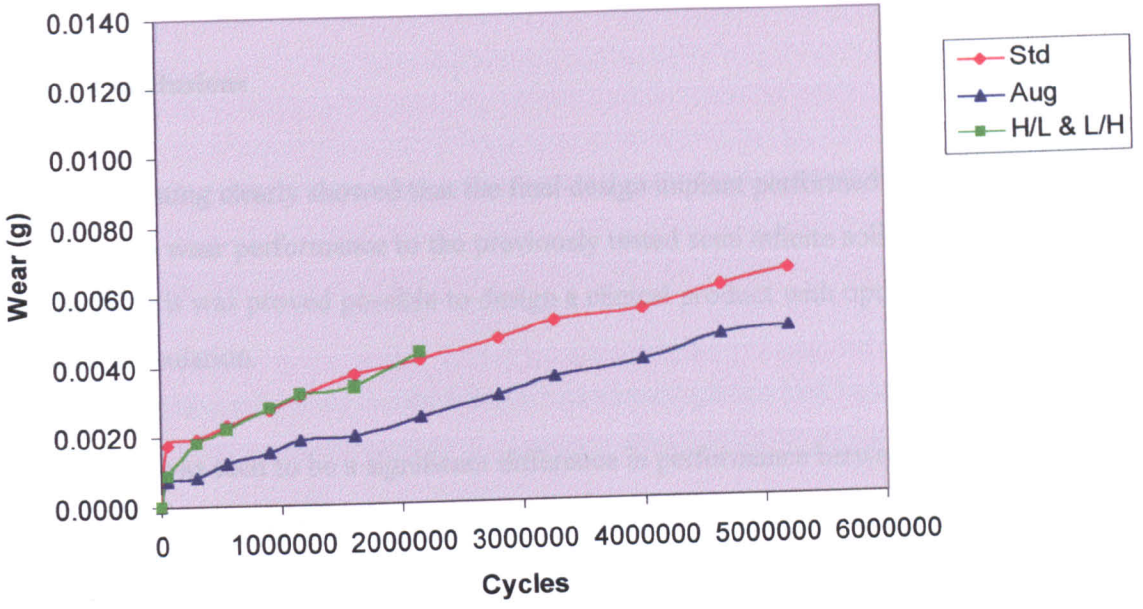

Figure 9.5: Mean Total Wear for Final Design Samples Compared to Previous Test

Figure shows weight loss against number of cycles of the hip simulator for the final design test samples compared to the same data for the high/low and low high carbon content test samples of chapter 7. The red curve represents the mean wear for standard and the blue curve for augmented samples and the green curve for the samples of chapter 7.

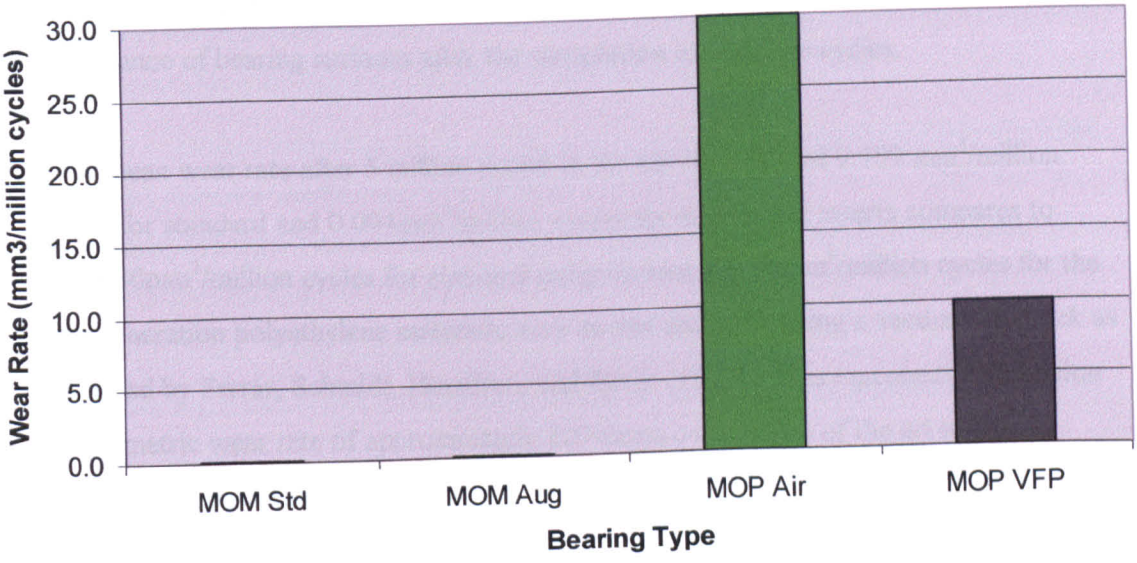

Figure 9.6: Wear Rate for MOM against that for MOP

Figure shows the wear rate for metal on metal designs compared with those for metal on polyethylene articulations either sterilized by gamma irradiation in air or in a vacuum foil pouch.

9.9 Conclusions

a. The testing clearly showed that the final design implant performed similarly with respect to wear performance to the previously tested semi infinite solid test samples. Therefore it was proved possible to design a clinical product with optimized metal on metal articulation.

b. There was seen to be a significant difference in performance between the standard and the augmented samples.

c. The size and form of post test bearing surfaces was only fractionally different to the pre test values (not including failed specimens) with maximum diameter change of 0.004mm and all parts meeting the 0.005mm pre test roundness limit. Therefore the test did not have a significant effect upon the geometry of the bearing surfaces.

d. The standard and augmented samples were seen to exhibit indistinguishable visual appearance of bearing surfaces after the completion of 5 million cycles.

e. A mean wear rate after 5 million cycles in the hip simulator of 0.109 mm^3/million cycles for standard and 0.094mm^3/million cycles for augmented inserts compares to about 30mm^3/million cycles for standard polyethylene and 10mm^3/million cycles for the new generation polyethylene materials such as that sterilized using a vacuum foil pack as described by Farrar, Schmidt, Hamilton, and Greer (1997). This represents a reduction in volumetric wear rate of approximately 100 times over a state of the art metal on polyethylene articulation.

CHAPTER 10

Conclusions of the Study, Discussion, and Recommendations for Further Work

10.1 Introduction

Metal on metal articulations were demonstrated through the 1960's and 70's to perform adequately and comparably to metal on plastic articulations being used at the same time. Through the late 1980's and the 1990's the concept of metal on metal bearings re-emerged as one potential solution to the long term clinical problems associated with polyethylene particle induced osteolysis in metal on polyethylene bearings. However, it is important that engineers and scientists optimise the design of metal on metal articulations for minimum bearing wear prior to clinical use, in order to extend the clinical lifetime of the prostheses. The main original contributions of this thesis are:-

a. The discovery that wear is strongly related to bearing clearance in practical tests.
b. That a lower limit of clearance exists due to deviations from perfect form which are unavoidable with current manufacturing technology.
c. That a band of clearance could be defined for 22, 28, and 35mm diameter bearings within which reduced wear is exhibited.
d. That steady state wear rates following the initial bedding in period, for the same head size with different diametral clearances, are generally equal regardless of total wear volume. Therefore starting clearance becomes less important if a non spherical geometry can be developed to mimic the bedding in phenomenon.
e. That high carbon against high carbon content cobalt chromium articulations do not produce the lowest wear contrary to previous studies in the literature.
f. That hardness difference between bearing surfaces may influence the wear performance of metal on metal articulations. This led to a patent application on the concept of a differential hardness ceramic on metal joint and an investigation by Firkins et al (August 2000).
g. That, using the above research findings, it was possible to design a clinical metal on metal bearing having modular femoral (head and stem) and acetabular (insert and shell) components with optimized metal on metal articulation.

10.2 Discussion

During the time that the work described in this thesis was being conducted and subsequently, other workers as well as the author himself have continued to explore the area of hard on hard (metal on metal, ceramic on ceramic, etc.) articulations. The most relevant of this work is discussed in the context of the research findings of this thesis.

Scott and Schroeder (1997) studied radial clearance in metal on metal articulations and produced results which supported the findings presented here. They showed bedding in and steady state wear rates consistent with the work in this thesis and also that as clearance was reduced, wear was also reduced. They did not show an increased weight loss at very small clearances as in the present work but did mention that this may occur.

In chapter 7, it was shown that contrary to the suggestions of other authors, there was no significant advantage in bearing couples where both surfaces were made from high carbon cobalt chromium alloy. However, during analysis of the data generated through simulator testing of high and low carbon samples, a general though not clear trend towards lower wear was observed with both increased mean hardness of the head and cup and increased differential hardness between the head and cup. It was recommended that a further study be carried out with a minimum of 10 HRC points difference between the head and cup. This concept lead to the invention of the ceramic on metal couple with patent applied for by Mr R Farrar and Professor J Fisher and to a ceramic on metal wear testing programme by Firkins et al (February 2000 and August 2000) . This testing lead to the conclusion that *"The differential hardness COM (ceramic on metal) pairings tested in this study showed dramatic reduction in wear rate, compared to MOM (metal on metal) pairings tested."* (Firkins et al, August 2000). Hence, the present work has lead to a program of further work which shows substantial potential for the further reduction of wear in hard on hard bearing systems.

In Chapter 7 it was shown that under certain configurations of bearing, when the wear patch reaches the lip of the cup, a high wear result may be obtained. In this case the edge contact was due to a manufacturing defect discovered through testing and led to

the recommendation of some design rules in relation to hard on hard articulation design. This is in direct agreement with the findings of Firkins (February 2000) who discovered that higher wear rates resulted when the head encroached onto the edge of the cup articulating surface during hip simulator testing. Furthermore, Nevelos et al (2000) have attempted to better simulate the wear marks seen on clinical ceramic on ceramic articulations by allowing the head to separate from the cup during the swing phase of the simulator gait cycle. This technique has produced higher wear in ceramic on ceramic articulations in vitro than was previously found and could be applied as a more severe test of metal on metal joints. In that case the edge contact phenomenon may be more likely and designers of clinical products may need to take these things into account. However, Dennis et al (2000) used fluoroscopy to demonstrate that whilst metal on polyethylene articulations show such separation of head from cup during clinical gait, such a phenomenon was far less pronounced if it occurred at all with a metal on metal device (actually the device described in Chapter 9).

Firkins et al (April 2000) looked at the difference in wear performance of the same metal on metal articulation in two kinematically different hip simulators. They found the wear rate to vary considerably between the simulators and concluded that *"This study has shown that the motion and kinematics of the contact were a critical determinant of the wear volume."*. This leads to a consideration that the results obtained during the present testing may be less close to the in vivo situation than may have been considered at the beginning of the study. It may be that the kinematics and indeed other features of the simulator have either shown less wear than the in vivo reality or have failed to pick up actual performance differences between bearings with different head sizes or material compositions for instance. With respect to simulations being closer to the in vivo conditions, Chan et al (1999) discussed the fact that the MMED simulator, which they and the present study used, could provide a better environment for fluid film lubrication because of the constant motions than the human body where periods of starting and stopping are much more frequent. It is then possible to conceive that a more realistic simulation would involve a duty cycle of force and motions varied to provide a more realistic replication of in vivo conditions. This would include walking, stair climbing, rising from sitting, and standing still for sufficient periods to allow the squeeze film effects to diminish. It might even be possible to

replicate shuffling or fidgeting whereby motion is not sufficient to generate fluid film lubrication but sufficient to generate wear through rubbing under load.

Clarke (personal communication from John Fisher dated December 2000 regarding presentation given by I. Clarke) has performed tests where he evaluated the effects of lubricant used in metal on metal simulations. In the present study the lubricant had a 90% serum concentration. However in the tests performed by Clarke, when only water was used the test had to stop due to complete failure of the articulation, but as concentration of the serum was increased from 25 to 90%, the wear volume reduced. Aspects of the conclusions reached in this study such as head diameter and material composition variations not yielding significant differences in wear performance may be challenged in the light of such findings. Indeed Smith, Dowson, and Goldsmith (2001) using a Prosim hip simulator and a 25% concentration of serum, have shown results for differential head diameter whereby lowest wear was obtained with 36mm, intermediate wear with 28mm and very much the highest wear with 22.225mm head diameter. Notwithstanding the fact that the 36mm samples were of a different material composition and subjected to different simulator loading and kinematics, the difference in wear performance is marked and the results are in clear contrast to those obtained in the present study.

The final element of work which deserves mention here is the ongoing research into wear particles generated by metal on metal articulations. The size, morphology, and quantity of metal wear particles is becoming of great interest. Firkins (February 2000) noted that *"MOM prostheses tested in a physiological simulator produced nanometer sized metal wear debris which were clinically relevant"* and that when the simulator kinematics were changed through use of different simulators Firkins et al (March 2000) noted that the mean particle size for both simulators remained the same at about 30nm and having similar uniform morphology. Wear debris analysis was outside the scope of this thesis but remains one of the most important pieces of the jigsaw as far as the effectiveness, particularly in the long term, of metal on metal bearings is concerned. Indeed, future studies of debris should be extended to incorporate cellular reactions and biocompatibility.

10.3 Recommendations for Further Work

a. In chapter 8 of the present study it was concluded that the hip simulator results at 2 million cycles for the 35mm samples had not yet demonstrated the bedding in process to yield a steady state wear curve. It was, and remains, a recommendation that the test be extended to 3 million cycles or beyond to establish the point if any at which a steady state wear curve is established.

b. Establish the influence of serum "protein" concentration on the wear of hard on hard articulations.

c. Establish more clinically relevant in vitro test conditions by defining a duty cycle in terms of time phased loading and kinematics for hip simulator testing. This may be facilitated by further investigation of the in vivo kinematics of metal on metal bearings in the hip using the methods of fluoroscopy.

d. Carry out further studies of differential hardness and high mean hardness articulations (typically through ceramic on metal) and thereby develop a clinical product.

e. Continue to study the reaction of the human body to wear debris from hard on hard bearings through appropriate biological studies.

f. Investigate the performance of non spherical bearing geometry in hard on hard articulations. These could replicate the bedded in state of existing bearings and so avoid the bedding in wear within the clinical environment.

g. In the longer term, compare the explanted bearings of the modern metal on metal designs with the results of hip simulator studies of the same. In the short term carry out hip simulator studies on the historical metal on metal designs, in particular the McKee-Farrar, and compare with explanted prostheses of the same design. This will help to create a correlation between in vitro and in vivo performance of the same prostheses.

BIBLIOGRAPHY

Andrew TA, Berridge D, Thomas A, Duke RNF, "Long term review of Ring total hip arthroplasty", Clin. Orthop, No 201, 111-122, 1985.

Almby B, Hierton T, "Total Hip Replacement: 10 Year Follow-Up of an Early Series", Acta Orthop Scand, 53, 398-406, 1982.

ASTM E112-96, "Standard Test Methods for Determining Average Grain Size", American Society for Testing and Materials, 100 Bar Harbor Dr., West Conshohocken, PA 19428, USA.

ASTM F75-98, "Standard Specification for Cobalt-28 Chromium-6 Molybdenum Casting Alloy and Cast Products for Surgical Implants (UNS R30075)", American Society for Testing and Materials, 100 Bar Harbor Dr., West Conshohocken, PA 19428, USA.

ASTM F799-87, "Standard Specification for Thermomechanically Processed Cobalt-Chromium-Moybdenum Alloy for Surgical Implants", American Society for Testing and Materials, 100 Bar Harbor Dr., West Conshohocken, PA 19428, USA. **Note that this specification was revised in 1995 to apply only to forged material. Wrought material was subsequently covered by a new specification ASTM F1537-94.**

ASTM F1537-94, "Standard Specification for Wrought Cobalt-28-Chromium-6-Molybdenum Alloy for Surgical Implants", American Society for Testing and Materials, 100 Bar Harbor Dr., West Conshohocken, PA 19428, USA.

August AC, Aldam CH, Pynsent B, "The Mckee-Farrar Hip Arthroplasty: A long- term study", JBJS, 68B, No4, Aug 1986.

Bentley G, Duthie RB, "A Comparative Review of the McKee-Farrar and Charnley Total Hip Prostheses", Clin Orthop, No 95, Sep 1973, 127.

Betteridge WW, "Cobalt and its Alloys", Chichester: Horwood, 1982.

Chan FW, Bobyn JD, Medley JB, Krygier JJ, Tanzer M, "Wear and Lubrication of Metal on Metal Hip Implants", Clin Orthop, No 369, Dec 1999, 10.

Chan FW, Medley JB, Krygier JJ, Bobyn JD, Podgorsak GF, Tanzer M, "Wear Performance of Cobalt-Chromium Metal-Metal Bearing Surfaces for Total Hip Arthroplasty", Trans. Orthop. Res. Soc., 21:464, 1996.

Chapchal G, Müller W, "Total Hip Replacement with the McKee Prosthesis", Clin Orthop, No 72, Sep-Oct 1970, 115.

Charnley J, Cupic Z, "The Nine and Ten Year Results of the Low-Friction Arthroplasty of the Hip", Clin. Orthop, No. 95, 9-25, 1973.

Courtois B, Variel R, Le Saout J, Kerboul B, Lefevre C, "Apropos of 87 Dislocations of Total Hip Prostheses" Int. Orthop. ,9(3):189-93, 1985.

Crowninshield RD, Brand RA, Johnston RC, Milroy JC, "The Effect of Cross-Sectional Geometry on Cement Stresses in Total Hip Reconstruction", Clin Orthop, No 146, 71, 1980.

Dennis D, Komistek R, Ochoa J, Northcut E, Hammill C, "In Vivo Determination of Hip Joint Separation in Subjects Having Either a Metal on Metal or a Metal on Polyethylene THA", Trans. Orthop. Res. Soc., 46:507, 2000.

Djerf K, Whalstrom O, "Total Hip Replacement Comparison between the McKee- Farrar and Charnley Prostheses in a 5 year Follow Up Study", Arch Orthop Trauma Surg, 105, 158-162, 1986.

Djerf K, Whalstrom O, Hammerby S "Loosening 5 Years after Total Hip Replacement A Radiological study of the McKee-Farrar and Charnley Prostheses", Arch Orthop Trauma Surg, 105, 339-342, 1986.

Farrar R, Schmidt MB, Hamilton JV, Greer KW, "The Development of Low Wear Articulations", Proceedings of the Societe Internationale de Recherche Orthopedique (SIROT) 97 Inter Meeting, Haifa, 1997.

Firkins PJ, "Wear Debris Generation in Metal on Metal and Metal on Ceramic Hip Prostheses", PhD Thesis, University of Leeds, February 2000.

Firkins PJ, Tipper JL, Ingham E, Stone MH, Farrar R, Fisher J, "A Novel Low Wearing Differential Hardness, Ceramic on Metal Hip Joint Prosthesis", submitted to Journal of Biomechanics, August 2000.

Firkins PJ, Tipper JL, Ingham E, Stone MH, Farrar R, Fisher J, "Influence of Simulator Kinematics on the Wear of Metal on Metal Hip Prostheses", Poster No 574, 46th Annual Meeting of the Orthopaedic Research Society, Orlando, March 2000.

Firkins PJ, Tipper JL, Ingham E, Stone MH, Farrar R, Fisher J, "Influence of Simulator Kinematics on the Wear of Metal on Metal Hip Prostheses", submitted to Journal of Engineering in Medicine April 2000.

Fowler JL, Gie GA, Lee AJC, Ling RSM, "Experience with the Exeter Total Hip Replacement Since 1970", Orthopedic Clinics of North America, Vol 19, No3, July 1988.

Freeman PA, "McKee-Farrar Total Replacement of the Hip Joint in Rheumatoid Arthritis and Allied Conditions", Clin Orthop, No 72, Sep-Oct 1970, 106.

Green RE (Editor), "Machinery's Handbook", 25th Edition, New York: Industrial Press Inc., 1996.

Greer A, "Statistics for Engineers", College Audience Trade Paper, Stanley Thornes (Publishers) Ltd, Bowker US, October 1988, ISBN 0-85950-495-6.

Hashemi-Hejad A, Goddard N, Birch N, "Current Attitudes to Cementing Techniques in British Hip Surgery", Annals of Royal College of Surgeons Engl, 76, 396-400, 1994.

Jacobsson SA and Djerf K, "20 Year Results of McKee-Farrar vs. Charnley Prosthesis", Clin Orthop, No 329S, S60, 1996.

Jin ZM, Dowson D, Fisher J, "Analysis of Fluid Film Lubrication in Artificial Hip Joint Replacements with Surfaces of High Elastic Modulus", Proc Instn Mech Engrs, Vol 211, Part H3, 247, 1997.

Langenskiold A, Paavilainen T, "Total Replacement of 116 Hips by the McKee-Farrar Prosthesis", Clin Orthop, No 95, Sep 1973, 143.

Malchau H, Herberts P, "Prognosis of Total Hip Replacement", Scientific Exhibition at 63rd AAOS, Atlanta, 1996.

McCalden RW, Howie DW, Ward L, Subramanian C, Nawana N, Pearcy MJ, "Observations on the Long-Term Wear Behaviour of Retrieved McKee-Farrar Total Hip Replacement Implants", Trans Orthop. Res. Soc., 242-40, 1995.

McKee G K, "Symposium: The Use of Metals in Bone Surgery", Proceedings of the Royal Society of Medicine, Vol.50, 837, 1957.

McKee G. K, Watson-Farrar J, "Replacement of Arthritic Hips by the Mckee-Farrar Prostheses", JBJS, 48B, No2, May 1966.

McKee G K, "Development of a Total Prosthetic Replacement of the Hip", Clin Orthop, No 72, 85, 1970.

McKee GK, "McKee-Farrar Total Prosthetic Replacement of the Hip", in M. Jayson, "Total Hip Replacement", JB Lippincott, Philadelphia, 1971, Ch3.

McKee GK, Chen SC, "The Statistics of the McKee-Farrar Method of Total Hip Replacement", Clin Orthop No 95, 26, 1973.

McKee GK, "The Norwich Method of Total Hip Replacement : Development and Main Indications", Annals of Royal College of Surgeons, Vol 54, 1974.

McKee GK, "Total Hip Replacement- Past, Present, and Future", Biomaterials, Vol 3, July, 130-135, 1982.

Medley JB, Chan FW, Krygier JJ, Bobyn JD, "Comparison of Alloys and Designs in a Hip Simulator Study of Metal on Metal Implants", Clin Orthop, 329S, S148, 1996.

Medley JB, Krygier JJ, Bobyn JD, Chan FW, Lippincott A, and Tanzer M, "Kinematics of the MATCO™ Hip Simulator and Issues Related to Wear Testing of Metal – Metal Implants", Proc. Instn Mech Engrs, Vol 211, Part H, 1997.

Medley JB, Krygier JJ, Bobyn JD, Chan FW, and Tanzer M, "Metal-Metal Bearing Surfaces in the Hip: Investigation of Factors Influencing Wear", Trans. Orthop. Res. Soc., 20:765, 1995.

Minakawa H, Stone M, Wroblewski BW, Ingham E, Fisher J, "Quantification of Third Body Damage, and its Effects on UHMWPE Wear with Different Types of Femoral Heads", Trans. Orthop. Res. Soc., 22:788, 1997.

Muller ME, "The Benefits of Metal-on-Metal Total Hip Replacements", Clin Orthop, No311, 54-59, 1995.

Nevelos J, Ingham E, Doyle C, Streicher R, Nevelos A, Walter W, Fisher J, "Microseparation of the Centers of Alumina-Alumina Artificial Hip Joints During Simulator Testing Produces Clinically Relevant Wear Rates and Patterns", The Journal of Arthroplasty, Vol 15, No 6, 2000.

Paul JP, PhD Thesis, University of Glasgow, 1967.

Ramamurti BS, Muratoglu OK, Bragdon CR, O'Connor DO, Jasty M, Harris WH, "How realistically Do Contemporary Hip Joint Simulators Reproduce Physiologic Gait Motion?", Trans. Orthop. Res. Soc., 21:457, 1996.

Ring P A, "Complete Replacement Arthroplasty of the Hip by the Ring Prosthesis", JBJS, 50B, No.4, 720, 1968.

Ring PA, "Total Replacement of the Hip", Clin Orthop No72, 161, 1970.

Ring PA, "Ring Total Hip Replacement in M. Jayson, Total Hip Replacement", JB Lippincott, Philadelphia, 1971, Ch3.

Ring PA, "Total Replacement of the Hip Joint", Clin Orthop No95, 451, 1973.

Ring PA, "Five to Fourteen Five to Fourteen Year Interim Results of Uncemented Total Hip Arthroplasty ", Clin Orthop No137, 87, 1978.

Ring PA, "Ring UPM Total Hip Arthroplasty", Clin. Orthop, No176, 115-123, 1983.

Ritter MA, Keating ME, Faris PM, Brugo G, "Metal-Backed Acetabular Cups in Total Hip Arthroplasty", JBJS, 72A, No 5, 1990.

Rolland JJ, "Metal on Metal Articulation", Snowbird, 1995.

Scott RA, Schroeder DW, "The Effect of Radial Mismatch on the Wear of Metal on Metal Hip Prostheses: A Hip Simulator Study", Trans. Orthop. Res. Soc., 22:764, 1997

Schmidt M, Weber H, Schon R, "Cobalt Chromium Molybdenum Metal Combination for Modular Hip Prostheses" Clin Orthop, 329S, S35, 1996.

Schmidt MB, Hamilton JV, "The Effects of Calcium Stearate on the Properties of UHMWPE", Trans. Orthop. Res. Soc., 21:4, 1996.

Semlitsch M, Striecher RM, Weber H, "Wear behaviour of cast CoCrMo Cups and Balls in Long Term Implanted Total Hip Prostheses", Orthopade, 18, 377-381, 1989.

Smith SL, Dowson D, Goldsmith AAJ, "The Effect of Femoral Head Diameter Upon Lubrication and Wear of Metal on Metal Total Hip Replacements", Proc. Instn Mech Engrs, Part H, 2001, In Press.

Streicher R, discussion session at the Metal on Metal Hip Symposium in Santa Monica, 2-5 November 1995.

Tillberg B, "Total Hip Arthroplasty Using the Mckee and Watson-Farrar Prosthesis: a Prospective Follow Up Study of 327 Arthroplasties", Acta Orthop Scand 53, 103-107, 1982.

Timoshenko SP, Goodier JN, "Theory of Elasticity", 3rd Ed, McGraw-Hill, 1970, ISBN 0-07-085805-5.

Unsworth A, Hall RM, "Friction and Wear of Prostheses", Unpublished report, Durham University, 1995.

Visuri T, "Long-Term Results and Survivorship of the McKee-Farrar Total Hip Prosthesis", Arch Orthop Trauma Surg, 106, 368-374, 1987.

Walker PS, Erkman MJ, "Metal On Metal Lubrication in Artificial Human Joints", Wear, 21, 377-391, 1972.

Walker PS, Gold BL, "The Tribology (Friction, Lubrication and Wear) of All-Metal Artificial Hip Joints", Wear, 17, 285-299, 1971.

Walker PS, Salvati E, Hotzler RK, "The Wear on Removed Mckee-Farrar Total Hip Prostheses", JBJS, 56A, 92, 1974.

Ward DM, "The Use of Fluorescence Markers to Record Prosthetic Wear Patterns", Journal of Audiovisual Media in Medicine, 19, 3, 123-129, 1996.

Weber BG, "Metal-Metal THR: Back to the Future", Z Orthop Ihre Grenzeb (GERMANY), Jul-Aug, 1992, 130 (4), 306-9.

Weber BG, "Metal/Metal Couple "Metasul" for Total Hip Replacement Implant: Development and First Results", Actualite, Maitrise Orthopedique, 12-17, 1995.

Wilson PD, Amstutz HC, Czerniecki A, Salvati EA, Mendes DG, "Total Hip Replacement with Fixation by Acrylic Cement", JBJS, 54A, No2, 1972.

Zaoussis A L, Patikas AF, "Experience with Total Hip Arthroplasty in Greece First 20 Years", Clin Orthop, No 246,39, Sept 1989.

Appendix A: Preliminary Wear Test

In order to make an initial assessment of the manufacturability of metal on metal cups using microfinishing technology, and of the performance of metal on metal articulations in a hip simulator, 5 test cups and heads were manufactured and tested. The test was carried out on a PM-MED 12 station hip simulator. The test was taken to 550,000 cycles at a simulator speed of 1.1 Hz using the loading curve described by Paul (1967) with maximum load of 2000N. The parts were cycled in bovine serum and measurements of wear were made as weight loss using a balance at 0, 50,000, 237,905, 443,534, and 554,711 cycles. The 5 samples with nominal head diameter 28mm were manufactured from CoCrMo alloy in accordance with ASTM F799 (This was wrought bar which has subsequently been redesignated as ASTM F1539). The geometrical details relating to articulating surfaces was recorded and are given in Table A.1.

Sample	Head Diameter (mm)	CMM Head Sphericity (mm)	Bore Diameter (mm)	CMM Bore Sphericity (mm)
1	27.835	0.0068	28.065	0.0033
2	27.815	0.0071	28.048	0.0047
3	27.777	0.0073	27.852	0.0032
4	27.776	0.0052	27.936	0.0030
5	27.761	0.0102	27.899	0.0035

Table A.1
Geometrical details of the articulating surfaces for the preliminary wear test samples

These heads and cups were paired to give an acceptable range of diametral clearance which is shown in Table A.2.

Sample Head	Sample Cup	Diametral Clearance (mm)
1	1	0.230
2	2	0.233
3	3	0.075
4	5	0.123
5	4	0.175

Table A.2
Wear test samples pairings to give variation in diametral clearance

The samples were of relatively thick section and so would be assumed to be semi infinite solids.

Cup and head pair 1 were run singly as a preliminary check on performance and simulator function and so only the remaining 4 samples were run together in the definitive test. The wear data is summarized in Tables A.3 and A.4, and in Figures A.1, A.2 and A.3.

Cycles		0	50000	237905	443534	554711
Cup Wear (g)						
Cup 2		0.0000	0.0010	0.0016	0.0015	0.0033*
Cup 3		0.0000	0.0007	0.0011	0.0010	0.0010
Cup 4		0.0000	0.0010	0.0014	0.0015	0.0015
Cup 5		0.0000	0.0015	0.0024	0.0024	**
Head Wear (g)						
Head 2		0.0000	0.0034	0.0050	0.0061	0.0068
Head 3		0.0000	0.0001	0.0008	0.0008	0.0010
Head 4		0.0000	0.0021	0.0049	0.0049	**
Head 5		0.0000	0.0017	0.0055	0.0058	0.0063
Total Wear (g)	Diametral Mismatch (mm)					
Head 2/Cup 2	0.233	0.0000	0.0045	0.0066	0.0076	0.0101
Head 3/Cup 3	0.075	0.0000	0.0008	0.0019	0.0018	0.0020
Head 4/Cup 5	0.123	0.0000	0.0036	0.0073	0.0073	**
Head 5/Cup 4	0.175	0.0000	0.0027	0.0069	0.0073	0.0078

* Sudden increase in wear rate was due to wear between the cup and a loose retaining set screw.
** Fluid loss during last test interval prevented weight loss being measured at 554711 cycles.

Table A.3
Preliminary hip simulator wear test results with wear in grams

And expressing the material loss as a volume with density for Cobalt Chromium Alloy calculated at 8331kg/m^3 Table A.4 is generated.

Cycles		0	50000	237905	443534	554711
Cup Wear (mm^3)						
Cup 2		0.0000	0.1200	0.1921	0.1801	0.3961*
Cup 3		0.0000	0.0840	0.1320	0.1200	0.1200
Cup 4		0.0000	0.1200	0.1680	0.1801	0.1801
Cup 5		0.0000	0.1800	0.2881	0.2881	+
Head Wear (mm^3)						
Head 2		0.0000	0.4081	0.6002	0.7322	0.8162
Head 3		0.0000	0.0120	0.0960	0.0960	0.1200
Head 4		0.0000	0.2521	0.5882	0.5882	+
Head 5		0.0000	0.2041	0.6602	0.6962	0.7562
Total Wear (mm^3)	Diametral Mismatch (mm)					
Head 2/Cup 2	0.233	0.0000	0.5402	0.7922	0.9123	1.2123
Head 3/Cup 3	0.075	0.0000	0.0960	0.2281	0.2161	0.2401
Head 4/Cup 5	0.123	0.0000	0.4321	0.8762	0.8762	+
Head 5/Cup 4	0.175	0.0000	0.3241	0.8282	0.8762	0.9363

* Sudden increase in wear rate was due to wear between the cup and a loose retaining set screw.
+ Fluid loss during last test interval prevented weight loss being measured at 554711 cycles.

Table A.4
Preliminary hip simulator wear test results with wear in mm^3

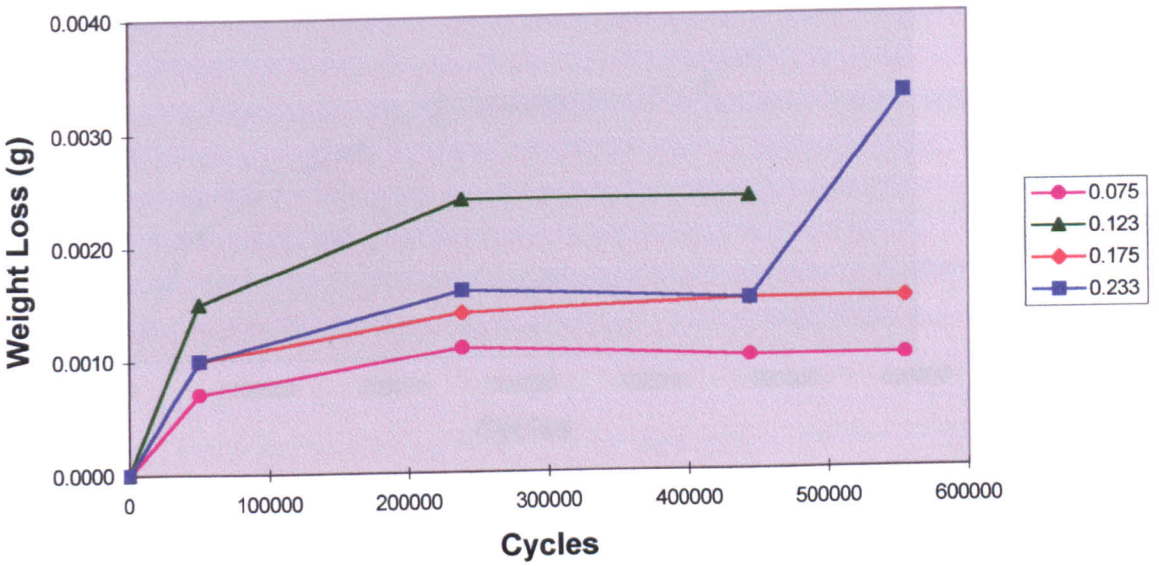

Figure A.1: Cup Weight Loss for Preliminary Wear Test
Figure shows cup weight loss against number of cycles of the hip simulator for the preliminary study wear test samples

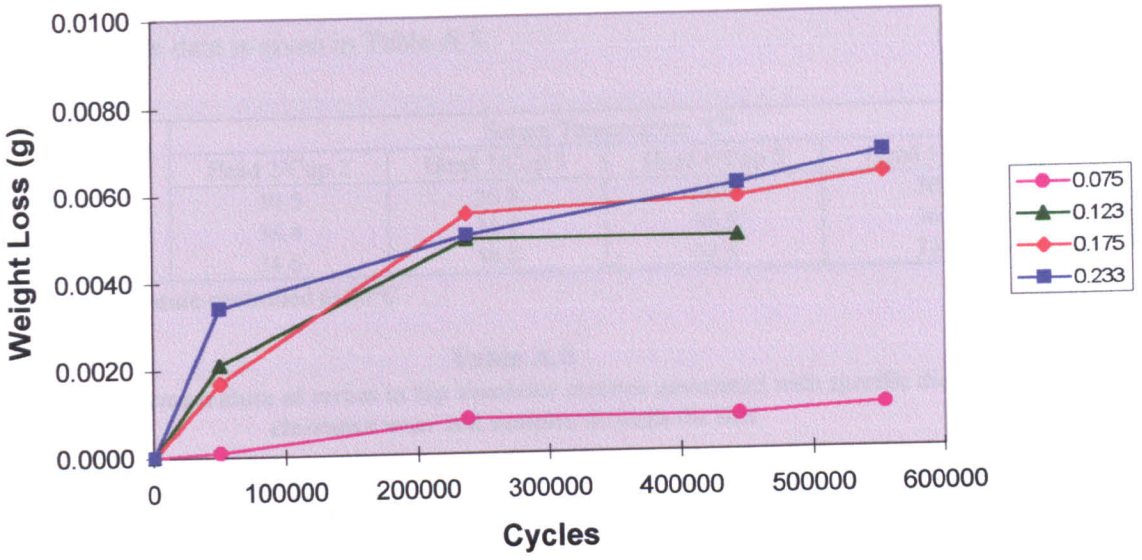

Figure A.2: Head Weight Loss for Preliminary Wear Test

Figure shows head weight loss against number of cycles of the hip simulator for the preliminary study wear test samples

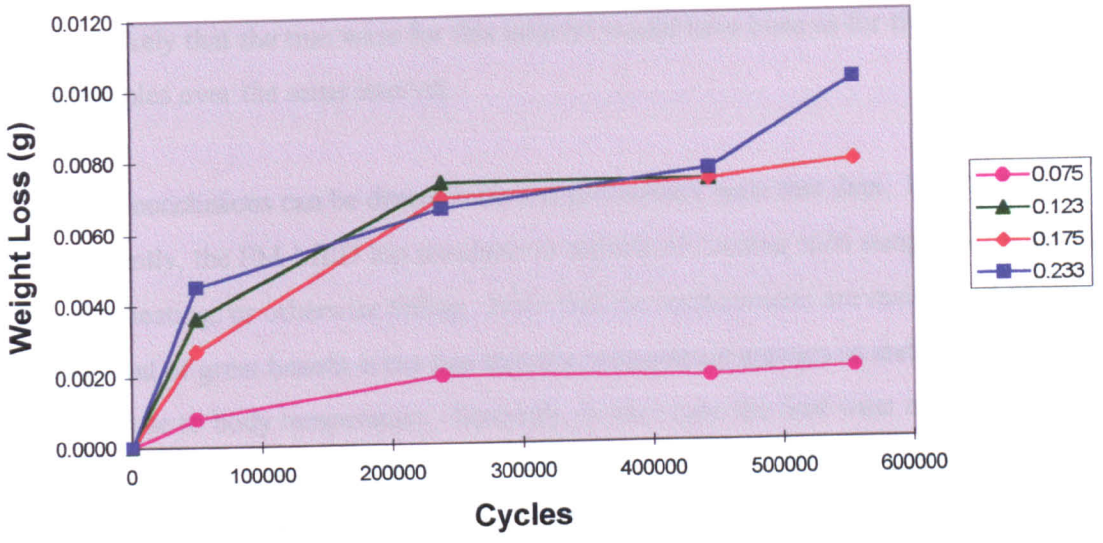

Figure A.3: Total Weight Loss for Preliminary Wear Test

Figure shows total weight loss against number of cycles of the hip simulator for the preliminary study wear test samples

As far as serum temperature was concerned, this was measured within each test sample chamber and the data is given in Table A.5.

Cycles	Serum Temperature °C*			
	Head 2/Cup 2	Head 3/Cup 3	Head 4/Cup 5	Head 5/Cup 4
4000	30.5	26.8	30.0	30.5
14000	36.4	31.2	35.5	36.3
29000	34.6	30.6	32.5	33.6

*Ambient temperature controlled to 20°C

Table A.5

Steady state temperature of serum in hip simulator stations associated with specific diametral clearance wear test samples through the test

Discussion and Recommendations

The sudden increase in wear in the 0.233mm clearance sample was due to a problem with the test set up whereby a clamping screw loosened and caused some wear on a non articulating surface of the cup. Clearly this last data point should be ignored and it is much more likely that the true wear for this interval would have been as for the .075 and .175mm samples over the same interval.

A number of conclusions can be drawn from this preliminary wear test data. Firstly, and most importantly, the PM-MED hip simulator is capable of running such samples without seizing, overheating, or otherwise failing. Note that the temperatures are maintained at a stable level and of great benefit is the fact that the temperature appears to stabilize reasonably close to body temperature. Secondly, in each case the final wear curve exhibits an initial high wear rate which then reduces, and in some cases the rate appears to tend to zero. It should be borne in mind that the samples were subjected to only around 0.5 million cycles and so bedding in may still be occurring. However, it may be that a metal on metal pair exhibit a "bedding in" type phenomenon with associated higher wear rate followed by bedded in wear with lower wear rate which in the limit may tend to zero. Thirdly, there appears to be a relationship between diametral clearance and wear. The data has established that the low clearance samples performed around 10 times better in terms of minimizing the weight loss of the pairing, with a loss of 0.002g (corresponding to about 0.24mm^3).

The clear recommendation of this preliminary work was that further work should be done using more samples with variations of geometrical and material factors to enable a scientific assessment of a more optimum metal on metal articulation.

Appendix B: Figures and Tables

Many of the figures and tables of data relevant to the chapters within the thesis have been produced in a separate appendix rather than the main body of the text to make the thesis easier to read. The figure numbers indicate the order in which the figures appear within the thesis. The table number indicates firstly the chapter and then where the table falls within that chapter. The designation B indicates that the figure or table is part of this appendix.

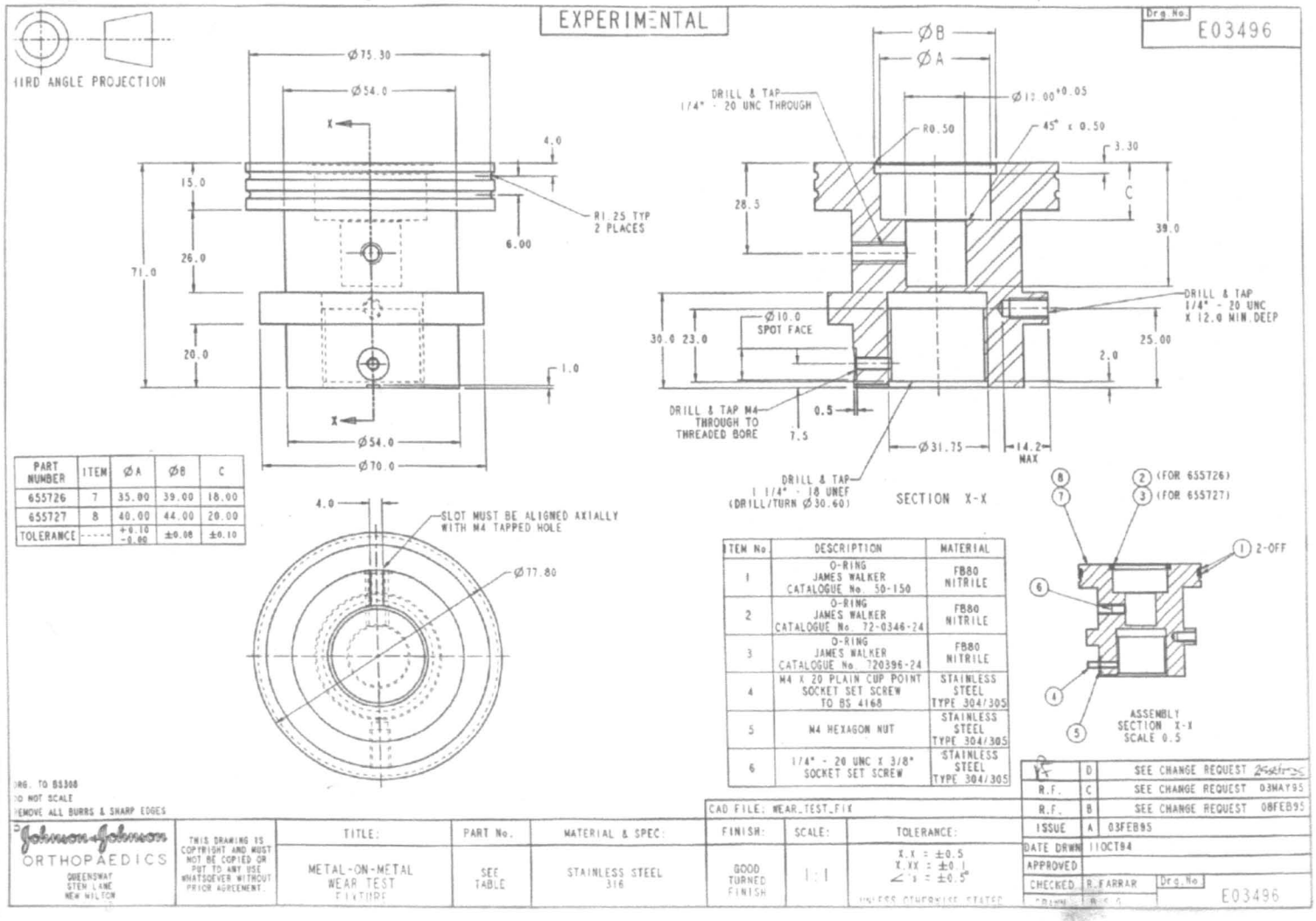

PART NUMBER	ITEM	ØA	ØB	C
655726	7	35.00	39.00	18.00
655727	8	40.00	44.00	20.00
TOLERANCE	-----	+0.10 -0.00	±0.08	±0.10

ITEM No.	DESCRIPTION	MATERIAL
1	O-RING JAMES WALKER CATALOGUE No. 50-150	FB80 NITRILE
2	O-RING JAMES WALKER CATALOGUE No. 72-0346-24	FB80 NITRILE
3	O-RING JAMES WALKER CATALOGUE No. 720396-24	FB80 NITRILE
4	M4 X 20 PLAIN CUP POINT SOCKET SET SCREW TO BS 4168	STAINLESS STEEL TYPE 304/305
5	M4 HEXAGON NUT	STAINLESS STEEL TYPE 304/305
6	1/4" - 20 UNC X 3/8" SOCKET SET SCREW	STAINLESS STEEL TYPE 304/305

Figure B5.15a: Hip Simulator Test Fixture Drawing (Base)

The test fixture base used for the hip simulator tests made in accordance with drawing E03496.

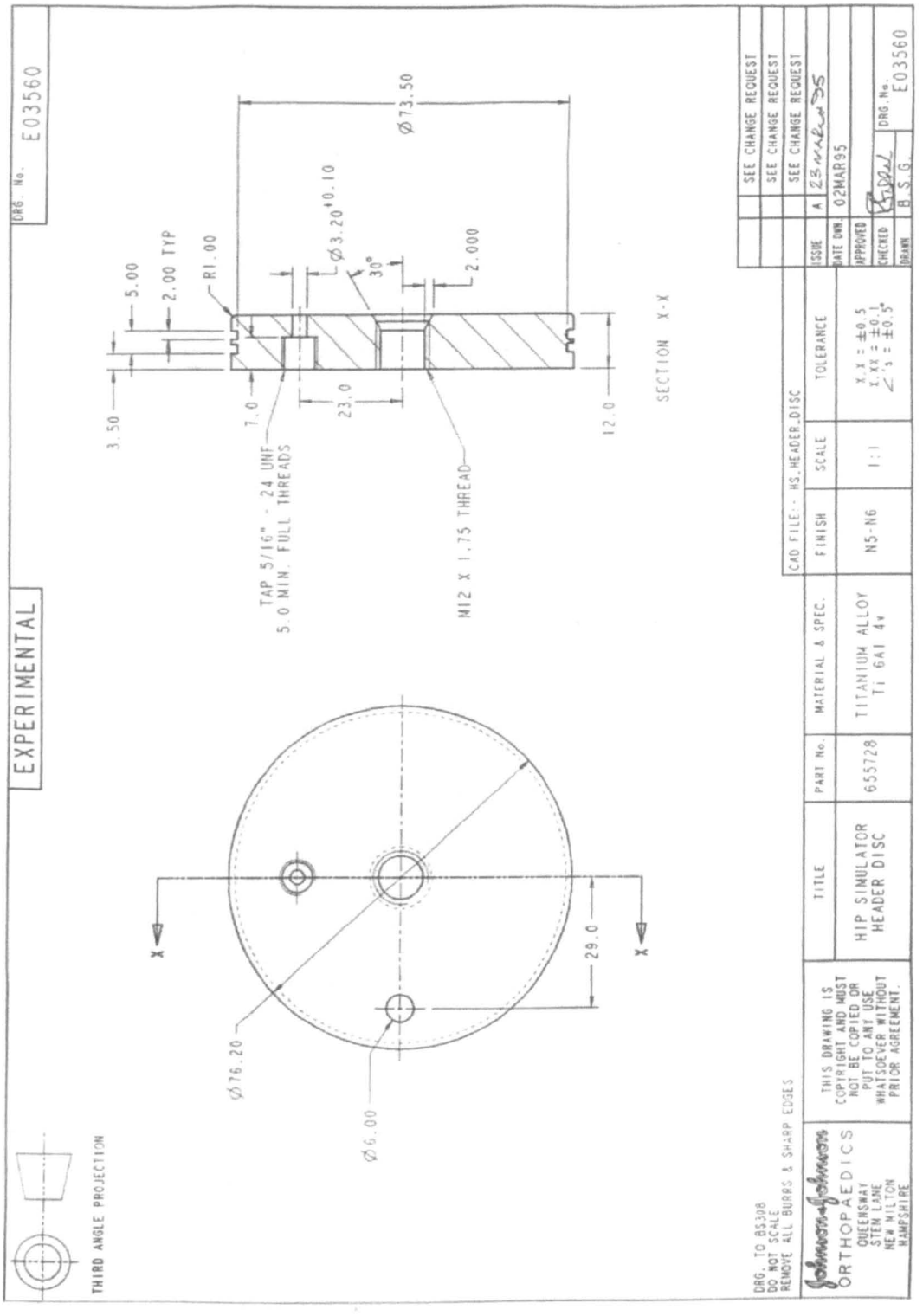

Figure B5.15b: Hip Simulator Test Fixture Drawing (Lid)

The test fixture header disc or lid used for the hip simulator tests made in accordance with drawing E03560.

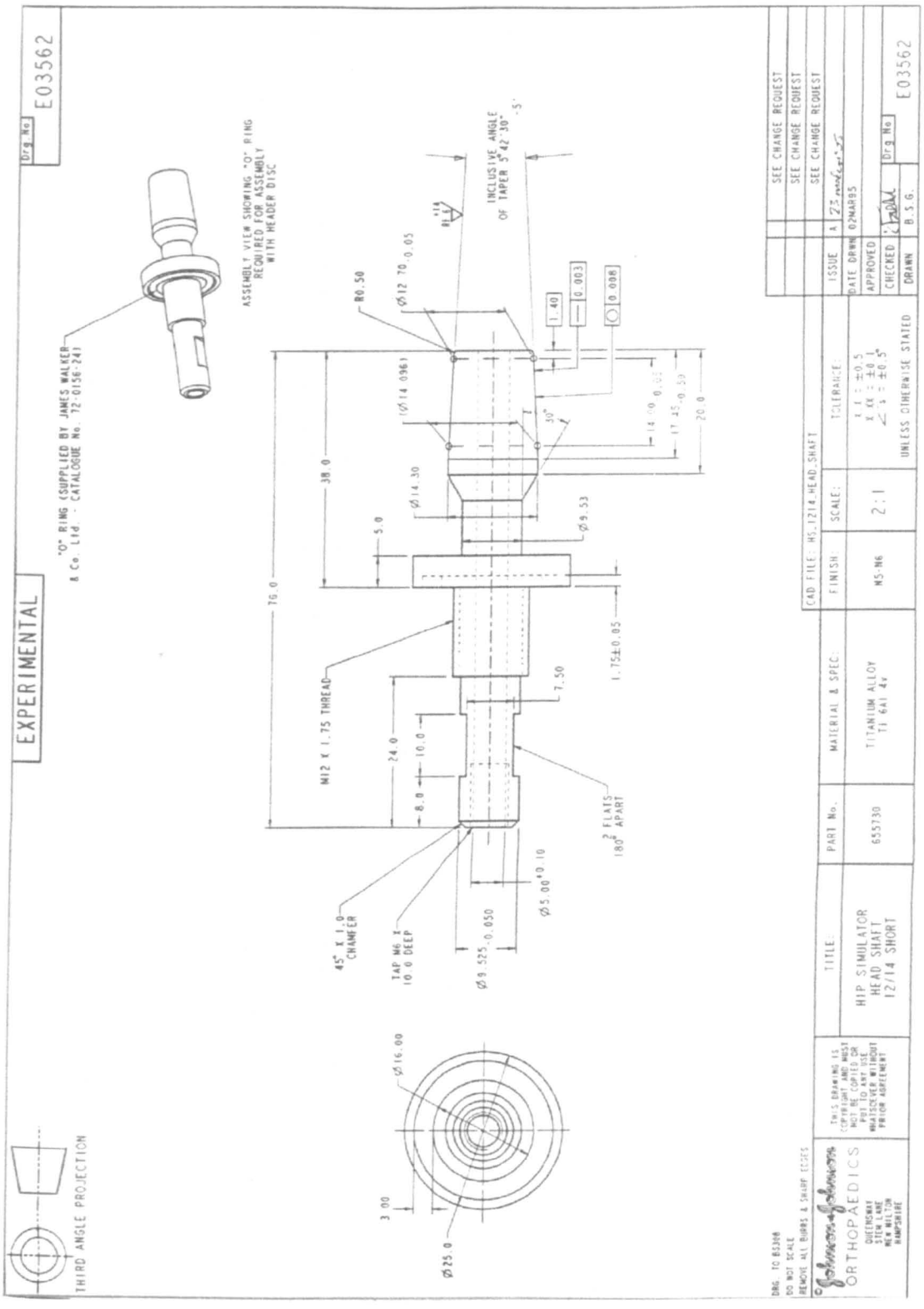

Figure B5.15c: Hip Simulator Test Fixture Drawing (Rod)
The test fixture head shaft or rod used for the hip simulator tests made in accordance with drawing E03562.

Figure B6.1b: Hip Simulator Test Cup Drawing

The test piece cups used for the hip simulator tests using wrought material were made in accordance with the test piece drawing E02931.

Heads	Ra (μm)	Rp (μm)	Ry (μm)	Rv (μm)	Rsk (μm)
MH005	0.008	0.030	0.070	0.030	-0.390
	0.012	0.070	0.090	0.040	0.570
MH006	0.008	0.030	0.080	0.050	-0.940
	0.008	0.030	0.070	0.040	-0.170
MH007	0.008	0.030	0.070	0.050	-0.440
	0.012	0.050	0.100	0.050	-0.060
MH008	0.014	0.070	0.100	0.050	0.680
	0.010	0.050	0.070	0.030	0.370
MH009	0.008	0.050	0.100	0.060	-0.220
	0.006	0.030	0.050	0.020	0.010
MH010	0.008	0.030	0.070	0.040	-0.320
	0.008	0.040	0.090	0.050	-0.210
MH011	0.008	0.030	0.050	0.030	-0.140
	0.008	0.030	0.060	0.030	-0.460
MH012	0.010	0.040	0.090	0.050	-0.120
	0.008	0.030	0.070	0.030	-0.600
MH013	0.008	0.030	0.070	0.050	-0.100
	0.010	0.030	0.080	0.050	-0.140
MH014	0.008	0.050	0.070	0.030	-0.160
	0.008	0.030	0.070	0.040	-0.020
MH015	0.010	0.030	0.070	0.040	-0.160
	0.010	0.040	0.070	0.030	-0.680
MH016	0.008	0.040	0.070	0.040	-0.160
	0.008	0.030	0.060	0.030	-0.310
Head Mean	0.009	0.038	0.075	0.040	-0.174
Head SD	0.002	0.012	0.014	0.010	0.349

Table B6.3a

Pre test surface finish data for 28mm diametral clearance variation wear test heads.

Cups	Ra (μm)	Rp (μm)	Ry (μm)	Rv (μm)	Rsk (μm)
MC005	0.014	0.100	0.230	0.130	0.150
	0.008	0.030	0.050	0.030	-0.230
MC006	0.008	0.030	0.070	0.040	-0.460
	0.010	0.030	0.070	0.040	-0.180
MC007	0.010	0.030	0.100	0.070	-1.090
	0.008	0.030	0.080	0.050	-0.360
MC008	0.010	0.040	0.070	0.050	-0.810
	0.010	0.030	0.070	0.040	-0.340
MC009	0.010	0.030	0.080	0.050	1.150
	0.010	0.030	0.070	0.050	-0.450
MC010	0.010	0.030	0.100	0.070	-0.930
	0.030	0.080	0.590	0.510	-4.610
MC011	0.010	0.030	0.140	0.120	-3.240
	0.022	0.120	0.590	0.470	-4.710
MC012	0.010	0.040	0.070	0.040	-0.420
	0.010	0.040	0.070	0.030	-0.710
MC013	0.020	0.090	0.280	0.200	-1.770
	0.010	0.030	0.070	0.030	0.400
MC014	0.018	0.060	0.180	0.120	-1.560
MC015	0.026	0.070	0.370	0.310	-3.320
	0.026	0.090	0.270	0.180	-1.660
MC016	0.012	0.050	0.120	0.070	-1.940
	0.014	0.040	0.150	0.120	-0.630
Cup Mean	0.014	0.050	0.169	0.123	-1.205
Cup SD	0.006	0.027	0.154	0.131	1.470

Table B6.3b

Pre test surface finish data for 28mm diametral clearance variation wear test cups.

Cycles	0	20000	53110	107325	284975	605010	1157280	1609800	2028204
Cup Wear (g)									
MC005	0.0000	0.0011	0.0028	0.0027	0.0028	0.0028	0.0031	0.0033	0.0048
MC006	0.0000	0.0010	0.0015	0.0010	0.0012	0.0015	0.0019	0.0020	0.0025
MC007	0.0000	0.0008	0.0019	0.0015	0.0015	0.0015	0.0015	0.0019	0.0023
MC008	0.0000	0.0030							
MC009	0.0000	0.0041							
MC010	0.0000	0.0014	0.0032	0.0040	0.0044	0.0065	0.0074	0.0079	0.0085
MC011	0.0000	0.0002	0.0015	0.0010	0.0014	0.0011	0.0013	0.0011	0.0018
MC012	0.0000	0.0012	0.0027	0.0023	0.0028	0.0027	0.0031	0.0032	0.0083
MC013	0.0000	0.0010	0.0022	0.0012	0.0019	0.0020	0.0022	0.0016	0.0027
MC014	0.0000	0.0018	0.0029	0.0025	0.0031	0.0031	0.0033	0.0033	0.0036
MC015	0.0000	0.0016	0.0038	0.0033	0.0033	0.0038	0.0038	0.0040	0.0042
MC016	0.0000	0.0003	0.0041	0.0063	0.0071	0.0070	0.0072	0.0081	0.0081
Head Wear (g)									
MH005	0.0000	0.0025							
MH006	0.0000	0.0016							
MH007	0.0000	0.0011	0.0016	0.0018	0.0020	0.0022	0.0024	0.0024	0.0029
MH008	0.0000	0.0012	0.0023	0.0029	0.0035	0.0045	0.0046	0.0049	0.0070
MH009	0.0000	0.0005	0.0008	0.0007	0.0011	0.0010	0.0011	0.0011	0.0011
MH010	0.0000	0.0016	0.0025	0.0030	0.0035	0.0043	0.0043	0.0042	0.0042
MH011	0.0000	0.0008	0.0011	0.0010	0.0012	0.0012	0.0012	0.0012	0.0014
MH012	0.0000	0.0012	0.0028	0.0036	0.0038	0.0040	0.0049	0.0050	0.0091
MH013	0.0000	0.0011	0.0023	0.0029	0.0036	0.0045	0.0045	0.0048	0.0048
MH014	0.0000	0.0014	0.0024	0.0035	0.0048	0.0085	0.0089	0.0091	0.0091
MH015	0.0000	0.0015	0.0032	0.0042	0.0068	0.0093	0.0094	0.0095	0.0108
MH016	0.0000	0.0022	0.0037	0.0076	0.0174	0.0220	0.0229	0.0230	0.0233
Total Wear (g)									
MH5/MC8	0.0000	0.0055							
MH6/MC9	0.0000	0.0057							
MH14/MC10	0.0000	0.0027	0.0056	0.0074	0.0091	0.0150	0.0163	0.0170	0.0176
MH9/MC6	0.0000	0.0015	0.0023	0.0017	0.0024	0.0025	0.0030	0.0031	0.0036
MH7/MC7	0.0000	0.0019	0.0035	0.0032	0.0035	0.0037	0.0040	0.0043	0.0051
MH11/MC11	0.0000	0.0010	0.0026	0.0020	0.0027	0.0023	0.0025	0.0024	0.0032
MH13/MC15	0.0000	0.0028	0.0060	0.0062	0.0068	0.0082	0.0082	0.0087	0.0089
MH10/MC13	0.0000	0.0025	0.0046	0.0042	0.0053	0.0063	0.0064	0.0058	0.0069
MH12/MC12	0.0000	0.0025	0.0056	0.0059	0.0067	0.0067	0.0081	0.0083	0.0174
MH8/MC5	0.0000	0.0024	0.0050	0.0056	0.0062	0.0073	0.0076	0.0082	0.0119
MH15/MC14	0.0000	0.0032	0.0060	0.0066	0.0098	0.0123	0.0126	0.0127	0.0143
MH16/MC16	0.0000	0.0024	0.0078	0.0139	0.0245	0.0289	0.0301	0.0310	0.0313

For volumetric wear (mm^3) multiply the weight loss values by 120 for material density of 8331kg/m^3

Table B6.5

28mm diametral clearance variation wear test results

Steady State Serum Temperature °C*										
	Diametral Clearance (mm)									
Cycles	.014	.033	.05	.074	.097	.121	.139	.156	.174	.322
30000	41.6	36.6	31.2	33.3	35.6	34.1	37.7	35.4	36.7	38.9
52990	45.6	42.7	36.9	40.5	42.7	38.4	38.9	38.3	38.7	44.0
107325	48.4	42.3	40.4	36.2	35.9	37.8	39.4	37.9	37.5	42.2
161305	39.0	41.4	39.2	37.8	36.5	37.8	39.2	38.5	38.3	**
196200	39.0	42.1	41.3	37.9	37.3	39.2	39.0	38.5	37.5	**
233357	39.2	42.1	42.0	37.9	37.9	39.7	39.2	38.5	38.2	**
267090	39.9	42.5	42.1	38.1	38.3	39.7	38.8	38.3	38.2	**
421360	45.4	38.6	36.2	35.1	33.5	35.4	34.6	35.0	34.3	33.4
1609800	47.1	42.1	41.1	37.0	36.0	37.3	38.6	38.9	35.6	35.5
1794170	48.5	42.3	37.0	40.6	36.9	37.7	39.3	39.4	35.9	38.0
1953235	47.1	41.3	39.2	40.8	36.8	37.6	39.0	42.3	41.1	38.2

*Ambient temperature controlled to 20°C.
** Probe malfunction.

Table B6.6

Steady state temperature of serum in hip simulator stations associated with specific diametral clearance wear test samples through the test.

Heads	Ra (μm)	Rp (μm)	Ry (μm)	Rv (μm)	Rsk (μm)
MH005	0.012	0.050	0.090	0.040	-0.310
	0.010	0.070	0.090	0.040	0.480
MH006	0.012	0.030	0.100	0.080	-2.680
	0.018	0.060	0.190	0.130	-0.210
MH007	0.048	0.120	0.560	0.440	-2.730
	0.010	0.040	0.070	0.040	-0.030
MH008	*	*	*	*	*
MH009	*	*	*	*	*
MH010	0.012	0.050	0.120	0.090	-0.490
	0.012	0.060	0.100	0.070	-0.070
MH011	0.014	0.040	0.120	0.090	-1.900
	0.016	0.050	0.160	0.110	-1.270
MH012	0.008	0.030	0.050	0.030	-0.320
	0.010	0.030	0.080	0.050	-0.140
MH013	0.012	0.050	0.140	0.090	-0.530
	0.018	0.090	0.200	0.120	-1.180
MH014	0.012	0.040	0.090	0.060	0.660
	0.066	0.250	1.450	1.200	0.720
MH015	0.010	0.040	0.090	0.060	-0.850
	0.010	0.030	0.070	0.040	-0.120
MH016	0.012	0.060	0.100	0.050	0.200
	0.008	0.030	0.060	0.030	-0.220
Head Mean	0.017	0.061	0.197	0.143	-0.550
Head SD	0.014	0.049	0.306	0.257	0.949

*Post test surface finish values not recorded for these samples.

Table B6.7

Post test surface finish data for 28mm diametral clearance variation wear test heads.

Cups	Ra (μm)	Rp (μm)	Ry (μm)	Rv (μm)	Rsk (μm)
MC005	*	*	*	*	*
MC006	*	*	*	*	*
MC007	0.008	0.030	0.070	0.060	0.310
	0.010	0.030	0.140	0.110	0.060
MC008	0.014	0.040	0.090	0.050	-0.250
	0.010	0.030	0.070	0.050	-0.570
MC009	0.010	0.040	0.080	0.050	1.030
	0.018	0.240	0.530	0.290	-1.540
MC010	0.012	0.050	0.190	0.140	-0.900
	0.010	0.030	0.070	0.040	11.220
MC011	0.016	0.050	0.150	0.120	-0.980
	0.018	0.080	0.160	0.090	-1.410
MC012	0.012	0.070	0.160	0.090	-0.100
	0.016	0.050	0.110	0.060	-0.100
MC013	0.012	0.040	0.100	0.070	-1.080
	0.010	0.050	0.090	0.040	0.070
MC014	0.014	0.050	0.090	0.050	0.190
	0.016	0.060	0.120	0.060	0.050
MC015	0.010	0.060	0.080	0.050	-0.570
	0.012	0.050	0.100	0.070	-0.030
MC016	0.008	0.030	0.060	0.030	0.060
	0.008	0.030	0.050	0.030	1.170
Cup Mean	0.012	0.056	0.126	0.078	0.331
Cup SD	0.003	0.045	0.100	0.057	2.587

*Post test surface finish values not recorded for these samples.

Table B6.7

Post test surface finish data for 28mm diametral clearance variation wear test cups.

Cycles	0	50750	128009	513710	780450	1199793	1675737	2036820
Cup Wear (g)								
MC017	0.0000	0.0002	0.0001	0.0012	0.0022			
MC018	0.0000	0.0002	0.0005	0.0006	0.0022	0.0028	0.0032	0.0031
MC019	0.0000	0.0003	0.0004	0.0009	0.0020	0.0024	0.0024	0.0027
MC020	0.0000	0.0002	-.0002	0.0005	0.0010	0.0014	0.0018	0.0020
MC021	0.0000	0.0004	0.0006	0.0024	0.0033	0.0036	0.0038	0.0040
MC022	0.0000	0.0004	0.0006	0.0009	0.0014	0.0024	0.0027	0.0029
MC023	0.0000	0.0003	-.0001	0.0003	0.0001	0.0012	0.0015	0.0015
MC024	0.0000	0.0010	0.0010	0.0010	0.0015	0.0020	0.0021	0.0021
MC025	0.0000	0.0002	0.0004	0.0006	0.0016	0.0021	0.0022	0.0021
MC026	0.0000	0.0000	0.0000	0.0005	0.0012	0.0015	0.0017	0.0016
MC027	0.0000	0.0004	0.0003	0.0007	0.0011	0.0016	0.0018	0.0019
MC028	0.0000	0.0008	0.0010	0.0012	0.0019	0.0031	0.0038	0.0039
Head Wear (g)								
MH017	0.0000	0.0000	-.0002	0.0000	0.0004			
MH018	0.0000	0.0000	-.0001	-.0001	0.0002	0.0002	0.0002	0.0003
MH019	0.0000	-.0001	-.00003	-.0002	0.0001	0.0002	0.0003	0.0004
MH020	0.0000	-.0002	-.0001	-.0001	0.0001	0.0003	0.0004	0.0004
MH021	0.0000	0.0000	0.0000	-.0002	0.0001	0.0004	0.0004	0.0004
MH022	0.0000	-.0001	-.0002	-.0002	0.0002	0.0003	0.0005	0.0006
MH023	0.0000	-.0001	-.0006	0.0002	0.0001	0.0003	0.0004	0.0004
MH024	0.0000	0.0001	-.0001	-.0001	0.0003	0.0003	0.0005	0.0005
MH025	0.0000	0.0000	0.0002	0.0001	0.0004	0.0007	0.0005	0.0007
MH026	0.0000	0.0001	0.0000	0.0000	0.0004	0.0006	0.0005	0.0006
MH027	0.0000	0.0000	-.0001	-.0001	0.0002	0.0003	0.0003	0.0004
MH028	0.0000	0.0001	-.0002	0.0003	0.0006	0.0006	0.0007	0.0008
Total Wear (g)								
MH/MC017	0.0000	0.0002	-.0001	0.0012	0.0026			
MH/MC018	0.0000	0.0002	0.0004	0.0005	0.0024	0.0030	0.0034	0.0034
MH/MC019	0.0000	0.0002	0.0001	0.0007	0.0021	0.0026	0.0027	0.0031
MH/MC020	0.0000	0.0000	-.0003	0.0004	0.0011	0.0017	0.0022	0.0024
MH/MC021	0.0000	0.0004	0.0006	0.0022	0.0034	0.0040	0.0042	0.0044
MH/MC022	0.0000	0.0003	0.0004	0.0007	0.0016	0.0027	0.0032	0.0035
MH/MC023	0.0000	0.0002	-.0007	0.0001	0.0011	0.0015	0.0019	0.0019
MH/MC024	0.0000	0.0011	0.0009	0.0009	0.0018	0.0023	0.0026	0.0026
MH/MC025	0.0000	0.0002	0.0006	0.0007	0.0020	0.0028	0.0027	0.0028
MH/MC026	0.0000	0.0001	0.0000	0.0005	0.0016	0.0021	0.0022	0.0022
MH/MC027	0.0000	0.0004	0.0002	0.0006	0.0013	0.0019	0.0021	0.0023
MH/MC028	0.0000	0.0009	0.0008	0.0015	0.0025	0.0037	0.0045	0.0047

For volumetric wear (mm^3) multiply the weight loss values by 120 for material density of 8331kg/m^3

Table B7.3a

28mm carbon content variation wear test results, Test 1 of 3

Cycles	0	58968	117560	250000	449597	1023912	1494037	2020822
Cup Wear (g)								
MC060	0.0000	0.0001	0.0003	0.0003	0.0005	0.0005	0.0007	0.0010
MC061	0.0000	0.0000	0.0003	0.0006	0.0006	0.0009	0.0012	0.0013
MC062	0.0000	0.0003	0.0006	0.0007	0.0007	0.0011	0.0017	0.0023
MC063	0.0000	0.0002	0.0005	0.0007	0.0007	0.0008	0.0013	0.0016
MC068	0.0000	0.0002	0.0003	0.0005	0.0005	0.0005	0.0008	0.0012
MC069	0.0000	0.0002	0.0004	0.0005	0.0006	0.0007	0.0010	0.0011
MC070	0.0000	0.0001	0.0003	0.0006	0.0007	0.0010	0.0013	0.0019
MC071	0.0000	0.0001	0.0003	0.0006	0.0005	0.0009	0.0015	0.0020
MC076	0.0000	0.0000	0.0004	0.0006	0.0005	0.0007	0.0013	0.0019
MC077	0.0000	-.0005	-.0001	0.0000	-.0001	0.0002	0.0006	0.0008
MC080	0.0000	0.0000	0.0001	0.0004	0.0004	0.0006	0.0008	0.0011
MC081	0.0000	0.0001	0.0007	0.0010	0.0011	0.0015	0.0021	0.0027
Head Wear (g)								
MH060	0.0000	0.0002	0.0002	0.0003	0.0006	0.0007	0.0016	0.0020
MH061	0.0000	0.0001	0.0001	0.0007	0.0011	0.0016	0.0021	0.0035
MH062	0.0000	0.0001	0.0001	0.0002	0.0001	0.0003	0.0004	0.0005
MH063	0.0000	0.0005	0.0008	0.0009	0.0008	0.0010	0.0016	0.0018
MH068	0.0000	0.0007	0.0011	0.0013	0.0016	0.0018	0.0022	0.0039
MH069	0.0000	0.0003	0.0004	0.0005	0.0005	0.0011	0.0021	0.0022
MH070	0.0000	0.0009	0.0009	0.0010	0.0010	0.0010	0.0016	0.0034
MH071	0.0000	0.0005	0.0012	0.0025	0.0027	0.0029	0.0045	0.0056
MH076	0.0000	0.0008	0.0023	0.0027	0.0029	0.0031	0.0041	0.0051
MH077	0.0000	0.0002	0.0006	0.0008	0.0011	0.0023	0.0033	0.0039
MH080	0.0000	0.0004	0.0010	0.0016	0.0016	0.0018	0.0022	0.0024
MH081	0.0000	0.0003	0.0004	0.0014	0.0017	0.0017	0.0026	0.0036
Total Wear (g)								
MH/MC060	0.0000	0.0003	0.0005	0.0006	0.0011	0.0012	0.0024	0.0030
MH/MC061	0.0000	0.0001	0.0004	0.0013	0.0018	0.0025	0.0033	0.0048
MH/MC062	0.0000	0.0003	0.0007	0.0009	0.0008	0.0014	0.0021	0.0028
MH/MC063	0.0000	0.0006	0.0013	0.0016	0.0014	0.0018	0.0029	0.0033
MH/MC068	0.0000	0.0009	0.0015	0.0018	0.0020	0.0023	0.0029	0.0051
MH/MC069	0.0000	0.0006	0.0008	0.0010	0.0010	0.0018	0.0032	0.0033
MH/MC070	0.0000	0.0010	0.0012	0.0017	0.0017	0.0020	0.0029	0.0053
MH/MC071	0.0000	0.0006	0.0015	0.0030	0.0032	0.0038	0.0060	0.0076
MH/MC076	0.0000	0.0008	0.0027	0.0033	0.0034	0.0038	0.0054	0.0069
MH/MC077	0.0000	-.0003	0.0005	0.0008	0.0010	0.0025	0.0038	0.0047
MH/MC080	0.0000	0.0004	0.0012	0.0020	0.0020	0.0023	0.0030	0.0035
MH/MC081	0.0000	0.0004	0.0011	0.0023	0.0027	0.0031	0.0047	0.0063

For volumetric wear (mm^3) multiply the weight loss values by 120 for material density of 8331 kg/m^3

Table B7.3b

28mm carbon content variation wear test results, Test 2 of 3

Cycles	0	67003	321993	734632	992950	1349162	1705210	2000414
Cup Wear (g)								
MC064*	0.0000	0.0008	0.0013	0.0015	0.0016	0.0017	0.0019	0.0018
MC065	0.0000	0.0014	0.0017	0.0024	0.0033	0.0036	0.0037	0.0038
MC066	0.0000	0.0014	0.0022	0.0025	0.0025	0.0030	0.0031	0.0032
MC067	0.0000	0.0012	0.0018	0.0020	0.0021	0.0024	0.0028	0.0030
MC072	0.0000	0.0007	0.0011	0.0013	0.0014	0.0015	0.0016	0.0015
MC073	0.0000	0.0007	0.0011	0.0013	0.0015	0.0016	0.0017	0.0016
MC074*	0.0000	0.0006	0.0010	0.0011	0.0011	0.0012	0.0013	0.0012
MC078	0.0000	0.0006	0.0010	0.0011	0.0011	0.0012	0.0013	0.0011
MC079	0.0000	0.0050	0.0090	0.0098	0.0103	0.0106	0.0109	0.0108
MC082	0.0000	0.0016	0.0022	0.0025	0.0025	0.0026	0.0027	0.0029
MC083	0.0000	0.0004	0.0007	0.0008	0.0009	0.0011	0.0018	0.0024
MC084	0.0000	0.0008	0.0012	0.0014	0.0016	0.0023	0.0025	0.0024
Head Wear (g)								
MH064*	0.0000	0.0006	0.0007	0.0007	0.0008	0.0009	0.0008	0.0007
MH065	0.0000	0.0013	0.0016	0.0017	0.0032	0.0034	0.0034	0.0032
MH066	0.0000	0.0023	0.0040	0.0042	0.0041	0.0053	0.0053	0.0056
MH067	0.0000	0.0014	0.0023	0.0025	0.0026	0.0028	0.0029	0.0029
MH072	0.0000	0.0009	0.0011	0.0011	0.0011	0.0013	0.0017	0.0020
MH073	0.0000	0.0006	0.0020	0.0019	0.0022	0.0032	0.0041	0.0039
MH074*	0.0000	0.0005	0.0008	0.0010	0.0017	0.0026	0.0026	0.0024
MH078	0.0000	0.0005	0.0007	0.0008	0.0009	0.0017	0.0017	0.0021
MH079	0.0000	0.0035	0.0066	0.0073	0.0076	0.0080	0.0081	0.0081
MH082	0.0000	0.0015	0.0018	0.0020	0.0021	0.0023	0.0025	0.0025
MH083	0.0000	0.0007	0.0012	0.0012	0.0013	0.0014	0.0016	0.0029
MH084	0.0000	0.0013	0.0017	0.0031	0.0033	0.0035	0.0042	0.0042
Total Wear (g)								
MH/MC064*	0.0000	0.0014	0.0020	0.0021	0.0023	0.0026	0.0027	0.0025
MH/MC065	0.0000	0.0027	0.0034	0.0042	0.0065	0.0070	0.0071	0.0069
MH/MC066	0.0000	0.0036	0.0063	0.0067	0.0067	0.0083	0.0084	0.0088
MH/MC067	0.0000	0.0026	0.0041	0.0045	0.0047	0.0051	0.0058	0.0059
MH/MC072	0.0000	0.0016	0.0022	0.0024	0.0025	0.0028	0.0033	0.0034
MH/MC073	0.0000	0.0014	0.0032	0.0033	0.0037	0.0048	0.0058	0.0055
MH/MC074*	0.0000	0.0012	0.0018	0.0021	0.0029	0.0038	0.0039	0.0036
MH/MC078	0.0000	0.0012	0.0017	0.0019	0.0020	0.0029	0.0030	0.0032
MH/MC079	0.0000	0.0084	0.0154	0.0172	0.0179	0.0186	0.0189	0.0189
MH/MC082	0.0000	0.0031	0.0040	0.0045	0.0046	0.0049	0.0052	0.0051
MH/MC083	0.0000	0.0011	0.0019	0.0021	0.0021	0.0024	0.0034	0.0053
MH/MC084	0.0000	0.0021	0.0029	0.0045	0.0048	0.0058	0.0067	0.0065

*Cleaning protocol not completely adhered to since the acid cleaning element was not carried out.
For volumetric wear (mm^3) multiply the weight loss values by 120 for material density of 8331kg/m^3

Table B7.3c

28mm carbon content variation wear test results, Test 3 of 3

Carbon Content (Head/Cup)	Mean Total Wear at 2 Million Cycles (g)	Number of Samples
H/H	0.003767	3
L/H	0.002500	2
H/L	0.002500	4
L/L	0.003500	2

Table B7.4a

28mm carbon content variation mean wear test results at about 2 million cycles, Test 1 of 3. Appendix C3 details the statistical method used.

Carbon Content (Head/Cup)	Mean Total Wear at 2 Million Cycles (g)	Number of Samples
H/H	0.005325	4
L/H	0.003475	4
H/L	0.004900	2
L/L	0.005800	2

Table B7.4b

28mm carbon content variation mean wear test results at about 2 million cycles, Test 2 of 3. Appendix C3 details the statistical method used.

Carbon Content (Head/Cup)	Mean Total Wear at 2 Million Cycles (g)	Number of Samples
H/H	0.004190	3
L/H	0.006020	4
H/L	0.005650	3
L/L	0.003230	1

Table B7.4c

28mm carbon content variation mean wear test results at about 2 million cycles, Test 3 of 3. Appendix C3 details the statistical method used.

Carbon Content (Head/Cup)	Mean Total Wear at 2 Million Cycles (g)	Number of Samples	Unbiased Estimator of Population Standard Deviation
H/H	0.004508	10	0.000984
L/H	0.004291	10	0.001600
H/L	0.004086	9	0.001350
L/L	0.004374	5	0.002186

Table B7.4d

28mm carbon content variation mean wear test results at about 2 million cycles, Sum of All 3 Tests. Appendix C3 details the statistical method used.

Carbon Content (Head/Cup)	Mean Total Wear at 2 Million Cycles (g)	Number of Samples	Unbiased Estimator of Population Standard Deviation
H/H	0.004508	10	0.000984
L/H and H/L	0.004196	19	0.000950
L/L	0.004374	5	0.002186

Table B7.4e

28mm carbon content variation mean wear test results at about 2 million cycles, Sum of All 3 Tests as Table B7.4d but combining the H/L and L/H samples. Appendix C3 details the statistical method used.

Carbon Content (Head/Cup)	Mean Total Wear at 2 Million Cycles (g)	Number of Samples	Unbiased Estimator of Population Standard Deviation
H/H	0.004508	10	0.000984
L/H and H/L	0.004196	19	0.000950
L/L	0.004221	8	0.001213

Table B7.4f

28mm carbon content variation mean wear test results at about 2 million cycles, Sum of All 3 Tests and including the 3 optimum clearance Low/Low samples from Chapter 6 (Figure 6.8). Appendix C3 details the statistical method used.

Cycles	0	113825	462794	1027502	1509464	2076464
Cup Wear (g)						
MC029	0.0000	0.00143	0.00221	0.00295	0.00485	0.00554
MC030	0.0000	0.00047	0.00090	0.00124	0.00181	0.00224
MC031	0.0000	0.00101	0.00168	0.00234	0.00264	0.00865
MC032	0.0000	0.00011	0.00074	0.00113	0.00659	0.00686
MC033	0.0000	0.00084	0.00123	0.00156	0.00226	0.00246
MC034	0.0000	0.00023	0.00035			
MC035	0.0000	0.00010	0.00018	0.00046	0.00092	0.00113
MC036	0.0000	0.00005	0.00069			
MC037	0.0000	-0.00003	0.00062	0.00130	0.00174	0.00207
MC038	0.0000	0.00023	0.00045	0.00077	0.00145	0.00160
MC039	0.0000	0.00049	0.00063	0.00111	0.00148	0.00182
MC040	0.0000	0.00103	0.00106	0.00143	0.00182	0.00205
Head Wear (g)						
MH029	0.0000	0.00230	0.00377	0.00555	0.00621	0.00626
MH030	0.0000	0.00166	0.00280	0.00308	0.00381	0.00388
MH031	0.0000	0.00180	0.00342	0.00416	0.00448	0.00474
MH032	0.0000	0.00064	0.00070	0.00106	0.00120	0.00144
MH033	0.0000	0.00035	0.00046	0.00076	0.00095	0.00111
MH034	0.0000	0.00032	0.00050			
MH035	0.0000	0.00059	0.00060	0.00110	0.00129	0.00128
MH036	0.0000	0.00109	0.00151			
MH037	0.0000	0.00107	0.00207	0.00249	0.00278	0.00301
MH038	0.0000	0.00182	0.00196	0.00230	0.00526	0.00517
MH039	0.0000	0.00305	0.00322	0.00338	0.00362	0.00374
MH040	0.0000	0.00303	0.00324	0.00435	0.00460	0.00463
Total Wear (g)						
MH/MC029	0.0000	0.00373	0.00598	0.00850	0.01106	0.01180
MH/MC030	0.0000	0.00213	0.00370	0.00432	0.00562	0.00612
MH/MC031	0.0000	0.00281	0.00510	0.00650	0.00712	0.01339
MH/MC032	0.0000	0.00075	0.00144	0.00219	0.00779	0.00830
MH/MC033	0.0000	0.00119	0.00169	0.00232	0.00321	0.00357
MH/MC034	0.0000	0.00055	0.00085			
MH/MC035	0.0000	0.00069	0.00078	0.00156	0.00221	0.00241
MH/MC036	0.0000	0.00114	0.00220			
MH/MC037	0.0000	0.00104	0.00269	0.00379	0.00452	0.00508
MH/MC038	0.0000	0.00205	0.00241	0.00307	0.00671	0.00677
MH/MC039	0.0000	0.00354	0.00385	0.00449	0.00510	0.00556
MH/MC040	0.0000	0.00406	0.00430	0.00578	0.00642	0.00668

For volumetric wear (mm^3) multiply the weight loss values by 120 for material density of $8331 kg/m^3$

Table B8.3a

22mm diametral clearance variation wear test results

Cycles	0	57415	237128	498418	719401	857600	1116825	1471677	2022343
Cup Wear (g)									
MC044	0.0000	0.00023	0.00032	0.00091	0.00115	0.00253	0.00303	0.00843	0.00923
MC045	0.0000	-0.00012	0.00019	0.00019					
MC046	0.0000	0.00000	0.00014	0.00023	0.00049	0.00101	0.00111	0.00171	0.00241
MC047	0.0000	0.00016	0.00021	0.00032	0.00057	0.00096	0.00156	0.00566	0.00776
MC048	0.0000	0.00012	0.00019	0.00030	0.00076				
MC049	0.0000	-0.00005	0.00005	0.00019	0.00057	0.00116	0.00156	0.00186	0.00316
MC050	0.0000	-0.00005	-0.00001	0.00012	0.00091	0.00165	0.00185	0.00195	0.00245
MC051	0.0000	0.00004	0.00010	0.00023	0.00044	0.00065	0.00125	0.00925	0.01095
MC052	0.0000	-0.00015	0.00010	0.00028	0.00044	0.00161	0.00301	0.00471	0.00581
MC053	0.0000	0.00005	0.00002	0.00029	0.00046	0.00075	0.00125	0.00965	
MC054	0.0000	0.00008	0.00020	0.00046	0.00074	0.00159	0.00239	0.00459	0.00559
MC055	0.0000	0.00025	0.00079	0.00329	0.00623	0.00680			
MC056[1]	0.0000	-0.00008	-0.00014	-0.00009	-0.00001	-0.00013	-0.00017	-0.00003	-0.00010
Head Wear (g)									
MH044	0.0000	0.00041	0.00084	0.00120	0.00167	0.00197	0.00277	0.00227	0.00247
MH045	0.0000	0.00001	0.00023	0.00029					
MH046	0.0000	0.00005	0.00012	0.00032	0.00109	0.00125	0.00195	0.00155	0.00165
MH047	0.0000	0.00107	0.00152	0.00157	0.00227	0.00263	0.00383	0.00353	0.00363
MH048	0.0000	0.00069	0.00082	0.00080	0.00211				
MH049	0.0000	-0.00001	0.00010	0.00015	0.00082	0.00087	0.00187	0.00157	0.00137
MH050	0.0000	0.00001	0.00007	0.00026	0.00053	0.00123	0.00233	0.00213	0.00193
MH051	0.0000	0.00006	0.00012	0.00020	0.00094	0.00088	0.00158	0.00118	0.00158
MH052	0.0000	0.00002	0.00010	0.00034	0.00049	0.00075	0.00285	0.00415	0.000465
MH053	0.0000	0.00000	0.00008	0.00031	0.00079	0.00094	0.00174	0.00124	
MH054	0.0000	0.000026	0.02910	0.03106	0.04002	0.04233	0.04753	0.04733	0.04793
MH055	0.0000	0.001970	0.00508	0.00550	0.00574	0.00625			
MH056[1]	0.0000	-0.00012	-0.00004	0.00007	0.00010	-0.00016	0.00054	0.00004	0.00014
Total Wear (g)									
MH/MC044	0.0000	0.00064	0.00116	0.00211	0.00282	0.00450	0.00580	0.01070	0.01170
MH/MC045	0.0000	-0.00011	0.00042	0.00048					
MH/MC046	0.0000	0.00005	0.00026	0.00055	0.00158	0.00226	0.00306	0.00326	0.00406
MH/MC047	0.0000	0.00123	0.00173	0.00189	0.00284	0.00359	0.00539	0.00919	0.01139
MH/MC048	0.0000	0.00081	0.00101	0.00110	0.00287				
MH/MC049	0.0000	-0.00006	0.00015	0.00034	0.00139	0.00203	0.00343	0.00343	0.00453
MH/MC050	0.0000	-0.00004	0.00006	0.00038	0.00144	0.00288	0.00418	0.00408	0.00438
MH/MC051	0.0000	0.00010	0.00022	0.00043	0.00138	0.00153	0.00283	0.01043	0.01253
MH/MC052	0.0000	-0.00013	0.00020	0.00062	0.00093	0.00236	0.00586	0.00886	0.01046
MH/MC053	0.0000	0.00005	0.00010	0.00060	0.00125	0.00169	0.00299	0.00819	
MH/MC054	0.0000	0.00034	0.02930	0.03152	0.04076	0.04392	0.04992	0.05192	0.05352
MH/MC055	0.0000	0.00222	0.00588	0.00880	0.01197	0.01306			
MH/MC056[1]	0.0000	-0.00020	-0.00018	-0.00002	0.00009	-0.00029	0.00071	0.00001	0.00001

[1]Control sample not wear tested

For volumetric wear (mm^3) multiply the weight loss values by 120 for material density of 8331kg/m^3

Table B8.3b

35mm diametral clearance variation wear test results

Cycles	0	51445	300100	553550	900850	1149800	1598450
Cup Wear (g)							
MC100	0.0000	0.00032	0.00053	0.00082	0.00091	0.00112	0.00133
MC101	0.0000	0.00076	0.00072	0.00094	0.00092	0.00110	
MC102	0.0000	0.00037	0.00045	0.00062	0.00069	0.00086	0.00105
MC104	0.0000	0.00040	0.00047	0.00073	0.00074	0.00114	0.00135
MC105	0.0000	0.00045	0.00074	0.00111	0.00129	0.00157	
MC106	0.0000	0.00084	0.00100	0.00124	0.00134	0.00151	
MC107	0.0000	0.00120	0.00152	0.00186	0.00190	0.00221	0.00258
MC108	0.0000	0.00110	0.00123	0.00150	0.00160	0.00174	
MC109	0.0000	0.00060	0.00064	0.00082	0.00102	0.00142	
MC110	0.0000	0.00134	0.00160	0.00180	0.00183	0.00239	
MC111	0.0000	0.00117	0.00121	0.00136	0.00142	0.00159	0.00169
MC112	0.0000	0.00097	0.00117	0.00159	0.00184	0.00213	0.00240
MC103[1]	0.0000	0.0000	0.00001	0.00005	0.00002	0.0000	0.00007
MC113[1]	0.0000	-0.00002	0.0000	0.00010	0.00002	0.00011	0.00015
Head Wear (g)							
MH100	0.0000	0.00012	0.00009	0.00025	0.00043	0.00050	0.00072
MH101	0.0000	0.00034	0.00027	0.00037	0.00064	0.00075	
MH102	0.0000	0.00019	0.00017	0.00031	0.00053	0.00060	0.00080
MH104	0.0000	0.00013	0.00009	0.00023	0.00036	0.00057	0.00066
MH105	0.0000	0.00013	0.00012	0.00037	0.00060	0.00077	
MH106	0.0000	0.00026	0.00025	0.00037	0.00059	0.00064	
MH107	0.0000	0.00030	0.00014	0.00046	0.00068	0.00082	0.00097
MH108	0.0000	0.00090	0.00095	0.00105	0.00135	0.00145	
MH109	0.0000	0.00024	0.00016	0.00019	0.00052	0.00057	
MH110	0.0000	0.00094	0.00105	0.00114	0.00132	0.00155	
MH111	0.0000	0.00076	0.00080	0.00094	0.00122	0.00129	0.00145
MH112	0.0000	0.00106	0.00114	0.00128	0.00166	0.00178	0.00207
MH103[1]	0.0000						
MH113[1]	0.0000						
Total Wear (g)							
MH/MC100	0.0000	0.00044	0.00062	0.00107	0.00134	0.00162	0.00205
MH/MC101	0.0000	0.00110	0.00099	0.00131	0.00156	0.00185	
MH/MC102	0.0000	0.00056	0.00062	0.00093	0.00122	0.00146	0.00185
MH/MC104	0.0000	0.00053	0.00056	0.00096	0.00110	0.00171	0.00201
MH/MC105	0.0000	0.00058	0.00086	0.00148	0.00189	0.00234	
MH/MC106	0.0000	0.00110	0.00125	0.00161	0.00193	0.00215	
MH/MC107	0.0000	0.00150	0.00166	0.00232	0.00258	0.00303	0.00355
MH/MC108	0.0000	0.00200	0.00218	0.00255	0.00295	0.00319	
MH/MC109	0.0000	0.00084	0.00080	0.00101	0.00154	0.00199	
MH/MC110	0.0000	0.00228	0.00265	0.00294	0.00315	0.00394	
MH/MC111	0.0000	0.00193	0.00201	0.00230	0.00264	0.00288	0.00314
MH/MC112	0.0000	0.00203	0.00231	0.00287	0.00350	0.00391	0.00447
MH/MC103[1]	0.0000						
MH/MC113[1]	0.0000						

[1]Control samples not wear tested

For volumetric wear (mm^3) multiply the weight loss values by 120 for material density of 8331kg/m^3

Table B9.3a

Final design wear test results from 0 to 2 million cycles

Cycles	2144465	2801630	3253720	3993400	4641100	5195220
Cup Wear (g)						
MC100	0.00163	0.00199	0.00243	0.00274	0.00320	0.00346
MC101						0.00233
MC102						
MC104	0.00163	0.00208	0.00232	0.00254	0.00304	0.00333
MC105						0.00339
MC106						0.00302
MC107	0.00285	0.00313	0.00351	0.00371	0.00399	0.00426
MC108						0.00363
MC109						
MC110						0.00351
MC111	0.00175	0.00188	0.00208	0.00208	0.00238	0.00242
MC112	0.00274	0.00306	0.00335	0.00350	0.00385	0.00403
MC103[1]	0.00013	0.00017	0.00019	0.00006	0.00015	0.00019
MC113[1]	0.00010	0.00019	0.00022	0.00010	0.00016	0.00016
Head Wear (g)						
MH100	0.00088	0.00107	0.00128	0.00155	0.00178	0.00197
MH101						0.00180
MH102						
MH104	0.00080	0.00092	0.00106	0.00114	0.00132	0.00148
MH105						0.00195
MH106						0.00162
MH107	0.00111	0.00140	0.00165	0.00171	0.00208	0.00237
MH108						0.00357
MH109						
MH110						0.00255
MH111	0.00157	0.00169	0.00186	0.00190	0.00212	0.00221
MH112	0.00241	0.00277	0.00308	0.00343	0.00385	0.00413
MH103[1]						
MH113[1]						
Total Wear (g)						
MH/MC100	0.00251	0.00306	0.00371	0.00429	0.00498	0.00543
MH/MC101						0.00413
MH/MC102						
MH/MC104	0.00243	0.00300	0.00338	0.00368	0.00436	0.00481
MH/MC105						0.00534
MH/MC106						0.00464
MH/MC107	0.00396	0.00453	0.00516	0.00542	0.00607	0.00663
MH/MC108						0.00720
MH/MC109						
MH/MC110						0.00606
MH/MC111	0.00332	0.00357	0.00394	0.00398	0.00450	0.00463
MH/MC112	0.00515	0.00583	0.00643	0.00693	0.00770	0.00816
MH/MC103[1]						
MH/MC113[1]						

[1]Control samples not wear tested

For volumetric wear (mm^3) multiply the weight loss values by 120 for material density of 8331kg/m^3

Table B9.3b

Final design wear test results from 2 to 5 million cycles

Cycles	Mean Wear (g)	Number of Samples	95% Confidence Limits on Mean
0	0.00000	6	0.00000
51445	0.00176	6	0.00054
300100	0.00194	6	0.00068
553550	0.00233	6	0.00074
900850	0.00273	6	0.00071
1149800	0.00316	6	0.00076
1598450	0.00372	3	0.00169
2144465	0.00414	3	0.00231
2801630	0.00464	3	0.00282
3253720	0.00518	3	0.00309
3993400	0.00544	3	0.00367
4641100	0.00609	3	0.00398
5195220	0.00654	5	0.00164

Table B9.4a

Standard insert final design mean wear data. Appendix C3 details the statistical method used.

Cycles	Mean Wear (g)	Number of Samples	95% Confidence Limits on Mean
0	0.00000	6	0.00000
51445	0.00072	6	0.00031
300100	0.00082	6	0.00028
553550	0.00123	6	0.00030
900850	0.00151	6	0.00036
1149800	0.00186	6	0.00035
1598450	0.00197	3	0.00026
2144465	0.00247	2	0.00051
2801630	0.00303	2	0.00038
3253720	0.00355	2	0.00210
3993400	0.00399	2	0.00388
4641100	0.00467	2	0.00394
5195220	0.00487	5	0.00066

Table B9.4b

Augmented insert final design mean wear data. Appendix C3 details the statistical method used.

Cycles	0	51445	300100	553550	900850	1149800	1598450	2144465
Total Wear (g)								
MH/MC019	0.0000	0.0002	0.0004	0.0009	0.0022	0.0025	0.0027	0.0032
MH/MC020	0.0000	0.0000	0.0000	0.0005	0.0013	0.0016	0.0021	0.0025
MH/MC023	0.0000	0.0002	-0.0003	0.0002	0.0012	0.0015	0.0018	0.0019
MH/MC024	0.0000	0.0011	0.0009	0.0010	0.0019	0.0022	0.0026	0.0026
MH/MC025	0.0000	0.0002	0.0006	0.0009	0.0022	0.0027	0.0027	0.0028
MH/MC026	0.0000	0.0001	0.0002	0.0007	0.0017	0.0020	0.0022	0.0022
MH/MC060	0.0000	0.0003	0.0007	0.0011	0.0012	0.0015	0.0025	0.0032
MH/MC061	0.0000	0.0001	0.0014	0.0019	0.0024	0.0027	0.0036	0.0052
MH/MC062	0.0000	0.0003	0.0009	0.0009	0.0013	0.0016	0.0022	0.0030
MH/MC063	0.0000	0.0005	0.0015	0.0015	0.0017	0.0021	0.0030	0.0034
MH/MC064	0.0000	0.0011	0.0020	0.0021	0.0022	0.0024	0.0027	0.0024
MH/MC065	0.0000	0.0021	0.0033	0.0037	0.0057	0.0067	0.0071	0.0068
MH/MC066	0.0000	0.0028	0.0061	0.0065	0.0067	0.0074	0.0084	0.0090
MH/MC067	0.0000	0.0020	0.0040	0.0043	0.0046	0.0049	0.0056	0.0059
MH/MC080	0.0000	0.0003	0.0020	0.0021	0.0022	0.0025	0.0031	0.0036
MH/MC081	0.0000	0.0003	0.0024	0.0028	0.0030	0.0035	0.0050	0.0067
MH/MC082	0.0000	0.0023	0.0039	0.0043	0.0046	0.0048	0.0051	0.0051
MH/MC083	0.0000	0.0008	0.0018	0.0020	0.0021	0.0023	0.0031	0.0062
MH/MC084	0.0000	0.0016	0.0028	0.0038	0.0047	0.0052	0.0064	0.0064
Mean Total Wear (g)								
	0.0000	0.0009	0.0018	0.0022	0.0028	0.0032	0.0034	0.0043

[1]Control samples not wear tested

For volumetric wear (mm^3) multiply the weight loss values by 120 for material density of $8331 kg/m^3$

Table B9.9

Mean wear data for the high/low and low/high carbon content samples of chapter 7 interpolated linearly to give data at the cycle intervals as used for the data of chapter 9.

Appendix C: Derivations and Calculations

C1: Calculation of Mean Linear Penetration for Mating Spheres

A simple method of estimating the linear penetration wear of the head and cup surfaces based on an estimate of the spread of wear over the respective surfaces and on the measured volumetric wear is presented.

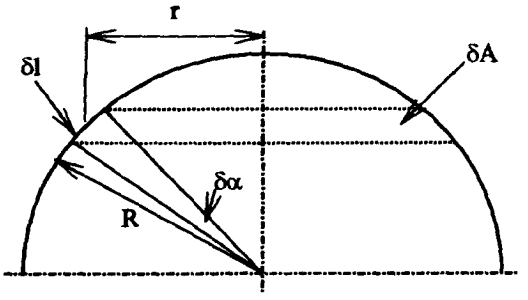

For the surface area of a sphere from first principles:-

$\delta A = 2\pi r \delta l$

$\delta A = 2\pi R \cos\alpha \delta l$

$\delta A = 2\pi R \cos\alpha r \delta\alpha$

$\delta A = 2\pi R^2 \cos\alpha \delta\alpha$

Therefore:-

$As = 4\sum \pi R^2 \cos\alpha \delta\alpha$ $\quad$ α from 0 to 90°

$$As = 4\pi R^2 \int_{\alpha=0}^{\alpha=\pi/2} \cos\alpha \delta\alpha$$

$As = 4\pi R^2 [\sin\alpha]$ $\quad$ α from 0 to $\pi/2$

$\underline{As = 4\pi R^2}$ $\quad$ Which can be confirmed in any mathematics formulae book.

And therefore the equation for the curved surface area of an hemisphere is:-

$Ah=2\pi R^2[\sin\alpha]$ α from 0 to $\pi/2$

Here any values of α between 0 and $\pi/2$ can be input to get the surface area for a portion of an hemisphere sphere.

Application to 28mm Diameter Components

Consider a spherical diameter 28mm and a contact patch under load extending 25° either side of the pole of the head forming a circular edged patch. Therefore α is from 65 to 90° for the head. Because the cup is inclined at 23° in the simulator, the bounds of the total wear area for the cup would be 48° either side of the pole and so α is from 42 to 90° for the cup. For head:-

$Ah=2\pi R^2[\sin\alpha]$ α from 65 to 90°

$Ah=2\pi R^2[\sin 90-\sin 65]$

$Ah=2\pi R^2[1-0.9063]$

$Ah=115mm^2$ for the head surface.

For the cup

$Ah=2\pi R^2[\sin\alpha]$ α from 42 to 90°

$Ah=2\pi R^2[\sin 90-\sin 42]$

$Ah=2\pi R^2[1-0.6691]$

$Ah=407mm^2$ for the cup surface

Therefore from Table B8.5 for MH007 and MC007:-

Component	Estimated Wearing Area (mm^2)	Volumetric Wear at 2028204 cycles (mm^3)	Estimated Linear Wear (mm)
MC007	407.0	0.276	0.0007
MH007	115.0	0.348	0.0030

C2: Calculation of Linear Penetration, Radius of Conforming Contact Patch, and Wear Volume for Overlapping Spheres

A more complex alternative method to C1 of calculating the linear penetration wear of spherical bearing surfaces by assuming that the wear takes place as if the spherical surfaces had intersected or overlapped. This method allows also for calculation of a radius of conforming contact surface radius, and output data is based on comparison of calculated and actual measured volumetric wear data.

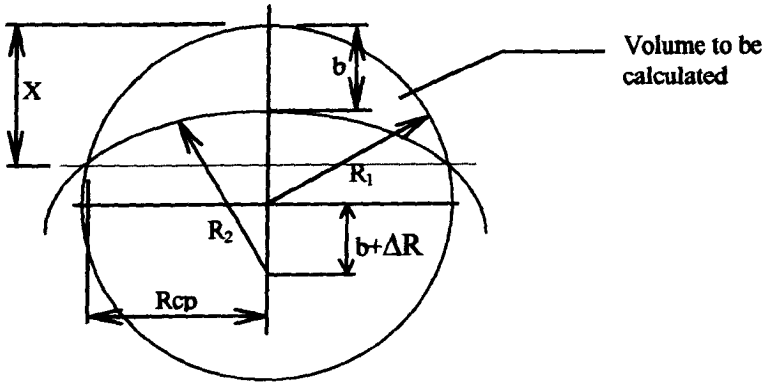

Given
R_1 =Radius of male sphere
R_2 =Radius of female sphere
b=linear penetration of R_1 into R_2
$\Delta R=R_2-R_1$

Required
Rcp= Radius of contact patch
V=Volume of intersection between the spheres

Rcp in terms of b, R_1 and R_2

$$\mathbf{Rcp^2=R_1^2-(R_1-X)^2} \qquad \textbf{Eq 1}$$

and

$$\mathbf{Rcp^2=R_2^2-(R_2-X+b)} \qquad \textbf{Eq 2}$$

Combining equations 1 and 2 to find an expression for X:-

$$R_1^2-(R_1-X)^2= R_2^2-(R_2-X+b)$$

So that X can be defined as:-

$$\mathbf{X=b(2R_2+b)/2(R_2-R_1+b)} \qquad \textbf{Eq 3}$$

Taking Eq 1 and substituting into Eq 3:-

$Rcp^2=R_1^2-(R_1- b(2R_2+b)/2(R_2-R_1+b))^2$

And therefore Rcp is defined as:-

$$\mathbf{Rcp= \left(\frac{b(2R_2+b)}{(R_2-R_1+b)}\left(R_1- \frac{b(2R_2+b)}{4(R_2-R_1+b)}\right)\right)^{0.5}} \qquad \textbf{Eq 4}$$

Calculation of Volume

The volume to be calculated by subtracting one from the other, the volume enclosed between the apex of R_1 and the plane defined by the intersection of the two spheres (V_{R1}) and the volume enclosed between the apex of R_2 and the same plane (V_{R2}).

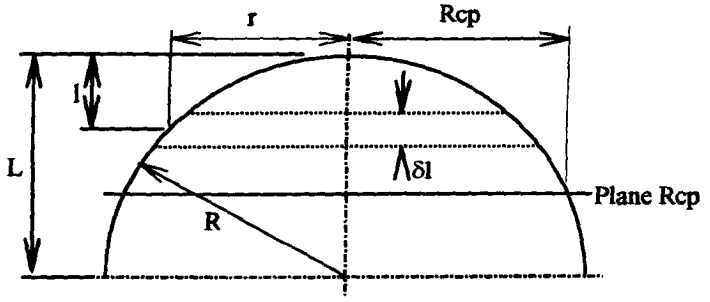

From first principles, the volume is defined as:-

$\delta V=\pi r^2 \delta l$

$V= \sum \pi r^2 \delta l$ l from 0 to L

Also:-

$R^2=r^2+(R-l)^2$

and therefore:-

$$\mathbf{r^2=2Rl-l^2} \qquad \textbf{Eq 5}$$

Substituting Eq 5 into the volume equation gives:-

$$V=\pi \int_{l=0}^{l=L} (2Rl-l^2)\delta l$$

Therefore:-

$$V=\pi \int_{l=0}^{l=L} 2Rl\delta l - \pi \int_{l=0}^{l=L} l^2\delta l$$

$$V=2\pi\left[\frac{Rl^2}{2}\right]_0 - \pi\left[\frac{l^3}{3}\right]_0$$

$$\mathbf{V=\pi L^2(R-L/3)} \qquad \textbf{Eq 6}$$

Now V_{R1} is found by substituting L=X into equation 6 where X is defined from equation 3:-

$$\mathbf{V_{R1}=\pi\left(\frac{b(2R_2+b)}{2(R_2-R_1+b)}\right)^2\left(R_1-\frac{b(2R_2+b)}{6(R_2-R_1+b)}\right)} \qquad \textbf{Eq 7}$$

For calculation of V_{R2}, from Eq 6 where $R=R_2$ and $L=X-b$ then:-

$$L=\frac{b}{2}\left(\frac{2R_1.b}{R_2-R_1+b}\right)$$

And therefore:-

$$\mathbf{V_{R2}=\pi\left(\frac{b(2R_1-b)}{2(R_2-R_1+b)}\right)^2\left(R_2-\frac{b(2R_1-b)}{6(R_2-R_1+b)}\right)} \qquad \textbf{Eq 8}$$

Finally, subtracting Eq 8 from Eq 7 gives the resultant volume required:-

$$\mathbf{V=\frac{\pi b^2}{4}\left(\left(\frac{2R_2+b}{R_2-R_1+b}\right)^2\left(R_1-\frac{b(2R_2+b)}{6(R_2-R_1+b)}\right)-\left(\frac{2R_1-b}{R_2-R_1+b}\right)^2\left(R_2-\frac{b(2R_1-b)}{6(R_2-R_1+b)}\right)\right)} \qquad \textbf{Eq 9}$$

The equations are easily validated by taking the case 2 spheres, where 1 sphere is infinitely bigger than the other and is therefore a flat plane, and the intersection is through the centre of the small sphere. The result should be the same as half the volume of the small sphere.

Eg R1=1
R2=1000000
b=1

The volume of a sphere is $Vs=4\pi R^3/3$

Therefore the half volume is 2.094395 units

Using equations 3, 4, and 9:-

X=1
Rcp=1
V=2.094396 units

Application to 28mm Diameter Components

Having established these equations then for a given head diameter, diametral clearance, and linear penetration, the radial spread of the theoretical conforming contact surfaces and the volumetric wear could be calculated.

Table C2.1 provides data on the theoretical wear volume and linear penetration for a range of values of Rcp up to about 7.2mm for three specific diametral clearances in a 28mm metal on metal bearing couple. For the purpose of the analysis the head is assumed to be exactly 28mm and the cup is oversized to create the required diametral clearance.

Wear Volume V for 0.014mm Diametral Clearance (mm^3)	Wear Volume V for 0.060mm Diametral Clearance (mm^3)	Wear Volume V for 0.322mm Diametral Clearance (mm^3)	Radius of Contact Patch Rcp (mm)	Linear Penetration b (μm)
0.00000	0.00000	0.00000	0.00000	0.0
		0.00004	0.49603	0.1
		0.00016	0.70117	0.2
		0.00062	0.99068	0.4
	0.00021		1.14147	0.1
		0.00139	1.21221	0.6
		0.00246	1.39844	0.8
		0.00385	1.56206	1.0
	0.00082		1.61030	0.2
		0.00553	1.70957	1.2
		0.00752	1.84484	1.4
		0.00981	1.97040	1.6
		0.01240	2.08800	1.8
		0.01528	2.19893	2.0
	0.00325		2.26600	0.4
0.00087			2.34201	0.1
		0.03418	2.68083	3.0
	0.00726		2.76170	0.6
	0.01282		3.17350	0.8
0.00342			3.27766	0.2
		0.09380	3.42974	5.0
	0.01991		3.53099	1.0
	0.02848		3.84950	1.2
	0.03852		4.13820	1.4
	0.04999		4.40310	1.6
0.01332			4.54168	0.4
	0.06287		4.64830	1.8
		0.36423	4.74442	10.0
	0.07713		4.87700	2.0
0.02918			5.45350	0.6
		0.79623	5.68797	15.0
	0.16829		5.83861	3.0
0.05055			6.17757	0.8
		1.37642	6.43367	20.0
0.07701			6.77942	1.0
		2.09284	7.05067	25.0
	0.44077		7.21882	5.0
		2.41512	7.27018	27.0
0.10819			7.29349	1.2

Table C2.1

Values of wear volume (V), radius of conforming contact patch (Rcp), and linear penetration (b) for a theoretical 28mm head diameter with diametral clearance of 0.014, 0.060, and 0.322mm. Data is colour coded to clarify which values of Rcp and b correspond to which diametral clearance.

C3: Calculation of Statistical Data Relating to the Wear Data

In measurement and interpretation of the wear data it was important to note that the sample sizes used were generally quite small. It was necessary to use appropriate statistical methods to ensure that the results were properly interpreted. The following is a discussion of the statistical methods used within this thesis (Greer, 1988).

A wear measurement was considered as one single sample from an *infinitely large* population or pool of such measurements. *Within this work*, when possible, samples from the pool were as large as possible. Even so, the total sample size taken from each infinite population of measurements was still quite small compared to the size of the population or pool. In statistics, when sample sizes are less than 30, it is not accurate to assume that the data generated fits a normal distribution but rather a "t" distribution. In this thesis, statistical samples were generally between 4 and 12 and so clearly fitted the t distribution.

A sample of n measurements from an infinite population of such measurements can provide an estimation of the true population mean and standard deviation. Indeed, the sample mean Ë should statistically be exactly the same as the population mean μ. The data for each sample of wear measurements was presented as a sample mean along with an error bar. This error bar represented the limits within which there was confidence that 95% of the time the true population mean fell.

The following example demonstrates how this analysis was performed.

Suppose there were 5 data points or measurements E_i and n was the sample size

1	0.0034
2	0.0045
3	0.0036
4	0.0040
5	0.0041
n	5

The sample mean Ë was calculated from

$\ddot{E}=\Sigma E_i/n=0.00392$

The sample standard deviation s was calculated from

$s=\sqrt{(\Sigma E_i^2/n-\ddot{E}^2)}=0.000387$

However, when the sample size was less than 30, it was important to calculate the "unbiased estimate of the population standard deviation" š :-

$\check{s}=s\sqrt{(n/(n-1))}=0.000432$

An estimate of closeness of the sample mean to the population mean was required and represented as the limits about the sample mean within which there was 95% confidence that the population mean lay. Using the "t" distribution table for 4 degrees of freedom (degrees of freedom being one less than the sample number) the appropriate number was selected from the table (two tail test):-

Significance Level	95% Level		99% Level	
Degrees of Freedom	One tail test	Two tail test	One tail test	Two tail test
1	6.314	12.706	*31.821*	*63.657*
2	2.920	4.303	6.965	9.925
3	2.353	3.182	4.541	5.841
4	2.132	2.776	3.747	4.604
5	2.015	2.571	3.365	4.032
6	1.943	2.447	3.143	3.707
7	1.895	2.365	2.998	3.499
8	1.860	2.306	2.896	3.355
9	1.833	2.262	2.821	3.250
10	1.812	2.228	2.764	3.169
11	1.796	2.201	2.718	3.106
12	1.782	2.179	2.681	3.055
13	1.771	2.160	2.650	3.012
14	1.761	2.145	2.624	2.977
15	1.753	2.131	2.602	2.947
16	1.746	2.120	2.583	2.921
17	1.740	2.110	2.567	2.898
18	1.734	2.101	2.552	2.878
19	1.729	2.093	2.539	2.861
20	1.725	2.086	2.528	2.845
21	1.721	2.080	2.518	2.831
22	1.717	2.074	2.508	2.819
23	1.714	2.069	2.500	2.807
24	1.711	2.064	2.492	2.797
25	1.708	2.060	2.485	2.787
26	1.706	2.056	2.479	2.779
27	1.703	2.052	2.473	2.771
28	1.701	2.048	2.467	2.763
29	1.699	2.045	2.462	2.756
30	1.697	2.042	2.457	2.750

With a t value of 2.776 the population mean was calculated from:-

$\mu = \ddot{E} \pm t\check{s}/\sqrt{n} = 0.00392 \pm 0.000536$

Therefore there was 95% confidence that the population mean was between 0.003384 and 0.004456. This was shown graphically as:-

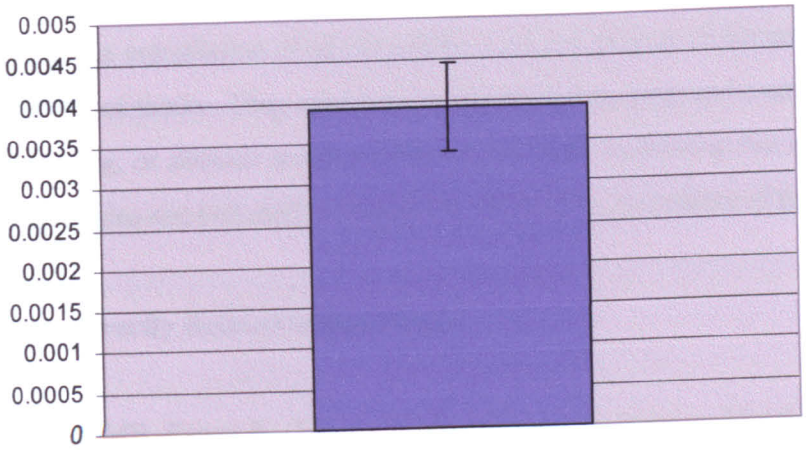

Graphical representation of the 95% confidence limits within which the population mean fell. The bar was the calculated sample mean.

Appendix D: Abstracts, Proceedings, *Papers, and Patents*

The following is a compilation of all the publications and patents of the author arising from the subject of thesis. They are listed in chronological order and a copy of each paper, proceeding, or abstract as appropriate is included. Following that are listed other publications (copies not included) of the author related to the subject of the thesis.

Publications Directly Related to the Thesis

1. Schmidt MB, Farrar R, "Effect of Diameter on the Wear of Metal-on-Metal Hips", Ninth Annual Symposium of the Intl. Soc. for Technology in Arthroplasty (ISTA), Amsterdam, 1996.

2. Farrar R, Schmidt MB, "The Effect of diametral Clearance on Wear Between Head and Cup for Metal on Metal Articulations", Trans. Orthop. Res. Soc., 22:71, 1997.

3. Farrar R, Schmidt MB, Hamilton JV, Greer KW, "The Development of Low Wear Articulations", Proceedings of the Societe Internationale de Recherche Orthopedique (SIROT) 97 Inter Meeting, Haifa, 1997.

4. Schmidt MB, Farrar R, "Characterisation of the Wear Behaviour of Metal-on-Metal Hip Components Using a Hip Joint Simulator", ASTM Symposium on Alternative Bearing Surfaces in Total Joint Replacement, San Diego, 1997.

5. Jacobs MA, Schmidt MB, Farrar R, "Comparison of Wear Rates for Metal on Polyethylene and Metal on Metal Hips", Journal of Arthroplasty, Vol. 12, No 2, Feb, 1997.

6. Jacobs MA, Schmidt MB, Farrar R, "The Effect of Clearance and Diameter on Debris Generation in a Metal-on-Metal Hip", Abstracts from the American Association of Hip and Knee Surgeons Seventh Annual Meeting, published in the Journal of Arthroplasty, Vol 13, No 2, Feb, 1998.

7. Nolan J, Farrar R, Schmidt MB, Phillips H, Tucker JK, "Effect of Head Size and Diametral Clearance on Wear Production of a New Metal on Metal Hip Prosthesis": Poster, 10th Meeting of the Combined Orthopaedic Associations of the English Speaking World, New Zealand, Feb, 1998.

8. European Patent Application EP0 841 041 A3, "Hip Joint Prosthesis", inventors R Farrar, ME Schmidt, Published 17 Mar 1999.

9. United States Patent 5 904 720, "Hip Joint Prosthesis", inventors R Farrar, ME Schmidt, granted 18 May 1999.

Publications by the Author of Relevance in the Thesis

1. European Patent Application EP0 811 360 A2, "Extraction Device", inventors B Hiernard, R Farrar, Published 10 Dec 1997.

2. United States Patent 5 938 701, "Extraction Device", inventors B Hiernard, R Farrar, granted 17 Aug 1999.

3. Tipper JL, Firkins PJ, Ingham E, Stone MH, Farrar R, Fisher J, "Quantitative Analysis of the Wear Debris from Low and High Carbon Content Cobalt Chrome Alloys used in Metal on Metal Total Hip Replacements", 8th Annual Meeting of the European Orthopaedic Research Society, May 7-10, 1998.

4. Firkins PJ, Tipper JL, Ingham E, Stone MH, Farrar R, Fisher J, "Quantitative Analysis of the Wear Debris from Metal on Metal Hip Prostheses Tested in a Physiological Hip Joint Simulator", Trans. Orthop.res. Soc., 45:49, 1999.

5. Tipper JL, Firkins PJ, Ingham E, Fisher J, Stone MH, Farrar R, "Quantitative Analysis of the Wear and Wear Debris from Low and High Carbon Content Cobalt Chrome Alloys used in Metal on Metal Total Hip Replacements", Journal of Material Science: Materials in Medicine, Vol. 10, 1999.

6. Firkins PJ, Tipper JL, Ingham E, Stone MH, Farrar R, Fisher J, "Influence of Simulator Kinematics on the Wear of Metal on Metal Hip Prostheses", Poster No 574, 46th Annual Meeting of the Orthopaedic Research Society, Orlando, March 2000.

7. Firkins PJ, Tipper JL, Ingham E, Stone MH, Farrar R, Fisher J, "A Novel Low Wearing Differential Hardness, Ceramic on Metal Hip Joint Prosthesis", submitted September 99.

8. Firkins PJ, Tipper JL, Ingham E, Stone MH, Farrar R, Fisher J, "Influence of Simulator Kinematics on the Wear of Metal on Metal Hip Prostheses", submitted to Journal of Engineering in Medicine March 2000.

9. Besong AA, Farrar R, Jin ZM, "Contact Mechanics of a Novel Metal on Metal Total Hip Replacement", Proceedings of the 12th Conference of the European Society of Biomechanics, Dublin, 2000.

10. Firkins PJ, Tipper JL, Ingham E, Stone MH, Farrar R, Fisher J, "A Novel Low Wearing Differential Hardness, Ceramic on Metal Hip Joint Prosthesis", accepted for Journal of Biomechanics, February 2001.

11. Jin ZM, Firkins P, Farrar R, Fisher J, "Analysis and Modelling of Wear of Cobalt Chromium Alloys in a Pin On Plate Test for a Metal On Metal Total Hip Replacement", Proceedings of the Institution of Mechanical Engineers, Journal of Engineering in Medicine, Volume214 Part H, 2000

EFFECT OF DIAMETER ON THE WEAR OF METAL-ON-METAL HIPS

M.B. Schmidt and R.Farrar*

Johnson & Johnson Professional, Inc. Raynham, MA USA
*Johnson & Johnson Orthopaedics, New Milton, Hants UK

INTRODUCTION: Clinical and simulator studies indicate that wear of polyethylene acetabular cups is dependent on femoral head size[1,2]. This relationship may not apply to metal-on-metal hip components, however, which contact over much smaller areas due to their lower compliance. The objective of this study was therefore to examine the effect of diameter on the wear performance of metal-on-metal hip components.
METHODS: Metal head and cup test samples with nominal diameters of 22 mm, 28 mm, and 35 mm were manufactured from ASTM F1537 (F799) CoCrMo alloy. Diametric clearances for all samples were 0.030-0.139 mm. Head and cup surfaces were polished to yield Ra values of 0.02 μm or better. For comparison, 28 mm polyethylene cups, gamma sterilized in vacuum-foil packaging, were also studied. Wear tests were performed using an MMED hip simulator. All tests were run at 1.1 Hz, using the Paul loading curve[3] with a 2000N peak load and serum lubrication. Wear was measured by weight loss and converted to volume loss by dividing by material density.
RESULTS: Head size did not have a significant influence on total wear of metal-on-metal components. Average total wear at 2 million cycles was 0.657 ± 0.472 mm^3, 0.607 ± 0.260 mm^3, and 0.864 ± 0.434 mm^3 for the 22 mm (n=5), 28 mm (n=5), and 35 mm samples (n=6), respectively. In contrast, the average total wear for the polyethylene acetabular components was 20.82 ± 3.84 mm^3 (n=6), which was significantly greater than all sizes of the metal-on-metal components.

[1] J. Livermore et al., *J. Bone Jt. Surg.* **72-A**:518, 1990.
[2] I.C. Clarke et al., unpublished data, 1995.
[3] J.P. Paul, *Proc. Inst. Mech. Eng.*, **181(3J)**:8, 1966.

THE EFFECT OF DIAMETRAL CLEARANCE ON WEAR BETWEEN HEAD AND CUP FOR METAL ON METAL ARTICULATIONS

Farrar R., Schmidt M.B.*
Johnson and Johnson Professional, New Milton, Hampshire, UK

RELEVANCE TO MUSCULOSKELETAL CONDITIONS: Minimization of particulate debris release from articulating surfaces is an important goal of prosthetic hip design.

INTRODUCTION: A theoretical study of the tribology of hard spherical bearing surfaces suggests that the potential for fluid film lubrication to develop between the articulating surfaces increases as the clearance between the surfaces is reduced[1]. As the lubrication regime tends towards full fluid film, the contact and, therefore, wear between the articulating surfaces should be reduced. The present study was carried out to investigate experimentally the relationship between diametral clearance and metal on metal wear for a 28mm head configuration.

MATERIALS AND METHODS: Twelve metal head and cup test samples with nominal diameter of 28mm were manufactured from ASTM F1537 (F799) CoCrMo alloy. Diametral clearances ranged from -0.074 to 0.322mm (Table 1). Head and cup surfaces were polished to Ra values of 0.02μm or better. The test was run on a 12 station hip simulator (MMED) for a total of 2028204 cycles at a frequency of 1.1Hz operating a Paul[2] loading curve with maximum load of 2000N. The parts were cycled in bovine serum and measurements of wear were made in terms of weight loss using a balance at 0, 20000, 53110, 107325, 284975, 605010, 1157280, 1609800, and 2028204 cycles. The weight loss data were converted to volume loss assuming a material density of 8331kg/m^3.

RESULTS: Table 1 shows the total volume loss at 2028204 cycles and graph 1 shows a three dimensional plot of wear against diametral clearance and number of cycles. These clearly demonstrate reducing wear with reducing diametral clearance down to about 0.080mm. However, with reductions in clearance below about 0.030mm an increase in wear occurs.

Considered individually, most samples demonstrated an initially higher wear rate reducing to a relatively low steady state level with increasing cycles.

DISCUSSION: A band of clearance can be defined for a 28mm head within which a metal on metal articulation should exhibit the lowest wear.

The reducing wear trend which is exhibited as diametral clearance is decreased from 0.322mm demonstrates good agreement with the theory. However, with further reductions in clearance below the "low wear" band, the reversal of the wear trend represents a departure from the theory. This is thought to be due to geometrical errors which are inevitable with any manufactured part but not present in a theoretical model. Where small clearances approach the order of the cumulative geometrical errors, contacts may develop much closer to the equator and the possibility of a simulated local negative clearance exists.

It is possible to simulate the so called "Equatorial Bearing" devices, such as the pre 1970 McKee-Farrar and Ring prostheses, on a hip simulator by having a negative or very low clearance. In this case the negative clearance samples reached about 20,000 cycles, exhibiting the highest wear rate, before seizing completely.

The generally low level of volumetric wear for these metal on metal articulations is in contrast to the much higher mean levels for metal on polyethylene articulations of 20.82 mm^3 under similar test conditions.

It is also noticeable that with the lower clearance samples, head and cup wear was similar, whilst with increased clearance the head wear was dominant.

Table 1: Samples ranked in order of increasing clearance and indicating volumetric wear at 2028204 cycles

Sample No	Diametral Clearance (mm)	Head Wear (mm^3)	Cup Wear (mm^3)	Total Wear (mm^3)
1	-0.074	a	a	a
2	-0.040	a	a	a
3	0.014	1.092	1.020	2.112
4	0.033	0.132	0.300	0.432
5	0.050	0.336	0.276	0.612
6	0.074	0.168	0.216	0.384
7	0.097	0.564	0.504	1.068
8	0.121	0.504	0.324	0.828
9	0.139	1.092	0.996	1.02
10	0.156	0.840	0.588	1.428
11	0.174	1.284	0.432	1.716
12	0.322	2.784	0.972	3.756

[a] Samples 1 and 2 failed at 20,000 cycles with total volume loss at 0.660 (0.300 cup, 0.360 head) and 0.684mm^3 (0.192 cup, 0.492 head) respectively.

Graph 1: The tabulated data are represented in three dimensions which also shows the incremental wear of each sample through the test.

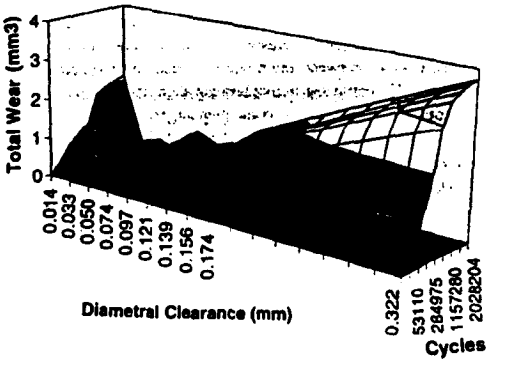

1. Jin ZM, Dowson D, Fisher J, Fifth World Biomaterials Congress, 787, 1996, Toronto.
2. Paul JP, PhD Thesis, University of Glasgow, 1967.

*Johnson and Johnson Professional Inc., Raynham, MA, USA

☒ One or more of the authors have received something of value from a commercial or other party related directly or indirectly to the subject of my presentation

☐ The authors have not received anything of value from a commercial or other party related directly or indirectly to the subject of my presentation.

FULL Name, Address, Phone, Fax, and E-Mail Numbers of Corresponding Author:
Richard Farrar
Research and Development Department
Johnson and Johnson Professional
Queensway, Stern Lane, New Milton, Hampshire
BH25 5NN, UK
Tel: 011 44 1425 624675, Fax: 011 44 1425 619923
E-Mail: rfarra@jppukc2.jnj.com

THE DEVELOPMENT OF LOW WEAR ARTICULATIONS

Farrar R*., Schmidt M.B., Hamilton J.V., Greer K.W.
Johnson and Johnson Professional, Raynham, Massachusetts, USA
*Johnson and Johnson Professional, New Milton, Hampshire, UK

INTRODUCTION

During the last 30 years, since the use of PTFE acetabular cups was shown to give poor results, ultra high molecular weight polyethylene (UHMWPE) has been used predominantly as a bearing surface with a metal or ceramic counter face. In the majority of cases during the last 20 years the material has been sterilized using gamma irradiation in air. The results for hip replacements with such articulations have been clinically successful, but concerns have been raised regarding the process and effects of oxidation on the UHMWPE material. Recent research and development investigations into types and treatments for UHMWPE materials have shown that much lower in vitro wear rates could be attained.

Throughout the 1960's and early 1970's metal on metal articulations became commonplace through prostheses such as the McKee-Farrar, Ring, and Sivash. Largely due to the perceived success of UHMWPE as an implant bearing material, these metal on metal devices were subsequently almost completely abandoned in favour of metal on UHMWPE articulations. However, with the realization that there were problems associated with the polyethylene debris shed from these articulations came a renewed clinical interest in the metal on metal articulations. It could be argued given the poor prosthetic designs utilized, that these early metal on metal devices did not perform too badly over a long period of clinical use. During the 1990's extensive research and development effort has been aimed at reducing the in vitro wear performance of such articulations .

This paper describes some of the work carried out by the authors into the improvement of in vitro wear performance of both, UHMWPE on metal, and metal on metal articulations, and the results achieved.

METHODS

A number of tests were carried out using pin on disc (POD) machines with a load of 132N (initial stress of 64MPa) for cobalt chromium alloy pins on UHMWPE discs. Further testing utilized a 12 station hip simulator (MMED) at a frequency of 1.1Hz operating a Paul[1] loading curve with maximum load of 2000N for both all metal (cobalt chromium alloy) and metal (cobalt chromium alloy) on UHMWPE articulations. All testing results were up to about 2 million cycles and were recorded as mass loss and converted to volume loss (ρ=940kg/m^3 for polyethylene and 8331kg/m^3 for CoCr). The POD testing was carried out on metal against UHMWPE combinations whilst the hip simulator tests were done on UHMWPE against metal and metal against metal articulations.

To establish the effects of material grade and sterilization by gamma irradiation (40 kGy), a series of tests were conducted on air sterilized, and vacuum sterilized (in foil pouches) UHMWPE. UHMWPE grades GUR 4150 and GUR 1120 having calcium stearate as a processing additive were used along with a calcium stearate free grade GUR 1020.

It has been suggested[2,3] that for metal on UHMWPE articulations there is a dependency between head diameter and total volumetric wear. Furthermore, a relationship between femoral head diameter and fluid film thickness has been predicted[4] (figure 1) in a study of the tribology of spherical bearing surfaces. Therefore a range of cobalt chromium alloy head and cup samples with nominal diameters 22, 28, and 35mm were tested to establish whether this dependency was seen to exist for metal on metal articulations in vitro.

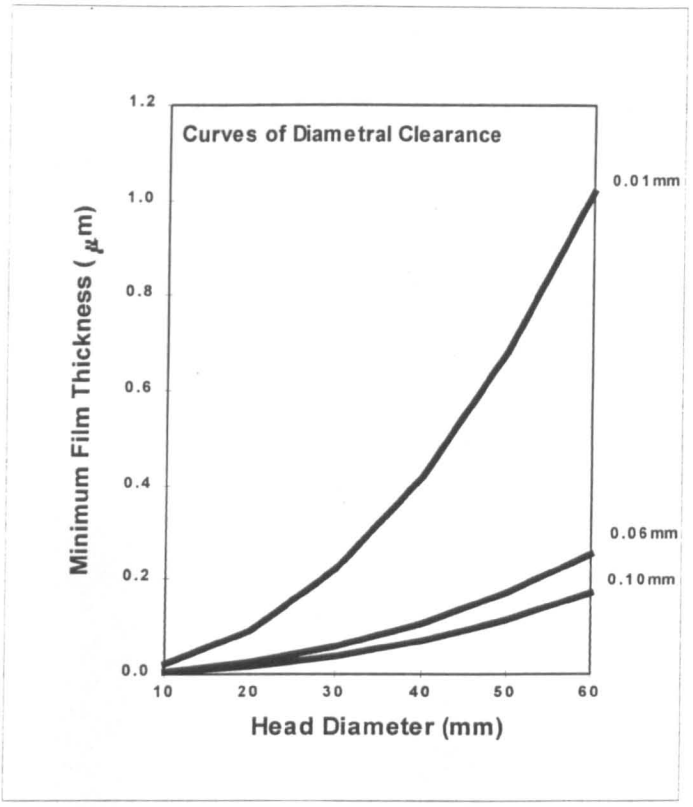

Figure 1: Predicted fluid film thickness against head diameter and diametral clearance[4]

Predictions based on tribological theory have also been made regarding variations in diametral clearance between heads and cups[4]. Therefore, for a 28mm nominal diameter, a range of diametral clearance values between -0.074 and 0.322mm were tested in vitro on a hip simulator.

It has also been suggested that in pin on disk testing of cobalt chromium alloy pairings, the lowest wear couples were ones where the alloy contained a relatively high carbon content[5] (figure 2). For a 28mm nominal diameter, a series of metal on metal articulations with varied material composition were tested using a hip simulator.

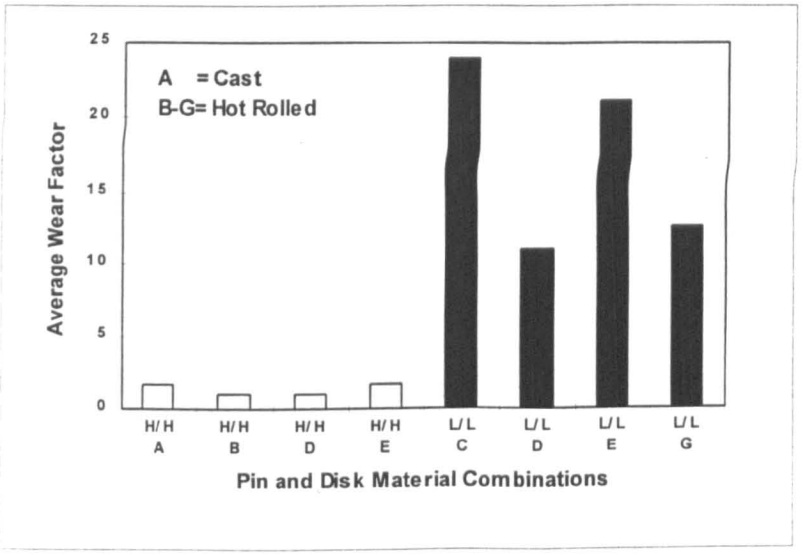

Figure 2: Pin on Disk Results Reported by Schmidt et al.[5]

RESULTS

Using the POD testing it was shown that 5 out of 8 samples of GUR 1120 which were sterilized by gamma irradiation in air exhibited pitting between 47,000 and 2 million cycles. By contrast none of the 12 samples of GUR 1020 sterilized in vacuum in a foil pouch exhibited any pitting within 2 million cycles[6].

Using the hip simulator, the lowest wear of 20.8mm^3 was exhibited by the calcium stearate free UHMWPE GUR 1020 sterilized vacuum packed in a foil pouch (figure 3). By contrast GUR 4150 and GUR 1120 material sterilized by gamma irradiation in air yielded a wear of more than double the lowest wear value[6] of 59.5 and 65.8mm^3 respectively.

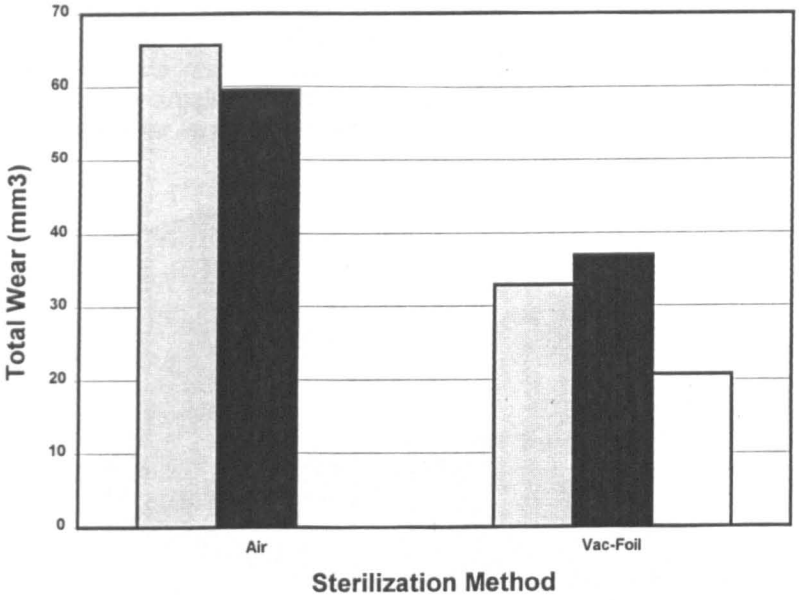

Figure 3: Hip simulator results for various UHMWPE types and sterilizations

In testing metal on metal samples in a hip simulator, there was very little difference in performance between 22, 28, or 35mm head diameters[7]. However, for 28mm samples with variation of diametral clearance there was substantial variation of wear between samples[8] (*maximum of 3.756mm^3 for 0.322mm* clearance compared with a minimum of 0.384mm^3 for a clearance of 0.074mm, figure 4).

When 28mm samples with variation of cobalt chromium material composition were tested, the combination of high carbon against low carbon articulations (0.485mm^3) yielded the lowest total wear compared with either the low against low (0.570mm^3) or the high against high (0.541mm^3) articulations (figure 5).

DISCUSSION

When tested in vitro on a POD machine it was clear that the material type and sterilization treatment could be varied to produce a material less susceptible to pitting. This result is thought to be of particular relevance to the knee since it is likely that pin on disc tests provide a similar type of pitting wear mechanism to that shown in knee replacement articulations having relatively low conformance between the surfaces. Here, fatigue of subsurface material leading to subsurface cracking and eventual loss of particles from the articulating surface is thought to be a dominant wear mechanism.

On the hip simulator it was clear that UHMWPE subjected to gamma irradiation in a vacuum foil pack exhibited less than half the wear at 2 million cycles than that sterilized conventionally by gamma irradiation in air. Calcium stearate free material performed even better.

The improvement in performance of the vacuum foil packaged GUR 1020 UHMWPE was due to the increase in cross linking and hydrogen recombination that resulted from gamma irradiation in an oxygen free atmosphere[6]. Additional improvement can be attributed to better consolidation of the calcium stearate free material during molding, which essentially eliminated the fusion defects typically found in UHMWPE containing calcium stearate[9].

Whilst nominal articulation diameter between 22 and 35mm did not appear to have *significant impact on the total wear* of metal on metal articulations, the variation of diametral clearance did demonstrate that some *optimum band of clearance exists* within which wear may be minimized. Theoretically, the lubrication regime is sensitive to *diametral clearance* for this type of hard spherical bearing (figure 1). As clearance decreases, fluid film thickness increases and as a result, contact and therefore wear between the articulating surfaces is reduced. At very small clearances, however, geometrical inaccuracies may come into play with increased wear as a consequence.

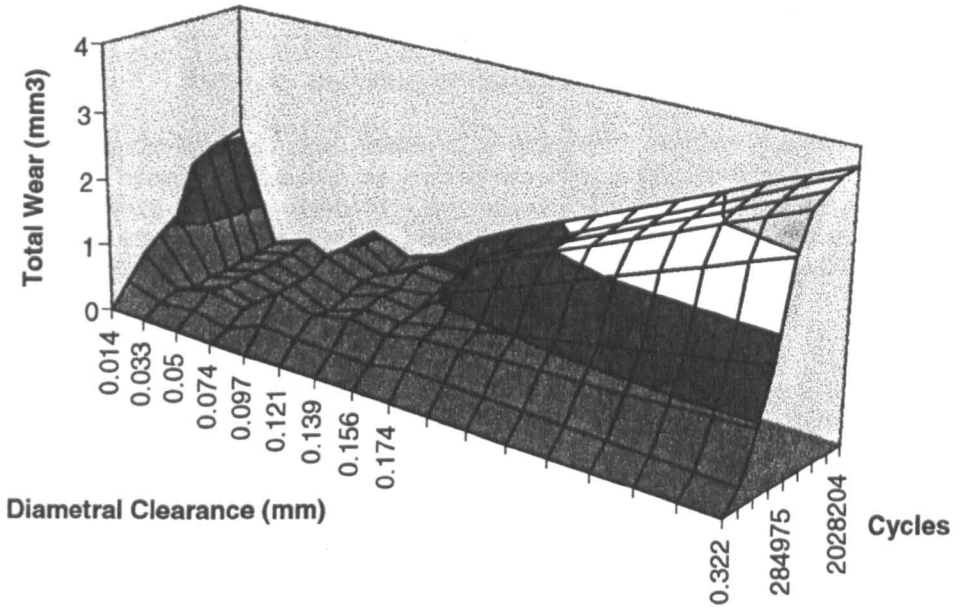

Figure 4: Variation of wear with diametral clearance

It was believed that within the range of nominal diameters tested, boundary or mixed lubrication regimes prevailed, at least for virgin components[8]. Operating largely outside of a full fluid lubrication regime means that contact between the articulating surfaces will occur. This means that the materials used for the wear couple can have an effect on wear performance. Indeed, the hip simulator tests reported here indicate that the use of high carbon (>0.18 wt. %) against low carbon (<0.07 wt. %) cobalt chromium alloy materials resulted in lower total wear than either high against high carbon or low against low carbon combinations (figure 5). This is in contrast to previously reported data from unidirectional wear screening tests (figure 2).

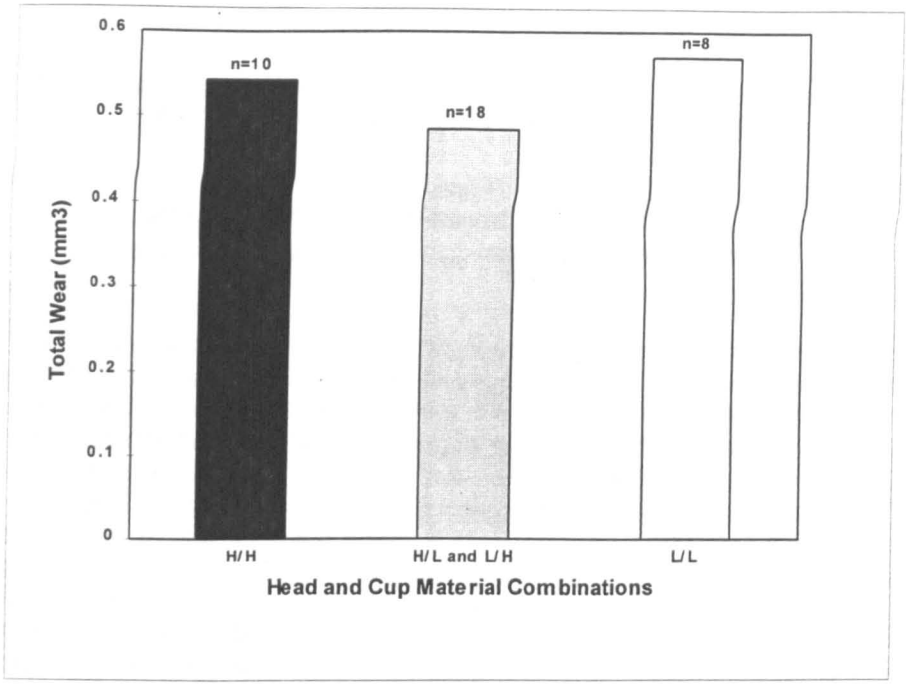

Figure 5: Material type data generated on hip simulator

The lowest overall wear was exhibited by the 28mm nominal diameter metal on metal articulation having one low and one high carbon component, being a factor of 69 times lower than the lowest metal on UHMWPE combination. This could have significant implications in the clinical environment where it is believed that all debris release has some effect on the surrounding environment and therefore a reduction in total volume could be beneficial.

CONCLUSION

Metal on UHMWPE articulations have performed well on the whole over a 30 year period compared to what existed previously. However, recently a significant step forward has been taken in reducing the wear of such articulations in vitro and it is also postulated that the new sterilization process results in a more stable material which should not suffer the levels of oxidative degradation exhibited by the usual material and treatment. This must be of benefit to the next generation of patients. However, it has also been demonstrated that use of metal on metal articulations tested under identical conditions have yielded results nearly two orders of magnitude lower in terms of wear volume. Such articulations are beginning to hold out the hope of increased longevity hip replacements in the years to come.

REFERENCES

1. Paul JP, PhD Thesis, University of Glasgow, 1967.
2. Livermore J, Ilstrup D, Morrey B, J. Bone Jt. Surg. 72-A, 518, 1990.
3. Clarke IC, Gustafson A, Jung H, Fujisawa A, Acta. Orthop. Scand., 67(2): 128, 1996.
4. Jin ZM, Dowson D, Fisher J, Fifth World Biomaterials Congress, Toronto, 1996
5. Schmidt M, Weber H, Schon R, Clin Orthop, 329S, 1996
6. Hamilton JV, et al., Trans Orthop. Res. Soc., 21:20, 1996 and 22:782, 1997.
7. Schmidt MB, Farrar R, Ninth Annual Symposium of the Intl. Soc. for Technology in Arthroplasty, Amsterdam, 1996.
8. Farrar R, Schmidt MB, Trans. Orthop. Res. Soc., 22:71, 1997.
9. Schmidt MB, Hamilton JV, Trans. Orthop. Res. Soc., 21:22, 1996.

CHARACTERIZATION OF THE WEAR BEHAVIOR OF METAL-ON-METAL HIP COMPONENTS USING A JOINT SIMULATOR

M.B. Schmidt and R. Farrar*
Johnson and Johnson Professional, Inc., Raynham MA
*Johnson and Johnson Professional, New Milton, Hampshire, UK

The objective of this study was to characterize and compare the wear behavior of metal-on-metal (MOM) and gamma sterilized metal-on-polyethylene (MOP) couples using a hip joint simulator. A twelve-station MMED hip simulator was used, which produces a biaxial rocking motion of the cup relative to the head. Calf serum with 0.2% w/v sodium azide and 20 mM EDTA was used to precondition UHMWPE cups and as a lubricant during testing. Due to concerns about the influence of inorganic precipitates on MOM lubrication, the effect of EDTA on MOM wear was assessed. Wear was measured at intervals throughout the 2 million cycle test by assessing weight loss of UHMWPE cups and total weight loss of MOM heads and cups combined. Cleaning techniques were adapted from McKellop et al.[1] for UHMWPE, with modifications for MOM samples. Control UHMWPE cups were soaked and weighed at identical intervals to correct for continued fluid absorption. Similar control MOM samples were used to confirm that the cleaning procedure did not affect the weight measurements.

Polyethylene wear consistently occurred in a nearly linear manner, with wear rates of 11.6-32.7 mm^3/million cycles, depending on the sterilization conditions used. In contrast, MOM samples characteristically exhibited biphasic wear curves, with a higher initial "wear-in" phase followed by substantially lower linear wear. Wear-in was nonlinear and the magnitude of wear during this period was dependent on head diameter and diametrical clearance between the head and cup. Volumetric wear rates for MOM samples during the second phase of wear were typically two orders of magnitude lower than MOP samples of the same diameter. EDTA was shown to have no significant effect on MOM wear rates.

In conclusion, this study demonstrates that joint simulators, together with weight loss measurements, may be successfully used to characterize the wear of alternative bearing couples such as metal-on-metal. Furthermore, simulator testing indicates that wear of this type of rigid bearing couple progresses in a fundamentally different manner than the more familiar MOP articulations. Efforts at further wear reduction for MOM articulations therefore should include decreasing the magnitude of the initial wear-in phase, as well as long-term wear.

---

[1] McKellop, H.A., and Clarke, I.C.: Degradation and wear of ultra-high molecular weight polyethylene. *Corrosion and degradation of implant materials: Second Symposium*, ASTM STP 859, A.C. Fraker and C.D. Griffin, eds. (Philadephia, PA: American Society for Testing and Materials), pp. 351-368, 1985.

PAPER # 25

*COMPARISON OF WEAR RATES FOR METAL-ON POLYETHYLENE AND METAL-ON-METAL HIPS

Michael A. Jacobs, MD, *Baltimore, MD*, Mary Beth Schmidt, PhD, Richard Farrar

Recent clinical studies suggest that polyethylene wear and associated debris may result in long-term problem for some total hip replacement patients. Sub-micron debris particles are thought to cause osteolysis in the surrounding bone leading to loosening and revision. The wear performance of polyethylene components my be improved through changes in the composition and processing of UHMWPE. Reexamining the potential of a metal-on-metal articulation is an alternative approach. The objective of this study was to compare the volumetric wear rates of several different metal-on-polyethylene bearing couples to that of a metal-on-metal couple under the controlled conditions provided by hip simulator testing.

The polyethylene acetabular components were divided into the following four groups based on sterilization method and grade of UHMWPE: 1) GUR412, gamma sterilized in air; 2) GUR412, sterilized using ethylene oxide gas; 3)GUR412, gamma sterilized in vacuum-foil packaging; and 4) GUR402, gamma sterilized in vacuum-foil packaging. GUR402 is identical to GUR412 but without the inclusion of calcium stearate as a processing additive. Calcium stearate has been shown to cause fusion defects within bulk UHMWPE. In all cases, 28mm wrought CoCrMo heads (ASTM F-1537) were used. The metal-on-metal components consisted of rigid hemispherical cups polished to implant-grade finish and standard 28mm femoral heads. All metal-on-metal components were made from wrought CoCrMo (ASTM-1537).

Wear testing was performed on a 12-station MMED hip simulator. This machine produces a biaxial rocking motion that is synchronized with variable compressive loads. Tests were run at 1.1 HZ using the Paul loading curve with peak loads of 2000 N for two million cycles. Samples were immersed in calf serum with 0.2% W/V sodium azide and 20 mm EDTA during testing. All UHMWPE components were preconditioned for 30 days in serum at room temperature to allow fluid absorption to stabilize. Wear was measured on the basis of weight loss, and the weight loss values for the polyethylene components were corrected for further absorption by adding the average weight gain of identical soaking control samples. Volumetric wear rates were subsequently calculated by linear regression of the weight loss data which were converted to wear volume by dividing by the material density and are reported in units of mm3 per million cycles.

The volumetric wear rate results for the metal-on-polyethylene couples are as follows: gamma/air/412 = 32.69±2.66mm3/million cycles (n=5); ETO/412 = 26.32±3.64 mm3/million cycles (n=6); gamma/vacuum-foil/412 = 16.96±2.18mm3/million cycles (n=5); gamma/vacuum/402 = 11.61±2.05 mm3/million cycles (n-8). In comparison, the average metal-on-metal wear rate was 0.12±0.07 mm3/million cycles (n=10). There were statistically significant differences among all of these values ($p<0.05$, one-way ANOVA, Scheffe multiple comparison test).

Early metal-on-metal hip components often suffered from problem related to the designs of both the articulating and nonarticulating surfaces. The results of this study, however, indicate that with current metallurgy and precision machining techniques, a metal-on-metal articulation couple may dramatically reduce the volume of wear debris generated in total hip replacements. In contrast, metal-on-polyethylene wear performance has been incrementally improved by recent processing changes such as sterilization method and atmosphere, and material grade.

PAPER # 7

*THE EFFECT OF CLEARANCE AND DIAMETER ON DEBRIS GENERATION IN A METAL-ON-METAL HIP

Michael A. Jacobs, MD, *Baltimore, MD*, Mary Beth Schmidt, PhD, Richard Farrar

Despite some successful clinical results with early metal-on-metal articulations, concerns about poor mechanical behavior and the effects of metal debris caused this concept to be abandoned. The purpose of this study is to reassess the potential application of metal-on-metal bearings for total hip arthroplasty, using a systematic approach to begin optimizing the wear performance of the articulating surfaces. The influence of clearance and diameter of the bearing couple on the amount of wear debris generated are specifically addressed.

Test samples consisted of rigid hemispherical cups, polished to implant-grade finish, and standard femoral heads with approximate diameters of 22 mm, 28 mm, and 35 mm. All components were fabricated from wrought CoCrMo (ASTM F-1537). The clearance between the heads and the cups was adjusted to provide up to twelve separate clearances for each size. For the 28 mm samples, diametral clearances ranged from 0.014 mm - 0.322 mm. The range narrowed to 0.01 mm - 0.15 mm for the 22 mm and 35 mm samples. Wear studies were performed using a multi-station MMED hip simulator. The simulator produces a biaxial rocking motion that is synchronized with variable compressive loads. All tests were run at 1.1 Hz, using the Paul loading curve, with a peak load of 2000 N, for two million cycles. Samples were completely immersed in calf serum with 0.2% W/V sodium azide and 20 mM EDTA during testing. At specific intervals, the heads and the cups were cleaned and the wear for each component was measured on the basis of weight loss. Total wear at each interval was calculated by adding the weight losses for the head and cup.

For all diameters, the smallest clearances (<0.015 mm) resulted in increased wear which may be caused by minor asphericities. Test results for the 28 mm samples indicate that total wear after two million cycles is positively correlated to clearance ($P = 0.0002$, $r^2 = 0.95$) over the range 0.033 - 0.322 mm. Total wear did not correlate as strongly with clearance for the 22 and 35 mm samples, over the decreased range of 0.02 - 0.15 mm (22 mm: $p = 0.48$, $r^2 = 0.075$; 35 mm: $p = 0.05$, $r^2 = 0.58$). The amount of wear debris generated for samples in the clearance range 0.02 - 0.15 mm was not statistically different for all 3 head sizes.

The results of this study indicate that clearance between the head and the cup plays a critical role in determining the wear performance of metal-on-metal articulations. In contrast, diameter does not appear to be as important. The failure of early metal-on-metal designs to identify the proper range of clearances and the inability to generate successful articulation couples within these demanding tolerances may have lead to increased wear in these designs. With the tighter manufacturing control afforded by current precision machining technology, the small clearances required to minimize debris generation can be consistently produced. Therefore, defining the relationship between clearance and wear is an essential step in the development of an optimal metal-on-metal design for total hip arthroplasty applications.

Effect of Head Size and Diametral Clearance on Wear Production of a New Metal-on-Metal Hip Prosthesis

JF Nolan* R Farrar† MB Schmidt# H Phillips* JK Tucker*

*Consultant Orthopaedic Surgeon, Norfolk and Norwich Hospital, Norwich, UK †Research and Development, Johnson and Johnson Professional, New Milton, UK #Applied Research, Johnson and Johnson Professional, Raynham, MA, USA

INTRODUCTION: The first generation of metal-on-metal hip replacements often failed for mechanical reasons associated with a poor understanding of bearing characteristics, and crude manufacturing tolerances. A revisiting of the metal-on-metal philosophy has occurred in the late 80's and through the 90's largely due to the fact that polyethylene debris production has been incriminated in the loosening of metal-on-plastic hip prostheses. In this study, the effect of head size and diametral clearance on wear of a metal-on-metal articulation was examined both theoretically and practically.

THE HISTORY OF METAL-ON-METAL IN NORWICH: Ken McKee was an orthopaedic surgeon at The Norfolk and Norwich Hospital, when in 1941, he began the development of the first metal-on-metal total replacement of the hip. In the late 1950's, and with the help of John Watson-Farrar, who joined him in Norwich in the early 1960's, the McKee-Farrar prosthesis was developed, the stem being a modification of the Thompson hemiarthroplasty geometry aimed at lessening the risk of impingement. In the late 1960's and the 1970's, the McKee-Farrar prosthesis was used widely around the world. Subsequent modifications to the articulation, including its conversion from an equatorial bearing to a polar bearing design, improved the tribological properties of the joint, which however remained very primitive by today's standards.

A poor understanding of the modes of failure of these prostheses, in some cases reportedly due to hypersensitivity to cobalt ions, and the mid-term success of Charnley's low friction arthroplasty, saw a withdrawal from use of the most popular of the early metal-on-metal joints. Many McKee-Farrar prostheses continued to function well, however, and in 1986, Charles Aldam and Adrian August, residents in orthopaedic surgery at The Norfolk and Norwich Hospital, with Pynsent, published the survivorship of 657 replaced joints[1]. Their study showed an 84% survival at 14 years! Longer term results have almost certainly been compromised by the inclusion in the analysis, of the earlier equatorial bearing prostheses.

In the 1990's, as the inevitable consequences of polyethylene debris have become more clearly defined the metal-on-metal concept has been revisited in Norwich. Retrieved McKee-Farrar prostheses have been re-examined and a new smaller articulation designed, based on the results of extensive in vitro testing, to establish the ideal Diametral Clearance and Head Size. Additionally, we have carried out further assays of metal levels in the surviving metal-on-metal joint replacement patients.

• THE THEORY

THEORY OF JOINT LUBRICATION: Jin, Dowson, and Fisher[2] analyzed the lubrication which should exist between mating spherical bearing surfaces. They derived a set of equations to predict the film thickness for any given articulating system.

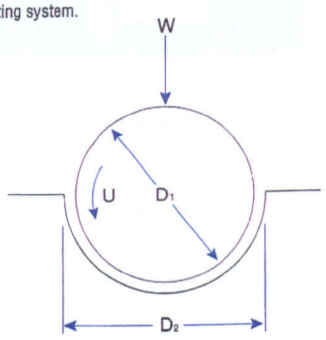

$$h_{min} = 1.64D\left(\frac{\eta u}{E'D}\right)^{0.65}\left(\frac{w}{E'D^2}\right)^{-0.21}$$

$$\lambda = \frac{h_{min}}{R_a}$$

$\lambda < 1$: Boundary Lubrication
$1 < \lambda < 3$: Mixed Lubrication
$\lambda > 3$: Fluid Film Lubrication

$$D = \frac{D_1 D_2}{D_2 - D_1}$$

$$E' = 2\left(\frac{(1-v_1^2)}{E_1} + \frac{(1-v_2^2)}{E_2}\right)^{-1}$$

$$R_a = \sqrt{R_{a1}^2 + R_{a2}^2}$$

h_{min} = minimum film thickness
D = equivalent diameter
η = lubricant viscosity
u = entraining velocity
E' = equivalent elastic modulus
w = load
R_a = combined roughness
Ra1 = Ra2 = 0.02µm

The theory suggests that the potential fluid film thickness which may be developed between the articulating surfaces increases as the clearance between the surfaces is reduced and as head size is increased. As fluid film thickness increases, the lubrication regime tends towards full fluid film so that the contact and therefore wear, between the articulating surfaces should be reduced.

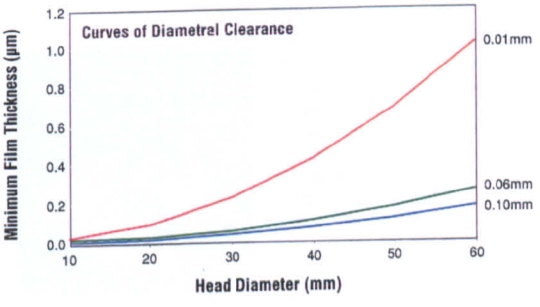

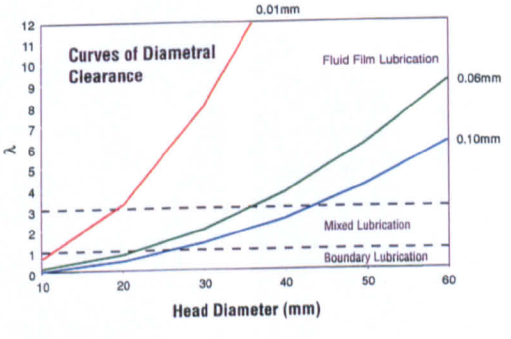

The first graph demonstrates the theoretical relationship between nominal head diameter, diametral clearance, and fluid film thickness. The second demonstrates the theoretical lubrication regime for combinations of nominal head diameter and diametral clearance. Obviously the truly no wear couple would only be possible if a "full fluid film" lubrication regime were achieved (ie. No contact between head and cup bearing surfaces). Both graphs indicate a greater sensitivity to variations in diametral clearance than to variations in head diameter.

MATERIALS AND METHODS: An M-MED 12 station hip simulator was used at a frequency of 1.1Hz and which employed a Paul[3] loading curve with maximum load of 2000N. All tests were carried out to about 2 million cycles and were recorded as mass loss and converted to volume loss (ρ=8331kg/m^3). All samples were cobalt chromium alloy with standard test piece configuration as shown.

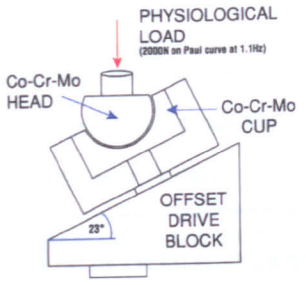

Typically run for 2 million cycles in Bovine Serum

Two separate tests were carried out. In one test, 12 samples at 28mm nominal head diameter but with variation of diametral clearance between -0.074 and 0.322mm were tested. In a second test, the effect of variation of head diameter but with constant diametral clearance was assessed by testing samples with 22, 28, and 35mm diameter.

RESULTS: The 3D wear plot clearly shows the reducing wear with reducing diametral clearance. However, below about 0.03mm an increase in wear occurs. For the variation of head size, the total wear at about 2 million cycles was not significantly different between the 22, 28, and 35mm diameter heads. This is demonstrated in the bar graph.

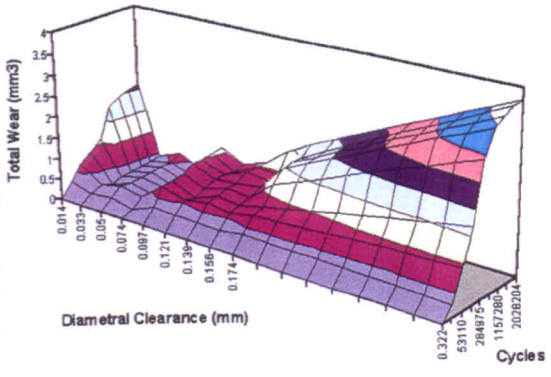

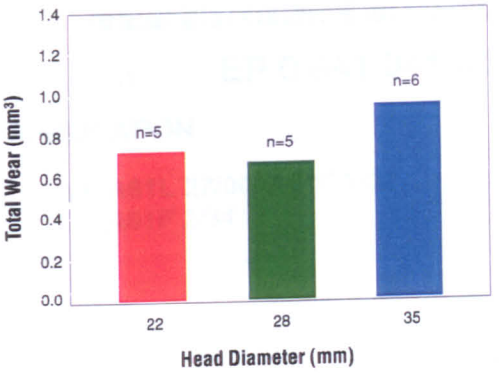

DISCUSSION: A band of clearance is clearly defined for a 28mm head diameter in which wear is minimized. Below about 0.03mm the wear is seen to increase and this is thought to be due to geometrical errors which start to have an effect when clearances are very small.

The little difference in wear results between 22, 28, and 35mm diameter articulations may point to all falling within the same mixed lubrication regime and bears out the lack of sensitivity of wear to head diameter predicted by the theory.

Based on these and other in-vitro studies, a clinical investigation product was designed utilizing an all metal cup with taper locking fit between a titanium alloy shell and a cobalt chromium alloy insert (as shown).

THE PROSTHESES: The result of this work has been the evolution of a prosthesis which relies on uncemented acetabular fixation, with elimination of polyethylene, not only from the articulation, but from the components, completely. The articulation itself, features a cobalt chromium insert, which fits via a friction locking taper into the porous coated titanium shell, the fixation of which has been proven in Norwich over the last decade.

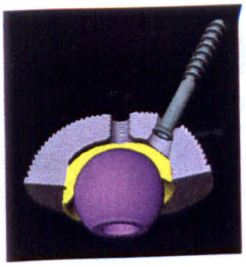

On the femoral side, a cemented cobalt chrome stem utilises the principles of the polished double-wedge taper. With the prosthesis ultimately being aimed at the younger population of hip replacement patients, serum metal levels are again being prospectively monitored.
Early clinical review, with follow-up just exceeding one year, is extremely encouraging and has identified no problems or concerns to-date.

REFERENCES
1. August A C, Aldam CH, Pynsent PB, JBJS 1986, 68B, 520-527.
2. Jin ZM, Dowson D, Fisher J, Fifth World Biomaterials Congress, 787, 1996, Toronto.
3. Paul JP, PhD Thesis, University of Glasgow, 1967.

(19) Europäisches Patentamt
European Patent Office
Office européen des brevets

(11) EP 0 841 041 A3

(12) EUROPEAN PATENT APPLICATION

(88) Date of publication A3:
17.03.1999 Bulletin 1999/11

(51) Int Cl.[6]: A61L 27/00, A61F 2/32, A61F 2/34

(43) Date of publication A2:
13.05.1998 Bulletin 1998/20

(21) Application number: 97309050.9

(22) Date of filing: 11.11.1997

(84) Designated Contracting States:
AT BE CH DE DK ES FI FR GB GR IE IT LI LU MC NL PT SE
Designated Extension States:
AL LT LV MK RO SI

(30) Priority: 12.11.1996 GB 9623540

(71) Applicant: Johnson & Johnson Medical Ltd.
Edinburgh EH2 4NH (GB)

(72) Inventors:
- Farrar, Richard
Lymington, Hampshire SO41 8AN (GB)
- Schmidt, Mary Elizabeth
Connecticut 06259 (US)

(74) Representative: Fisher, Adrian John
CARPMAELS & RANSFORD
43 Bloomsbury Square
London WC1A 2RA (GB)

(54) Hip joint prosthesis

(57) A joint prosthesis, such as an artificial hip joint (1), comprises a first component (12) and a second component (14), the articulating surfaces (20,16) of the two components (12,14) being formed from a cobalt chromium alloy. The alloy of one of the articulating surfaces (20,16) has less than 0.1% carbon by weight, while the other comprises at least 0.18% carbon by weight.

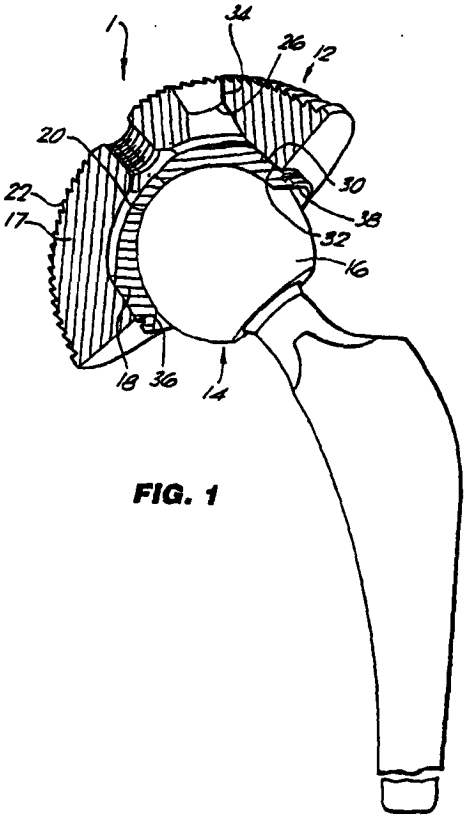

FIG. 1

EP 0 841 041 A3

US005904720A

United States Patent [19]

Farrar et al.

[11] Patent Number: 5,904,720

[45] Date of Patent: May 18, 1999

[54] **HIP JOINT PROSTHESIS**

[75] Inventors: **Richard Farrar**, Lymington, United Kingdom; **Mary Elizabeth Schmidt**, Pomfret Center, Conn.

[73] Assignee: **Johnson & Johnson Professional, Inc.**, Raynham, Mass.

[21] Appl. No.: **08/909,619**

[22] Filed: **Aug. 12, 1997**

[30] **Foreign Application Priority Data**

Nov. 12, 1996 [GB] United Kingdom 9623540

[51] **Int. Cl.**[6] ***A61F 2/36***

[52] **U.S. Cl.** 623/22; 623/18; 623/20; 623/19

[58] **Field of Search** 623/16, 18, 19, 623/20, 22, 23, 66

[56] **References Cited**

U.S. PATENT DOCUMENTS

3,744,061	7/1973	Frost	623/22
3,865,585	2/1975	Rademacher	623/66
4,631,082	12/1986	Andrews et al.	75/235
4,714,468	12/1987	Wang et al.	623/16
4,718,908	1/1988	Wigginton et al.	623/23
4,904,267	2/1990	Bruce et al.	623/18
5,549,699	8/1996	MacMahon et al.	623/18
5,571,193	11/1996	Kampner	623/18

FOREIGN PATENT DOCUMENTS

1126961	9/1968	United Kingdom .	
9716138	5/1997	WIPO	A61F 2/30
WO 9738650	10/1997	WIPO	A61F 2/32

OTHER PUBLICATIONS

R. Varano, J.D. Bobyn, and S. Yue. 1997. Characterization of Co–Cr–Mo Alloys Used in Hip Implant Articulating Surfaces, Materials Research Society Symposium Proceedings. 441:481–486.

Steicher, RM et al. "Investigation of the Tribological Behaviour of Metal–on–metal Combinations for Artificial Hip Joints," *Biomedizinische Technik*, vol. 35 No. 5/1990, pp. 3–7.

Protek AG, "Metasul, 'Metal–on–Metal Articulation'" Edition Feb. 1994, pp. 1–8.

Metasul®, Technical Information, Copyright 1993 by Allo Pro Ag, Lit. No. 1912e—Ed. Apr. 1994, 16 pp.

Semlitsch, M., et al., Long–Term Results with Metal/Metal Pairing in Artificial Joints, pp. 62–67. (Publication date unknown.)

R. M. Streicher et al., "Metal–on–metal articulation for artificial hip joints: laboratory study and clinical results,"210 Proc. Instn. Mech. Engrs. 223–232 (1996).

M. Schmidt et al., "Cobalt Chromium Molybdenum Metal Combination for Modular Hip Prostheses,"3295 Clinical Orthopaedics and Related Research 536–547 (1996).

Primary Examiner—Michael J. Milano
Assistant Examiner—Tram A. Nguyen
Attorney, Agent, or Firm—Nutter, McClennen & Fish, LLP

[57] **ABSTRACT**

A joint prosthesis having two mutually articulating components that are made of a metal alloy. One of the components is made of an alloy having a low carbon content (0.03 to 0.10 wt. %) and the other component is made of an alloy having a high carbon content (0.18 to 0.35 wt. %). The articulating components may be, for example, a hip head prosthesis and an acetabular cup prosthesis.

11 Claims, 3 Drawing Sheets

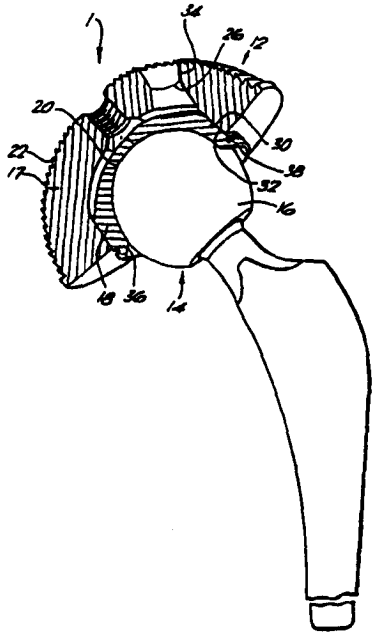

Appendix E: Procedure for Operation of Surfanalyzer 5000 Profilometer

The following is the protocol for operation of the Surfanalyzer 5000 profilometer which specifically includes guidance on selection of optimum settings, to ensure accurate and repeatable readings, for a variety of potential component forms and finishes. Additional information on profilometry and suface texture can be found in the 25th edition of Machinery's Handbook.

i. Calibration (if required)

Follow directions for Auto Calibration in Manual. The machine must be calibrated whenever probes are changed. Pre-test calibration is optional. Test the calibrated roughness standard kept in the drawer. If there are any doubts regarding the accuracy of the roughness readings obtained during testing, this could give an indication if the profilometer is yielding a proper roughness measurement. This standard is a fairly rough standard and is not calibrated to 3 decimal places like the smallest probe range, so if the samples are polished the standard may not help.

ii. Cutoff Filters

Three types of filter are available:-

Standard ANSI RC: Typically used on relatively flat surfaces
***ANSI* RC P/C:** Typically used on curved surfaces
50% Gaussian P/C: Typically used on curved surfaces and often on *flat surfaces*

For curved surfaces, if not sure which filter should be used on a given curved surface, take a trace with any one of the filters. Then, without taking another trace, recalculate that same trace using the other two filters. The most level trace, with the smallest peaks or valleys at the beginning and/or the end, is the most accurate one to use. These distortions at the beginning and/or end of the roughness trace are a result of the

processor's unsuccessful attempt to filter out the curvature of the sample. Be aware that although the standard ANSI filter is usually used on flat surfaces, it may also be used on curved surfaces. Also, both Federal Products Co. and J&J have had problems with ANSI P/C filter on curved surfaces. **Therefore, the two most popular filters on curved surfaces are the standard ANSI and the 50% Gaussian filters.**

iii. Cutoff Filter Length

The ultimate criterion for selecting a roughness cutoff filter length is to choose the shortest length with 5 - 40 roughness features (tool marks for example) per cutoff length. This indicates that the trace is long enough to accurately measure the sample, yet not long enough for any unwanted waviness to enter into the calculations. For roughness measurements, the waviness cutoff length is not operational, therefore it really doesn't matter what it is set at. Typically it is set at the same value as the roughness cutoff.

To estimate the roughness cutoff length for new samples the following table may be used. Keep in mind, however, the table is only an estimate and that ultimately the shortest cutoff distance that will give 5 - 40 tool marks is required to ensure an accurate measurement. (Note: When the drive speed is changed from 0.01"/s (0.25 mm/s) to 0.1"s (2.5 mm/s), the cutoff filter lengths increase by a factor of 10)

Average Roughness vs. estimated Cutoff Length

Average Roughness		Surface Type	Roughness	Cutoff Length
µin	µm		in	mm
0-3	0-0.076	Highly Polished	0.003	0.080
4-9	0.102-0.229		0.010	0.250
10-150	0.254-3.81	Machined	0.030	0.800
>150	>3.81		0.100	2.500

iv. Traverse Mode and Drive Speed

There are 3 traverse mode settings available:-

5-Cutoff: Use this mode for most surface roughness measurements. The program actually uses a trace 7 cutoffs long and ignores the first and last cutoffs

Traverse Length: Transverse Chisel Tip/Stylus: Use for sharp edges where the probe moves parallel to the sharp edge. Use this mode when the length that needs to be evaluated is either greater than or less than 5 cutoffs. However, check the roughness parameters to make sure you understand how they will be calculated

Stop-to-Stop: Similar to the Traverse Length Mode except that the actual traverse distance is determined solely by the safety switches on the drive unit. Use this selection when the curvature or waviness of the surface is beyond the largest sensitivity range possible. Check the roughness parameters to make sure you understand how they will be calculated.

The drive speed affects the data spacing and the maximum length over which data may be gathered as defined in the table:-

Effect of Drive Speed on Data Spacing

Drive Speed	Data Spacing	Max. Length of Data Gathered
0.25mm/s or 0.010"/s	1.25 μm or 50 μin	100mm or 4.0"
2.5mm/s or 0.100"/s	6.25 μm or 250 μin	500mm or 2.0"

Although there are two drive speeds available, the slower one (0.01"/s or 0.25 mm/s) is probably applicable for the range of surface roughness normally encountered for smoother surfaces. When the faster drive speed (0.1"/s or 2.5 mm/s) is used, the cutoff filter lengths increase by a factor of ten and the data spacing increases, thus making it less sensitive.

v. Curve Adjusting Skid (CAS)

The curve adjusting skid is for use on surfaces with a radius of curvature between 9.5mm and 38mm and having a roughness average (Ra) value of about 16 μin (0.40 μm) or less. If the surface has a rougher Ra value than 16 μin, the trace may still be accurately measured without the skid if a relatively straight line can be obtained on the roughness plot. Any one of the three filters may be used to eliminate as much of the curve as possible. Often, experimenting with the position of the sample so the most level area is traced allows for acceptable results. If the surface has a radius of curvature less than 9.5mm, it may not be able to be accurately measured with this machine. If the surface has a radius of curvature greater than 38mm, the curve adjusting skid is no longer needed. However using it should not affect calculated parameters.

For curved surfaces where the radius of curvature is unknown or is in question, the radius can be estimated (prior to performing the roughness evaluation) using the **"Crown Drop"** method. The Crown Drop method can be found in the Analyze menu under **"Crown Drop"** (when performing the crown drop method it may be necessary to enable off scale data under **"System 1"** in the Configure menu).

From some preliminary evaluations, it has been determined that the Crown Drop method should be used over the longest trace possible in order to determine the correct radius of the area evaluated. This long trace may be independent of the trace used for the roughness evaluation depending on the cutoff length and vertical sensitivity used.

For components with a fine surface finish, the following guidelines are in place for the Crown Drop method. Make a trace approximately 10X longer than needed for the roughness trace. In levelling this longer trace, it is OK to use the least sensitive vertical probe range (±500 μm or ±20,000 μin). Although the calculated roughness parameters would not be as accurate under these conditions for such a finish, it will not affect the radius of curvature calculation. After levelling this 10X longer trace, press the start button to begin collecting data. Go to the Crown Drop option under the Analysis menu from the main screen. Accept a **Centreline** (CL) value half of the overall trace

distance. Set **Evaluation Range** (ER) to approx. 90-95% of CL value. Look at the radius of curvature values for **Evaluation Distance** (ED) values ranging from 75-100% of IR, and use them to determine whether or not to use the curve adjusting skid. Use reverse polarity to analyze the radius of curvature on concave surfaces.

vi. Probe Tip/Stylus

There are 3 probe tips currently available in house although many others can be purchased from the profilometer supplier:-

High Resolution Tip/Stylus: Use for all flats with limited curvature and without a lip on the edge.
Groove Bottom Tip/Stylus (L-shaped): Use for curved surfaces, grooves, hole bottoms or flats with a lip on the edge. The groove bottom tip is used with the curve adjusting skid. There are two groove bottom tips, one with a 55 degree included angle on the diamond tip and one with a 90 degree included angle.
Transverse Chisel Tip/Stylus: Use for sharp edges where the probe moves parallel to the sharp edge.

vii. Waveform Display

there are 4 choices of Waveform Display available:-

Unlevelled Profile: Shows the total profile of the sample as is without centreing it on the vertical axis. This mode is not applicable when using the curve adjusting skid.
Levelled Profile: This takes the total profile and centres it on the vertical axis. This mode is not applicable when using the curve adjusting skid.
Filtered Roughness: This takes the profile and filters out any irregularities greater than the roughness cutoff and centres the trace on the vertical axis. Use when the roughness parameters are to be determined.

Filtered Waviness: This takes the profile and filters out any irregularities which are smaller than the waviness cutoff. Use when waviness parameters are to be determined. This mode is not applicable when using the curve adjusting skid.

viii. Parameters

Prior to taking the measurement, choose the desired parameters to be printed out from the Setup menu as follows (see Surfanalyzer Manual sections 1.4-1.6 for detailed descriptions):-

"Parameters 1"

Roughness (group 1) parameters: Ra, Rq, Rt, Rz, Rzi, R3z, R3zi, R3zm, Rp, Rpi, Rpm, and Rmax

Roughness (group 2) parameters: Rsk, Rku, Ry, Rv, Rp*(ISO), tp, S, Sm, Pc, Lq, Dq, and HSC

Waviness parameters: Wa, Wq, Wt, Wp, Wv, Lq, Dq, TIR1, and TIR2

Profile parameters (group 1): PRa, PRq, PRp, PRv, Pt, Ptp, Rz (note: this is a profile parameter and must not be confused with the roughness parameter in group 1), TIR1, and TIR2

Profile parameters (group 2): PRsk, PRku, PS, PSm, PPc, PLq, PDq, PHSC

"Parameters 2"

Roughness (group 3): Ra mx, Ra mn, Ry av, Ry mn, Rz*(ISO), and Rk...

Additional parameters can be printed out after the trace is made and saved, provided there are no specific requirements for the calculations which have been violated by the parameters under which the trace was run.

ix. Graduation Scales

The x-axis and y-axis scales for the trace printout can be changed over a large range. Make sure they are sufficient to show the roughness and/or profile features of interest.

This screen may also be opened by touching the button with the magnifying glass at the bottom of the screen.

If you change the graduation scales after a trace has been run, you can print them out, but when you save any trace, it will be saved with the same graduation scales which were specified when the trace was run. If you want to save the trace with the new graduation scales, you must rerun the trace with the new scales.

x. Report Printout (i.e. Report Header)

The report printout (i.e. the report header) is where the identification information which goes on the top of each printed trace is recorded. Typically this **"header"** area will be used to record information which will be constant for all the samples in a group (the specific part I.D. and trace direction can be recorded in the file name).

If the **"header"** is changed after the trace has been run, the trace can be printed with the corrected header, but, if the trace is saved, it will be saved with the original header. To save the trace with the new header, it must be rerun with the new header.

xi. Levelling and Probe Sensitivity

The samples should be levelled as per the directions on levelling in section 5.4 of the Surfanalyzer 5000 manual. The length of the trace must not exceed the length of the sample. **If the stylus or CAS goes off the edge of the sample or into a hole or ridge, damage to the equipment could occur.** In all modes including 5 cutoff and traverse length, the length of the probe travel during levelling and testing is defined by the mechanical stops on the drive unit. Ensure that the **HOME** position, which is the starting point for the trace, is observed. Sometimes during the levelling procedure (e.g. when a trace is aborted) the stylus/probe does not automatically return to the **HOME** position. If the sample is repositioned when the probe is not in the **HOME** position, the stylus may be forced into a problem area or off the edge of the

sample. If the levelling procedure proceeds without aborting, it should return to the **HOME** position each time.

Start levelling in the least sensitive probe range (i.e. Low) and keep increasing the sensitivity until the desired range for measuring the surfaces is reached. There are three probe sensitivity levels/probe ranges as follows:

Low: (±500μm or ±20000μin)
Normal: (±50μm or ±2000μin)
High: (±12.5μm or ±500μin).

Vertical probe sensitivity is directly related to the sensitivity of the results of your trace. Therefore, for surface roughness measurements, the most sensitive vertical probe range possible should be utilized. See table below for Ra resolution for each range.

Ra Resolution for each Vertical Probe Range

Range	Sample Rate (4096 bits/total range)	Ra Resolution
±500 μm or ±20000 μin: Low	0.2μm/bit or 10μin/bit	0.1μm or 5.0μin
±50 μm or ±2000 μin: Normal	0.02μm/bit or 1.0μin/bit	0.01μm or 0.5μin
±12.5μm or ±500 μin: High	0.005μm/bit or 0.25μin/bit	0.002μm or 0.1μin

For roughness or waviness traces, the part does not have to be exactly levelled. Levelled profile traces should be exactly levelled to give the proper perspective. When using curve adjusting skid, levelling is done with the set screw on the top of the skid. Do not level with the knob on the top of the drive box which is used for levelling skidless operations. Because the set screw has a relatively coarse thread, it may be preferable to utilize the **"offset"** to get the final levelling, especially on the Normal and High sensitivity ranges. For detailed instructions see section 5.3 of the Surfanalyzer Manual. When levelling is complete, leave the levelling screen by pressing **DONE**, then run the trace by pressing **START** on the main screen and then pressing **START** again to take the measurement.

xii. Saving and Printing of Traces

In order to save the trace, go to the **"Load/Save"** option in the Setup menu. Give the trace a file name which is unique and identifies the part and the trace direction measured. The file name can have up to 14 characters, but cannot contain any spaces. Save the trace, which stores it on the C-drive (i.e. hard drive) of the computer. When the trace has been saved, it can be printed out by touching the Printer button in the lower right corner of the screen. It will print out at the thermal recorder or printer selected under **"System 1"** in the Configure menu. Change from the thermal recorder (i.e. Recorder) to an external printer (i.e. Printer) by changing the **"COPY DEVICE"** from Recorder to Printer under **"System 1"** in the Configure menu. Printouts may also be made by using the Printer button on the "Profile" screen under the Analyze menu. In this case, the printout can be configured to show either one or two graphs at the same time. For one graph to be printed, **PLOT 1** and **PLOT 2** (see "Waveform Displays" under the Configure menu) should list the same graph. For two graphs to be printed, **PLOT 1** and **PLOT 2** should list different graphs. For more detail see Surfanalyzer Manual section 4.4.3.

Save file to a floppy disk if requested. A previous trace may be loaded by going to **"Load/Save"** in the Setup menu and either loading it from the hard disk (drive C) or from a floppy disk (drive A). To transfer a trace from the hard disk to a floppy disk, it must first be loaded, then it can be saved to the floppy disk.